Mesozoic deformations of the southwestern Transdanubian Range: the role of Triassic – Jurassic inherited normal faults in the development of Cretaceous folding and thrusting

Héja Gábor Herkules

Dissertation submitted to the Ph.D. program for Geology and Geophysics at the Ph.D. School of Earth Sciences, Eötvös Loránd University, Budapest
in partial fulfilment of the requirements for the degree of
Philosophiae Doctor

Supervisor:
Dr. Fodor László
scientific advisor

Head of the Ph.D. School: **Dr. Bartholy Judit**
Chair of the Ph.D. Program: **Dr. Harangi Szabolcs**

2019

Eötvös Loránd University
MTA-ELTE Geological, Geophysical and Space Science Research Group
Budapest, Hungary

1. Introduction

1.1. General background of the research

Pre-existing normal faults have an increasing role in the structural interpretation of thrust and fold belts (Butler et al. 2006). Several balanced sections show that the retro-deformed original stratigraphy cannot be considered as a layer-cake and prominent pre-orogenic deformation can be recognized (Perez et al. 2016; Yagupsky et al. 2008, De Vicente et al. 2009).

Identification, investigation and understanding of these early structures have primary importance. On one hand, pre-existing normal faults may represent important map-view structures, which basically determine the basin geometry of the subsequently shortened succession. On the other hand, these early structures may have significant effect on the final geometry of subsequent folding and thrusting, and pre-existing normal faults are inherited in several ways in compressional deformation.

Pre-orogenic normal faults develop mostly during continental rifting, subordinately during passive margin evolution or even during foreland basin evolution; in the latter case due to the flexure of the subducting lower plate (Butler et al. 2006; Billi & Salvini 2003).

Investigation of pre-orogenic normal faults is often complicated, since such structures can be strongly overprinted by later contractional deformation in thrust belts. However, pre-orogenic syn-sedimentary structures are often accompanied by secondary features, which may survive the basin inversion. Such features are abrupt facies changes (Bertotti et al. 1993; Jadoul et al. 2005) reflecting significant changes in depositional environment (e.g. deepening) and characteristic sediments and sedimentary structures related to fault activity, such coarse-grained talus cone breccias (Bertotti et al. 1993; Ortner et al. 2008) or soft-sediment deformation (Bergerat et al. 2011). Nevertheless, syn-sedimentary extension creates facies change only in those cases, when the rate of extension-related subsidence of the hanging wall is significantly larger than the rate of deposition. If the deposition keeps pace with the subsidence of the hanging wall, both the hanging wall and the footwall can have the same environment, and thus the fault cannot be identified solely on the basis of facies changes. In this case, thickness variation of the pre-orogenic succession can be an indicator of syn-sedimentary normal faulting, which can be detected by several techniques including balanced cross-sections (e.g. Behrmann & Tanner 2006).

Irregularities in thrust-and-fold belts can be often traced back to inheritance of pre-existing normal faults (Butler et al. 2006). Different types of structural inheritance appear both in section and map view. Such inheritances are, for example, when a footwall ramp of a thrust

or a buckling fold is localized by an early normal fault (Figs.1.1a, b and f; Schedl & Wilitschko 1987; Wilitschko and Eastman 1983). In many cases, structural inheritance is responsible for the development of backthrusts (Fig.1.1e; Colpron et al. 1998; Gelabert et al. 2004 Bonini et al. 2012), or young-on-older thrusts (Fig.1.1d; Pace et al. 2014). Pre-existing normal faults can also suffer simply compressional reactivation or inversion (Fig.1.1c; Bonini et al. 2012).

Pre-existing normal faults are often responsible for the development of compressional transfer zones. These structures link areas characterized by different amount of shortening (Moustafa & Khalil 2016). Transfer zones are oblique or lateral to the general trend of thrust and fold belt, and they are represented by curved thrusts (Marschak 2004), oblique and lateral ramps (Corrado et al. 1998; Ustaszewski & Schmid 2006) or tear faults (Said et al. 2011). These oblique/lateral structures are often localized along pre-existing normal faults, whose strikes are oblique or perpendicular to the future shortening.

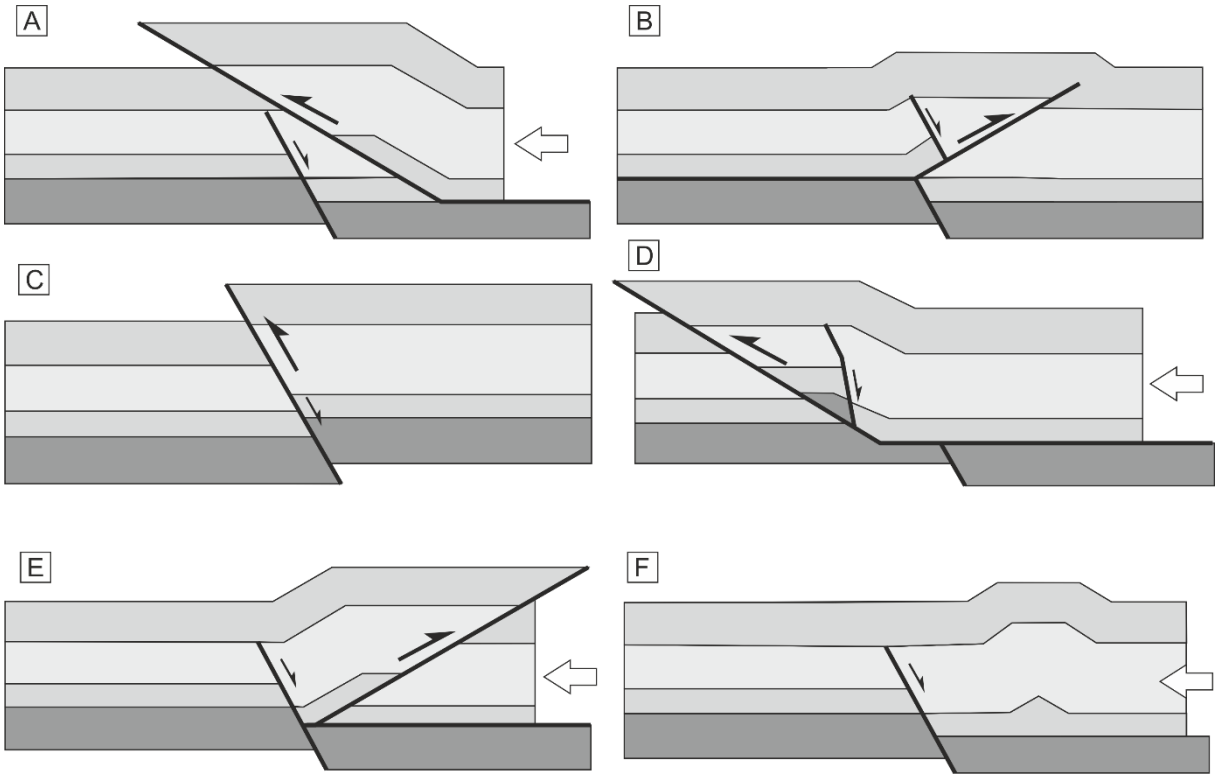

Fig.1.1: Models for different types of control of pre-existing normal faults on late contractional deformation. Note reactivation of old normal faults or localization of thrust faults by the old normal fault.

The study area is the southwestern part of the Transdanubian Range, which is situated in the well-investigated Pannonian Basin (Fig.1.2). Based on previous works, Mesozoic evolution of the Transdanubian Range can be characterized by Triassic – Jurassic extension followed by Cretaceous folding, thus this area can be a good candidate to study this interaction. This is one of the main topics I concentrated during my PhD research. Researches of the last century accumulated considerable amount of structural data and concept about the evolution of the Transdanubian Range and the Pannonian Basin in general.

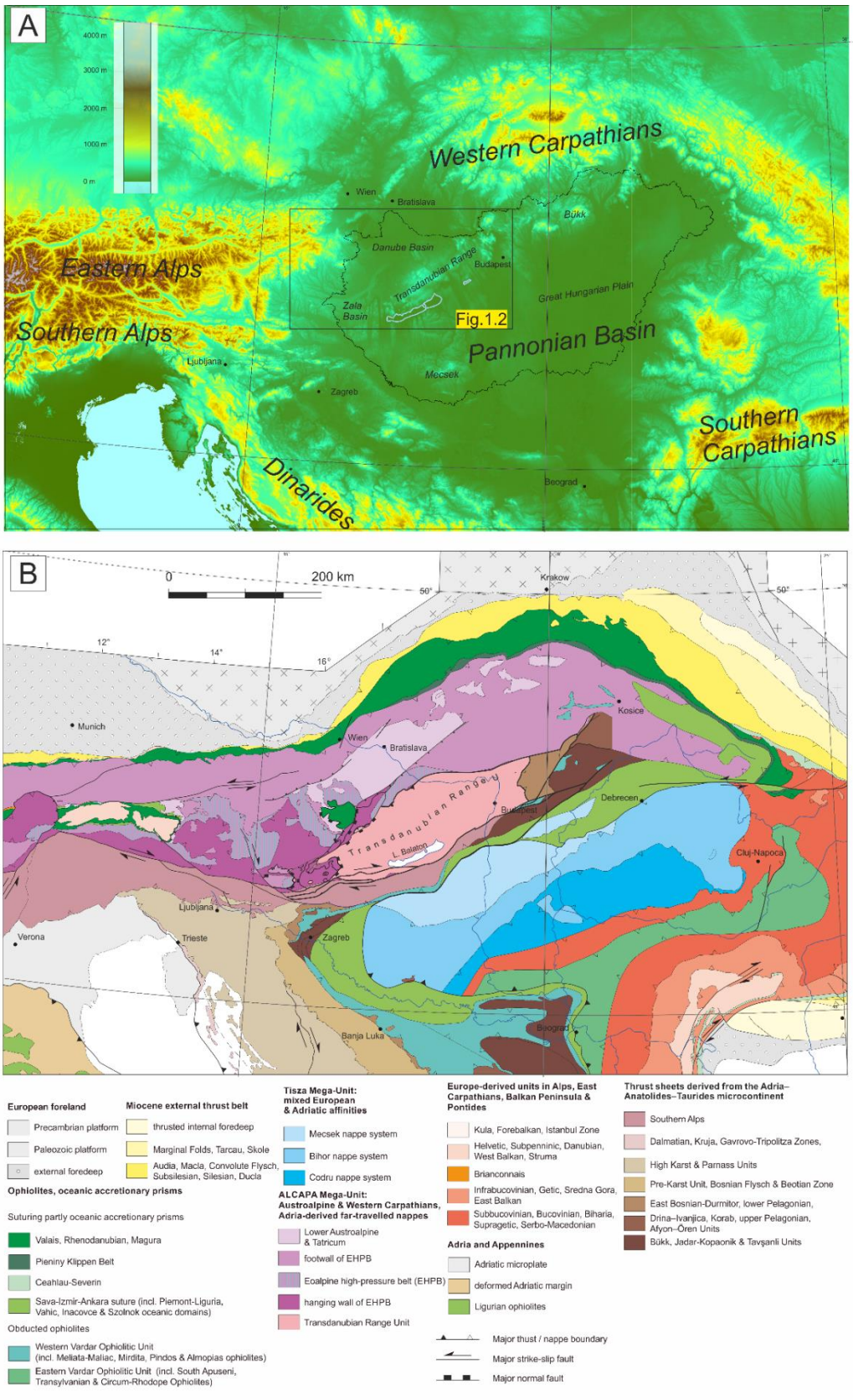

Fig.1.2: (a) Topographic image of the Pannonian Basin and surrounding mountain belts; (b) The position of the Transdanubian Range Unit within the Alpine–Carpathian–Dinaridic units (Schmid et al. 2016 modified by Fodor et al. 2017).

A schematic and simplified view is given on Figure 1.3., and can be compared to my results and concept, given in the last part of this work.

The Miocene extensional Pannonian basin is a famous example of back-arc basins, and it provides important analogy for other back-arc basins of the world (e.g. Balázs et al. 2017). Its Miocene evolution is the topic of a huge amount of studies since the 1980s till most recent works (Horváth & Berckhemer 1982; Balla 1988b; Royden 1988; Rumpler & Horváth 1988; Csontos et al. 1991, 1992; Tari et al. 1992; Horváth 1993; Tari 1994; Csontos 1995; Horváth & Cloething 1996; Fodor et al. 1999; Horváth et al. 2006, 2015; Balázs et al. 2017). However, pre-Cenozoic evolution of the basement of the Pannonian Basin is poorly known, and much more controversial (Fig.1.2b). Nevertheless, investigation of the pre-Miocene basement is important in respect of hydrocarbon exploration, since Mesozoic deformations determined many features of important source rocks and reservoirs (Badics & Vető 2012, Csizmeg et al. 2016). Therefore, I concentrated in this work mostly on the Mesozoic structural evolution of the study area, but of course, I could not ignore Cenozoic deformations, which strongly overprinted Mesozoic structures. Thus during the first steps of my research, I needed to determine the effect of Cainozoic deformation, then go on with the older structures.

It is known that the Transdanubian Range was affected by repeated pre-orogenic extension before Cretaceous folding (Galácz & Vörös 1972; Galácz 1988; Budai & Vörös 1992, 1993, 2006; Haas 1993b; Csillag et al. 1995; Vörös & Galácz 1998; Budai et al. 2001), but the

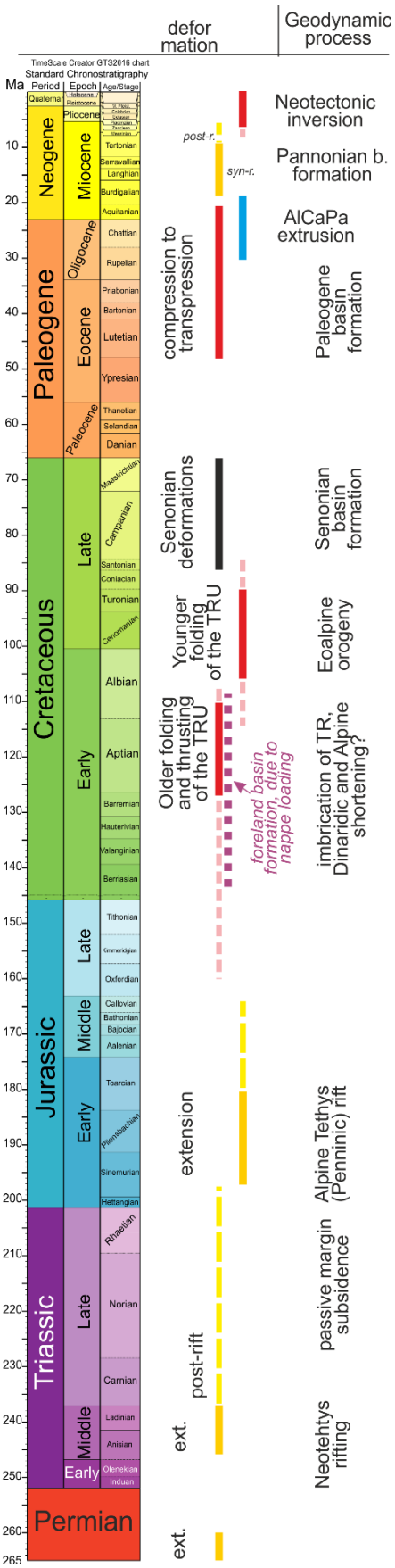

Fig.1.3: Main deformations, structural phases and possible geodynamic links in the Transdanubian Range Unit. For sources see the text of Chapter 1 and 2

related map-view structures are just poorly identified and they have not been interpreted on seismic sections or illustrated on geological cross sections, yet. This early extensional deformation is postulated mainly based on abrupt facies changes (Fig. 1.3). However, pre-orogenic syn-sedimentary faults are just rarely observed directly (Lantos 1997; Fodor et al. 2013a). In this work, I make a first attempt to identify map-view pre-orogenic normal faults in the southwestern Transdanubian Range based on modern 2D seismic sections, 3D cubes, and balanced cross-sections. I will add surface observation to the seismic interpretation, and I try to give a coherent view of Mesozoic extensional structures in the whole southwestern Transdanubian Range (Héja et al. 2015, 2018). During field work, I refine my surface observation made during my master works (Héja 2015a, c).

One of the major deformations of the Transdanubian Range is its folding during the Cretaceous (e.g. Haas et al. 1984; Tari 1994), although the geometry, the style of deformation and the number of folding phases are strongly controversial in different works (Fig. 1.3). Cretaceous compressional structures show various trends, which is traditionally explained by two or even three phases of folding events in the Transdanubian Range (Tari 1994; Pocsai & Csontos & Vörös 2004; Csontos et al. 2005; Sasvári 2008, 2009; Tari & Horváth 2010). In contrast, my results show that deviations of fold trends can be explained rather by inheritance of Triassic and Jurassic pre-orogenic normal faults than multiphase folding (Héja et al. 2016, 2017a). In this topic, I also combined surface maps and observations with subsurface mapping; in this way I could prepare a detailed structural map of the Cretaceous contractional structures (Héja et al. 2015, 2018).

The nature of the compressional structures is also not clear; several authors propose the presence of internal thin-skinned nappes within the Transdanubian Range (Tari 1994; Tari & Horváth 2010; Csontos et al. 2005; Sasvári 2009), which corresponds to large-scale allochtonity and large amount of internal shortening. On the other hand, other authors calculate with smaller amount of internal shortening (Dudko 1996; Fodor et al. 2013a; Fodor et al. 2017). I tried to clarify this issue based on construction of regional cross-sections and their balancing. In this respect, I broadly followed cross sections of Fodor et al. (2013a), but choose a direction better supplemented by modern and good-quality seismic data. The different data sets and combined approaches permitted a more detailed interpretation. Balancing the main regional section gives additional constraints in structural interpretation, the base of detachment, and the amount of shortening (Héja et al. 2017b).

1.2. Position of the Transdanubian Range in the Pannonian Basin

The Transdanubian Range (TR) is a mountainous-hilly region and comprises a series of important inselbergs of the Pannonian Basin. It forms a NE-SW trending morphological range in the western part of the Pannonian Basin (Fig.1.2a). This range can be separated into more or less isolated inselbergs by Miocene extensional grabens or the remnants of the former Paleogene basin. The pre-Cenozoic suite is built up by low-grade metasediments and metavolcanites, metamorphosed during the Variscan orogeny, and Permian to Upper Cretaceous non-metamorphosed succession. These successions form the basement of Miocene sub-basins surrounding the Transdanubian Range, namely the Zala and Danube Basins; therefore, the term 'Transdanubian Range Unit' (TR) is used as a structural unit (Fig.1.2b) including surface outcrops and pre-Cenozoic subsurface extension up to its tectonic boundaries.

The north-easternmost Mesozoic outcrops of the Transdanubian Range are located in the eastern side of the Danube (Csővár Hills, Fig.1.4).

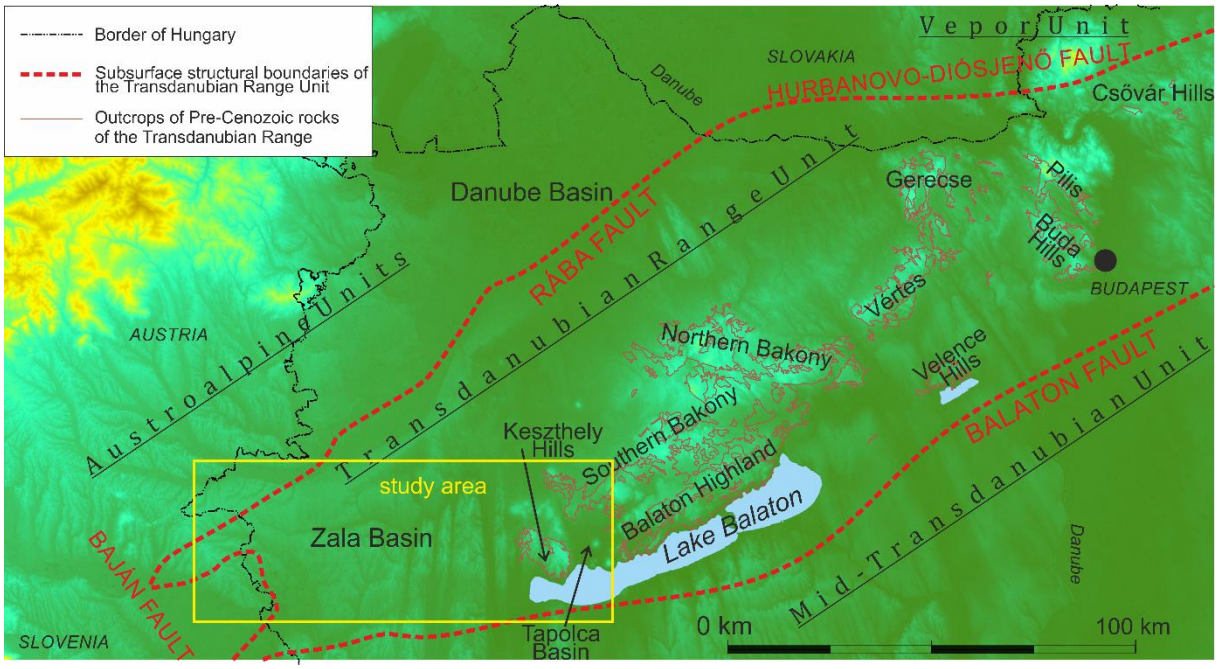

Fig. 1.4: Topographic view of the Transdanubian Range showing its inselbergs and structural boundaries.

On the western side of the Danube, the inselbergs of the Gerecse, Pilis and Buda Hills are situated. The Vértes, Velence Hills and the northern Bakony Mts. composes the central part of the TR. The Southern Bakony, the Balaton Highland and the Keszthely Hills are situated in the south-western part of the TR (Fig.1.4).

Several fault zones buried beneath Cenozoic sediments bound the TR (Fig.1.2b; Fig.1.4). These faults had variable kinematics and were active in different time spans (Balla 1999; Fodor & Koroknai 2000). The north-western boundary of the TR is the NE-SW striking Rába fault (Kőrössy 1958), which joins in the south with the curved Baján fault (Fig.1.2b;

Fig.1.4). These boundaries are southeast- to northeast-dipping normal faults of Miocene age, which reactivated or crosscut the Cretaceous thrusts (Tari et al. 1992; Horváth 1993; Tari 1994; Fodor et al. 2003, 2013a). In the footwall of these detachment faults deeper Austroalpine nappes occur (Horváth 1993; Tari 1994), such as the Koralpe-Wölz and Drauzug-Gurktal nappe systems (Fig.1.2b; Schmid et al. 2004, 2008; Fodor et al. 2013b).

The south-eastern NE-SW striking boundary of the TR is the Balaton fault (Balla et al. 1987), which separates the TR from the Mid-Transdanubian Unit; this latter is made up by rocks with South Alpine and Dinaric affinity (Haas et al. 2000b; Haas et al. 2010; Schmid et al. 2008) (Fig.1.2b; Fig.1.4). In an alternative interpretation, the Mid-Transdanubian Unit corresponds to a major, complex fault zone, altogether also known as Mid-Hungarian fault Zone (MHFZ) (Balla 1988). This fault zone was mainly active during Late Oligocene – Early Miocene (Csontos et al. 1992; Tari 1994), during the so-called extrusion phase (Fig. 1.3.). This zone accommodated significant dextral shear (Kázmér and Kovács 1985; Balla 1988; Balla and Dudko 1989; Csontos et al. 1992; Tari 1994) estimated around 300–350km. The northern branch of the wide fault zone, the Balaton fault represents the southern boundary of the relatively rigid TR (Balla et al. 1987). It can be interpreted as a system of strike-slip duplex (Fodor et al. 1998, 2013b) while other parts of the MHFZ are considered as a narrow thrust-and-fold belt (Csontos and Nagymarosy 1998).

The northern E-W striking boundary of the TR is the Diósjenő-Hurbanovo fault, whose age and kinematics is poorly known (Balla 1989) (Fig.1.2b; Fig.1.4). Koroknai et al. (2001) suggested Late Cretaceous age, Fodor & Koroknai (2000) extensional kinematics, whereas Tari (1994) interpreted the fault as an Oligocene thick-skinned backthrust. Boreholes reached the crystalline basement of the Vepor Unit (thick-skinned nappe of the Western Carpathians) in the northern side of the Diósjenő-Hurbanovo fault (Koroknai et al. 2001; Haas et al. 2010).

1.3. Position of the study area in the Transdanubian Range

The study area is the westernmost part of Transdanubian Range Unit (Fig. 1.4). Here, the Mesozoic basement is gradually submerging westward below Cenozoic cover (Fodor et al. 2013b). Consequently, Mesozoic rocks crop out in the eastern part of the study area, in the westernmost inselbergs of the Transdanubian Range (Keszthely Hills, Balaton Highland, Southern Bakony). I made detailed structural mapping only in the Keszhely Hills, however, I used the former geological maps of the Balaton Highland and Southern Bakony for cross-section construction.

The Zala Basin, where the Mesozoic basement is under thick Cenozoic cover, represents the western part of the study area (Fig. 1.4). It can be investigated by 2D and 3D seismic and well data. Existing high-quality data sets give good opportunity for comparison and combined analyses of 2D – 3D seismic and surface data sets in the Transdanubian Range.

2. Stratigraphy and structure of the study area

2.1. Stratigraphy of the study area

2.1.1. Permian to Early Cretaceous succession

Apart from a few exceptions, the Permian to Middle Triassic succession has not been reached by any wells in the Keszthely Hills and Zala Basin (Kőrössy 1988), even so its presence can be proposed in the whole study area. The stratigraphy of this time span is projected from the Balaton Highland which represents the easternmost part of the study area (Fig.1.4).

The several km thick Paleozoic shales of the Transdanubian Range was affected by low-grade Variscan metamorphism (Lelkes-Felvári et al. 1994; Fülöp 1990, Lelkes-Felvári 1998). This succession is covered by the upward-fining Upper Permian red continental siliciclastics (Balatonfelvidék Sandstone Formation, Fig.2.1a; Majoros 1983). After the Induan transgression a north-eastward deepening shallow water ramp developed on which mixed siliciclastic-carbonatic formations were deposited during the Early Triassic (Haas et al. 2012). In the study area the Induan is represented by the Köveskál Dolomite deposited in a hypersaline lagoon (Haas et al. 1988; Budai et al. 1999a). Due to the increased terrigenous input, shallow water siliciclastic sandstone deposited during the Olenokian (Hidegkút Formation, Zánka Sandstone Member) (Fig. 2.1a). This event is interpreted as the result of a humid pulse (Broglio Loriga et al. 1990) or the uplift of the hinterland (Budai et al. 1999a). The recovery of arid climate resulted in the deposition of the lagoonal to peritidal Hidegkút Dolomite Mb. during the Middle Olenokian (Haas et al. 1988). Due to the next transgression phase, the deposition of the Csopak Marl Fm. occurred on a deeper outer ramp environment (Fig. 2.1a).

As the siliciclastic input decreased a carbonate ramp developed during the Early Anisian (Budai et al. 1993). The Aszófő Dolomite deposited in a tidal flat. Its cellural structure represents the dissolution of evaporites. The formation is overlain by the laminated Iszkahegy Limestone Fm. which formed in a restricted ramp or inner shelf basin. It first becomes thin-layered and bioturbated upward, then it is overlaid by the thick-bedded Megyehegy Dolomite Fm. which represents a normal saline carbonate platform environment (Budai & Vörös 1992) (Fig. 2.1a).

Intense facies differentiation occurred in the Balaton Highland during the Middle Anisian (Budai & Vörös 1992, 2006) which led to the formation of deepwater basins (Buchenstein Group). These basins were separated by highs where carbonate platforms still continued to grow (Budai et al. 1993) – in the central Balaton Highland this was the isolated

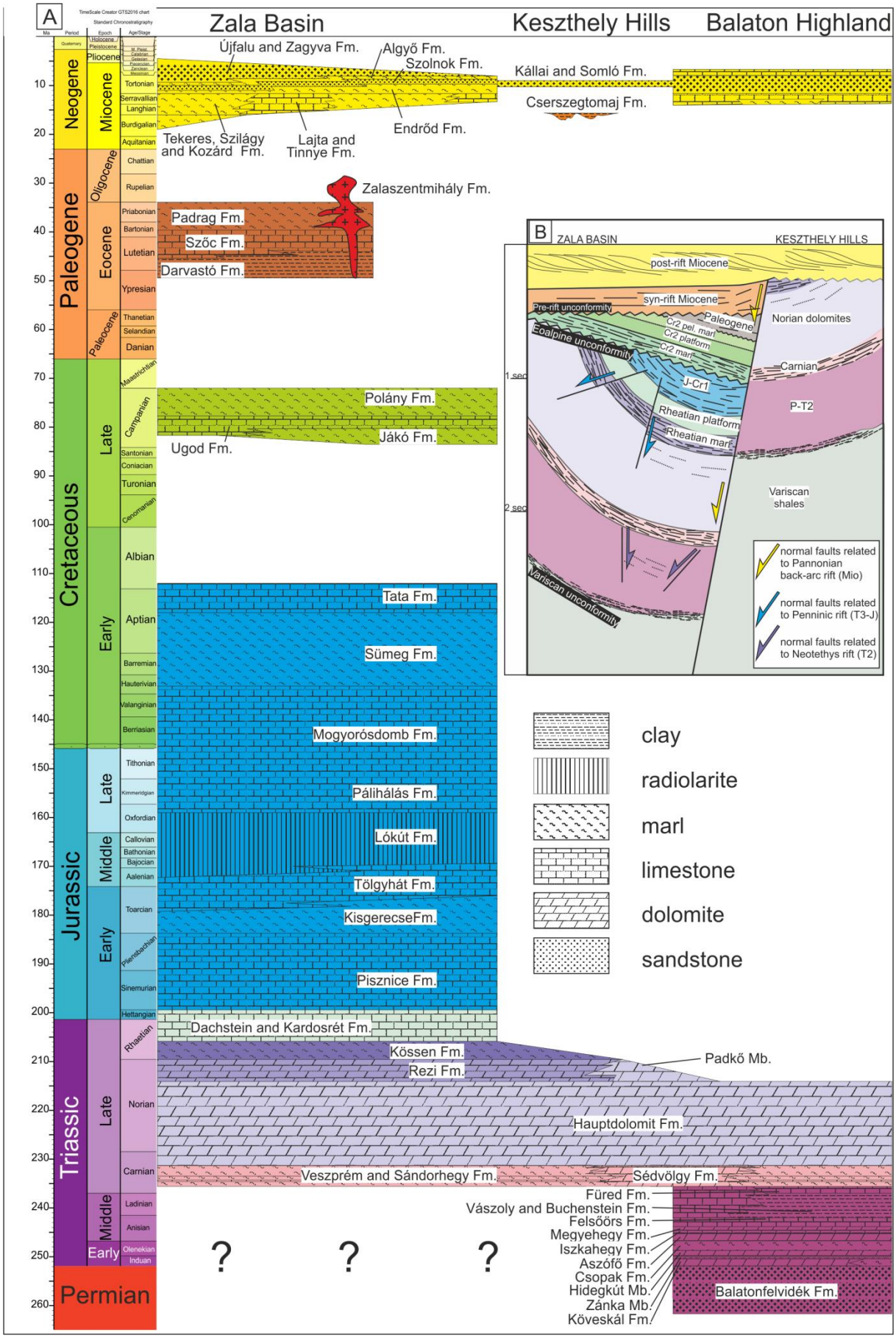

Fig. 2.1: (a) Stratigraphic chart of the study area based on Budai et al. 1999a; Vörös & Galácz 1998; Siegl-Farkas & Haas (2002) and Fodor et al. (2013a) (b) Idealized seismic section showing characteristic, high amplitude reflections of the study area.

Tagyon platform which finally drowned during the terminal part of the Anisian (Budai et al. 1993; Budai & Vörös 2006) (Fig. 2.1a). In contrast to this dissected paleotopography, the central Transdanubian Range (Eastern and Northern Bakony, Fig.1.4) is characterized by a broad carbonate platform during the Middle and Late Anisian which continued to grow during most of the Ladinian (Budaörs Dolomite). Nagy et al. (2014) described another Ladinian platform progradation in the Tapolca basin (Fig.1.4) which can be related to an additional platform further to the west from the Balaton Highland (Fig. 2.1a).

In the intraplatform basins a well-bedded dark cherty limestone (Felsőörs Fm.) deposited during the Middle Anisian which is overlain by rhyolitic and trachitic tuffs, as well as the crinoidal-bioclastic limestones of the Vászoly Formation (Fig.2.1a; Budai et al. 1999a, Vörös et al. 1997, Budai & Vörös 2006). The Ladinian nodular limestones and tuffitic intercalations (Buchenstein Formation) of the basinal development laterally interfinger with the propagational tounges of the coeval Budaörs platform (Budai et al. 2001). The Buchenstein Formation is overlain by the well-bedded Füred Limestone (Böckh 1872) which deposited around the Ladinian/Carnian boundary (Budai et al. 1999a; Fig. 2.1a).

The Middle Triassic basins were filled up by the Carnian mixed carbonatic-siliciclastic succession which indicates humid climate (Haas et al. 2012). The Veszprém Formation is built up by monotonous marls (Mencshely and Csicsó Marl), dissected by a nodular limestone member (Nosztor Limestone Mb.).

Finally, these basins were filled up by the Sándorhegy Formation (Csillag & Haas 1993) which is made up by the alternation of limestones, marls and dolomites (Fig. 2.1a). In the Keszthely Hills, small occurrences of oncoidal limestone is interpreted as Sándorhegy Formation; the specific development indicate deposition between the platform and the basin (Csillag et al. 1995).

The Carnian basinal formations laterally interfingers with the coeval carbonate platform (Ederics Formation) (Csillag et al. 1995) which was partly dolomitized (Sédvölgy Dolomite) in the Keszthely Hills (Haas et al. 2014) (Fig. 2.1a). Limited occurrences of transitional breccias were documented in the Keszthely Hills (Csillag et al. 1995).

From the end of the Carnian the depositional environment became uniform and the Hauptdolomit Formation was deposited on a huge carbonate platform (Fig. 2.1a). The formation is built up by a thin-layered bituminous dolomite in the study area. Occasionally microbialite intercalations occur. The formation was deposited in ultra-back-reef lagoon environment (Fruth and Scherreiks 1984), indicating the recovery of arid climate again (Haas 1993a, Haas et al. 2012).

From the end of Middle Norian (Budai and Kovács 1986) intraplatform basins opened again, and some of them persisted in the Rhaetian. These intraplatform basins were filled up by the late Middle to Upper Norian Rezi Dolomite and the latest Norian–Rhaetian Kössen Marl (Budai & Koloszár 1987; Budai & Kovács 1986; Budai et al. 1999a; Csillag et al. 1995; Haas 1993b, 2002). Budai & Koloszár (1987) subdivided the Rezi Formation into three members. The lower member is composed of dark-grey cherty bituminous laminated dolomites. The middle member is an alternation of thin-layered and thick-layered porous dolomites which often contain redeposited green algae fragments (Fig. 2.1a). This middle member can be interpreted as the progradation tongue of the coeval platform (Padkő Member). The upper member is similar to the lower member. Another dolomite breccia lithofacies of the Rezi Dolomite was identified by Csillag et al. (1995) in the Csókakő quarry (Keszthely Hills). This dolomite breccia is made up by dolomite blocks redeposited from coeval platform into a laminated dolomite matrix.

The Rhaetian Kössen Marl Formation (Fig. 2.1a) is poorly exposed, therefore, it is mostly known from wells (Haas 1993b). Dark-grey to black shales with high organic matter content constitute the main part of the formation. Thin-bedded fossiliferous limestone intercalations occur frequently within the shale which is strongly folded due to slumping (Budai & Koloszár 1987). The formation probably indicates another humid event which increased the terrigenous influx. This is also reflected in the composition and derivation of organic matter particles (Haas 2002; Haas et al. 2012; Hetényi 2002).

Based on well data the Kössen Marl interfingers with the limestone of the coeval Rhaetian Dachstein platform towards NE (in the southern Bakony, Fig.1.4). Consequently, the Kössen Marl pinches out northeastward (Haas 1993b; Haas 2002). Platform progradation of the few hundred metres thick Dachstein Formation can also be observed above the Kössen Marl in several wells of the Zala Basin (Kőrössy 1988). The formation is made up by cycles of thick-bedded limestones, stromatolites and paleosols (Haas et al. 1988, Mindszenty & Deák 1999).

Jurassic formations are not known on the surface within the study area, with the exception of Sümeg (Haas et al. 1984). However, general trends form the TR and borehole data form the Zala basin (Kőrössy 1988) permit to draw a schematic description. The carbonate platform environment still persisted in the earliest Jurassic (Kardosrét Fm.), however, it drowned at the beginning of the Sinemurian (Fig. 2.1a). During Early Jurassic facies differentiation occurred which fundamentally determined the Early and Middle Jurassic sedimentation (Galácz 1988; Vörös & Galácz 1998). Hiatus or condensed sedimentation occurred on the top of the submarine highs while thin pelagic formations with variable lithologies deposited between these swells (Galácz & Vörös 1972; Haas et al 1984). Along the

transition of these depositional areas (the margin of submarine highs) bioclastic Hierlatz Limestone was deposited during the Early Jurassic.

The Sinemurian is characterized by a red well-bedded bioturbated limestone (Pisznice Formation) in the Zala Basin (Vörös & Galácz 1998), however, near Sümeg (southern Bakony, Fig.1.2) grey cherty crinoidal limestone also occurs with partly the same age (Isztimér Limestone; Haas et al 1984). Red nodular Tűzkövesárok Limestone was deposited during the Pliensbachian which is overlain by the Toarcian red nodular Kisgerecse Marl in the Zala Basin (Vörös & Galácz 1998). During the Toarcian and Aalenian red nodular Tölgyhát Limestone was deposited in the Zala Basin (Vörös & Galácz 1998), however, near Sümeg (Southern Bakony, Fig.1.4) a cherty limestone with Bositra fossils represents the Aalenian and Bajocian stages (Haas et al. 1984). According to Vörös & Galácz (1998), the deposition of Lókút Radiolarite possibly started during the Aalenian in the Zala Basin and lasted until the Oxfordian (Fig. 2.1a).

The Upper Jurassic formations seal both the pre-existing highs and "basins" (Vörös & Galácz 1998; Haas et al 1984). This succession is made up by the Oxfordian to Tithonian red nodular Pálihálás Limestone and Tithonian white pelagic cherty Mogyorósdomb Limestone (maiolica facies) whose deposition lasted until the Hauterivian. From the Hauterivian to the Aptian Ammonitic deep-marine Sümeg Marl deposited. Siltstone and sandstone intercalations occur upward. The formation shows gradual transition into the Aptian to earliest Albian shallow marine crinoideal Tata Limestone (Haas et al. 1984; Szives 1999). This Tata Limestone represents the youngest member of Permian–Early Cretaceous sedimentary cycle. This succession was folded during the late Early Cretaceous and early Late Cretaceous. The number of folding phases and the exact age of the deformation(s) is controversial in different works, therefore, I summarize the theories regarding that in Chapter 2.2.5.

2.1.2. Senonian succession

During the middle Cretaceous compressional deformation, the whole Transdanubian Range was uplifted and sub-aerially exposed. On the tropic climate denudation surfaces formed, occasionally with bauxites. These are the pre-Middle Albian Alsópere Bauxites in the Northern Bakony (Császár 1986) and the pre-Senonian Halimba Bauxite in the Southern Bakony (Mindszenty et al. 2000).

The pre-Senonian succession is discordantly overlain by Senonian deposits (Haas et al. 1984; Fodor et al. 2017) which is well visible in the Sintérláp quarry near Sümeg. The Late Cretaceous sedimentation started on an articulated topography. In the Southern Bakony NE-SW trending paleo-highs developed (Haas et al. 1984). In the elongated sub-basins, the

deposition of the fluvial Csehbánya Formation and the Ajka Coal Formation started in the Santonian (Haas 1999). The shallow marine Jákó Marl with Gryphea fossils deposited due to the Late Santonian transgression (Fig.2.1a). Sedimentation started just by the end of the Santonian on the paleohighs separating the sub-basins. There, elongated platforms of the Ugod Limestone evolved which contains lot of rudist shells (Haas et al. 1984; Haas 1999). In the basins the Jákó Marl is overlain by the Santonian-Campanian deep-marine Polány Marl which often contains Inoceramus shells. The presence of Jákóhegy Breccia suggests that the Polány Marl and the Ugod Limestone was interfingering during Early Campanian. The upper member of the Polány Formation is a silty marl. The related increase of terrigenous influx may have been responsible for the drowning of Ugod platform during the middle Campanian (Haas 1999).

A somewhat different situation is outlined in the Zala Basin (Kőrössy 1988). Here the NE-SW trending platforms and sub-basins cannot be traced while the Jákó Marl is overlain everywhere by Ugod Limestone. Note, that there are also some places where the Senonian succession starts with Ugod Limestone (Siegl-Farkas and Haas 2002). Thick platform originated limestone intercalations occur frequently in the Jákó Marl which is also a different feature compared to the occurrences of the Southern Bakony (Boldogh 2003; Siegl Farkas & Haas 2002). The Senonian sedimentation started later in the Zala Basin than in the Southern Bakony, just during the Campanian (Siegl Farkas and Haas 2002). During the end of Cretaceous –Early Paleogene the whole Transdanubian Range was uplifted and exposed on the surface.

2.1.3. Paleogene succession

A more than one km thick Eocene succession was preserved in the so-called Bak-Nova graben in the Zala Basin (Kőrössy 1988). The Ypresian(?)–Lutetian shallow marine clays with limestone intercalation (Darvastó Formation) are overlain by the Lutetian–Bartonian Nummulitic Szőc Limestone (Fig. 2.1a). It is covered by a thick volcano-sedimentary succession which interfingers with the Lutetian–Priabonian shallow bathyal Padrag Marl (Kőrössy 1988; Báldi 1986). The igneous rocks are represented by andesite pyroclastic rocks, andesite, basaltic andesite and dacite (Kőrössy 1988, Benedek 2002). K/Ar ages measured on intrusive and effusive rocks suggest a younger Oligocene (26.0–34.9 Ma) age, therefore, the relationship of sediments and volcanic rocks is not clearly understood (Benedek et al. 2004). The younger (Early Oligocene) age of most of the effusive rocks would suggest their shallow subvolcanic character, instead of their interfingering with Eocene sediments (Benedek et al. 2004). South of the Bak-Nova graben tonalite and diorite intrusions are Early Oligocene in age and are parts of the magmatic suite along the Periadriatic – Balaton fault zone (Benedek et al. 2004). Although a late Oligocene clastic sedimentation could be postulated (as elsewhere in the

TR), this was not preserved in the study area. The Paleogene sedimentation was followed by a regional uplift, which caused sub-aeral exposure in the study area probably during the early Miocene.

2.1.4. Neogene succession

The next cycle of sediments deposited in the Pannonian back-arc basin which formed during the Miocene. The first syn-rift deposits are represented by even 2 km thick late Early Miocene (Karpatian) mostly marine succession which is made up by marls with sand intercalations (Kőrössy 1988; Fodor et al. 2013a). Conglomerate occurs along major syn-rift normal faults (Fodor et al. 2013a). The above-mentioned succession occurs on the western part of the Zala Basin, in the deepest sub-basins. The transgression reached the western foreland of the Keszthely Hills only during the Badenian (Fig. 2.1a). Depending on the paleo-topography created by the Miocene extensional deformation Badenian marine marls (Tekeres and Szilágy Formation) and shallow marine Lajta (Leitha) Limestone deposited there (Fodor et al. 2013a). Continental Cserszegtomaj Kaolinite deposited in karstic holes of the denudation surface in the Keszthely Hills (Bohn 1979; Csillag & Nádor 1997; Budai et al. 1999a) which is Badenian in age (Kelemen 2018). During the Sarmatian, the Kozárd Formation deposited in most of the Zala Basin. The formation is made up by clays, marls and sands. In the foreland of the Keszthely Hills shallow-water Tinnye Limestone represents marginal carbonate deposits (Fig. 2.1a).

The Pannonian Basin was occupied by the brackish to fresh-water Lake Pannon during the Late Miocene (Pannonian). The lake was filled up by a south to south-eastward prograding delta system, therefore, the formation boundaries are not isochron and they gets younger towards the SW (Pogácsás 1985, Uhrin et al. 2009; Magyar et al. 2013; Fodor et al. 2013a). The lower basinal marls (Endrőd Fm.) are covered by turbidites which deposited on the basin floor (Szolnok Formation). Algyő Formation consists of mostly siltstones and it represents the slope deposits. It is covered by the Újfalu and Zagyva Formations (Fig.2.1a). The latter two represent sediments of the distally-sourced deltas that prograded across the clastic shelf and the overlying alluvial plain deposits (Sztanó et al. 2016). In the flank of the Zala Basin (e.g. Keszthely Hills) and in the Tapolca graben a more reduced Miocene succession occurs (Budai et al. 1999a; Csillag et al. 2010; Sztanó et al. 2010), which is represented by Pannonian gravels (Kálla Fm.), sands and sandstone (Somló Fm.). The Miocene succession is discordantly overlain by Quarternary fluvial and aeolian deposits (Budai et al. 1999a; Fodor et al. 2013a).

2.2. Mesozoic deformation in the Transdanubian Range: a review of previous works

2.2.1. Middle Triassic extension in the Balaton Highland

Partial drowning of the Anisian platforms and the development of isolated platforms and deepwater basins in the Balaton Highland were explained by syn-sedimentary movement along NW-SE striking normal faults (Budai & Vörös 1992, 1993, 2006). According to the observations of Budai et al. (1999a) and Budai & Vörös (1993) normal faulting started during the Pelsonian (middle Anisian). The Illyirian (late Anisian) Vászoly Fm. locally seals major normal faults (Fig.2.2).

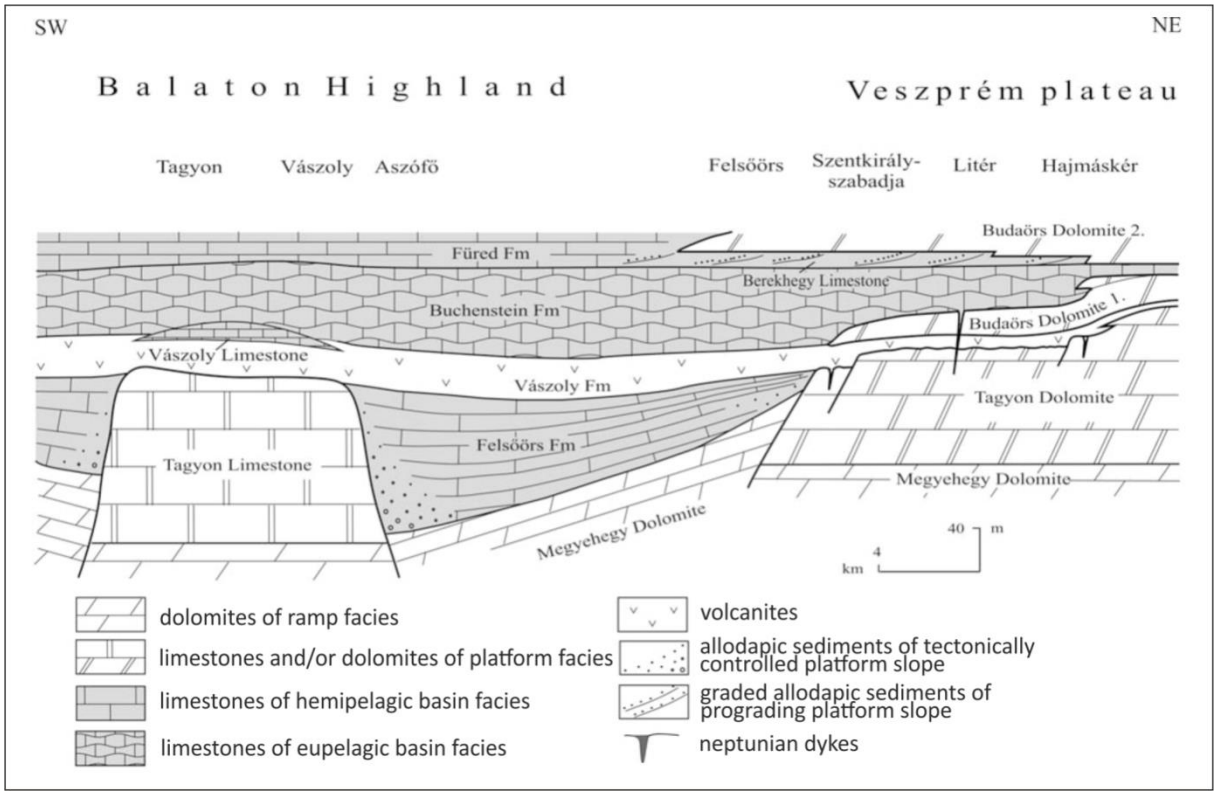

Fig.2.2: Relationship between Middle Triassic platform carbonates and basin facies on the Balaton Highland and the Veszprém plateu (Budai & Vörös 2006).

Several outcrop-scale syn-sedimentary normal faults were described by Csicsek (2015) and Fodor et al. (2017) in the eastern part of Balaton Highland. These structures have similar NW-SE strike and they suggest that extensional deformation continued, at least locally, from the Anisian up to the Ladinian/Carnian boundary.

2.2.2. Late Triassic extension

Intraplatform basins formed in the southwestern (Zala Basin and Keszthely Hills) and northeastern parts (Buda Hills, Pilis, Csővár Hills, Fig. 1.4) of the Transdanubian Range during the Late Triassic (Haas 2002; Hips et al. 2015). Although based on sudden lithological changes or dolomitisation the normal faults were always postulated along the basin margins, they have not been directly observed so far.

Former observations led to a vaguely defined model which was never properly figured, although a number of elements were published. Additionally, I have good input ideas from personal communications (Csillag G., Haas J., Budai T.). In the Keszthely Hills the Rezi Dolomite was deposited in a syn-sedimentary extensional basin (Budai et al. 1999a). The dolomite breccia of the Csókakő quarry (Keszthely Hills) is an important point in the evolution of the ideas about Triassic deformation, and fault-related origin of this breccia was gradually accepted (Csillag et al. 1995; Budai et al. 1999a). However, the exact location, geometry and the strike of the controlling normal faults has not been given.

Csillag et al. (1995) and Budai et al. (1999a) documented that the platform dolomites and basinal laminated dolomites interfingers, and the platform dolomite prograded into the basin from the NE. Despite all this data the exact basin geometry has not been clearly described and figured, although Csillag (pers.com.) suggested a half-graben geometry. I tried to formulate this geometrical model in map view and cross section already in my master works (Héja 2015a, b) and elaborated it further in the present study.

Deposition of the Kössen Marl is also considered to have occurred in an extensional basin according to numerous previous works (Haas 1993b; Budai et al. 1999a). However, due to the lack of outcrops, the basin geometry is even more difficult to determine.

Late Triassic intraplatform basins of the north-eastern Transdanubian Range are suggested to be fault-controlled as well (Haas et al. 2005, 2010). The Middle to Late Norian Feketehegy Basin developed at the same time or slightly earlier than the onset of deposition of the Rezi Dolomite. Deep-marine environment has already existed from the Carnian in the case of the intraplatform Csővár Basin in the north-easternmost end of the TR (Csővár Hills, Fig.1.4) and Hármashatárhegy Basin in the Buda Hills (Fig.1.4) (Haas et al. 2000a; Haas 2002). Hips et al. (2015) explained the presence of soft breccia (plasticlasts) and partial dolomitization of the Hármashatárhegy basin by fluids which were guided by syn-sedimentary normal faults.

2.2.3. Jurassic deformations

Jurassic normal faulting has been long known from the TR (Fig.2.3). Thickness variations, facies changes and the presence of sedimentary breccias and other redeposited sediments were explained by syn-sedimentary normal faulting (Galácz & Vörös 1972; Galácz 1988; Vörös & Galácz 1998). Several outcrop-scale Jurassic syn-sedimentary faults and Neptunian dykes were reported from the Bakony (Albert 2000; Kiss 2009); Vértes (Császár & Peregi 2001; Fodor 2008) and Gerecse (Lantos 1997; Bada 1994; Fodor et al. 2013a; Fodor et al. 2013b). Although the direction of these structures show big dispersion but the (W)NW-(E)SE striking structures are dominant. According to Vörös & Galácz (1998) and Fodor et al. (2013a) extensional deformation started during the Sinemurian and was present probably throughout the Middle Jurassic. Upper Jurassic (Tithonian) sediments seem to seal extensional horsts (Vörös & Galácz 1998). Considering the thickness of Jurassic succession which is approximately 40 m in the Gerecse (north-eastern TR) and 400 m in the Bakony (central TR), the offset of related syn-sedimentary faults probably did not exceed few hundred meters.

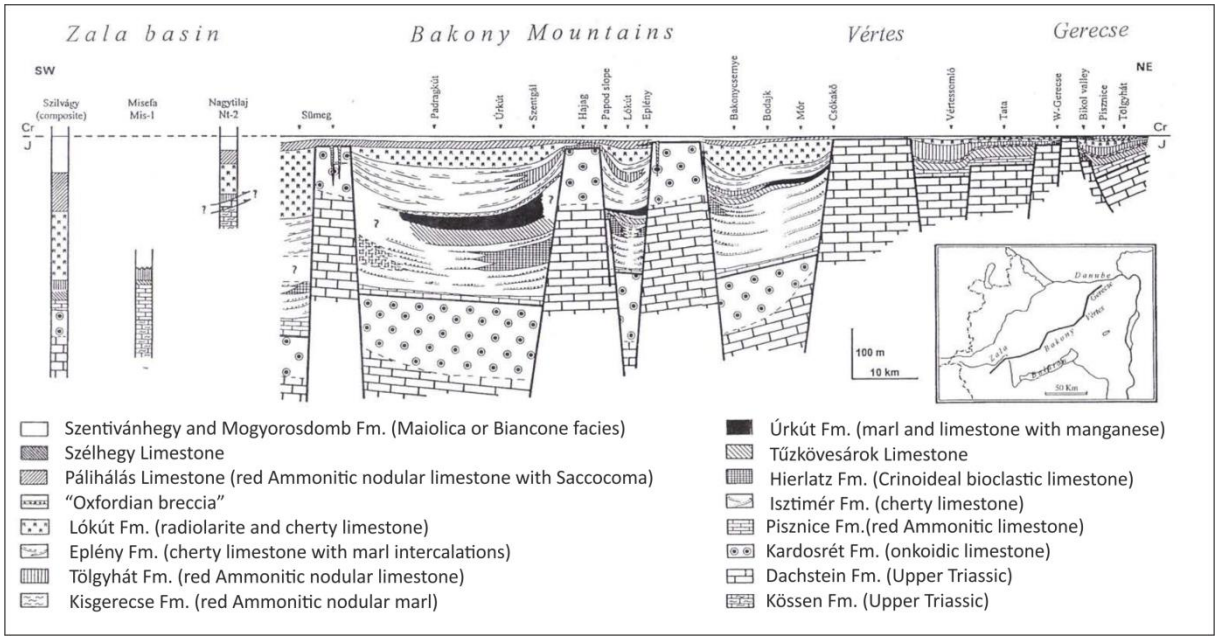

Fig.2.3: Jurassic formations of the Transdanubian Range showing their thickness variation along a SW to NE profile (Vörös & Galácz 1998). The figure is 10 times vertically exaggerated.

The interpretation of sedimentary breccia of Oxfordian age in the Gerecse and Pilis (Palotai et al. 2006a; Fodor et al. 2013b) and Kimmeridgian/Tithonian age in the Bakony (Palotai et al. 2006b) is controversial. Some authors raise the possibility that the deposition of Late Jurassic breccias was controlled by compressional deformation (Bárány 2004; Palotai et al. 2006a,b; Csontos and Vörös 2004; Csontos et al. 2005) and they represent the first signs of orogenic movements, very similarly to the coeval compressional deformation model of

Northern Calcareous Alps (Gawlick et al. 1999). Other authors relate the Late Jurassic sedimentary breccias to normal faulting (Fodor et al. 2013b).

2.2.4. Early Cretaceous Gerecse foreland basin of the Transdanubian Range

An Early Cretaceous (Berriasian to Aptian) siliciclastic basin developed in the northeastern part of the Transdanubian Range (Gerecse; Fig. 2.4.c) which was filled up by an upward coarsening turbiditic succession (Fülöp 1958; Sztanó 1990; Császár & Árgyélán 1994; Tari 1994; Fogarasi 1995a). Sedimentary transport directions range from NNE to ENE (Fogarasi 1995b; Sztanó 1990). The geochemistry of detrial chromium-spinel suggests that the Gerecse foreland basin developed in the front of ophiolitic nappes (Császár & Árgyélán 1994; Árgyelán 1996). Tari (1994) recognized that this basin represents a foreland basin formed due to the loading of the overlying nappe stack. The central Transdanubian Range was a non-depositional area during the Early Cretaceous. At this time the area of the Transdanubian Range is interpreted as a forebulge, bordering the Gerecse foreland basin from the SW (Tari 1994; Mindszenty et al. 1994; 2000;). The study area (southwestern Transdanubian Range) was in a back-bulge position during the Early Cretaceous where the deposition of micritic pelagic limestone and marl (Biancone) continued (Fig. 2.1a). The facies pattern of Early Cretaceous formations (Császár 1995) suggests that the orogenic load was located NNE or ENE from the Transdanubian Range, and migrated slowly toward the SW (Tari 1995; Mindszenty et al. 1995; Mindszenty et al. 2000). The Late Aptian termination of sedimentation in the Gerecse foreland basin can reflect the arrival of foreland-related deformation front (Szives et al. 2018). On the other hand, according to Mindszenty et al. (2000) the related forebulge still existed during the Albian and the Albian bauxite indicates the location of the forebulge. After these authors the overlying Albian succession of the Northern Bakony Mts. was still deposited on this migrating forebulge.

It is still a question if the latest Aptian to earliest Albian Tata Limestone was part of the Early Cretaceous clastic basins, as its marginal deposits, or it represents a separate tectono-sedimentary cycle. Csontos et al. (2005) and Pocsai & Csontos (2006) interpreted this formation in the former, Szives et al. (2018) in the latter concept. It is to note that Palotai et al. (2006a) placed the onset of the NE–SW shortening somewhat older than the onset of the Cretaceous clastic sedimentation, namely to the Late Jurassic.

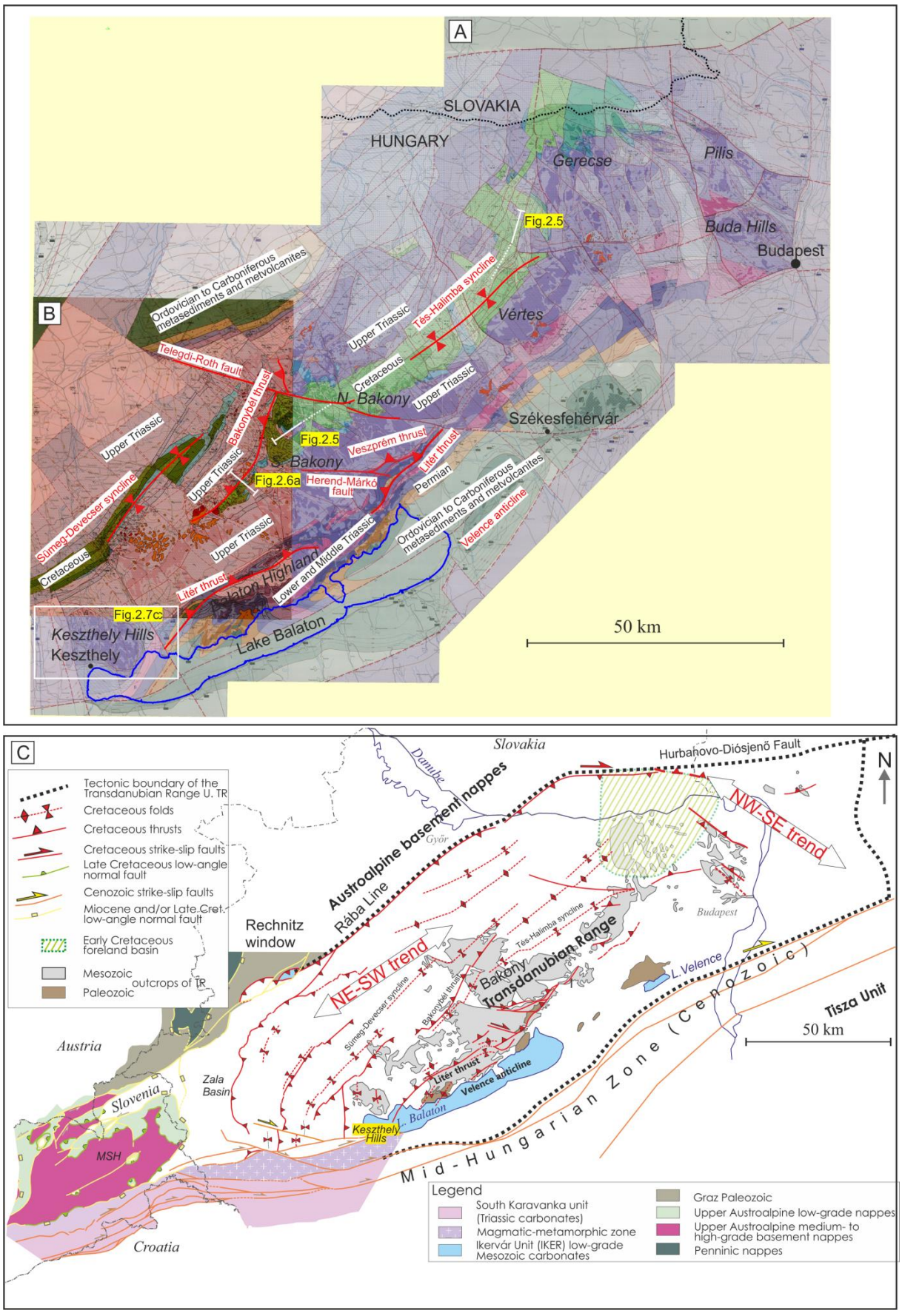

Fig.2.4:(a) pre-Cenozoic map of the Transdanubian Range (Császár et al. 1978) (b) pre-Senonian map of the western Transdanubian Range (Haas and Jocháné Edelényi 1978) (c) geometry of major map-view Cretaceous compressional structures of the Transdanubian Range (Fodor et al. 2017 modified).

2.2.5. Late Early – early Late (middle) Cretaceous folding of the Transdanubian Range

The main compressional structures of the Transdanubian Range show complex geometry with variable trends (Fig. 2.4.c). The northeastern Transdanubian Range (Gerecse, Pilis, and Buda Hills) (Fig.1.4) is dominated by NW-SE trending compressional structures (Wein 1977; Fodor et al. 2013b;).

The main structural elements of the central Transdanubian Range are NE-SW trending synclines in the Bakony and southeast-vergent thrusts in the Balaton Highland – they were described in papers and represented in maps (Császár et al. 1978; Fülöp & Dank 1987; Budai et al. 1999a, Császár 1986; Budai et al. 1999b; Kiss 2009; Fodor 2010, respectively). Further to the west, in the Zala Basin, the trend of the main compressional structures is N-S (Fodor et al. 2013a) or even NNW-SSE (Tari 1994). Folds with similar N-S strike were identified in the Keszthely Hills by Dudko (1996) and Budai et al. (1999a).

These variable trends are traditionally explained by two phases of perpendicular folding (Tari 1994; Tari & Horváth 2010). According to this model, southwest-vergent thrusts and folds constitute the first deformation phase while the second corresponds to the development of major NE-SW trending synclines and thrusts of the Transdanubian Range.

The age of transition between these two phases is controversial, and represents the target of ongoing debate and research. It can be given around the Aptian – Albian boundary (Tari 1994). According to Sasvári (2008, 2009) the transition between the two events is manifested in an individual phase of E-W compression in the Gerecse, and the direction of compression was gradually rotated.

2.2.5.1. NW-SE trending compressional structures in the northeastern and central Transdanubian Range

NW-SE trending compressional structures are clearly present and locally are the dominant structures in the northeastern part of the TR (Gerecse; Pilis; Buda Hill), although locally other contractional features do occur as well. Tari (1994, 1995) was the first who connected the NE–SW shortening with the formation of the Gerecse foreland basin, and he explained the subsidence and basin migration by the orogenic load of the nappe stack. Following this pioneer study, the small-scale contractional features were considered as parts of this foreland basin evolution while the folding was logically considered as the final phase of shortening. Csontos et al. (2005) and Palotai et al. (2006a) suggested the Late Jurassic as the starting point of the contraction while Sasvári (2008, 2009) strengthened the Aptian onset of

deformation. On the other hand, newer analyses suggested the Early Albian (Fodor et al. 2013b) or Latest Aptian onset of folding (Szives et al. 2018).

It is important to note that in the northeastern Transdanubian Range the oldest cover of these compressional structures is only Eocene in age, thus there is no direct time constraint for these structures (Budai et al. 2018).

The most detailed studies about the folds of the Gerecse Hills described three different directions of folds, two of them correspond to this phase; WNW–ESE and NNW–SSE in direction (Sasvári 2008, 2009; Fodor et al. 2018).

Several authors found evidences for (E)NE-(W)SW compression in the central Transdanubian Range where perpendicular NE-SW trending map-scale structures are dominant. It is to note that the timing of these structures, their importance and sometimes their kinematics are contested by other authors. Thus here I give only a list of such features and try to formulate my opinion in chapter 5. Albert (2000) described NNW-SSE trending folds from the Bakony (Central Transdanubian Range) which were discordantly sealed by Middle Albian deposits. Pocsai & Csontos (2006) supposed the presence of map-scale SW-vergent thrusts based on the finding of sedimentary breccias and thickness variation of the Late Aptian–Earliest Albian Tata Limestone (Fig. 2.5). According to this model, the NE-SW compression is coeval with the deposition of Tata Limestone, shortening is present in the Vértes and northern Bakony within the TR (Fig. 2.5).

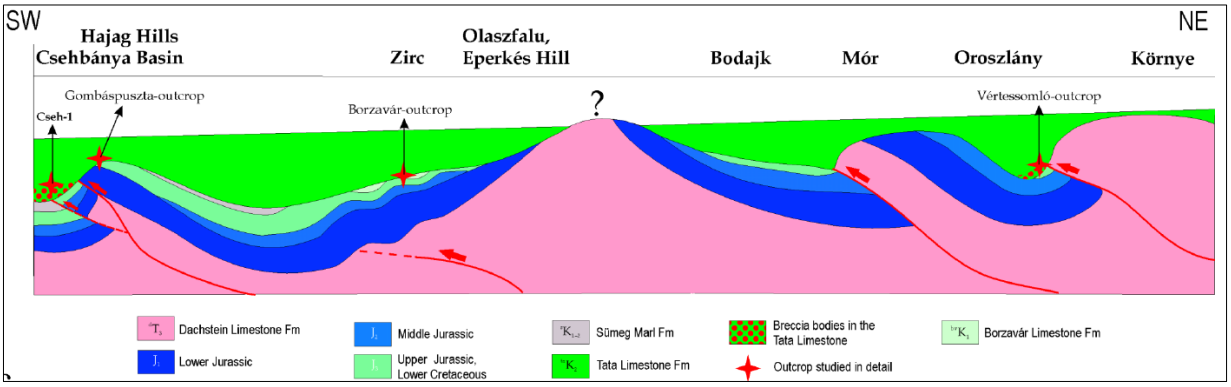

Fig. 2.5: NE-SW conceptional section along the axis of Tés-Halimba syncline, Transdanubian Range (Pocsai & Csontos 2006). For location of the section see Fig.2.4a and b

Dudko (1996) mentioned several compressional structures in the Balaton Highland which are perpendicular to the main SE-vergent thrusts. However, she considered them as part of the NW-SE compressional phase, representing only local features with specific shortening history.

In contrast, several authors do not accept the presence of this NE-SW compression preceding the main NE-SW trending folding in the central Transdanubian Range (Fodor 2008; Kiss 2009; Csicsek 2015). For example, Fodor (2008, 2010) did not find fault-slip data

supporting the presence of NE–SW shortening outside the northeastern TR, namely in the Vértes and Bakony areas; such stress field should characterize the supposed contractional structures.

In the southwestern part of the TR, Tari (1994) and Tari & Horváth (2010) observed W or WSW-vergent thrusts in the Zala Basin (Figs. 2.4.c and 2.7a,b). They claim that these thrusts could be related to this NE–SW shortening. Tari (1994) suggested that the deposition of the Late Aptian to Earliest Albian Tata Limestone seems to postdate this deformation.

To summarize, on one hand several authors (Tari 1994; Csontos et al. 2005; Pocsai & Csontos 2006; Sasvári 2008, 2009 and Tari & Horváth 2010) propose that the whole Transdanubian Range was involved in an Aptian (E)NE-(W)SW compression while on the other hand, other authors suppose that this deformation was restricted only to the northeastern Transdanubian Range and NE–SW shortening was not present further to the SW (e.g. Fodor et al. 2013a and b). Finally, as a third opinion, while Dudko (1991, 1996) accepted the presence of NE–SW compressional structures within the Balaton Highland, she considered these features as local ones, belonging to the other (younger) shortening phase.

2.2.5.2. NE-SW trending compressional structures in northeastern and central Transdanubian Range

Most authors agree that the NW-SE compression resulted in the major folds and thrusts of the central TR (Bakony, Vértes; Fig. 2.4). These folds are represented by two en-echelon synclines: the Tés-Halimba and Sümeg-Devecser synclines (Tari 1994) which are already outlined on the subsurface geologic map of Császár et al. (1978; Fig.2.4.a) and Haas & Jocháné Edelényi (1978; Fig.2.4.b). Balla & Dudko (1989) added the Velence anticline at the southeastern margin of the TR.

According to Tari (1994) the two synclines are separated by the SE-vergent Bakonybél thrust (Fig.2.4). The SE-vergent Litér and Veszprém thrust of the Balaton Highland developed probably during this deformation as well, as interpreted by a number of authors (Erdélyi-Fazekas 1940; Teleki 1936, 1941; Budai et al. 1999b, Dudko 1996), although the oldest cover is just Miocene in age (Fig. 2.4). Variscan low-grade rocks are exposed or are subsurface along the Lake Balaton below the generally NW dipping Permian to Triassic succession of the Balaton Highland (Fig.2.4b). According to Balla & Dudko (1989) and Tari (1994) this NW-ward tilted succession represents the northwestern limb of the thick-skinned Velence anticline (Fig.2.4). Variscan shales are exposed in the core of this anticline, whereas its southwestern limb is dissected by the Cenozoic Balaton fault (Balla & Dudko 1989; Tari 1994).

Regarding the age of folding, Late Aptian – Earliest Albian Tata Limestone occurs in the core of the Tés-Halimba and Sümeg-Devecser synclines whereas the Tés-Halimba syncline and the Bakonybél thrust are discordantly sealed by Middle Albian fluvial sediments (Tés Fm.; Császár 1986; Fodor 2010; Fodor et al. 2017; Fig.2.6a). It means that the main deformation occurred during the Early Albian (Fodor et al. 2017). On the other hand, thickness variation of the Albian-Cenomanian sediments in the Bakony Hills suggests that compressional deformation was still active during their deposition (Tari 1994, Héja 2015b; Fig. 2.6b).

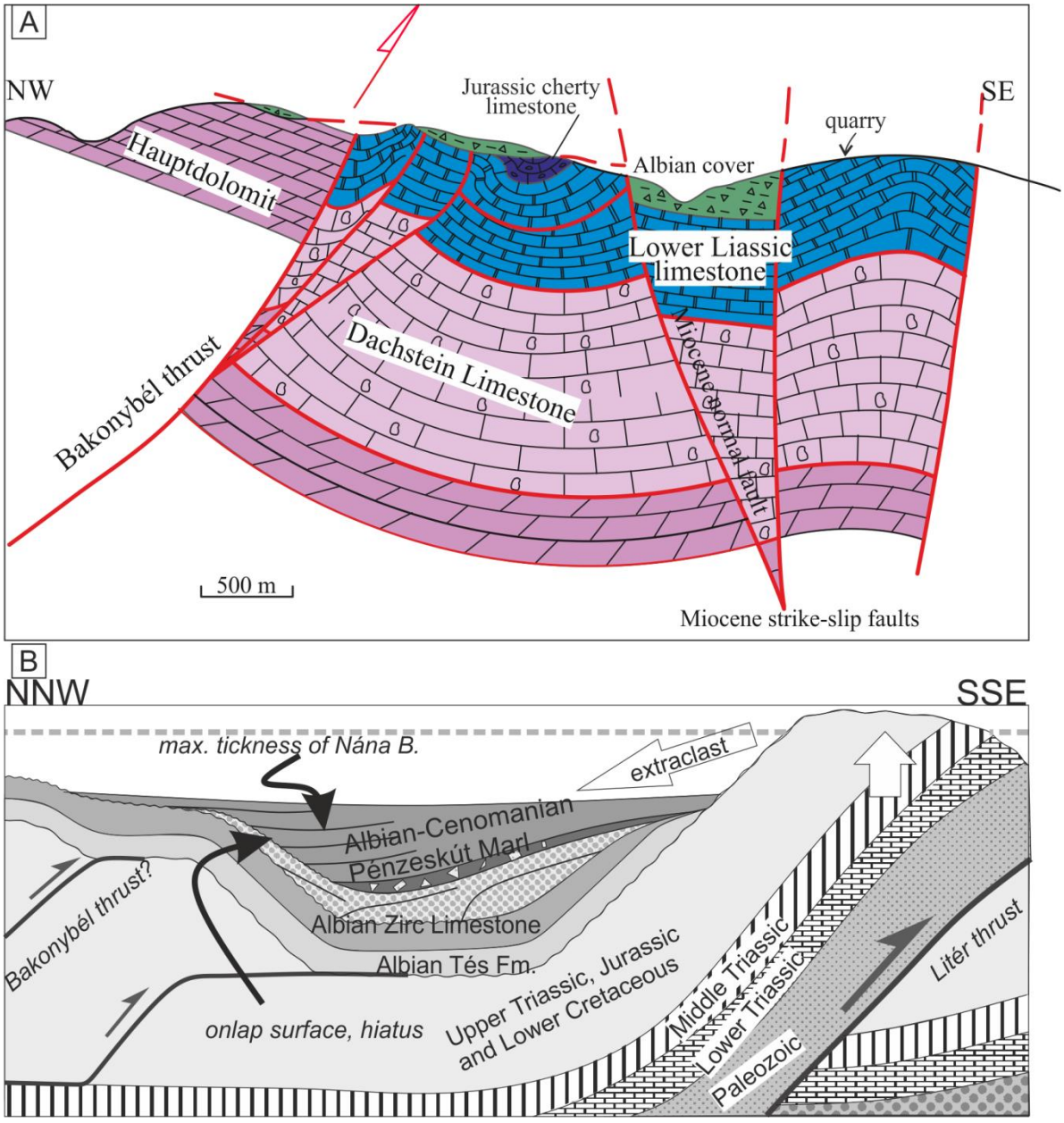

Fig. 2.6: (a) Section across the Bakonybél Thrust and related folds, covered by middle Albian Tés Fm. (Fodor 2010; Fodor et al. 2017). For location of the section see Fig.2.4a; (b) Schematic model for the Late Albian formations on a NNW–SSE cross-section across the Tés-Halimba syncline (Héja 2015b modified): thickness-variations suggest syn-sedimentary folding.

The Albian–Early Cenomanian succession is truncated at deep marine sediment and the eventual filling of the basin is not preserved. While these sediments are preserved only in the

core of the Tés-Halimba syncline (Kiss et al. 2009), the NW-SE compression continued and possibly represented the Late Cenomanian to Coniacian time span, although the termination of the middle Cretaceous shortening is poorly constrained. The deformed sequence was exposed to denudation and the bauxite formation indicate subtropical weathering. Santonian deposits discordantly cover the middle Cretaceous folds in the Southern Bakony (Haas et al. 1984; Fodor et al. 2017).

While the deformation continued across the boundary of the Early and Late Cretaceous it is confined to the middle part of the Cretaceous. I will refer to this phase as middle Cretaceous, indicating its "central" temporal position within the Cretaceous. Although the term "middle Cretaceous" is not correct according to the present-day subdivision of Cretaceous, I only use it in this study for the sake of simplicity.

WNW-ESE trending dextral faults (e.g, Telegdi-Roth fault on Fig.2.4), which were described by Mészáros (1983) as Miocene structures, were probably already active during the Cretaceous NW-SE compression as dextral tear faults (Tari 1994; Linzer and Tari 2012). According to Csicsek (2015) one of these dextral faults, the Herend-Márkó fault represents the southern termination of the Veszprém thrust, accommodating its offset as a tear fault (Fig.2.4).

2.2.5.3. Geometry of Cretaceous compressional structures in the south-western TR

The major NE-SW trending compressional structures of central TR (Bakony) change their strike gradually towards N–S strike in the Zala Basin (Tari 1994; Fodor et al. 2013b). Major folds and thrusts become N-S or NNW-SSE trending in the western part of the study area.

Same, N-S trending map-scale folds were mapped by Budai et al. (1999b) in the Keszthely Hills which represents the eastern part of the study area. Rezi Dolomite and Kössen Marl are preserved in the core of the western Rezi syncline whereas the eastern Vállus syncline is outlined based on the Rezi Dolomite (Fig. 2.7c). The Rezi and Vállus synclines are separated by the broad Várvölgy anticline (Fig. 2.7c). The Rezi syncline is bordered by the enigmatic Héviz thrust from the west (Fig. 2.7c) which has also a N-S strike (Fodor et al. 2013a). Its presence was proposed based on wells penetrating the Miocene cover. Besides that, second-order folds with NE-SW and NW-SE trends were described by Dudko (1996) and Budai et al. (1999b) in the Keszthely Hills.

Tari (1994) proposed that W-vergent thrusts of the Zala basin change their strike further toward SE, forming a 180° curvature, and they can be connected to the SE-vergent thrusts of the Balaton Highland (Fig.2.7a). According to this concept, Tari (1994) considered the Litér thrust going through the Keszthely Hills with NE-SW strike. Consequently, the SE-vergent

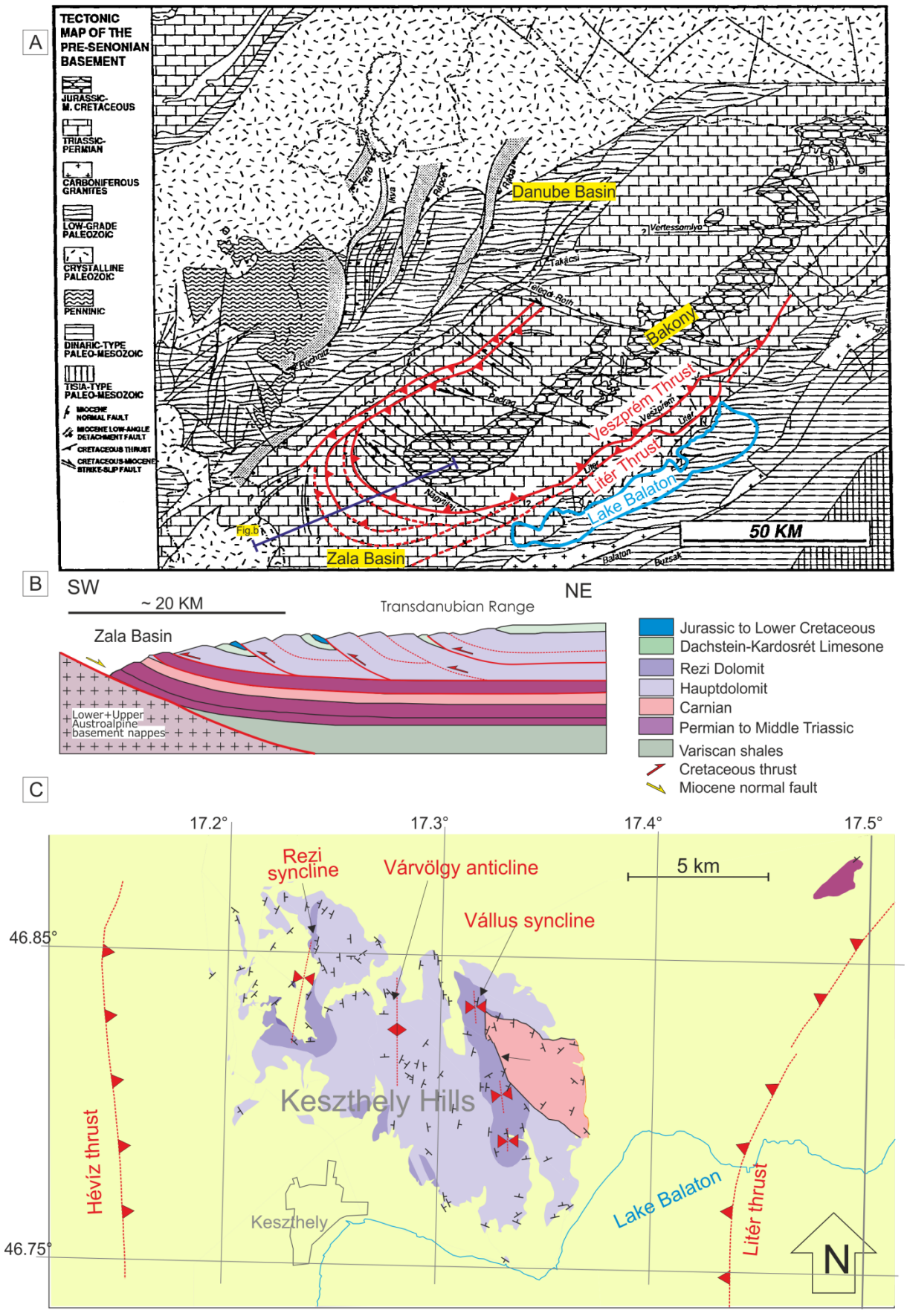

Fig. 2.7: (a) Tectonic map of the pre-Senonian basement in the Transdanubian Range (Tari 1994 redrawn) (b) Idealized cross section across the Zala Basin (Tari 1994 redrawn), interpreted TR as a thin-skinned thrust and fold belt. (c) Geologic map of the Keszthely Hills. Lithology, dips are after Budai et al. (1999b), major folds after Budai et al. (1999a) and Fodor et al. (2013a). For location of the map see Fig.2.4.a and b

thrusts of the Balaton Highland and the W-vergent thrust of the Zala Basin can be connected through a curved thrust front. Tari (1994) and Tari & Horváth (2010) suggested that this curved thrust front is developed due to interference of Aptian ENE-WSW and perpendicular Albian NNW-SSE compression (Fig.2.7a).

In contrast, Császár et al. (1978) and Fodor et al. (2013b) suggested that the Litér thrust cannot be traced in the Keszthely Hills, and that its continuation is running east of the Keszthely Hills, under the Miocene infill of the Tapolca Basin (Fig.2.4).

The Upper Norian to Lower Cretaceous succession is preserved only in a few synclines of the Zala Basin (Tari 1994, Fodor et al. 2013a). These synclines were interpreted by Tari (1994) and Tari & Horváth (2010) as the hanging wall synclines of W-vergent fault-bend folds which developed above a shallow décollement level at the base of Hauptdolomit, within the Carnian clastic formation. Tari (1994) supposed the duplication of the Triassic succession below this décollement and interpreted it as the far-travelled internal thin-skinned nappes of the TR (Fig. 2.7b). Fodor et al. (2013a) also interpreted the synclines of the Zala Basin as hanging-wall synclines of fault bend folds. However, they didn't assume internal nappes in the Mesozoic succession but proposed a deeper décollement for the fault-bend folds in the Variscan shales.

2.2.6. Structural background of the Senonian Basins

The Senonian succession was deposited on a strongly articulated surface which is evidenced by abrupt facies changes (Haas et al. 1984; Haas 1999). The NE-SW trending elevated areas and sub-basins are outlined in the Southern Bakony based on facies distributions which are suggested to be normal fault controlled (Haas 1999). According to Haas (1999) these normal faults are NE-SW striking, nevertheless Nyíri (2017) identified NW-SE striking Senonian normal faults in the western part of Zala Basin based on seismic data. Kiss (2009) observed a few outcrop-scale Senonian syn-sedimentary normal faults in the Southern Bakony, also in NW-SE strike. All these structures suggest (E)NE-(W)SW extension.

In contrast, Tari (1992, 1994), Tari & Horváth (2010) and Tari & Linzer (2018) suggest compressional origin of the Senonian Basins, since the NE-SW trend of paleohighs of the southern Bakony can be better explained by the reactivation of Middle Cretaceous (Eoalpine) thrusts which show similar NE-SW strike in the central Transdanubian Range (Bakony and Danube Basin).

2.2.7. Structural background of the Maastrichtian – Paleocene uplift

During the Maastrichtian – Paleocene interval the whole Transdanubian Range was uplifted and sub-aerially exposed which is evidenced by the widespread bauxites (Mindszenty

et al. 2000). However, the structural background of this sub-areal event is not well known. Fodor (2010) and Fodor et al. (2013b) estimated (E)NE-(W)SW compression during the time span of exposure and denudation. This phase was observed on Senonian rocks but it is missing from Paleogene rocks (Fodor et al. 2013b). Despite the temporal coincidence of denudation and the stress field, they did not connect the two data sets. Sasvári et al. (2007) proposed the presence of similar stress-field based on fault slip data from the Bakony (central TR).

3. Data and methods

The study area is the western part of the Transdanubian Range including the Keszthely Hills in the east and the Zala Basin in the west (Fig.3.1).

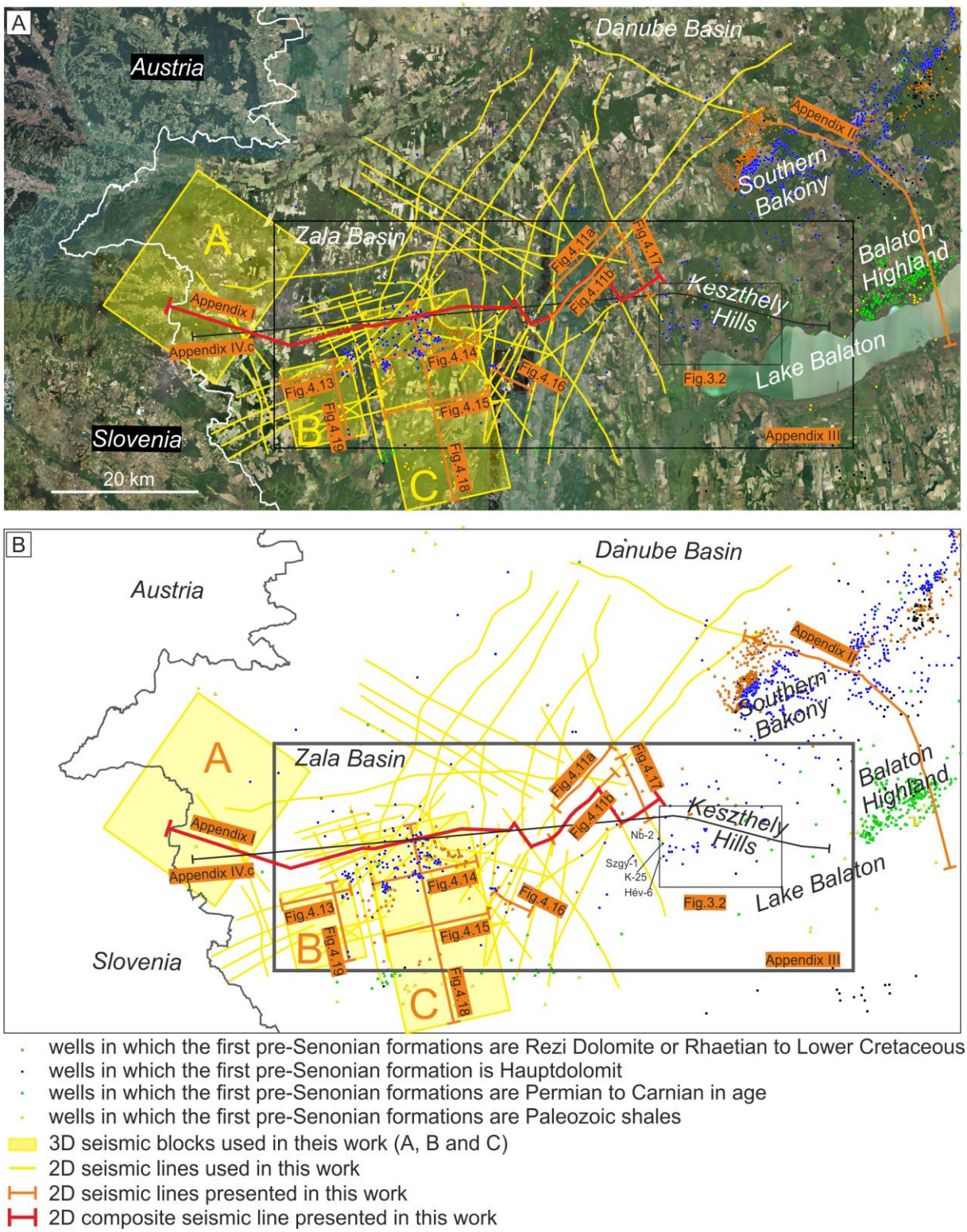

Fig.3.1: (a) Satellite image and (b) simplified topographic map of the study area indicating the location of the used 2D and 3D seismic data and boreholes.

In the huge quarries of the Keszthely Hills the folded Mesozoic basement is exposed, and field observations have been done there (for location see Table I. and Fig. 3.2a). In the Zala Basin the Mesozoic basement is under Cenozoic cover, and was investigated on 2D seismic sections, 3D seismic blocks and well data (Fig. 3.1).

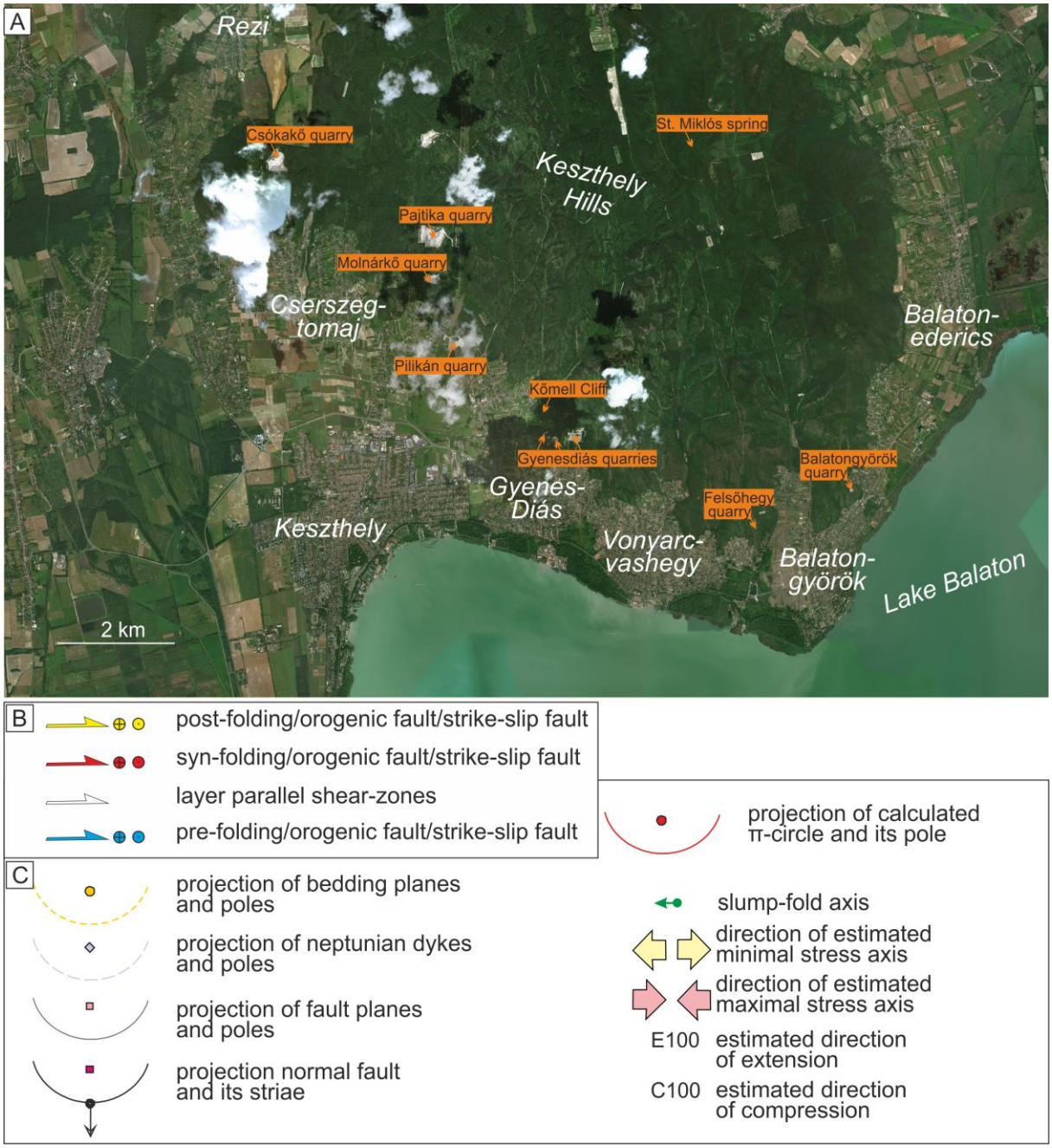

Fig.3.2: (a) Location of described quarries/outcrops on a satellite image of the Keszthely Hills (b) Legend of structures interpreted on field and on seismic (Fig.4.1-4.19) (c) Legend of the sterepots.

3.1. Interpretation of outcrop photos

Name of the outcrop	latitude	longitude	Name of the outcrop	latitude	longitude
Csókakő quarry	46.82219	17.23101	Gyenesdiás middle quarry	46.77851	17.29167
Pajtika quarry	46.80990	17.26448	Gyenesdiás eastern quarry	46.77929	17.29630
Molnárkő quarry	46.80354	17.26469	Felsőhegy quarry	46.76542	17.33641
Pilikán quarry	46.79337	17.27255	Balatongyörök quarry	46.77088	17.35539
Kőmell Cliff	46.78421	17.28789	St Miklós spring	46.82416	17.32267
Gyenesdiás western quarry	46.77971	17.28958			

Table I: Location of the investigated quarries/outcrops; Projection datum is WGS84.

The described structures are marked by colors and numbers (Fig. 3.2b). In general, I signed with blue arrows those faults, which were interpreted as pre-folding/pre-orogenic structures. Middle Cretaceous syn-folding/orogenic structures are marked by red color, whereas yellow arrows show post-folding/orogenic structures (Fig. 3.2b). Layer-parallel shear zones were widely observed on field, which I marked by dotted lines and white arrows. The classification of structures is not explained in the description of the outcrops (Chapter 4), however, it is described in a separated chapter, including interpretation of the observations (Chapter 5).

I started the numbering of faults from the beginning in the individual quarries, since correlation of these small structures are impossible between the outcrops. The names of the faults include the initial(s) of the names of the quarries. For example, Fpil2 means fault no. 2 in the Pilikán quarry. I gave similar names for folds, where A means anticline and S means syncline. Quarry-scale folds were named after the quarry.

3.2. Stereoplots

Several types of structural data were measured in outcrops of the Keszthely Hills, which were plotted by the software of Angelier (1990) (for legend see Fig. 3.2c). The data were illustrated by stereoplots, with lower hemisphere equal area projection.

Fault-slip inversion was not carried out, since detailed fault-slip analyses has been done by Héja (2015a). I made tilt test on some of the conjugate normal fault pairs by the modul of "Rotilt" (Angelier 1990), if the beds had significant dip. The basic assumption during tilt-test was, that the tilting of the strata is mostly the result of Cretaceous folding. Pre-orogenic structures were back tilted by the dip of the beds, to get a better view on the original geometry. Consequently, tilt test gave a relative chronology with respect to tilting/folding. In the case of positive tilt-test, I interpreted the fault pair as pre-orogenic or pre-folding structure.

I identified several second-order outcrop-scale folds in the dolomite quarries of the Keszthely Hills. Since I supposed the presence of cylindrical folds, therefore, I suit a best fitting great circle (π-circle) for the sets of bedding poles by the software InnStereo developed by Tobias Schönberg in 2015. The pole of this great circle represents the axis of the fold.

3.3. Seismic data

The featured 2D seismic sections were acquired and processed by GES Geophysical Services Ltd in 2001 using vibroseis source with 8-90 Hz sweep frequency. Coverage of 100 and 12.5 m distance between CDPs ensured the proper lateral resolution and a good signal/noise ratio. These acquisition parameters represented an advanced technology that time. This facilitated a good image of basement structures. The processing was standard time processing including a challenging static correction due to hilly terrain, DMO correction and post-stack migration.

Seismic block A was acquired by Geophysical Services Ltd (GES) in the winter of 2006-2007. Vibroseis source with 8-90 Hz were used with a few dynamite infill records. Coverage of 36 and 25x25 m bin size ensured the proper lateral resolution and a good signal/noise ratio even in the shallow part. These acquisition parameters represent a standard technology that time. The data have been reprocessed by Geoinform Ltd and Dana Energy (Iran) in 2018. Both processing performed a standards PSTM workflow with minor differences in statics calculation and noise attenuation.

Seismic block B was acquired by Geophysical Services Ltd (GES) in two stages in autumn of 1996 and autumn of 1997. The source was dynamite with 4kg charge. Coverage of 20 and 20x20 m bin size ensured the proper lateral resolution and a good signal/noise ratio even

in the shallow part. These acquisition parameters represent a standard technology that time. The survey was reprocessed by Shearwater (UK) in 2017. Standard PSTM processing flow was applied focused on statics and noise attenuation.

Seismic block C was acquired by GES Geophysical Services Ltd in two phases in autumn of 2008 and summer of 2010 using mostly vibroseis source with minor dynamite infill. Sweep frequency was 8-100 Hz. Coverage of 42 and 20x20 m bin size ensured the proper lateral resolution and a good signal/noise ratio even in the shallow part. These acquisition parameters represent a standard technology that time.

The data were processed by GES Ltd and Tricon Ltd little bit later. Both processing run a standards PSTM workflow with minor differences in statics calculation (uphole based statics vs GLI refraction statics) and noise attenuation.

The featured sections were not time-depth converted, and the vertical scales show two ways travel time is sec. An exception is L-L' seicmic section, in which I connect seismic and surface data (Appendix II). In this case I made a very simple time-depth conversion: I calculated with average seismic velocity of 6500 m/sec, based on data of Dohr (1981) (see details in chapter 3.5)

3.3.1. Interpretation of seismic data

Seismic and well data were loaded and interpreted in Landmark Decision Space software. The particular seismic units are characterized and described in Chapter 4.2.1. The described structures were colored and numbered by a similar way as in the case of outcrops (Fig.3.2b). I distinguished pre-orogenic (marked by blue), middle Cretaceous orogenic (marked by red) and post-orogenic (marked by yellow) structures. Interpretation of larger-scale faults facilitated their correlation. Therefore, I didn't start the numbering of faults from the beginning in the individual sections. The same fault number in individual sections indicates the same fault-zone. Fault and horizon surfaces were generated after seismic interpretation and correlation of 67 2D lines and 3 cuboids of 3D seismic blocks. I used the original name in the cases of structures, which had already been described by previous authors (e.g., Bakonybél thrust).

3.4. Well data

Huge number of well data was available from the database of MOL Oil and Gas Plc. and the Hungarian Geological Survey. Wells deriving from the database of MOL Oil and Gas Plc., are indicated by coded name (e.g, Well A, Well B, Well C…etc.), since the Zala Basin still represents active area for hydrocarbon exploration. However, I used the original name of wells, which derives from the database of the Hungarian Geological Survey, since it represents public data. These wells are located mostly in the Bakony, Balaton Highland and Keszthely Hills.

I made a data filtering, and I took into account only those wells which reached the Mesozoic basement (Fig. 3.1b). Most of the wells were drilled more than 30 years ago, and they were reinterpreted by the experts of the MOL Oil and Gas Plc. and the Hungarian Geological Survey several times based on well descriptions. Sometimes there are significant contradictions in the different reinterpretations. For example, any type of dolomite was frequently interpreted as Hauptdolomit, note the distinction of Triassic Dolomites is highly problematic. There are examples, where a core is interpreted both as Rhaetian Kössen Marl and Carnian Veszprém Marl. Therefore, I used these problematic well data carefully, and I chose those well reinterpretations which fit better with seismic data.

3.5. Construction of restored cross sections

Based on zig-zag composite seismic section across the Zala Basin (Appendix I) and field data from the Keszthely Hills a straight regional cross-section was constructed across the Southwestern Transdanubian Range (Appendix IV.c). The section, which was restored in two steps (Appendix IV.a and b), connects seismic data of the Zala Basin and surface data of the Keszthely Hills.

The straight regional section was created based on the intersecting fault planes and horizon surfaces. The next step was time-depth conversion of straight regional section. In this step I used a very simple velocity model, in which I calculated with average velocity of 2913 m/sec in the case of Upper Cretaceous and Cenozoic succession, and with 6500 m/sec average velocity in the case of pre-Senonian rocks.

Average velocity of the Upper Cretaceous – Cenozoic succession was calculated based on 15 wells along the regional section (Appendix IVc). The TWT depth of top pre-Senonian basement in time was adopted from seismic interpretation (Appendix I), and the average velocity was calculated based on the ratio of real depth in meter and interpreted OWT depth in time.

Most of these wells are penetrating only the upper few tens of meters of pre-Senonian rocks, therefore, time-depth conversion of pre-Senonian basement was problematic. Triassic-Jurassic stratigraphy of the Northern Calcareous Alps and Transdanubian Range show many similarities (Haas et al. 1995). Therefore, I applied average seismic velocity (6500 m/sec) for the pre-Senonian basement based on measurements of Vorderriß-1 well, which penetrated the whole nappe-system of the Northern Calcareous Alps (Dohr 1981). I used the same velocity in the case of L-L' 2D seismic section (Appendix II), in which seismic data are connected with surface data.

Kinematic restoration was carried out by using software Midland Valley Move. The structures were restored in two step: first post-orogenic normal faults were restored by using 2D Move on fault – Simple Shear module (White et al. 1986). The restored section was simplified and redrawn using kink folds, and after that it was unfolded by using 2D flexural-slip unfolding module (Suppe 1983).

For the sake of simplicity, I ignored the effects of compaction and Miocene post-rift thermal subsidence. Moreover, NE-SW direction of post-orogenic extension and E-W direction of orogenic compression (discussed in details in chapter 5) resulted, that plane strain could not be applied on E-W striking plane of the section (Elliott 1983). Therefore, section of the present study (Appendix IV) can be rather considered as a "quasi"-restored section or sketches of tectonic evolution. Nonetheless the section provide important new findings about the structural development of the Transdanubian Range.

4. Oservations

4.1. Keszthely Hills

4.1.1. Csókakő quarry

In the Csókakő quarry (Fig. 3.2a), Upper Norian Rezi Dolomite is exposed, which is covered by Upper Miocene (Pannonian) conglomerate and sand. The most spectacular part of the quarry is its eastern wall (Fig.4.1a). Two main facies types of the Rezi Dolomite are visible here: thin-layered or laminated dolomite and dolomite breccia. Laminated dolomite occurs in the northern part of the eastern wall with sub-horizontal dip. Southward-thickening dolomite breccia tongues can be observed between the laminated dolomite layers, further to the south. These strata dip already moderately toward NNE. Further south, the dark grey laminated dolomite intercalations pinch out, and in the southern edge of the quarry only massive dolomite breccia is present (Fig.4.1a).

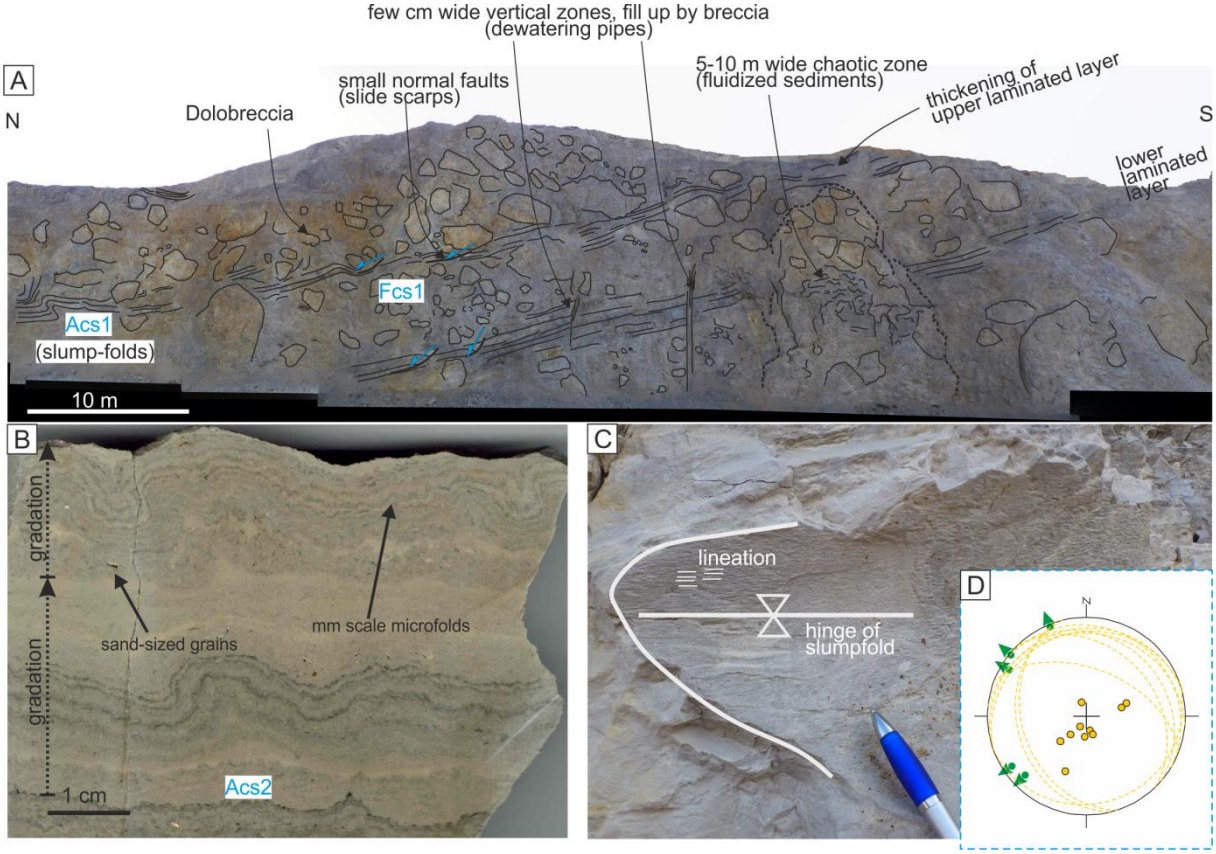

Fig. 4.1: Eastern wall of the Csókakő quarry. (a) Dolomite breccia and two laminated dolomite intercalations; Fluidized zones cross-cut the dolomite breccia layers; (b) cm-scale slump-folds with mm-scale microfolds; (c) lineation is visible parallel to the cm-scale slump fold axis; (d) stereonet of the measured slump fold axes and bedding. For location of the outcrop see Fig. 3.2a and Table I. For legend of the stereoplot see Fig. 3.2c.

The laminated unit is characterized by dark grey, strongly bituminous dolomite (Figs. 4.1a,b,c). Two laminated dolomite intercalations are visible between the dolomite breccia

tongues in the middle part of the eastern wall (Fig. 4.1a). Occasionally, sand-sized dolomite lithoclasts can be observed at the base of the laminated dolomite layers (Fig. 4.1b). These layers show normal gradation (Fig. 4.1b).

The clasts of the dolomite breccia are up to few meters in size (Fig. 4.1a). They are thick bedded or massive, white or light grey boulders, which often contain green algae, molluscs and gastropods. Stromatolitic, intertidal dolomite represents another clast-type of this dolomite breccia.

The matrix of the dolomite breccia is gradually changing southward. In the northern, distal part of the breccia-tongues, the matrix of this breccia is laminated dolomite. In contrast, in the southern part of the breccia tongues the matrix is made up by massive, light-grey dolomite, containing the same platform-derived fossils as the fossil-rich clasts of the dolomite breccia itself.

Folds are present both in the thin-layered, laminated unit (Acs1 and Acs2 on Fig. 4.1), and in the laminated matrix of the dolomite breccia. First, I describe folds of the laminated unit: the wavelength of these folds range from few centimetres to up to meter (Fig.4.1a and b). Tightness of the folds varies between open to even tight (Fig.4.1b). The folds are rounded, and the limbs are not fractured, the folds show continuous deformation. Thickness changes along the fold limbs are frequent. Folds are symmetric to slightly asymmetric, with vertical or plunging axial trace (Fig.4.1b). Folds of the laminated unit are frequent mostly in the northern part of the eastern wall.

Folds with slightly different geometry occur in the laminated matrix of the dolomite breccia; these folds are more chaotic around and/or between the redeposited large dolomite blocks. These folds are asymmetric, sometimes overturned or even recumbent with horizontal axial trace.

The measured fold axes of the folds show significant dispersion; nevertheless, WNW-trend is most frequent (Fig. 4.1d). Closely spaced (0.5-2 mm) few cm long lineation was observed on the bed surfaces of some of the folds, which is parallel to the fold-axis (Figs. 4.1b,c). On the polished surfaces of the sample it is visible that this lineation represents hinges of very fine micro-folds (in the scale of 0.5-2 mm).

Small-scale normal faults are frequent in the laminated dolomite unit, mostly in the middle and southern part of the eastern wall (Fcs1 fault set on Fig. 4.1). These normal faults detach at the base of the laminated unit, creating roll-overs in the hanging wall. The layers are thicker in the hanging wall of the faults, and the faults are sealed by upper beds of the laminated dolomite.

The gently NNE dipping beds are cross-cut by several, few centimetre-wide vertical zones (Fig. 4.1a). The infill of these zones is few mm- up to few cm-sized dolomite breccia clasts sitting in dolomite matrix. The lower laminated dolomite layer is interrupted by a 5 to 10-meter-wide sub-vertical chaotic zone, where dark-grey dolomite matrix is mixed with huge, light-grey dolomite blocks (Fig. 4.1a). The dark-grey dolomite probably originally represented the same material as the laminated one, but its original sedimentary features (lamination) were disappeared later, therefore, the primary lamination cannot be recognized (Fig. 4.1a). The upper laminated dolomite intercalation downbends and became thicker above this zone (Fig. 4.1a).

4.1.2. Molnárkő quarry

Most of the quarry is made up by Hauptdolomit, while in the southeastern corner thin layered, laminated Rezi Dolomite occurs (Fig. 4.2a). In the Rezi Dolomite few decimeter wide folds occur. One of these folds is an isoclinal synform, which is outlined only in a laminated dolomite intercalation (Sm1 on Fig. 4.2d). Despite isoclinal folding, the laminite is not fractured, and shows continuous deformation. This laminated dolomite intercalation pinches out toward southeast, between two layers of dolomite. The axial plane of the synform is dipping steeply toward SE, and it is folded into a rounded, open NE-SW trending antiform (Am1 on Fig. 4.2d). This antiform is slightly asymmetric, with northeastern vergency. This antiform can also be outlined based on the thin dolomite layer, which is covering the laminated intercalation; the thickness of this layer is changing on the limbs of the antiform. However, the dolomite layer, underlying the laminated intercalation is not affected by these folds (Fig. 4.2d).

A few meters wide dolomite breccia body can be found in the Hauptdolomit on the southern wall (Figs. 4.2a and e). The breccia body has subvertical sharp contact with the bedded Hauptdolomit. In contrast with the previous outcrop, this breccia body does not appear as a layer or wedge. The breccia is grain supported, however, dolomite matrix is visible, as well. The material of the clasts is dolomite, with different colors (from light gray to dark gray). The size of the clasts is from mm up to few decimeters. The clasts are angular, and their contact is sharp. In several cases the clasts are in fact breccias, composed of angular clasts of 1-3cm (Fig. 4.2e).

Due to the relatively poor outcrop conditions, any marker beds can be hardly followed along the entire quarry walls. Based on dip data a 200 m wide segment of the NE-SW trending Molnárkő anticline was recognized (Fig. 4.2c). The hinge of the Molnárkő anticline intersects the western edge of the southern wall (Fig. 4.2a), and the eastern edge of the northern wall (Fig.

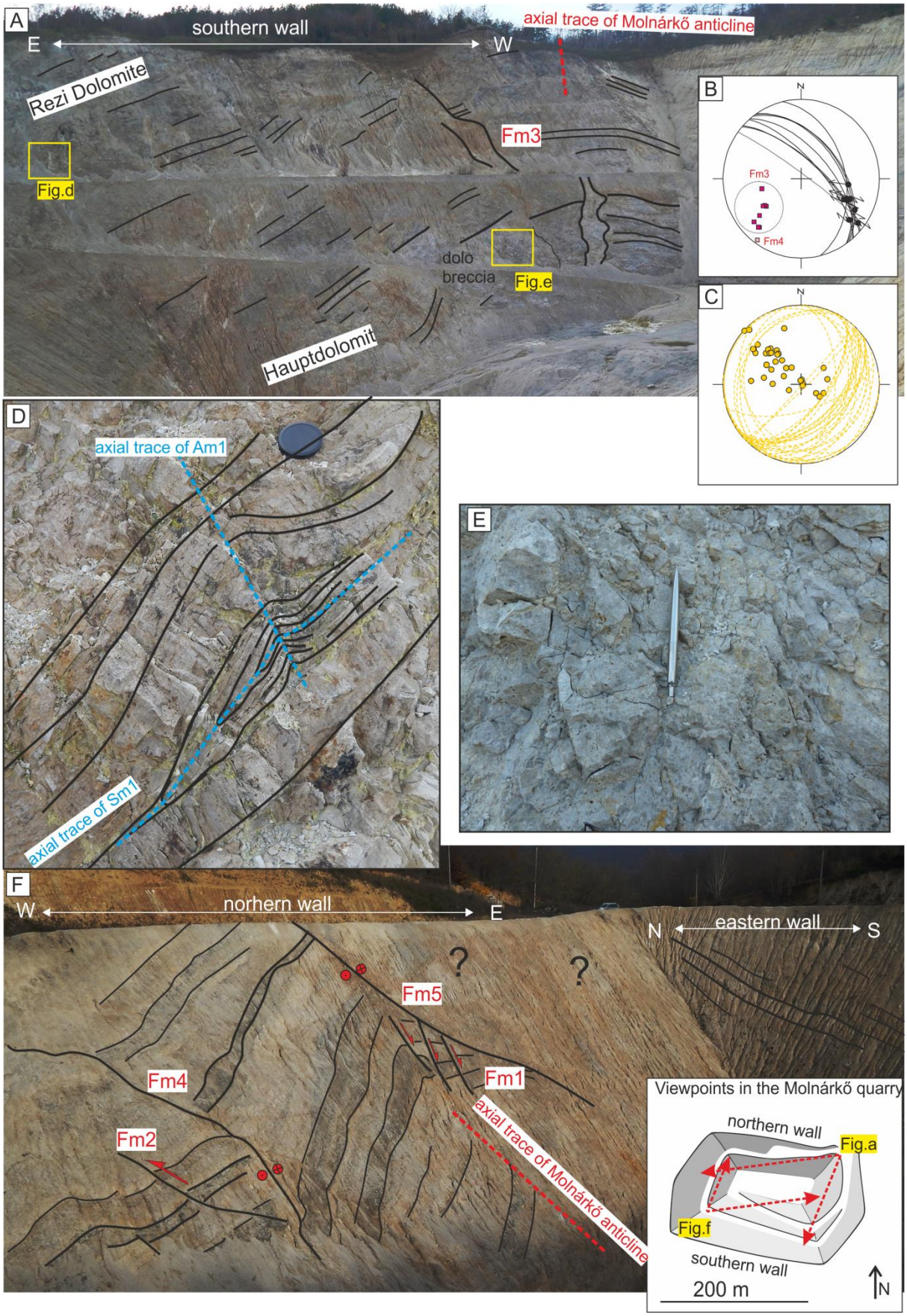

Fig.4.2: Molnárkő quarry; (a) southern wall of the quarry; (b) stereoplot of Fm3 and Fm4 faults (c) stereoplot of bedding dip data (d) slump in Rezi Dolomite (e) dolomite breccia (f) northern wall of the quarry. For location of the outcrop see Fig. 3.2a and Table I. For legend of the interpreted structures see Fig.3.2b. For legend of the stereoplot see Fig. 3.2c.

4.2f), so cut the entire quarry diagonally. The anticline is rounded and gentle on the southern wall (Fig. 4.2a), whereas it is represented by a narrower open fold on the northern wall (Fig. 4.2f). There, the hinge of the anticline is angular/sharp (Fig. 4.2f). The limbs of the Molnárkő anticline are much steeper on the northern wall (Fig. 4.2f), than in the southern wall (Fig. 4.2a). Consequently, the interlimb angle of the anticline is decreasing northeastward.

The hinge of the Molnárkő anticline is dissected by small normal faults on the northern wall (Fm1 faults on Fig. 4.2f). The northwestern limb of the Molnárkő anticline consists of two kink bands on the northern wall. The western kink band shows more gentle dips, than the eastern kink. A small, apparently west-vergent thrust is running from the kink band boundary (Fm2 on Fig. 4.2f).

The Molnárkő anticline is dissected by three NW trending steep faults (Fm3; Fm4; Fm5). Fm3 fault is exposed on the southern wall (Fig. 4.2a). On Fm3 fault plane oblique sinistral-inverse, and dextral-normal striae are preserved (Fig. 4.2b). Steeper, oblique sinistral-inverse slicken lines are overprinting subhorizontal sinistral slicken lines on the same plane (Fig. 4.2). The middle steep fault (Fm4 on Fig. 4.2f) is NW-SE striking (Fig. 4.2b), and shows apparent reverse offset, which may also refer to left-lateral movement. F5 cut the F1 set of faults, and, being parallel to F4, also can be considered as sinsitral fault.

4.1.3. Pajtika quarry

The huge quarry is made up by Hauptdolomit (Fig. 3.2a). The strata dip steeply towards northwest to southwest in general (Figs.4.3c and). On the east-facing walls of the quarry a 300 m wide segment of the gentle, rounded Pajtika syncline is outlined (Fig.4.3d). Dip data suggest, that the axis of this syncline is plunging significantly toward WSW (Fig. 4.3c).

On Figure 4.3a, the southern wall of the quarry can be seen. The layers are crosscut by a number of post-tilt normal faults (Fpaj1 set on Fig.4.3a), and a minor thrust (Fpaj2 on Fig. 4.3a). The latter one is probably coeval with the folding/tilting. Occasionally, layer-parallel slickenlines also occur. A steep NE-trending fault (Fpaj3 on Fig. 4.3a and b) can be traced on the southern wall of the quarry. The fault core is represented by a 1.5-meter-wide powdered dolomite zone (Fig. 4.3a). The hanging wall of the fault is built up by strongly fractured dolomite representing a few-meter-wide damage zone of Fpaj3 fault. In contrast to the hanging wall, the footwall of Fpaj3 is deformed less intensively. The west dipping beds show strongly different dips on two sides of F1 fault (Fig. 4.3a). In the northwestern part of the fault beds are dipping moderately toward west, whereas at the opposite side beds are sub-vertical (Fig. 4.3a). These sub-vertical beds represent the steep western limb of the rounded Apaj1 anticline. There is no information about the eastern limb of this anticline, since the quarry terminates at the crest

of the fold (Fig.4.3a). The Apaj1 anticline is dissected by several minor thrusts (Fpaj4 set on Fig. 4.3a).

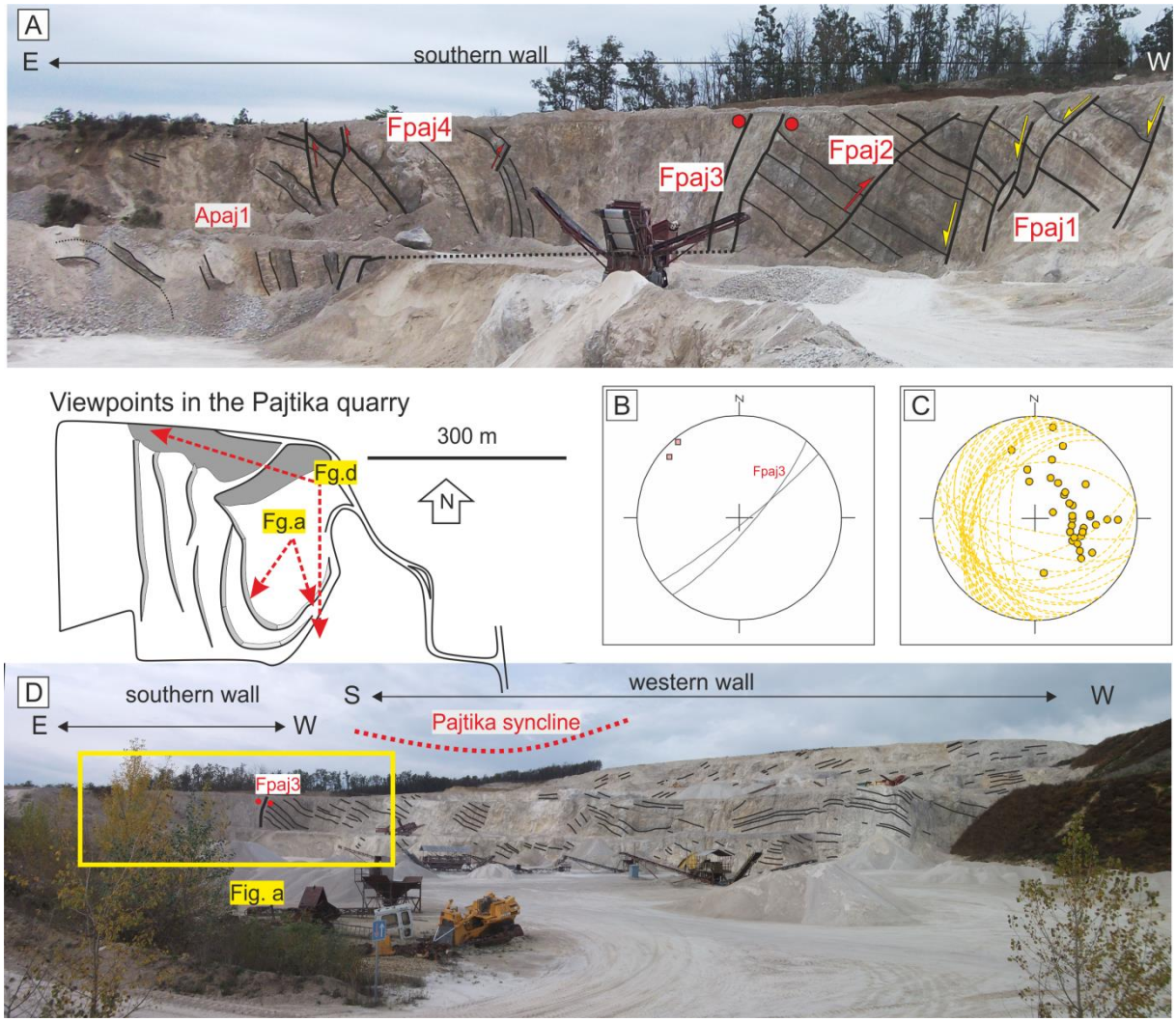

Fig. 4.3: Pajtika quarry (a) southern wall of the quarry; (b) stereplot of Fpaj3 fault; (c) stereoplot of dip data; (d) western wall of the quarry. For location of the outcrop see Fig. 3.2a and Table I. For legend of the interpreted structures see Fig.3.2b. For legend of the stereoplot see Fig. 3.2c.

4.1.4. Kőmell Cliff

Near Gyenesdiás, Rezi Dolomite can be observed at the Kőmell Cliff (Fig. 3.2a). The lower part of the cliff is built up by massive dolomite; layering is not visible. The top of the cliff is built up also by massive cherty dolomite, however, up to 0.5 m blocks of laminated dolomite occur in that massive dolomite matrix, Consequently, it could be also considered as dolomite breccia (Fig. 4.4a). On the northern part of the top of the crag, thin-bedded dolomite crops out in several small cliffs. The dip azimuth of the beds in individual crags are generally toward the NNE, however, strongly different dip values suggest that this part of the cliff is built up by dolomite breccia, and the individual crags of the well-bedded dolomite represents single blocks (Figs 4.4a and b). At the northeastern side of the cliff the WNW-ESE trending

asymmetric, overturned, closed Ak1 anticline was observed (Fig 4.4c). The fold gradually smoothens upward, and it is covered by homocline beds.

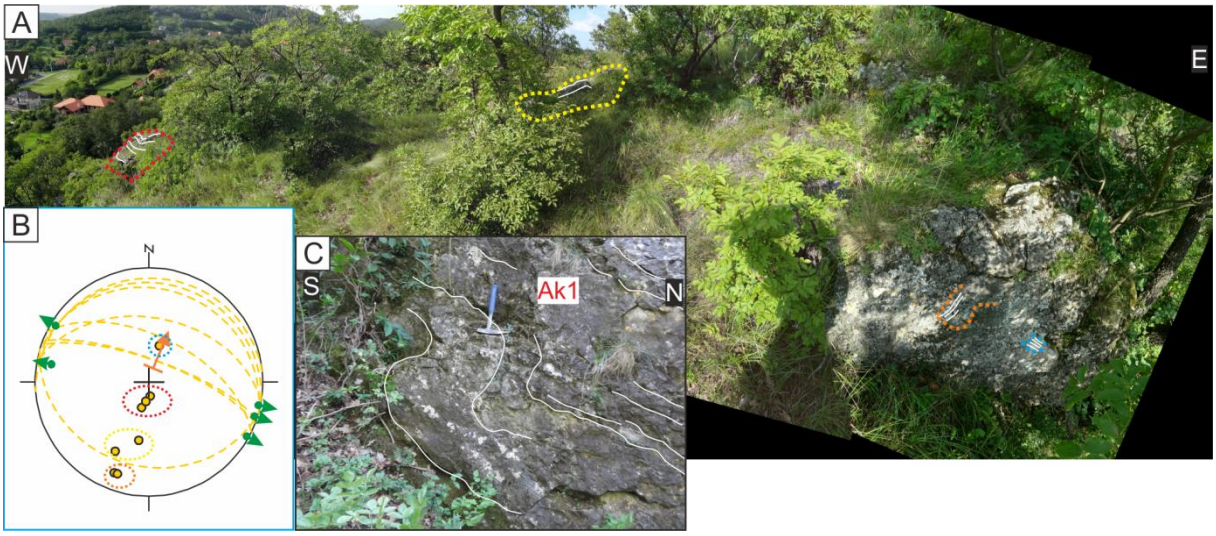

Fig.4.4. Kőmell Cliff (a) individual crags at top of the Kőmell Cliff show significantly different dips (b) stereoplot of bedding dip data; dasched circles assign different blocks (c) slumpfold in the northern side of the cliff. For location of the outcrop see Fig. 3.2a and Table I. For legend of the stereoplot see Fig. 3.2c.

4.1.5. Pilikán quarry

Thin-bedded to laminated, dark-grey, bituminous dolomite (Rezi Fm.) crops out in the Pilikán quarry (Fig. 3.2a). Along the eastern wall of the quarry, a 3 m thick dolomite breccia intercalation was observed (Fig. 4.5a). The clasts are significantly smaller than those of the Csókakő quarry; their maximum size is from mm up to few dm (Fig. 4.5b). The clasts are made up of light grey to dark grey dolomite. The breccia is grain supported, but similarly to the Csókakő quarry dolomite matrix occurs here, as well. The contact of the breccia bed and the underlying dolomite is a wavy erosional surface.

Another type of breccia was identified in the north-western corner of the quarry. This breccia appears in a few decimetres thick light grey beds. There dark grey clasts float in slightly lighter grey dolomite; the breccia is matrix supported. The clasts do not have sharp contact; they are rather obscure.

The breccia bed of the eastern wall is dissected by a number of normal faults (Fpil1; Fpil2; Fpil3 and Fpil4 on Fig. 4.5a). The offset of these faults decreasing upward, and finally they are sealed by covering dolomite beds, without any flexure or distortion at the upper bed contact.

On the southern quarry wall small faults dissect a dark grey marker bed, with a few cm offset; the overlying layers seal these structures (Fpil5 and Fpil6 on Fig. 4.5c). The NW-SE trending faults show mostly normal offset, however, some of the faults are steep reverse faults (Fpil5 on Figs. 4.5c and d).

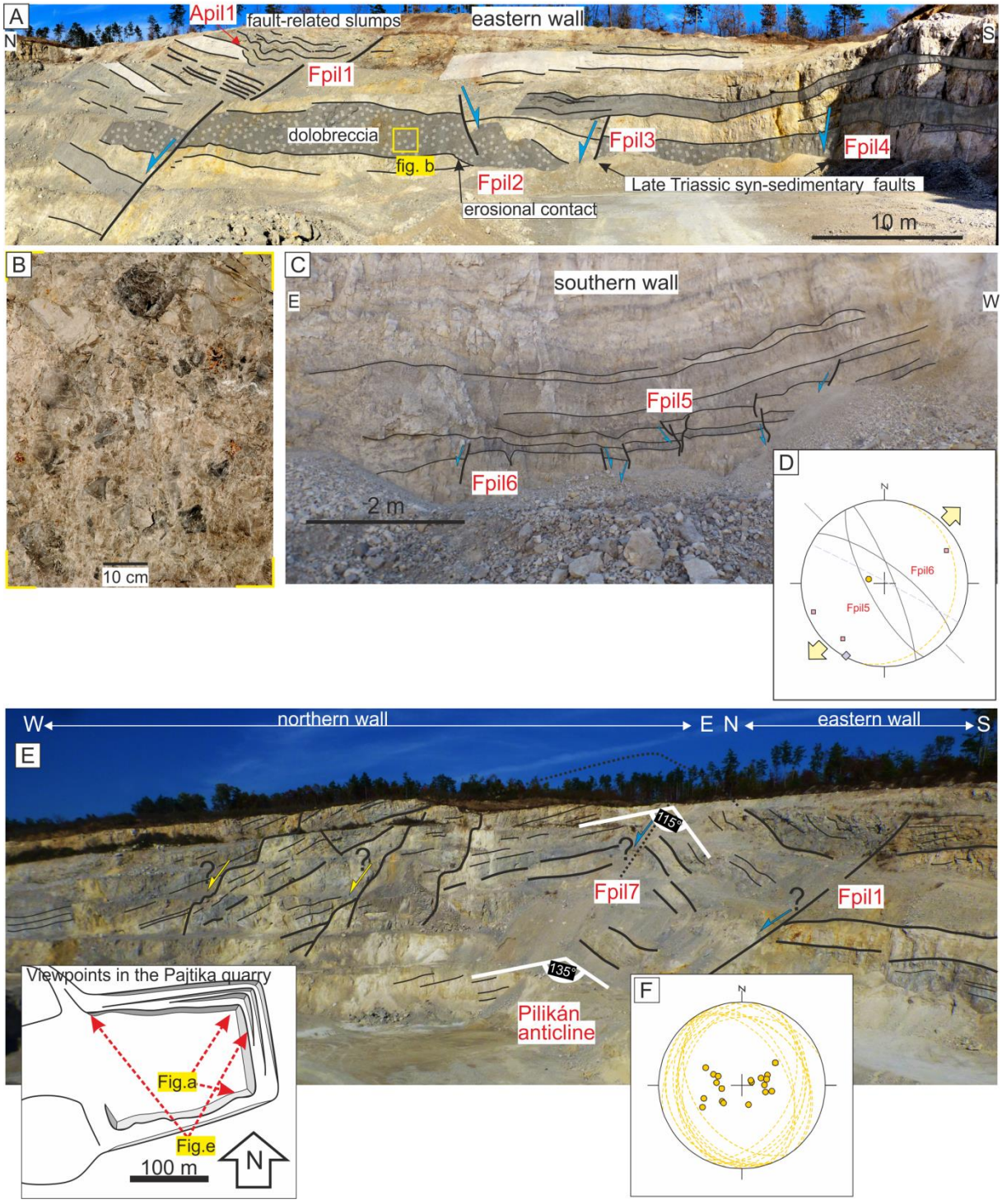

Fig.4.5. Pilikán quarry (a) eastern wall of the quarry (b) dolomite breccia (c) syn-sedimentary normal faults on the southern wall (d) their projection on stereoplot (e) Pilikán anticline on the northern wall (f) stereoplot of bedding dip data. For location of the outcrop see Fig. 3.2a and Table I. For legend of the interpreted structures see Fig.3.2b. For legend of the stereoplot see Fig. 3.2c. fault-related slumps

In the upper part of the eastern wall meter sized symmetric, rounded folds occur (Apil1 on Fig. 4.5a). Noticeable thickness variations along the limbs of the folds can be observed.

The most dominant structure of the quarry is the approximately 200 m wide N-S trending, angular Pilikán anticline (Fig 4.5e and f). The axial trace of the asymmetric anticline is plunging toward west on the northern wall. The hectometric fold is dissected by a number of

faults, although the relative age of these structures is unclear with respect to folding. One of these structures, with only a few meters of normal offset, is situated along the axial trace of the anticline (Fpil7 on Fig. 4.5e). Another larger normal fault occurs along the axial trace which separates the eastern steep limb from the subhorizontal beds of the eastern wall (Fpil1 on Fig. 4.5e). Another important feature of the anticline is that the limbs steepen upward. Consequently, the anticline has gradually increasing amplitude, and decreasing interlimb angle upward (Fig. 4.5e).

4.1.6. Gyenesdiás quarries

NNW-SSE trending Gyenesdiás anticline is exposed in the three yards of the Gyenesdiás quarries (Fig. 3.2a, Figs. 4.6d and g). The three yards expose different parts of this anticline. The yards are described in the following chapters one after another.

4.1.6.1. Gyenesdiás, eastern quarry

Steeply ENE ward dipping beds are dominant in this dolomite quarry, therefore, a relatively thick tilted succession is visible. In general, all types of the outcropping dolomites are highly fractured. In the western wall of the quarry thick beds of Hauptdolomit occur, whereas the southern wall exposes the Rezi Dolomite (Figs. 4.6a, b and d). The latter is thin-bedded, laminated, dark grey bituminous dolomite, in which gentle NW-SE trending symmetric folds were observed, with approximately 1-meter wavelength (Agy1). The folds affect only a 0.5-meter-thick succession of laminated dolomite, and it is covered by homocline beds. Thick bedded, light grey dolomite intercalations occur upward, and they dominate the eastern part of the southern wall, whereas along the easternmost side laminated dolomite is present again (Figs. 4.6a and b).

On the southern wall of the quarry, several second-ordered structures are visible, which are described one after another. A few meters wide pop-up structure is visible on the eastern part of the southern wall, where the steep beds start moderately dipping (Fig. 4.6a). The pop-up structure is bordered by several conjugate thrusts (Fgy1 fault set), which have only a few ten cm of off-set. The pop-up anticline is more remarkable in the upper level, whereas it gradually disappears down-ward. The bedding surfaces are represented frequently by powdered dolomite. I interpret these powdered zones as layer-parallel shear zones. Powdered dolomite zones are intersected by small thrusts, which could be related to the pop up structure. On the other hand, an upper powdered dolomite zone jumps to a higher level across the pop-up structure (Fgy1), which suggests that this layer-parallel shear zone postdates the pop-up structure (Fig. 4.6a).

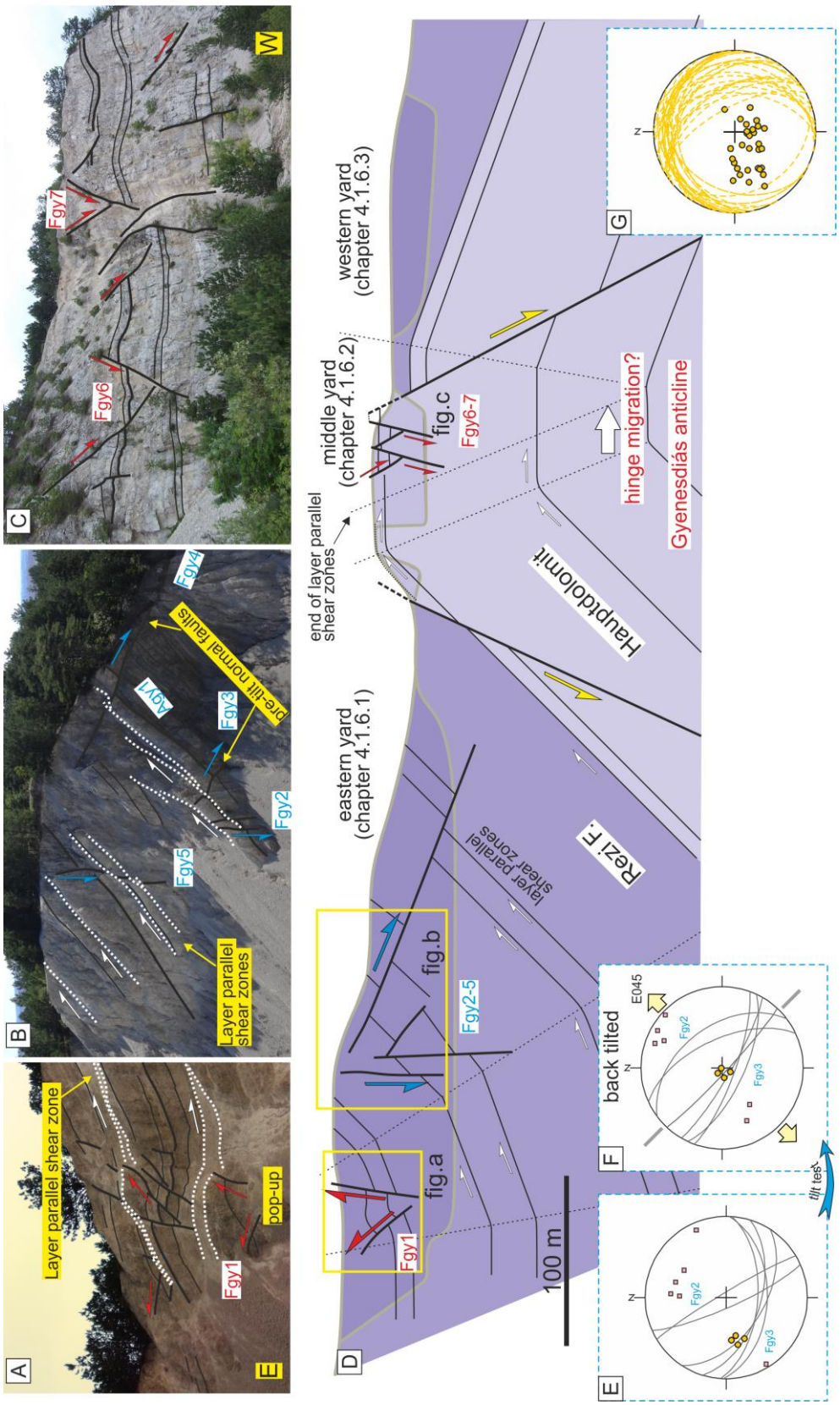

Fig.4.6. Gyenesdiás quarries (a) pop-up structure on the southern wall of the eastern yard (b) tilted normal faults on the southern wall of the eastern yard (c) conjugate normal faults in the middle yard, note the photo is mirrored (d) simplified crossection across the Gyenesdiás quarries (e) stereplots of tilted normal faults on fig.c (f) the same normal faults on a back-tilted stereoplot. (g) NNW-SSE trending anticline is outlined based in dip data of the quarries. For location of the outcrop see Fig. 3.2a and Table I. For legend of the interpreted structures see Fig.3.2b. For legend of the stereoplot see Fig. 3.2c.

Further west, the steep beds are dissected by tilted conjugate normal fault pairs (Fgy2-5 on Figs. 4.6b, e and f). Here, the boundaries of the beds are also frequently marked by powdered dolomite. Some of the pre-tilt faults are dissected by these powdered zones, while some of the powdered layers pinch out towards the pre-tilt normal faults. In some cases, the powdered dolomite zone is forking into two branches along pre-orogenic tilted normal faults (Fig. 4.6b).

4.1.6.2. Gyenesdiás middle quarry

In the middle yard of the Gyenesdiás quarries, beds of the Hauptdolomite are subhorizontal (dipping gently towards NNE). Powdered dolomite zones appear only along the eastern side of the quarry, whereas they are missing in the western side (Fig.4.6d). Similarly, the eastern side of the quarry yard is much more fractured than the western side (northern wall). The beds are dissected by several conjugate normal faults (Fgy6-7), which do not deform the denudation surface (Fig. 4.6c).

4.1.6.3. Gyenesdiás, western quarry

This outcrop is situated in the western vicinity of the previously described quarry (Fig. 4.6d). It is built up by thin bedded, laminated dark grey Rezi Dolomite. Meso-scale normal fault was identified with a few tens of cm offset (Fgy-8 on Fig. 4.7a). Several displaced beds are thicker in the hanging-wall, and the displacement of the small fault decreases upwards. There is an upward smoothing extensional fault-related fold, a very gentle flexure above the upper fault tip point. Within the flexure minor normal faults are layer-bounded (Fig. 4.7b). These minor faults are only expressed by very small steps on bedding planes, while the fault planes are not visible. The faults suggest WNW-ESE extension (Fig. 4.7c).

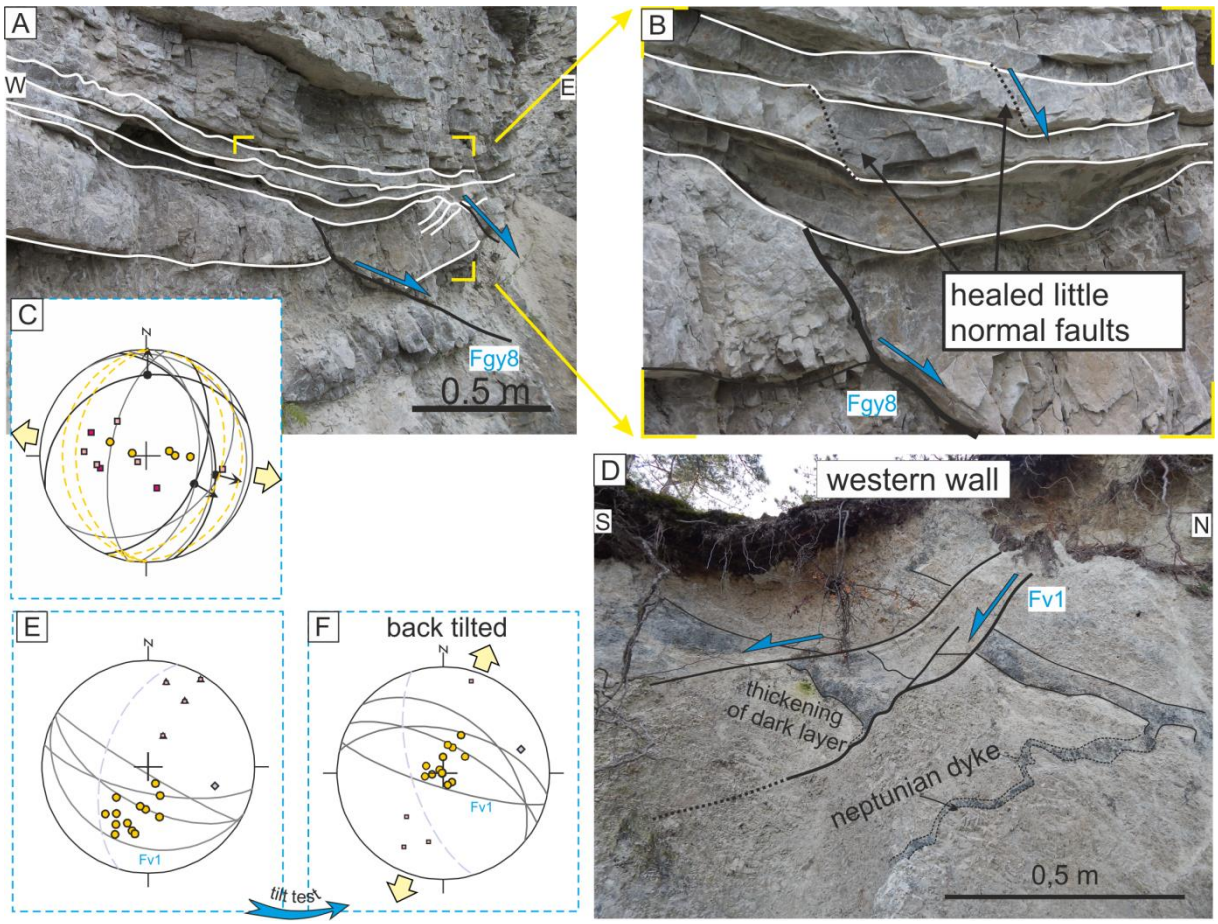

Fig.4.7. (a) Oblique view to syn-sedimentary normal fault in the western yard of Gyenesdiás quarries; (b) healed normal faults in the western yard of Gyenesdiás quarries (c) stereoplot of the faults (d) syn-sedimentary normal fault in the Felsőhegy quarry; (e) stereplots of tilted normal faults on fig.d (f) the same normal faults on a back-tilted stereoplot. For location of the outcrop see Fig. 3.2a and Table I. For legend of the interpreted structures see Fig.3.2b. For legend of the stereoplot see Fig. 3.2c.

4.1.7. Felső Hill quarry

This quarry exposes the NNE-ward tilted beds of the Hauptdolomit Fm. (Fig. 3.2a, Fig. 4.7d). Thick bedded, light-grey dolomite is the most common, but occasionally, few cm thick, black, bituminous dolomite interbeds also occur locally. They contain small, angular clasts of light-grey dolomite. On the western wall, tilted normal faults were observed (e.g, Fv1 on Fig. 4.7d). A dissected, bituminous, dark grey interlayer/intercalation has increased thickness in the hanging wall. A neptunian dyke, which is running parallel to the fault is present in the footwall. It is filled by dark grey, bituminous dolomite and show strong undulations along dip; this is probably due to post-emplacement vertical shortening and compaction. These structures suggest NE-SW extension (Fig. 4.7e and f).

4.1.8. Balatongyörök quarry

Steeply north – northeast-ward dipping Hauptdolomit is exposed in this quarry (Fig. 3.2a, Fig.4.8a and b). Microbialitic interbeds occur frequently between thick massive dolomite beds. These dolomite interbeds are often powdered; in this case, the original microbial laminites cannot be recognized. The dolomite beds in the vicinity of the powdered zones are strongly fractured. I interpreted this powdered zones as layer-parallel shear zones. Deformation along these shear zones made the dolomite powdered, because deformation gradually decreases from powdered zone core both upward and downward into massive dolomite beds. Several SW-dipping (Fig.4.8b) thrusts (Fb1-4) are cross-cutting the tilted beds. The off-sets of these thrusts are less than a metre. All the mentioned thrusts are dissected by layer-parallel shear zones, on the other hand in some cases the shear zones are faulted by the thrusts (e.g., uppermost signed shear zone is faulted by Fb2 on Fig. 4.8a).

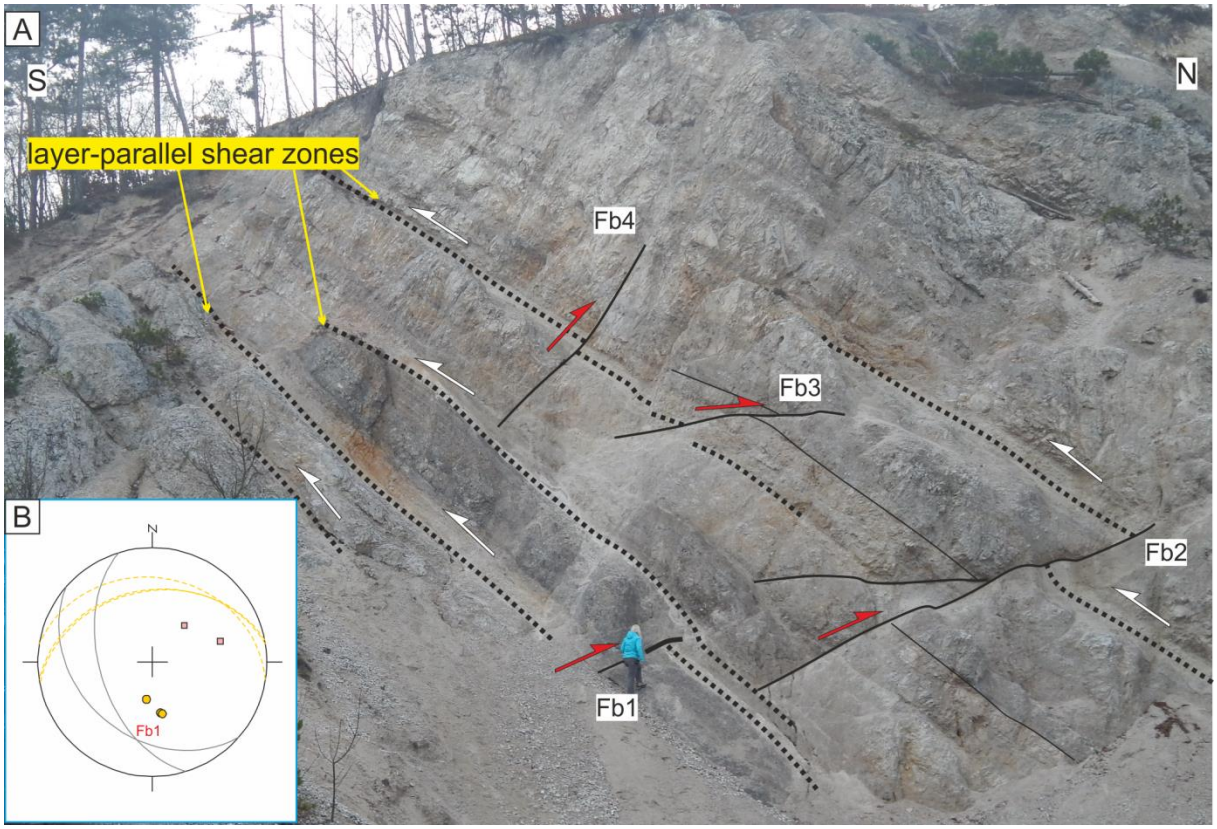

Fig.4.8 (a) Layer-parallel shear zones and thrusts in the Balatongyörök quarry. (b) Stereoplot of Fb1 thrust and bedding planes. For location of the outcrop see Fig. 3.2a and Table I. For legend of the interpreted structures see Fig.3.2b. For legend of the stereoplot see Fig. 3.2c.

4.1.9. Szent Miklós spring, couloir

This outcrop is located in the Eastern Keszthely Hills, near the Ederics platform (Fig. 3.2a). East of the Szent Miklós spring the Csicsó Member of the Carnian Veszprém Formation is exposed in a small ravine (Csillag et al. 1995). The deformed beds are consisted of well-

bedded marly limestone and thin-layered to laminated marl. A meter-wide tight anticline is outlined in the thin-layered – laminated beds. The eastern limb of the anticline is vertical or overturned, and it is crosscut by a small reverse shear zone with a few centimeters of off-set (Fig.4.9a and b).

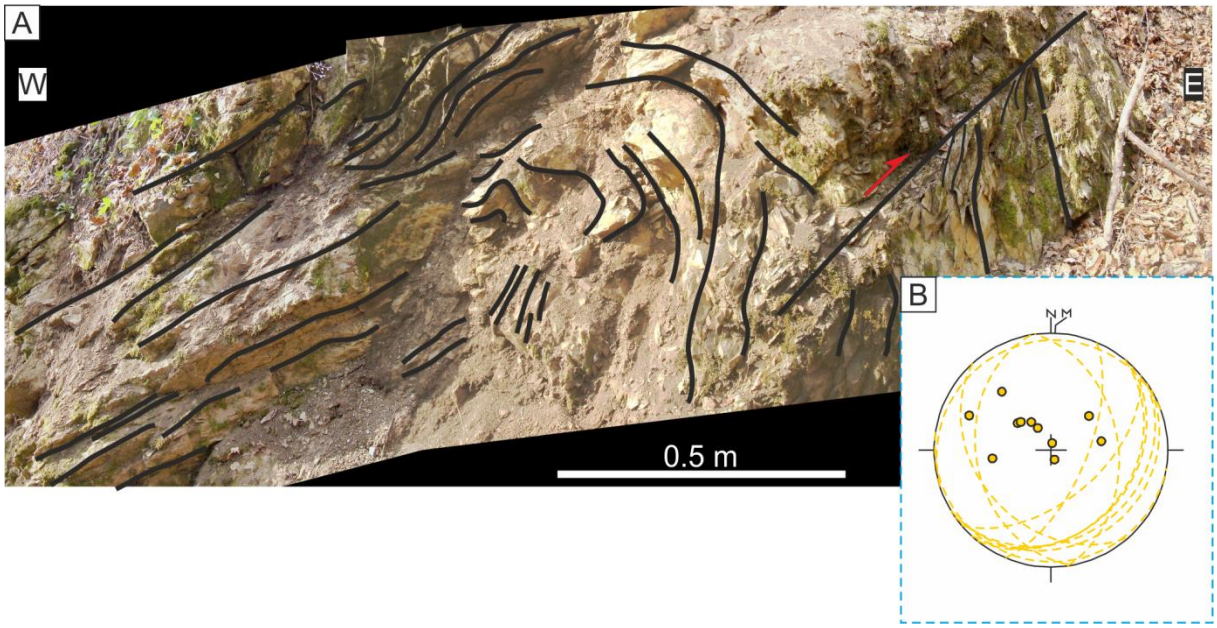

Fig.4.9. (a) Folded Carnian Veszprém Marl near Szent Miklós spring, eastern Keszthely Hills; (b) NNE-SSW trending anticline is outlined on stereoplot of dips. For location of the outcrop see Fig. 3.2a and Table I. For legend of the interpreted structures see Fig.3.2b. For legend of the stereoplot see Fig. 3.2c.

Immediately east of this fold, the beds are dipping moderately toward west (out of the photo), similarly like in the western limb of the anticline (Fig.4.9a). This suggests that the eastern vertical/overturned limb of the anticline is turning back into a syncline directly east of the anticline. Consequently, the anticline has a longer western, and a shorter eastern limb. The axial plane of the fold is dipping westward, and altogether the anticline shows asymmetry and eastern vergency (Figs. 4.8a and b).

4.1.10. Büdöskút anticline

On the eastern limb of Várvölgy anticline (Fig.2.7c) I identified a second-order anticline, which is referred as Büdöskút anticline in the present study (Fig. 4.10). The Büdöskút anticline is outlined by dip variations of the Hauptdolomit (Fig. 4.10) observed in scattered outcrops by mapping geologists (Budai et al. 1999a and b), and along forest roads by myself. The anticline is N-S trending; however, it becomes NW-SE trending along the southern edge of the Keszthely Hills. I suppose that the western limb of the Büdöskút anticline is dissected by the west-vergent Büdöskút thrust (Fig. 4.10). This structure can be detected only where the Hauptdolomit is thrust over the Rezi Dolomite. The anticline observed in the Pilikán quarry (Fig. 4.5e) and the anticline of the Gyenesdiás quarries (Fig.4.6d) are situated in the front of

this thrust. The relatively steep NNE-dipping limb of the southern, NW–SE-trending segment of the Büdöskút anticline is exposed by small quarries (Felsőhegy quarry on Fig.4.7d, Balatongyörök quarry on Fig.4.8a). East of the anticline, the Vállus syncline is outlined based dip values in the Rezi Dolomite (Fig.4.10)

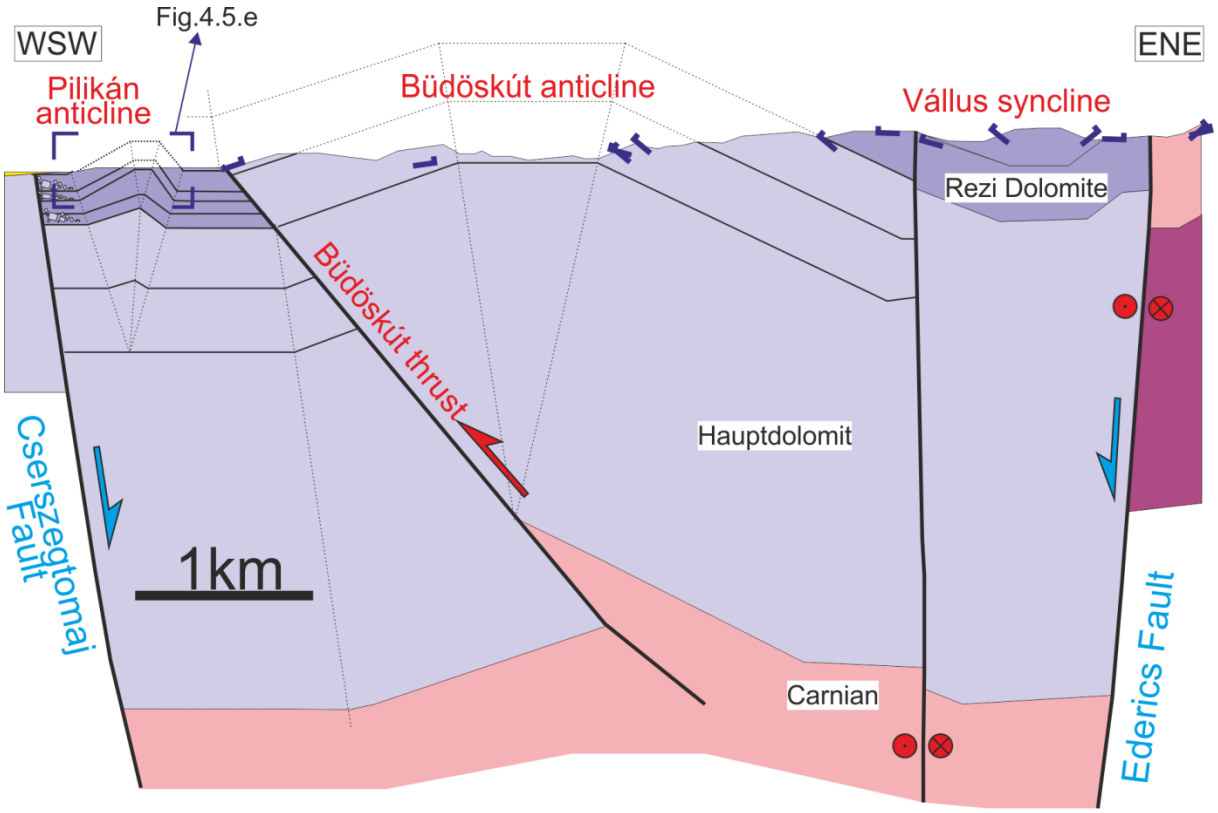

Fig.4.10. The Büdöskút anticline and its relation to the anticline observed in the Pilikán quarry. For location of the section see Fig. 5.8.

4.2. Seismic sections

4.2.1. Seismic facies of Mesozoic succession

The pre-Senonian basement is represented by characteristic architecture and texture of reflections and reflection package features (Figs. 2.1b).

The deepest reflections appear as a part of a maximum 0.5 sec thick package. These reflections are characterized by low to medium amplitudes. Reflections are laterally short, and they cannot be followed protractedly. This reflection package was not reached by any wells in the Zala Basin. Most probably they represent the contact of Variscan shales and Permian sandstone (Variscan unconformity). This assumption is suggested based on L-L'-Balatonszepezd-Kapolcs section (Appendix II). The position of this section is sticking out a little bit from the area of other interpreted seismic data. However, in this section I can connect deep seismic data to a geological section, which was constructed based on tilted and outcropping Permo-Triassic succession of the Balaton Highland. On the basis of this section, thickness estimation of the Permian – Middle Triassic succession is approximately equal to the non-reflective seismic unit, which is overlying these deep reflections based on time-depth converted seismic section.

These lowermost reflections are overlain by a 0.4-0.8 sec thick quasi non-reflective seismic unit. Occasionally, laterally short, low-amplitude reflection occurs. I correlated this seismic unit with the Permian to Middle Triassic succession. The relatively strong reflection-package above it is equivalent to the Carnian Veszprém Marl, which was drilled by several wells (e.g., well H on Appendix I). It is characterized by low to high amplitude; reflectors laterally often fades away (Fig. 2.1b), which may represent interfingering with coeval platforms (Ederics and Budaörs Fm.). Above this formation, a significantly thick unit (0.5-1.2 sec) without any strong reflections occurs. This unit is interpreted as the Hauptdolomit and the Rezi Dolomite; and the two formations are considered as one seismic unit in this work. Occasionally, pale reflection can be observed in the upper part of this seismic unit. These pale reflections may represent the laminated intercalations of the Rezi Dolomte. The strong continuous reflections above the Hauptdolomit – Rezi Dolomite seismic unit corresponds to the Kössen Marl (Fig. 2.1b). The medium to high amplitude are related to the significant impedance contrast between the marl and the limestone intercalations. Thin, non-reflective unit above the Kössen Marl was interpreted as the Upper Rhaetian-Hettangian prograding tongue of the Dachstein and Kardosrét Fm. Consequently, the strong reflections of the Kössen Marl are sandwiched between two, relatively monotonous platform carbonates without reflections (Fig. 2.1b). The Jurassic–Early Cretaceous succession, which is made up by thin formations with variable lithologies (see 2.1.1.

chapter), shows again relatively strong continuous reflectors. These reflectors can be characterized by low to high amplitude (Fig. 2.1b).

This Upper Triassic – Lower Cretaceous succession is unconformably overlain by Senonian shallow marine marl with limestone intercalations (Jákó Marl), platform limestone (Ugod Limestone) and finally monotonous deep-marine marl (Polány Marl.; Figs. 2.1a, b). The variable lithology of the Jákó Marl causes again continuous reflectors with high amplitude (Fig 2.1b), while the relatively monotonous Ugod and Polány Formations show low-amplitude reflectors.

4.2.2. A-A' section

The NE-trending section is running in the northwestern foreland of the Keszthely Hills. The most prominent structure of the section is an extensional graben, which is sealed by the Senonian deposits (Cr2 on Fig. 4.11a). The graben has a segmented southwestern, NE-dipping boundary fault (F1) and a northeastern, SW-dipping boundary fault (F2). The graben is dissected in the middle by an additional NE-dipping fault (F3), separating two sub-grabens. Deposition of Senonian strata postdates the main activity of these faults, but F1 and F3 show minor off-set on base Senonian (Fig 4.11a). The Kössen Marl forms SW-ward thickening half-grabens above the gently SW-ward tilted blocks (Fig. 4.11a). In the southwestern sub-graben offlap surface within the Kössen Marl occurs (Fig. 4.11a). The contact between the Dachstein Limestone and the Kössen Marl is also an offlap surface. In the vicinity of the major faults the seismic image of the Kössen Marl shows poor quality, and in the hanging-wall of the faults wedge-shaped bodies are outlined (Fig. 4.11a). I interpreted these bodies as fault-bounded talus breccia. The thickening trend of the Kössen Marl toward the faults suggests that F1 and F3 were dominantly active during its deposition (Fig. 4.11a). The Dachstein and Kardosrét Limestone gradually get thicker towards F2 (Fig. 4.11a). Only minor offset of these formations can be observed along the other two faults (F1 and F3). Therefore, the fault activity retreated onto F2 during the deposition of the Dachstein and Kardosrét Limestone. If the Senonian re-activation of F1 and F3 is restored, it seems that Jurassic – Lower Cretaceous strata sealed these faults. However, Jurassic – Lower Cretaceous deposits occur only in the hanging wall of F2, which suggests, that the fault was active during or after deposition of Jurassic – Lower Cretaceous succession as well, but before the deposition of Senonian rocks.

The section is situated in the core of the mid-Cretaceous Sümeg-Devecser syncline, and it is subparallel to the axis of the syncline. The Sümeg-Devecser syncline can be nicely seen in the perpendicular K-K' section (Fig.4.17). In contrast, no major middle Cretaceous contractional structures are visible on this section. However, minor thrusts and

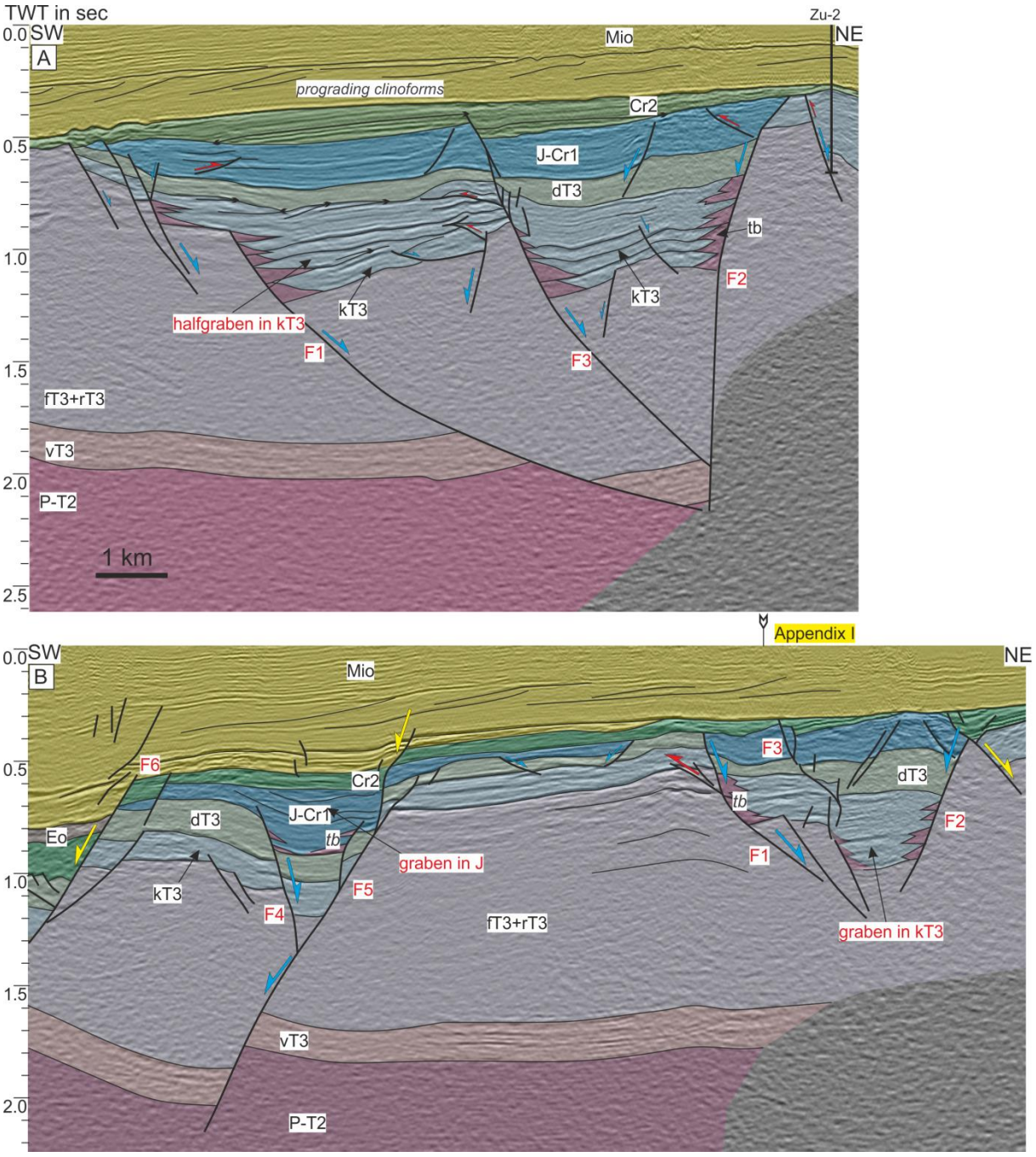

Fig. 4.11: (a) Interpretation of A-A' section (b) Interpretation of B-B' section. For location see Fig. 3.1. P-T2: Permian to Middle Triassic; vT3: Veszprém and Sándorhegy Fm., fT3 and rT3: Hauptdolomit and Rezi Dolomite, kT3: Kössen Fm., dT3: Dachstein and Kardosrét Fm., J-Cr1: Jurassic to Lower Cretaceous; Cr2: Senonian (Upper Cretaceous); Eo: Eocene; Mio: Miocene; tb: talus breccia.

related folds occur in the pre-Senonian rocks (Fig.4.11a). It is interesting, that these structures are localized along the above described faults (F1-3). In the case of F1 and F2, antithetic small thrusts developed in the proximal hanging-wall of the faults within the Jurassic –Lower Cretaceous succession. Above / near the F3 fault, on top of a small horst small double-verging thrusts developed in the Kössen Marl, which made a gentle anticline in the Dachstein – Kardosrét Limestone. These compressional structures are sealed by Senonian deposits.

4.2.3. B-B' section

The NE-trending section is running parallel to the previous section, therefore, their structures can be correlated. The same pre-Senonian extensional graben can be traced on the northeastern part of the section as in section A-A', but it is much narrower there (Fig. 4.11b). The graben shows more symmetric geometry compared to the previous section. F2 seems to be cut by a younger NE dipping fault, which has an off-set on Senonian, but it is sealed by Miocene deposits (Fig. 4.11b). The Dachstein and Kardosrét Limestone gradually get thicker towards F2, which is well illustrated on this section. On the southwestern part of the section another probably Jurassic graben is enclosed by F4 and F5 (Fig. 4.11b). The Kössen, Dachstein and Kardosrét Formations do not have any thickness changes related to these faults. On the other hand, the Jurassic – Lower Cretaceous succession is thicker in the graben, and reflections of this seismic unit seals F4 fault. Base Senonian and Miocene is dissected by F5 fault, however, it shows significantly larger pre-Senonian offset (Fig. 4.11b).

Small normal faults are visible on the horst between F5 and F1 faults. These faults cross cut only the Dachstein and Kardosrét Limestone, and they probably detach on the Kössen Marl. These structures possibly bound a large slide unit (Fig. 4.11b).

The section is also running in the core of the mid-Cretaceous Sümeg-Devecser syncline, and it is subparallel to its axis. Therefore, no major mid-Cretaceous contractional structures are visible on this section, similarly to the previous section. A small reverse fault is running across the footwall of F1 fault.

Thicker Senonian and Paleogene strata are visible on the hanging wall of F6. The Middle Miocene succession is also thicker on the southwestern side of F6 (Fig. 4.11b). Small fault segments are emerging up to the Upper Miocene (Pannonian) succession.

4.2.4. Regional composite section

This E-W trending zig-zag composite section (Appendix I) is situated W of the Keszthely Hills (Fig. 3.1). The section is composed of 2D and slices of 3D seismic data (Block A and C). The section has two segments, which lack any seismic data, there the interpretations (F13; F7; F8; F6) were projected from neighboring/adjacent, parallel seismic sections (Fig. 3.1, Appendix I). A short segment of the section is described in details in the previous section (chapter 4.2.3).

One of the main characters of this section is that the pre-Miocene formations are in deeper and deeper position westward, thus they form a half graben (Appendix I). This half graben, which is filled up by Miocene sediments, is developed in the hanging wall of the Baján detachment fault (Fodor et al. 2013a). The Koralpe-Wölz nappe system and the Transdanubian

Range have a tectonic contact along this important fault zone (Fodor et al. 2013a). In the footwall of the Baján fault reflections presumably image the probably extension-related foliation (Appendix I); similar fault-parallel package was observed and interpreted along the Rechnitz detachment by Tari et al (1992) and Tari (1994).

As it was mentioned, the base Miocene horizon is deepening stepwise west-ward, due to mostly SW dipping Miocene normal faults (F5; F6; F7; F8; F12). Nevertheless, NE-dipping Miocene faults also occur (Viszák fault; F13; F10). Fault F6 shows strange "N"-shaped intersection, due to the fact that the more or less flat fault plane is cut three times by the zig-zag section (Appendix I), creating such strange apparent geometry. Senonian and occasionally Eocene deposits occur in the hanging-wall of some of these faults (F10; F8; F6). In contrast, other faults are sealed by Senonian or the offset of pre-Senonian horizons is larger, than the post-Senonian movement (F12; F11; F5; F1).

The Cretaceous compressional structures are outlined mostly based on the reflections of the Carnian Veszprém Marl (Appendix I). These compressional structures are represented by broad anticlines, synclines and thrusts, which are discordantly sealed by Senonian deposits.

The Sümeg-Devecser syncline appears in the eastern segment of the section. In the core of the syncline the reflections of the Kössen Marl and the Jurassic – Lower Cretaceous succession are visible, and are unconformably covered by Senonian strata (Appendix I). The syncline is probably narrower than imaged, while the NE-SW trending segment of the section is running parallel to the Sümeg-Devecser syncline (this part overlaps with B-B' section). The syncline is outlined based on deeper reflections, such as the reflections of Veszprém Marl and even the Variscan unconformity.

The Sümeg-Devecser syncline is probably bounded from the east by the enigmatic Héviz thrust, which is mapped mostly based on well data (Fodor et al. 2013a). According to the cited work, the Hévíz thrust is N-S striking. Carnian Veszprém Marl and Sándorhegy Fm. were drilled by Hévíz K-25 and Hév-6 wells in the eastern side of the fault, whereas Norian Hauptdolomit and Rezi Dolomite are reached by Nemesbük Nb-2 and Szentgyörgyvár Szgy-1 wells in the western side of the fault. The enigmatic west-vergent thrust should appear on the easternmost edge of the seismic section. Unfortunately, it is not visible due to the poor quality of the section edge. Despite this fact, I illustrated its postulated geometry.

The Sümeg-Devecser syncline is bordered from the west by the Pölöske anticline. It is well visible, that the Variscan unconformity is tilted toward west on the western limb of the anticline. Consequently, the pre-Variscan basement is involved in this folding (Appendix I). The thickness of the Permian to Middle Triassic succession is 0.4 sec on the western limb, while

under the core of the Sümeg-Devecser syncline the thickness of the same series reaches 0.8 sec thickness (Appendix I).

Reflections of Carnian Veszprém Marl dip steeply toward west in the easternmost edge of the 3D slice (block C), therefore, I suggest that this segment also represents the western limb of the Pölöske anticline. Due to the western dip of Veszprém Marl, it is emerging eastward close to the base Senonian surface. Nevertheless, Well E drilled younger sediments under Senonian deposits (Rhaetian Kössen Marl) within the segment of sesimic data gap between the eastern and middle segment of the composite sections (Appendix I). Therefore, I propose the presence of a NE dipping F9 normal fault, along which Kössen Marl in the hanging wall is down-faulted beside Veszprém Marl in the footwall. F9 fault is covered by Senonian based on well data (e.g. Well D, E and F), therefore, I propose that F7 and F8 faults, which deform Senonian and Miocene rocks, cross-cut the F9 older structure.

West of the Pölöske anticline the Nagylengyel syncline is outlined based on the reflection of Carnian Veszprém Marl. In the core of the syncline thin, eroded beds of the Kössen Marl was drilled by several wells (e.g. Well D), however, the quality of seismic does not allow to interpret the base of this formation. The Nagylengyel syncline is the trailing syncline of the west-vergent Nagylengyel thrust. The Nagylengyel thrust is nicely visible based on the displaced/repeated reflections of the Carnian Veszprém Marl (Appendix I). The thrust has a sub-horizontal flat segment at the base of the Carnian Veszprém Marl, then emerges upward along a footwall ramp. The geometry of this thrust is described in details in the next chapter. There is a NW-trending extensional horst between faults F12 and F11, west to the Nagylengyel thrust. Carnian Veszprém Marl is cut by F11 fault, on the other hand, the fault is covered by Miocene. Fault 12 has a significant offset on the base of the Miocene succession, although the fault must have an older activity, since the separation of the Veszprém Marl is bigger, than that of the base Miocene horizon.

In the western part of the section the Permo-Triassic succession gently dips toward the east under the west-dipping base of Miocene horizon, which may represent the eastern limb of a next anticline. In the westernmost part of the section, small patches of Senonian is drilled by wells (e.g, well B and C). Separation of this Upper Cretaceous succession from Miocene is problematic here based on seismic data, therefore, I gave an uncertain interpretation for the top of Senonian in this part of the section. Due to the discordancy, gradually older and older Mesosoic rocks can be seen under the base-Miocene or base-Senonian denudation surface on the western part of the section. Well C reached Middle Triassic rocks, Well B reached Lower Triassic succession. Well A reached 300 m thick mylonitic shear zone (Lelkes-Felvári et al. 2002) which represents the Baján detachment fault itself (Fodor et al. 2013a).

4.2.5. 3D Geometry of the Nagylengyel thrust

4.2.5.1. Aim of detailed description

The Nagylengyel thrust and the extensional horst, which is situated west of this structure are mentioned in the description of regional composite section (previous chapter). The Nagylengyel thrust is situated in the 3D seismic block C, which has the best quality in the study area. On the basis of this modern 3D seismic block description of detailed 3D geometry of the Nagylengyel thrust is possible. In this chapter, I describe the Nagylengyel thrust and its relation to the extensional horst bordered by F12 and F11 faults, based on four oblique vertical slices of the 3D block (Fig.4.12a-d).

4.2.5.2. C-C' section

This northernmost ENE-WSW striking section is running subparallel to the regional composite section (Appendix I.). Consequently, a very similar geometry is outlined (Fig.4.12a). Reflections of the Carnian Veszprém Marl and the base of Miocene are down-faulted by the SW-dipping F12 normal fault in the western part of the section. The dissected Veszprém Marl shows larger offset, than the dissected Miocene strata. The NE-dipping F11 fault normal fault crosscuts the Veszprém Marl, however, it is sealed by Miocene, or the base Miocene is just slightly deformed by this fault (Fig.4.12a). The Nagylengyel thrust is outlined based on the reflections of the Veszprém Marl. The Veszprém Marl thrust onto the Hauptdolomit along the footwall ramp of the Nagylengyel thrust. This structure continues toward east with a flat segment, at the base of Veszprém Marl. The thrust shows WSW-vergency in this section, with an approximate 1 km of horizontal offset. The tilted Veszprém Marl in the hanging is discordantly covered by Senonian deposits (Fig.4.12a). This Upper Cretaceous succession is present only in the hanging wall of the NE dipping F10 normal fault. The base of Miocene is also dissected by F10 fault, which runs downward probably along the base of Hauptdolomit.

4.2.5.3. D-D'' section

This NE-SW striking section is situated south of the previous described one. In this section thin remnants of the Upper Cretaceous succession were drilled by Wells I and J, both in the hanging wall and footwall of F12 normal fault (Fig.4.12b). F12 fault has a more remarkable off-set on the reflection of Veszprém Marl, than on the base of Senonian. F11 fault has a more pronounced displacement on the Veszprém Marl compared to the previous section.

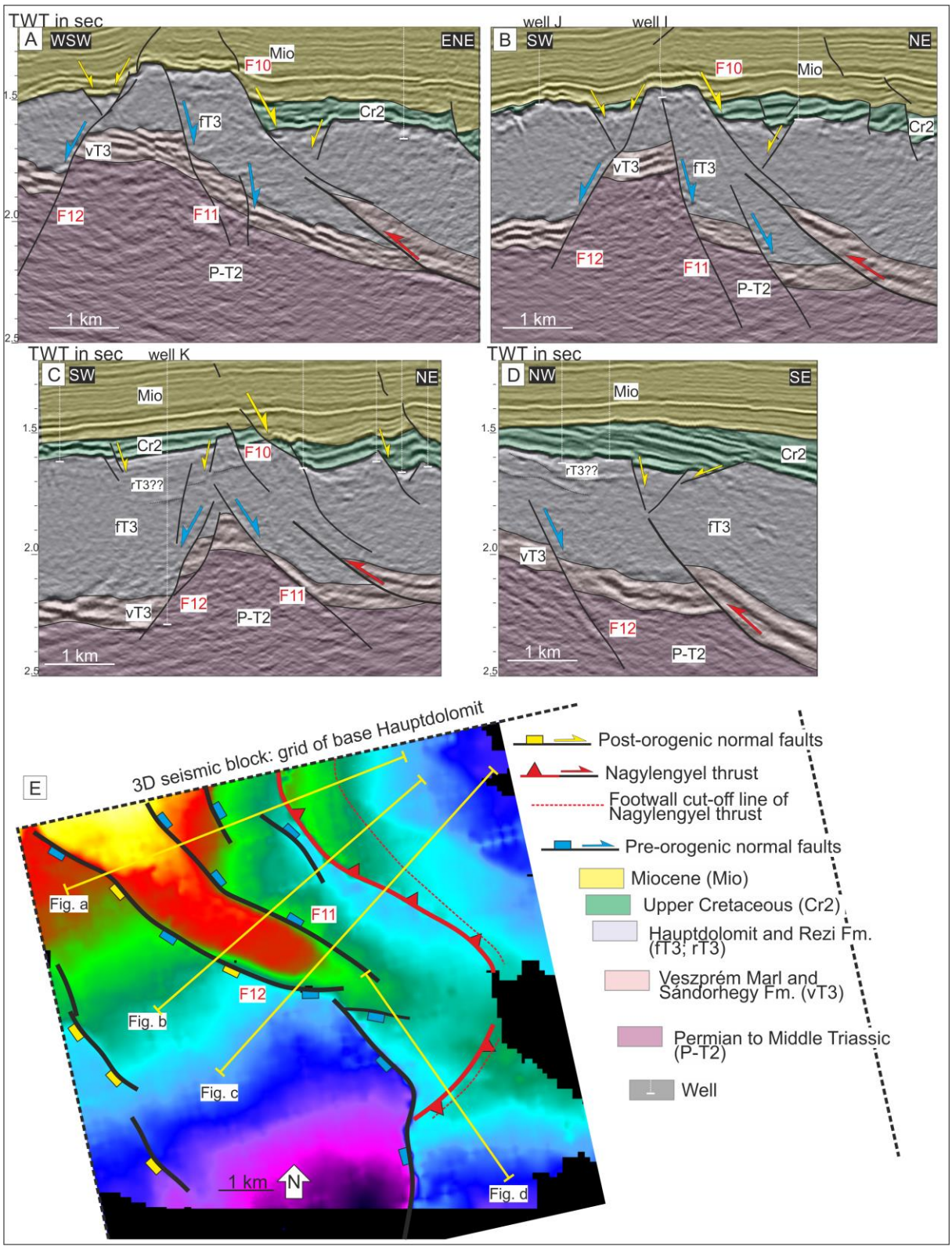

Fig.4.12: Interpretation of C-C' (a); D-D' (b); E-E' (c); F-F' (d) slices of 3D seismic block C. (e) Time-depth map of the base Hauptdolomit horizon in the northwestern part of 3D seismic block C.

This fault is probably sealed by erosional remnants of Upper Cretaceous strata in this section (Fig.4.12b). The Nagylengyel thrust has a very similar geometry as in the previous section, but it is situated much more close to F11.

4.2.5.3. E-E' section

This NE-SW trending section is situated further southeast, and parallel to the previous section. Pale reflection appears in the thick body of Upper Triassic Dolomites (Fig.4.12c). Based on well K, this reflection represents most probably the base of Rezi Dolomite (Fig.4.12c). F12 fault has minor off-set on the base-Senonian in this section, however, the Hauptdolomit, is significantly thicker in the hanging-wall, than in the footwall. F11 is covered by the reflection of base-Rezi Dolomite. The Nagylengyel thrust is present in this section as well, however, its horizontal displacement (500 m) is smaller, compared to the previous sections.

4.2.5.4. F-F' section

This southernmost, NW-SE striking section is running perpendicular to the previous ones. The F12 normal fault is visible on the northwestern edge of the section (Fig.4.12d). The fault has minor off-set compared to previous sections. The Nagylengyel thrust can be observed in the hanging wall of F12 fault. The Nagylengyel thrust is seemingly NW-vergent here, and its horizontal displacement is only 200 metres (Fig.4.12d).

4.2.6. G-G' section

The E-W section derives from the 3D seismic block B (for location see Fig. 3.1.). The base of Miocene is significantly dipping towards the west, similarly to the regional composite section (Appendix I). The base Miocene horizon is cut by only one normal fault (F16). The tilting of Miocene strata is related to the activity of Baján detachment fault (Appendix I). Timing of this tilting is possible based on offlap and onlap surfaces, which occur in the lower part of the Miocene succession (Fig. 4.13).

There is a thin Senonian succession under the Miocene in the eastern part of the section. The Upper Cretaceous succession is truncated, and pinches out westward.

Under the base-Senonian horizon, the non-reflective unit of the Hauptdolomit and relatively strong reflections of the Carnian Veszprém Marl can be seen. The pre-Senonian reflections are horizontal or dipping gently toward the east. Taking into account the significantly westward tilted base of Miocene, the today quasi-horizontal pre-Senonian strata were east dipping below the "back-tilted" or flattened base-Miocene. The Veszprém Marl and the Hauptdolomit are imbricated by the west-vergent F14 thrust. The thrust has a flat segment at the base of Carnian Veszprém Marl (Fig. 4.13), then it emerges up to the base-Senonian reflector, which

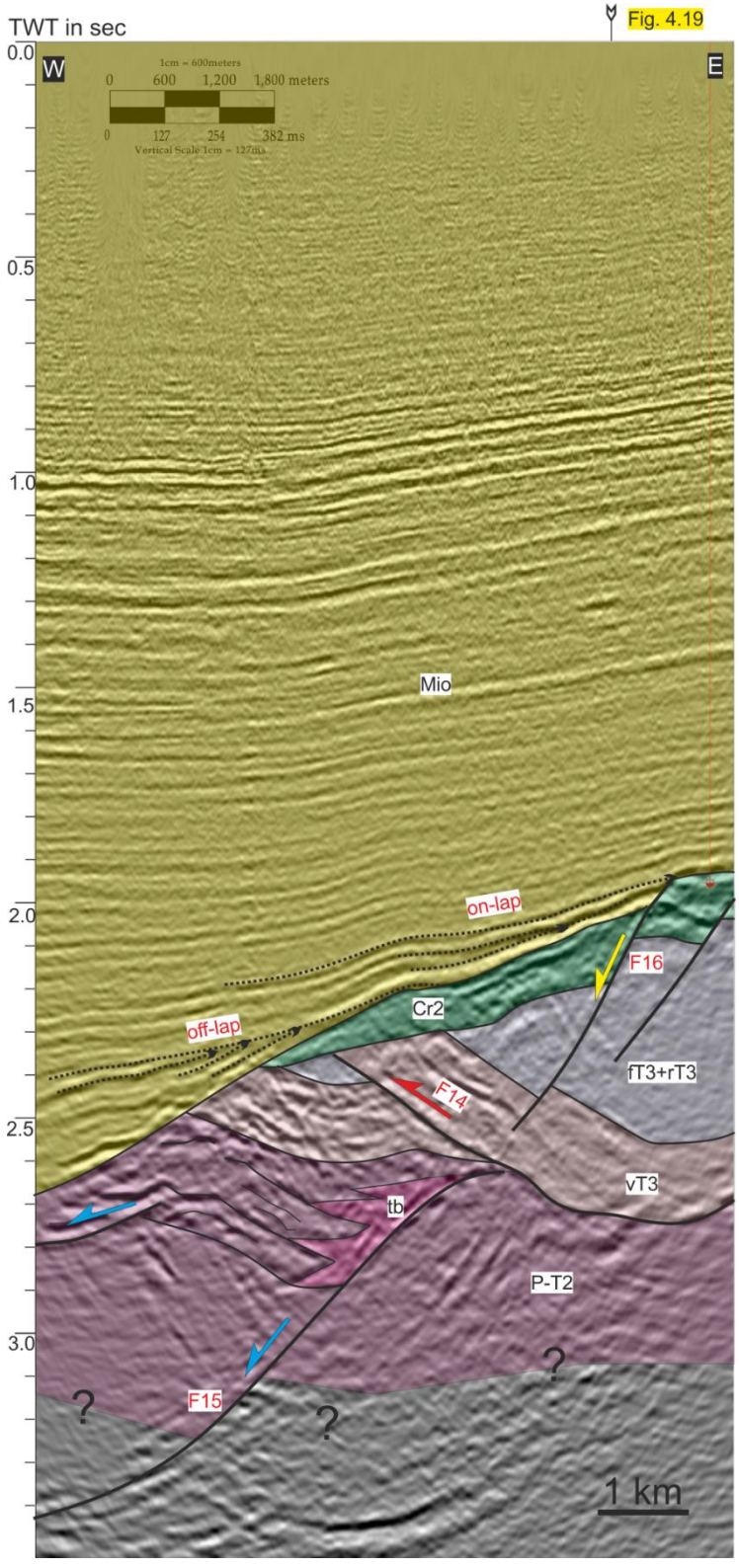

Fig. 4.13: Interpretation of G-G' slice of 3D seimic block B. For location see Fig. 3.1.

discordantly covers the F14 thrust. In the footwall of F14 thrust the Veszprém Marl and a thin eroded slice of Hauptdolomit can be seen.

A strong steeply west-dipping reflection is running down from the footwall cut-off point of F14 thrust. I interpreted this reflection as a normal fault (F15), which is truncated by F14 thrust. The seismic facies on the two side of F15 are strongly different. The footwall of F15 is non-reflective under the Carnian Veszprém Marl. In the hanging-wall of F15, there are several strong reflections which fade away approaching F15. Wedge-shape bodies are interpreted as talus cone breccia (Fig.4.13).

4.2.7. H-H' section

The E-W section derives from the 3D seismic block C (for location see Fig. 3.1). The base of Senonian is strongly dissected by several normal faults (Fig.4.14). Some of these faults

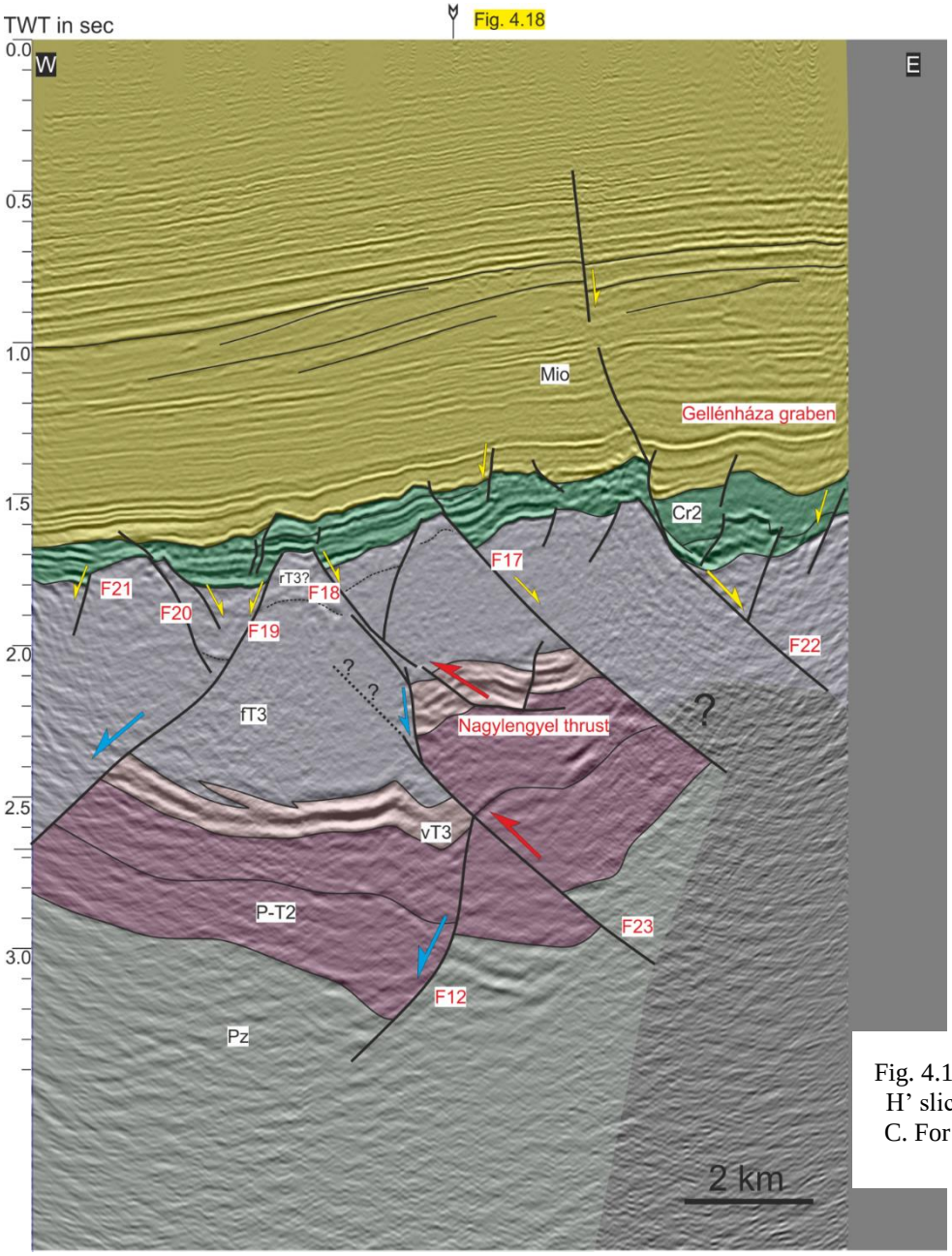

Fig. 4.14: Interpretation of H-H' slice of 3D seimic block C. For location see Fig. 3.1.

are sealed by intra-Senonian reflections (e.g. F21; F18). In the hanging wall of F17 a half graben developed, the Senonian infill of this half graben is thinning away from the fault. In the eastern part of the section fault F22 represents the southeastern boundary of the Gellénháza graben. The Senonian is thicker in the graben as in the footwall of F22. At several cases, faults have minor offsets on the base of the Miocene (F20; F17; F22). These Miocene reactivations are often accommodated by an individual fault segment. Fault segments cut up high into the Upper Miocene (Pannonian) succession above F22 (Fig.4.14).

Below the Senonian, the non-reflective seismic unit of the Hauptdolomit and Rezi Dolomite is visible. A single pale horizon between F17 and F20 may represent the base of the Rezi Dolomite, indicated by dashed grey line on Fig.4.14. The strong reflection of the Veszprém Marl can be traced under the Hauptdolomit. In the western part of the section the upper reflection of the Veszprém Marl is gradually disappearing westward. I interpreted this geometry as the interfingering of the overlying dolomite and the Veszprém Marl – Sándorhegy Formation. In the middle of the section the repetition of the Carnian Veszprém Marl is well visible, which suggests an east-dipping thrust (F23). On the other hand, the geometry of the Permian-Middle Triassic seismic unit and an intra-Triassic horizon suggests a west-dipping normal fault. In addition, the termination of the Veszprém Marl is not along the F23 thrust fault, but along a presently vertical fault, which I interpret as the higher segment of fault F12. This normal fault represents the southern N-S trending continuation of F12 introduced earlier on the regional composite section (Appendix I). According to my interpretation, the F12 fault is dissected by F23 thrust. Both structures are sealed by Senonian.

In the hanging wall of F12 an anticline – syncline pair can be traced based on the reflection of Carnian Veszprém Marl. In the hanging wall of F23 thrust the southern segment of the Nagylengyel thrust occurs, which slightly displaces the reflection of the Carnian Veszprém Marl (Fig.4.14). Based on fault mapping, and a perpendicular section M-M' (Fig. 4.18), the Nagylengyel thrust is NNW-vergent here, thus the section cuts it obliquely. However, the small displacement can suggest a near tip point location along the Nagylengyel thrust.

4.2.8. I-I' section

This slice of the 3D seismic block C is running parallel to the axis of the Bak-Nova graben. A very important feature of this section is the total lack of normal faults crosscutting the base-Miocene (Fig.4.15). The Miocene strata are onlapping on the denudation surface of the top-Paleogene horizon. The thick Paleogene and Senonian successions are cut by only few normal faults (e.g. F39). It seems that there is no pronounced angular discordance between the Paleogene and Upper Cretaceous (Fig.4.15).

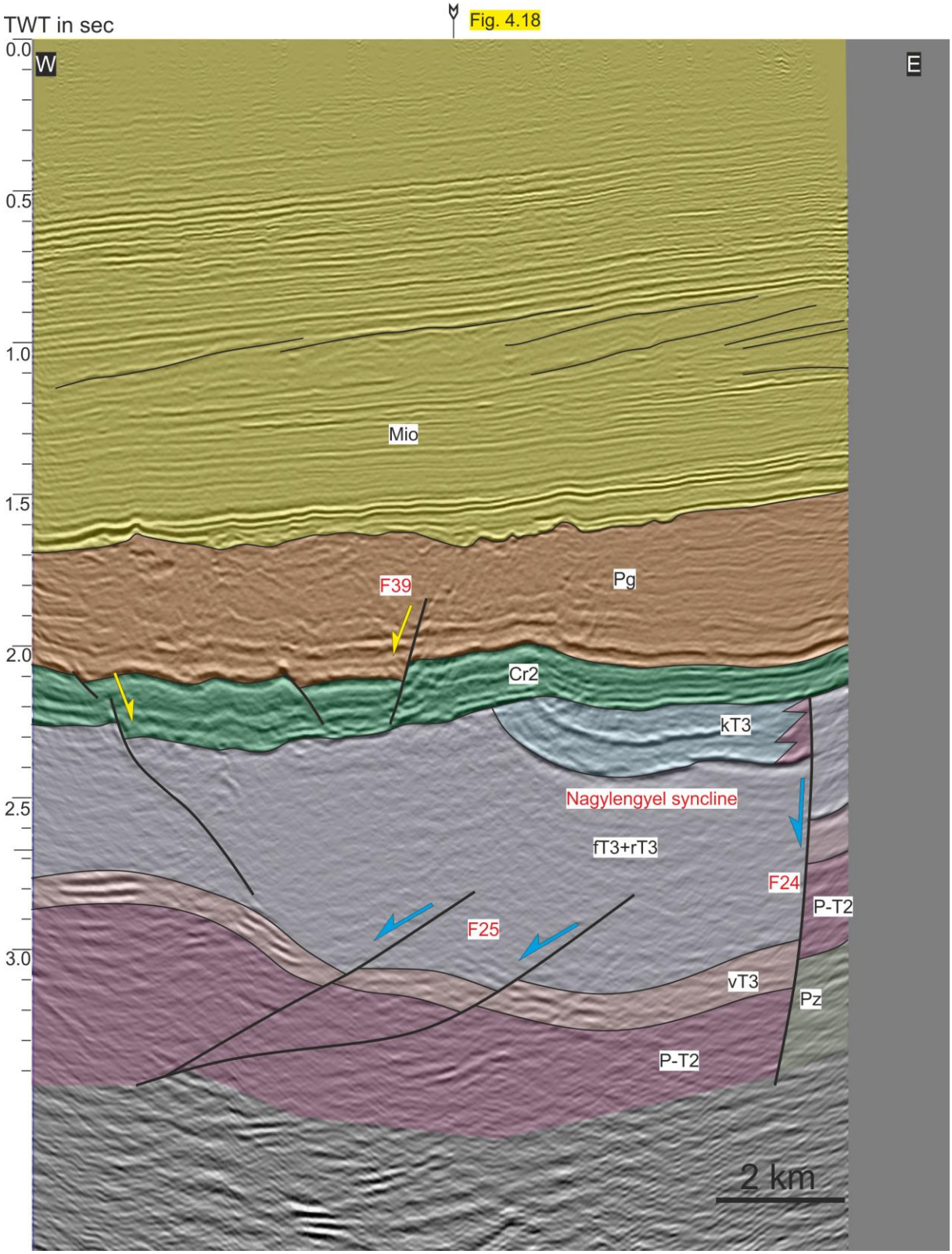

Fig. 4.15: Interpretation of I-I' slice of 3D seimic block C. For location see Fig.3.1.

On the other hand, the Senonian is discordantly overlying the folded Triassic rocks. The Nagylengyel syncline is nicely outlined based on the reflection of the Kössen Marl. The syncline can also be recognized based on the reflections of the Veszprém Marl under the non-reflective Hauptdolomit (Fig.4.15). The Hauptdolomit is thickening westward in the hanging-wall of tilted normal faults (F25 fault set). A normal fault sealed by Senonian is visible in the

eastern edge of the section (F24). Poorly imaged wedge-shape bodies in the Kössen Marl are interpreted as talus breccia cones in the hanging wall of F24 (Fig.4.15).

4.2.9. J-J' section

This 2D seismic line is running parallel to the axis of Bak-Nova graben. The Miocene is separated from the thick Paleogene succession with a gentle angular discordance surface. There is apparently no angular discordancy between Senonian and the Paleogene strata. Similar to the I-I' section, this section also lacks any normal faults in the Upper Cretaceous – Cenozoic succession (Fig. 4.16).

The southernmost continuation of Nagylengyel syncline can be seen under the base of Senonian. An important east-dipping normal fault is crosscutting the syncline, the fault is sealed by Senonian. I correlate this fault with the enigmatic F9 fault of the regional composite section (Appendix I). Kössen Marl and probably pale reflection of Rezi Dolomite is visible on the footwall side of F9 fault. In the hanging-wall strong reflections of Kössen Marl and moderately pronounced Jurassic succession can be seen with the thin, non-reflective Dachstein – Kardosrét Limestone intercalated between them. This succession is drilled by Well L (Fig.4.16).

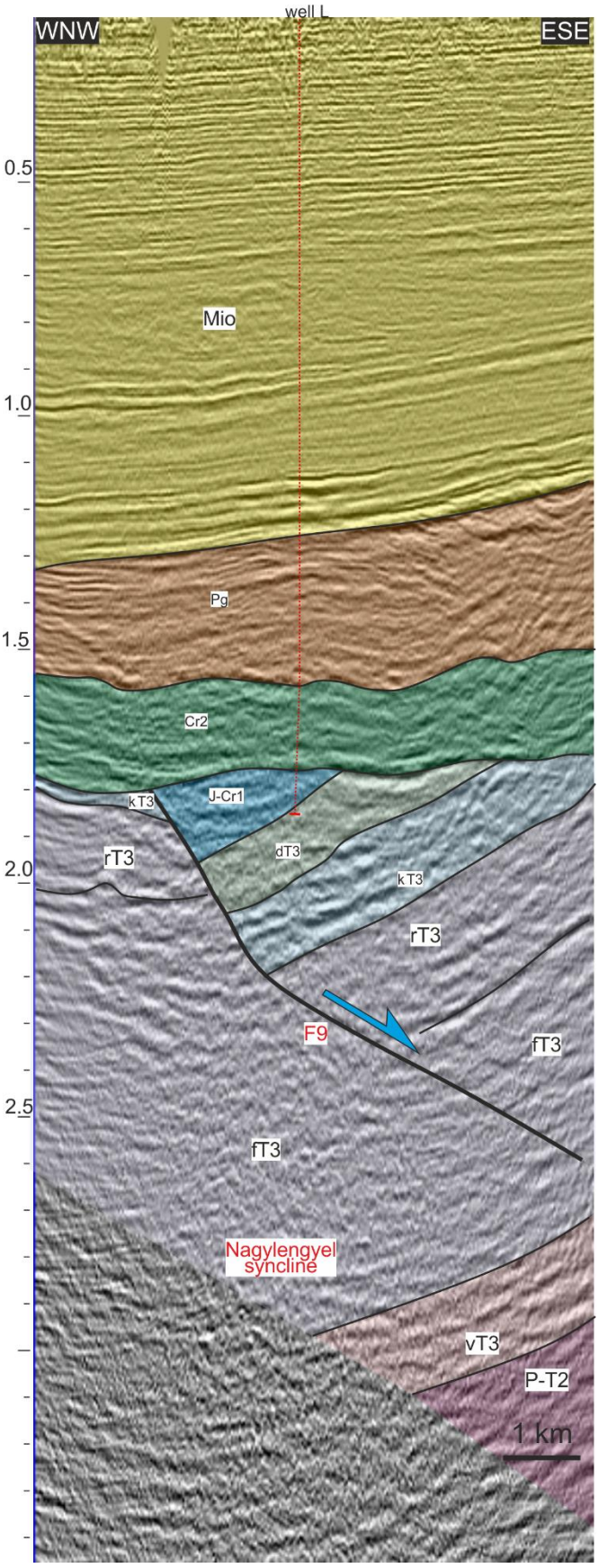

Fig. 4.16: Interpretation of J-J' seismic section. For location see Fig. 3.1.

4.2.10. K-K' section

This NW trending 2D seismic section is situated in the northwestern foreland of the Keszthely Hills (Fig.3.1). It is more or less perpendicular to the Sümeg-Devecser syncline, which is described by several authors (e.g., Tari 1994, Tari 1995). The syncline is outlined by the reflections of the Kössen Marl, and it is discordantly covered by Senonian strata (Fig. 4.17).

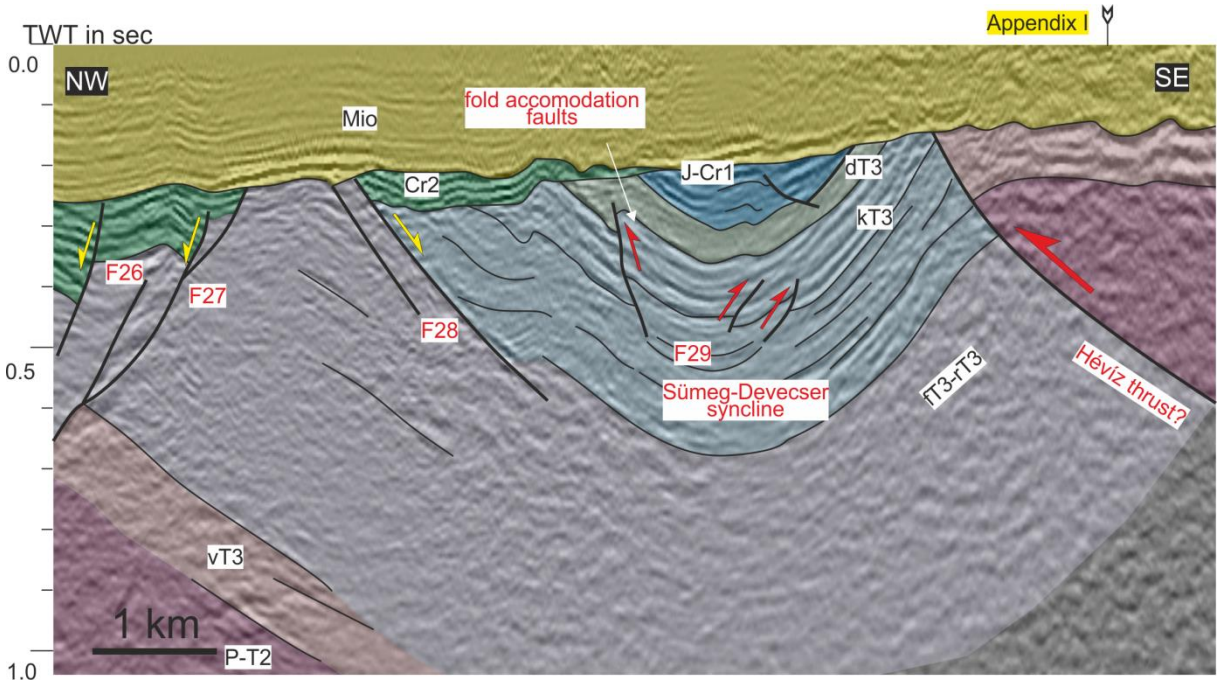

Fig. 4.17: Interpretation of K-K' seismic section. For location see Fig. 3.1.

On the NW limb of the syncline pale reflections of the Carnian Veszprém Marl occur below the non-reflective Hauptdolomit – Rezi Dolomite unit. The Sümeg-Devecser syncline is bounded from the east by the enigmatic Héviz thrust; which was generally postulated by well data (e.g., Fodor et al. 2013a). Here, the non-reflective hanging wall is in strong contrast to reflective footwall, thus the thrust can be fairly well documented on this seismic section.

In the core of the syncline minor internal compressional structures can be observed, which are also covered by the Senonian sequence. Steep NW- and SE-vergent thrusts crosscut the Kössen Marl in the core of the Sümeg-Devecser syncline (F29 fault set). These thrusts have a downward decreasing off-set, and they do not cut across the pale upper reflections of the Hauptdolomit – Rezi Dolomite unit. In the core of the Sümeg-Devecser syncline a small anticline is visible on the basis of Jurassic reflections (Fig.4.17). A less visible structure occurs slightly northwestward, where reflections of the Kössen Marl seems to depict an asymmetric northwest-vergent anticline. The relationship of this fold to an axial-planar thrust fault, similar to previous examples, is not obvious on the seismic data. The western limb of the Sümeg-Devecser syncline is dissected by a number of faults, which have normal offsets on the base of Senonian (F26; F27; F28 on Fig.4.17). These structures area sealed by Miocene deposits.

4.2.11. L-L'—Kapolcs–Balatonszepezd section

This combined section is composed of the WNW-ESE trending L-L' 2D seismic section and the Kapolcs – Balatonszepezd geological section (Appendix II), which was constructed based on surface data (using the map of Budai et al. 1999b) and wells. I made a simple time-depth conversion on L-L' seismic section in order to connect it to the surface data. I calculate with 6500 m/sec velocity in the case of pre-Senonian basement (for more detailed explanation see chapter 3.5.).

The Upper Cretaceous, Paleogene and Miocene successions are relatively thin, therefore, they were interpreted on seismic as one merged unit (Appendix II). This Upper Cretaceous – Miocene succession is bounded to the southeast by F30 normal fault. In the Balaton Highland, thin Miocene deposits and Mio-Pliocene basalt are discordantly lying on Triassic succession, without any significant faults (Appendix II).

The Permian to Lower Cretaceous succession is relatively strongly deformed by folds and thrusts. These compressional structures are discordantly sealed by the Upper Cretaceous – Cenozoic succession. I describe the related compressional structure one after another from west to east.

In the westernmost part of the section the Sümeg-Devecser syncline is outlined based on the reflections of Kössen Marl —Jurassic–Lower Cretaceous succession in its core. In depth, the syncline can be imaged by the reflections of Carnian Veszprém Marl as well (Appendix II).

The Sümeg-Devecser syncline is the trailing syncline of a SE-vergent thrust, which is situated east of the syncline. Hauptdolomit is thrusted over Kössen Marl by this thrust. The thrust has a well visible offset on Veszprém Marl, and it is running at the level of the base of Veszprém Marl. The thrust does not cut down in deeper stratigraphy. The thrust occupies the same structural position with respect to the Sümeg-Devecser syncline as the Bakonybél thrust of the northern Bakony (approximately 50 km to NE). Tari (1994) named this structure as Bakonybél thrust, and it was extensively confirmed by Kiss (2009). Despite the considerable distance, I suggest correlation of the thrust of the section with the Bakonybél thrust.

It is important to note, that the Bakonybél thrust does not continue into a flat décollement: The Veszprém Marl is folded into the Ajka anticline below the Bakonybél thrust. This anticline probably detaches above Paleozoic shales, since they are not involved in folding.

In the footwall of the Bakonybél thrust the westernmost termination of the Tés-Halimba syncline can be recognized with Kössen Marl in its core (Appendix II). The eastern limb of this syncline emerges steeply southeastward, while it is flattened further to the southeast. The Sümeg-Devecser and the Tés-Halimba synclines are not outlined by the reflections of the Variscan unconformity, as two individual synclines. These deep reflections show only one

broad syncline which is referred as Bakony syncline in this work. The Tés-Halimba and the Sümeg-Devecser ssynclines are sitting in the core of the Bakony syncline. Similar geometry was proposed already by Tari (1994), which is confirmed by the present section.

The SSE-vergent Litér thrust is situated further to the east of this flat segment, and it duplicates a considerable part of the Triassic succession. In this section, Middle Triassic Iszkahegy Limestone juxtaposes Norian Hauptdolomit at the surface. Similar to many other authors (e.g. Dudko 1996; Csicsek 2015), I propose that the Litér thrust has a horizontal décollement within the Variscan shales. There is a hundred-meter scale small syncline in the hanging-wall of Litér thrust. According to my opinion, this second-ordered fold can be related to internal flat segments of the Litér thrust in the level of Iszkahegy Limestone (iT2). The second order fault-bend fold is the result of complex flat-ramp-flat-ramp-flat geometry of the Litér thrust (Appendix II).

The Permian emerges to the surface in the southeastern edge of the section, in the core of an anticline. According to my opinion this anticline represents the Velence anticline, which was described by Balla & Dudko (1989).

The Veszprém Marl provides strong reflections in the hanging wall of the Bakonybél thrust, whereas in its footwall it can be traced hardy by pale/weak reflections. In my view this difference can be explained by the interfingering of Carnian basinal and coeval platform deposits. Such interfingering is widespread on surface, and documented by Haas & Budai (1999). Wells Sz-710 and Kapolcs-27 drilled Carnian platform formations (Budaörs Dolomite) at the hanging wall of Litér thrust, whereas Budai et al. (1999b) mapped Veszprém Marl in the footwall of the thrust.

One of the most important aspects of this section is that the deep reflection data from the Southern Bakony can be correlated to surface data of the Balaton Highland. The time-depth converted thickness of non-reflective unit below the strong reflection of the Veszprém Marl at the eastern part of L-L' section is approximately 1.5 km thick. This is equal to the thickness of Permian to Middle Triassic succession exposed on the northwestern limb of the Velence anticline (Appendix II). Consequently, this section provides a good evidence for one of my basic assumptions, that the lowermost strong reflection package far below the Veszprém Marl represents the contact of Paleozoic shales and Permian sandstone. Note, this Permian to Middle Triassic seismic unit has no uniform thickness based on L-L' seismic section, since it is significantly thicker in the hanging wall of F31 normal fault (Appendix II).

4.2.12. M-M’ section

This NNW-SSE trending section is a slice of 3D seismic block C. This section exhibit complex structures, which belong to several phases; I will describe them successively. A key-element of this section is the Petri fault, which is a sub-vertical fault in the center of the section. The fault cuts through the basal Miocene reflection. Probably, the Petri fault is responsible for

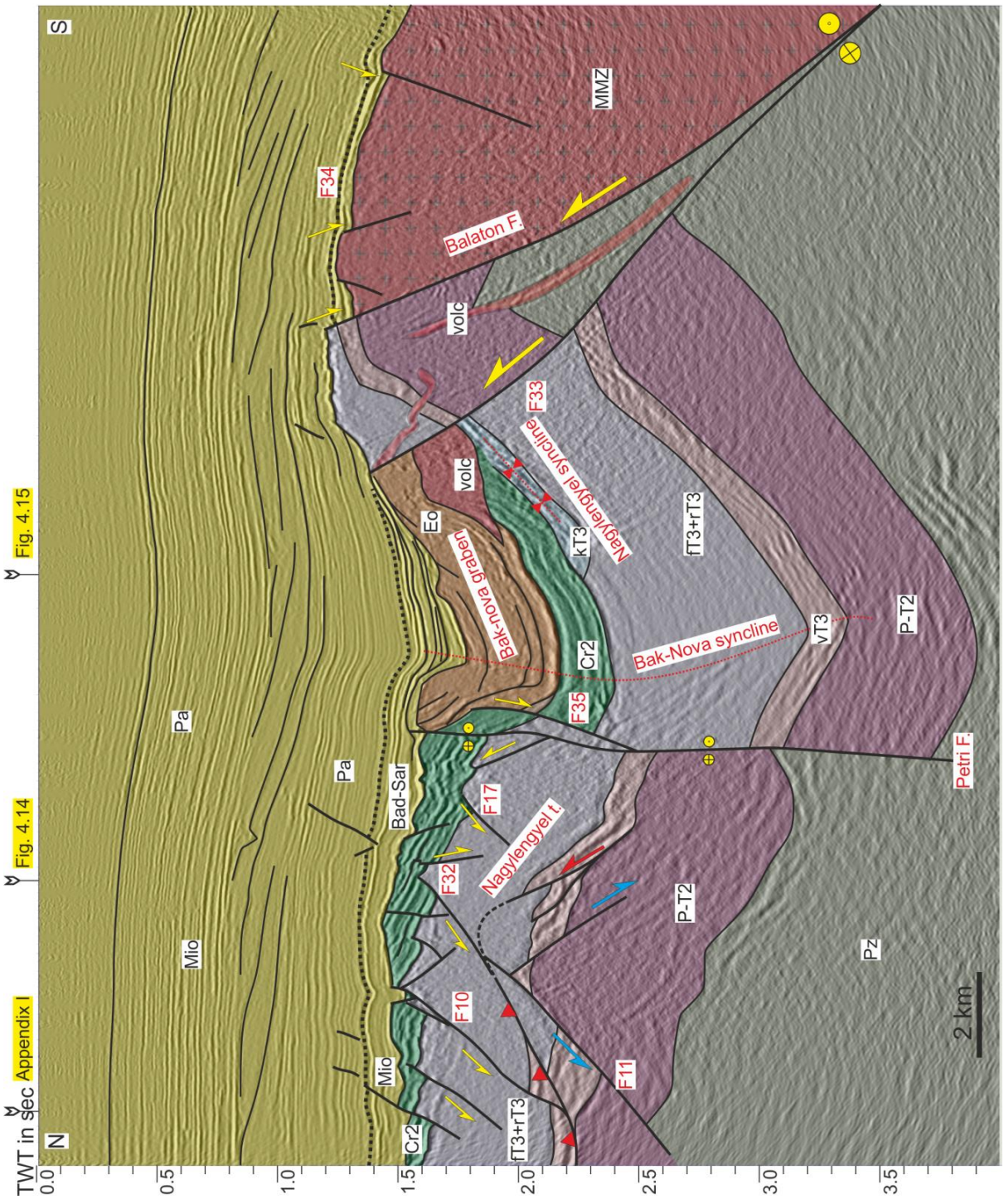

Fig. 4.18: Interpretation of M-M’ slice of 3D seismic block C. For location see Fig. 3.1.

the development of the antiform or dome-like structure in its southern side. Even Pannonian (Upper Miocene) horizons are deformed by this folding. As it will be demonstrated in chapter 4.3, the Petri fault is an important WNW-ESE striking dextral strike-slip fault.

North of the Petri fault several normal faults (e.g, F10) are crosscutting the base-Miocene horizon, which are well visible in the perpendicular slices as well (Appendix I, Fig. 4.14). In contrast, the area immediately south of the Petri fault lacks any normal faults in the Miocene succession, similarly to the perpendicular section (Fig. 4.15). South of the Petri fault the base of Miocene horizon is folded into an open syncline. Intra-Miocene / Badenian-Sarmatian horizons onlap onto the limbs of this syncline, consequently, this syncline can be considered as a growth syncline. South of this syncline, an anticline with complex internal structure follows. It is dissected by small-scale Miocene normal faults (F34 on Fig. 4.18).

The syncline immediately south of Petri fault appears in the underlying Paleogene sediments as well, with a larger amplitude. Therefore, the base Miocene is discordantly covers the truncated beds of Palogene succession. This geometry shows that repeated folding was active for a long interval, before and during the Miocene sedimentation.

The Paleogene succession is bounded from the south by the NNW-vergent F33 thrust, which juxtaposes Triassic and Paleogene formations. The F33 thrust is sealed by Miocene sediments. The Triassic reflections show a relatively narrow anticline which is bounded from the south by a non-reflective unit. This non-reflective unit is drilled by several wells, and the penetrated rocks represents the so-called “Magmatic-metamorphic-zone”, which consist of low-grade Palaeozoic metamorphic rocks and Palaeogene magmatic rocks (Jósvai et al. 2005). The steep fault which separates the Magmatic-metamorphic-zone from Triassic rocks is probably the Balaton fault (Fodor et al. 2013a).

The Paleogene formations are mostly restricted to the southern side of the fault F35, which is situated immediately south of Petri fault. The lower reflections of the Paleogene are dragged along F35, while the upper horizons onlap on these dragged strata. The F35 fault, which is a steep thrust in its recent geometry, represents the northern boundary fault of The Bak-Nova graben. The infill of this graben is characterized by Paloegene sedimentary succession, which laterally interfingers with volcano-sedimentary rocks (Körőssy 1988). The section exhibits several occurrences of Paleogene magmatic bodies, studied from petrological and geochemical point of view by Benedek (2002) and Benedek et al. (2004). A large cone-shaped body in the southern part of the section is interpreted as a complex volcano (‘volc’ on Fig.4.18). In its vicinity, strong, zig-zag-shaped reflections cutting through the reflections are interpreted as sub-volcanic dykes. A straight, string reflector just in the hanging-wall of F33 thrust is considered as conduit channel for the magma.

A number of normal faults dissect the southward tilted horizon of base-Senonian north of the Petri fault. These faults are sealed by inta-Senonian reflections (e.g, F32 and F17), and they represent tilted conjugate pairs with respect to the southward tilted Senonian succession (Fig. 4.18).

The pre-Senonian formations (e.g, Veszprém Marl) are also folded into a syncline, like the Senonian and Cenozoic succession. The angular discordance at the base of Senonian is not as pronounced as in the perpendicular sections (Appendix I, Fig 4.14, Fig 4.15). In the footwall of the F33 thrust the Kössen Formation depicts a small syncline eroded by the Senonian sequence. The small amplitude of this fold may suggest that this section cuts the fold near its termination, while map view permits its correlation with the Nagylengyel syncline. Different locations of fold axial traces clearly show that the pre-Senonian fold has been refolded by the large-amplitude Bak-Nova fold (Fig. 4.18).

On the northern side of the seismic slice, a strange intersection of the northern segment of the Nagylengyel thrust can be seen (Fig. 4.18). Above the F11 normal fault the Nagylengyel thrust is visible in strike, with a gentle apparent northward dip. From map view (Fig. 4.12e) and perpendicular sections (Figs. 4.12a-d) it is clear that this section is cutting obliquely the thrust with respect to its local strike; this explain its apparent northerly dip and its southerly vergency. South of F11 the southern NNW-vergent segment of the Nagylengyel thrust can be seen (for a map-view see Fig.4. 12e).

4.2.13. N-N' section

This NNW-SSE trending section is a slice of the 3D seismic block B. The section crosses the westernmost edge of the Paleogene Bak-Nova graben. Normal fault F36 represents the northern boundary of the graben here (Fig. 4.19). The Senonian succession and the lower part of the Paleogene are significantly dragged along F36. This drag is truncated by the base of the Miocene succession.

Late Triassic succession is thrust on Paleogene and Senonian infill of the Bak-Nova graben by a NNW-vergent thrust (F33). The two 3D volumes and intervening 2D lines permit the correlation of this thrust to F33 of the previous section (Fig. 4.18). These structures are sealed by Middle Miocene strata, however, on the southern part of the section already the Late Miocene strata onlap on the northward tilted (folded) denudation surface (Fig. 4.19). In the footwall of the F36 fault, steeply southward tilted reflections of the Veszrém Marl can be seen. Toward north, the Veszprém Marl jumps down along F37 fault. Based on 3D mapping, the F37 represents the southern boundary of west-vergent F14 thrust (see in perpendicular section G-G', Fig. 4.13); thrusting is transferred by this E-W trending vertical fault (F37). Displacement

along the F14 thrust cannot be seen in this section; it was mapped on the basis of the perpendicular G-G' section. This combined view suggests that the present section is strike-parallel to F14 thrust. While F37 is sealed by Senonian (Fig. 4.19.), the connected F14 should also have the same age, as shown on perpendicular section G-G' (Fig. 4.13).

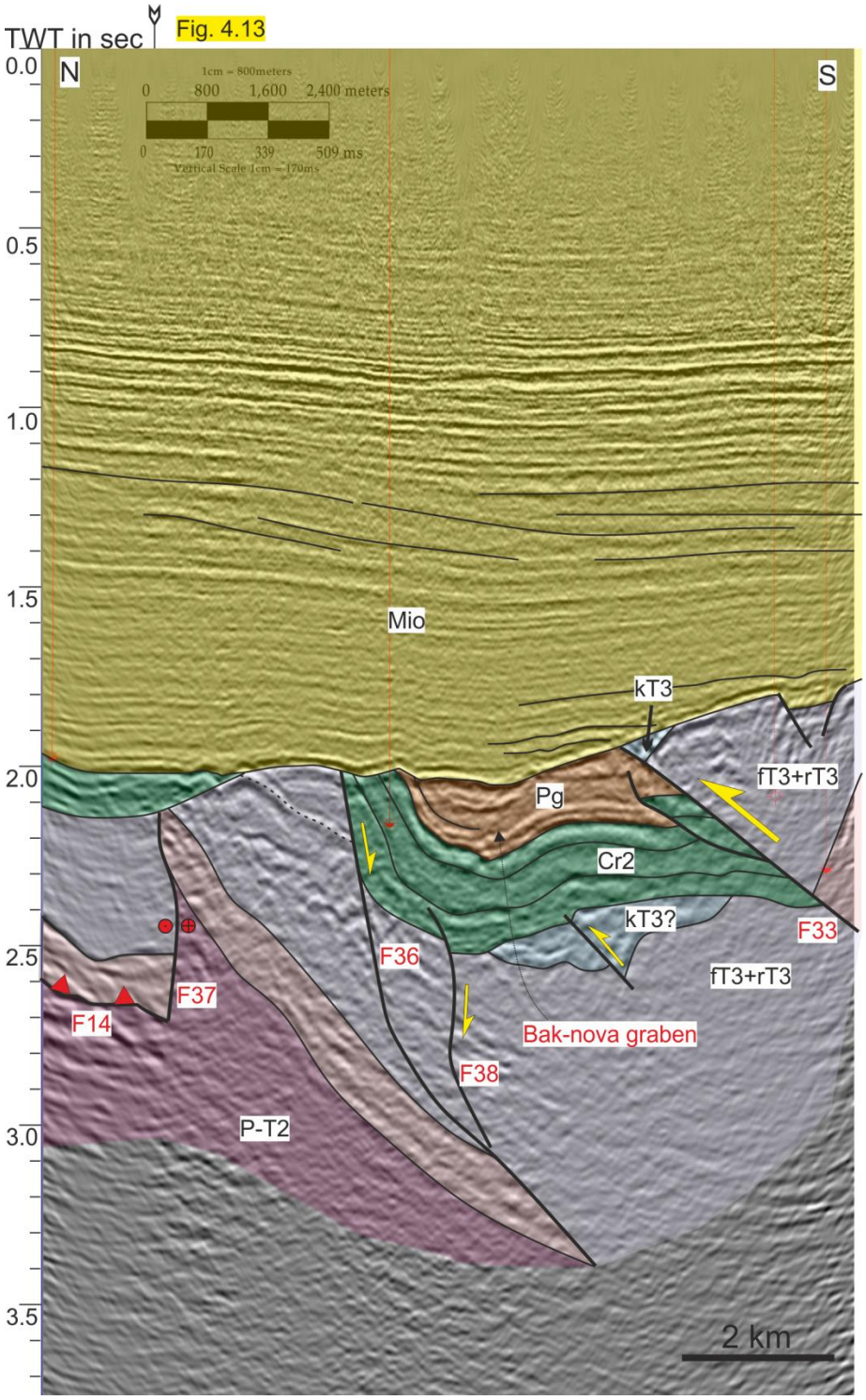

Fig. 4.19: Interpretation of N-N' slice of 3D seismic block B. For location see Fig. 3.1.

4.3. Map-view geometry of the structures of the Zala Basin

Pre-Senonian geological map (Appendix III.a) and depth map of the top pre-Senonian basement in TWT time (Appendix III.b) have been constructed based on 2D and 3D seismic data and well data indicated on Fig. 3.1. Of course, I was not able to introduce all the interpreted seismic sections of the study area, therefore, the maps are mostly based on that kind of data, which are not described in this work in details.

Most of the old normal faults and Cretaceous compressional structures are not visible on the depth map of the top pre-Senonian basement, since these structures are discordantly covered by Senonian. Faults which were active during and after the onset of Senonian sedimentation are nicely outlined.

Several indications (e.g. thickness-variation along fault) support that development of pre-Senonian normal faults of the study area preceded Cretaceous folding (See details in next chapter). These structures have generally NW-SE strike (e.g, F11, F12 on Fig.4.12; F9 on Appendix I, Appendix III.a and Fig.4.16; F2-5 on Figs.4.11a and b), although deviations from this strike occur. For example, F24 (Fig.4.15, Appendix III.a) and the southern continuation of F12 fault (Fig.4.14, Appendix III.a) are almost N-S striking, whereas F1 (Figs.4.11a and b, Appendix III.a) is approximately E-W striking.

Pre-Senonian folds strongly determine the position of the erosional remnants of Upper Triassic to Lower Cretaceous rocks. These formations appear only in the core of Cretaceous synclines, therefore, these formations outline the map-view geometry of these folds (Appendix III.a). Furthermore, folding of pre-exisiting normal faults resulted in strange map-view geometries. The NE-SW trending Sümeg-Devecser syncline of the Southern Bakony can be traced further southwest-ward in the western foreland of the Keszthely Hills. The syncline gradually changes its trend from NE-SW to NNE-SSW and finally N-S. The axis of the Sümeg-Devecser syncline terminated at the F2 fault, further northeast it steps eastward, where it is crossed by K-K' seismic section (Fig.4.17). On one hand, it is possible that this step is related to F2 fault, on the other hand, the two segments of the Sümeg-Devecser syncline may represent two individual en-echelon folds.

The Nagylengyel syncline runs from the Danube Basin into the study area with a NE-SW trend (Fodor et al. 2013a). The syncline changes its strike gradually in a similar way like the Sümeg-Devecser syncline. Starting with NW-SW trend in the NE, it becomes N-S trending further southwest. According to my observations, the Nagylengyel syncline is not bordered from the east or southeast by any thrusts, as it was proposed by Tari (1994) and Fodor et al. (2013), but by a simple anticline (Pölöske anticline). The southern segment of the Nagylengyel

syncline is dissected by the Petri fault. Approximately 5 km dextral offset of this strike-slip fault is nicely visible on Appendix III.a. Mapping of this southern segment of the Nagylengyel syncline was quite straightforward. According to my observations, it is clear that the Nagylengyel syncline does not turn back further south, as it was proposed by Tari (1994), therefore, these compressional structures cannot be connected to the NE-SW trending compressional structures of the Balaton Highland, as it was suggested by Tari (1994). The termination of the N-S trending southern segment of the Nagylengyel syncline is represented by the north-vergent post-Paleogene F33 thrust, which transports Hauptdolomit onto the Nagylengyel syncline and covering Upper Cretaceous and Paleogene sediments. The N-S trending Nagylengyel syncline is refolded by the approximately E-W trending Bak-Nova syncline, which is developed in the footwall of the F33 thrust after the Paleogene (Appendix III.a).

Based on well data and uncertain interpretation of seismic sections (e.g, N-N' section; Fig.4.19) a next pre-Senonian syncline, the Szilvágy syncline is present west of the Nagylengyel syncline. I was not able to determine the exact geometry of this syncline, due to the poor quality of seismic data on this area.

Normal faults, which deform the base-Senonian horizon, show characteristic pattern. Such normal faults are N-S or even NNE-SSW striking at the northwestern corner of the study area (F13 and Viszák fault on Appendix I and appendix III). Further to the east-southeast, these normal faults gradually turn into NW-SE (e.g, F10, F22, F7, F8 on Appendix III) or even WNW-ESE strike (F19, F6 on Appendix III). The southern limit of these normal faults is the WNW-ESE striking Petri fault. The area south of this strike-slip lacks any normal faults, except the northern boundary faults of the Paleogene Bak-Nova graben (e.g, F32, F36, F35 on Appendix III.) The northern border of the Bak-Nova graben is fault controlled; it has irregular zig-zag shape. The WNW-ESE striking F36 and F32 faults are running into a NE-SW striking fault, which represents the western border of the Bak-Novas graben. The F35 fault is ENE-WSW striking, and it is dissected by the Petri fault.

The Bak-Nova graben is bounded from the south by the F33 thrust system (Fig. 4.18, Fig.4.19, Appendix III). The western segment of this thrust (above Szilvágy syncline) gradually changes its strike from E-W at the west to WNW-ESE on the east. This segment probably represents an oblique ramp or tear fault. The eastern segment of the F33 thrust is E-W or even ENE-WSW striking above the Nagylengyel syncline (Appendix III).

5. Interpretation of data

I separated the observed structures into the following seven deformation phases, based on criteria, which I will demonstrate throughout this chapter. At first, I list these phases with a very brief definition. I will discuss the geometry and timing of the structures in the sub-chapters. The significance of observed structures in the geodynamic evolution of the Transdanubian Range is discussed in chapter 6.

D1) Pre-orogenic extension: Structures related to this phase are coeval with the deposition of different parts of the Triassic – Jurassic succession and / or they certainly predate Cretaceous compression (D2). The related faults are WNW-ESE striking (Fig.5.1). These structures had very important role in the evolution of Transdanubian Range, since they strongly influenced the geometry of later deformations.

D2) middle Cretaceous compression: This deformation caused overall folding of the study area. Structures related to this phase are discordantly sealed by Senonian strata. On the surface (Keszthely Hills) only the Miocene Cserszegtomaj Kaolinite covers D2 structures, thus it only offers a very wide constraint. D2 structures developed due to E-W shortening in the study area (Fig.5.1), however, these structures show various trends, which I explain by structural inheritance of D1 normal faults (Chapter 5.2.7.)

D3) Senonian extension: This phase is represented by Senonian syn-sedimentary faults observed mostly on seismic data sets. The related faults are WNW-ESE or NW-SE striking (Fig.5.1).

D4) Paleogene transtension: This phase is represented by Paleogene syn-sedimentary faults, which were observed only on seismic sections. These structures are responsible for the development of the Paleogene Bak-Nova graben. The related faults show two main populations in strike: WNW-ESE and NE-SW. I will give two possible explanations in order to explain this geometry.

D5) Late Oligocene – Early Miocene transpression: This phase is represented by a narrow E-W striking fold and thrusts belt, which overprints Paleogene and Senonian rocks, while it is

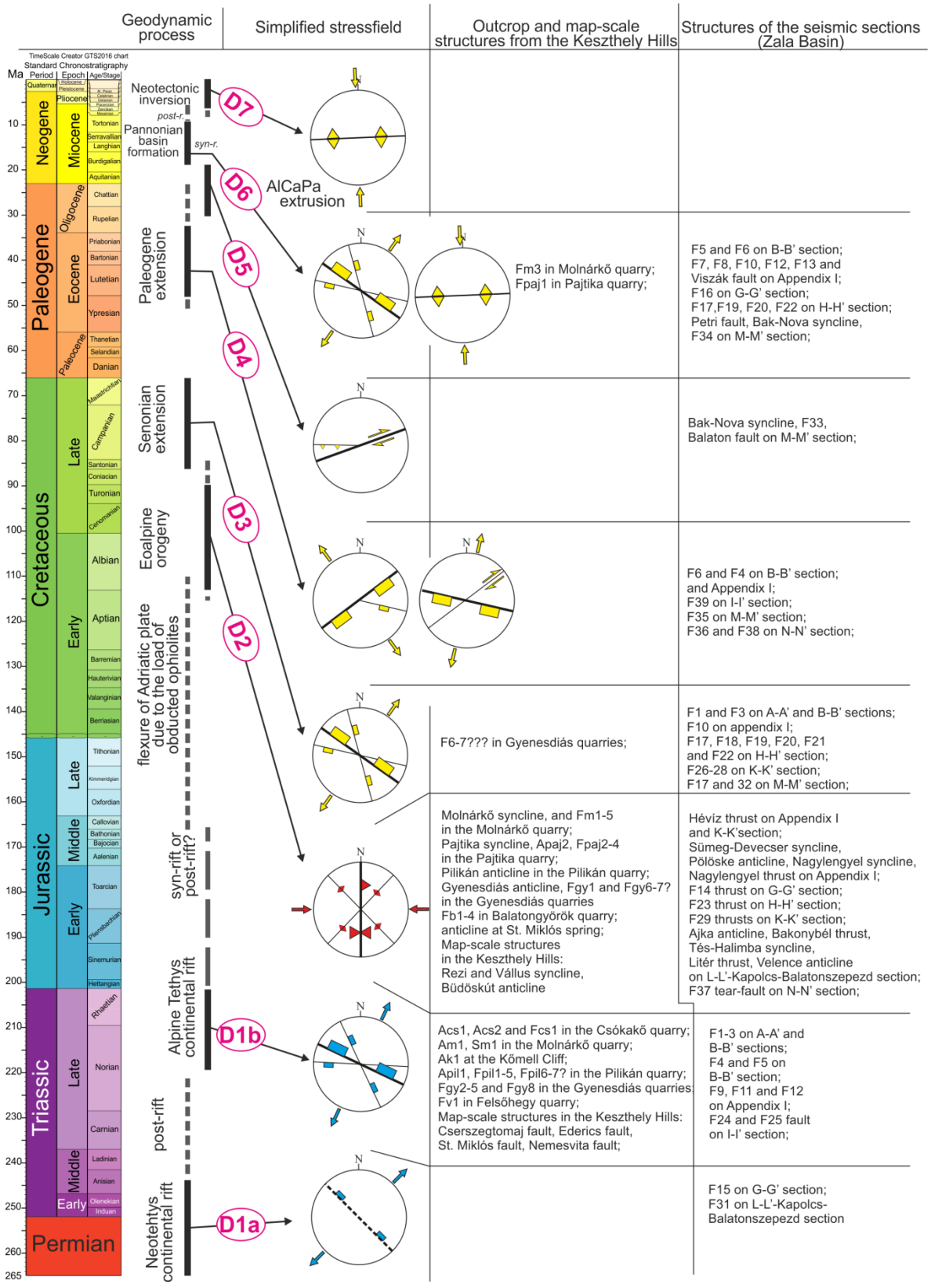

Fig.5.1. Supposed age range, simplified stereoplots and summary of the observed and separated deformation phases. The structures described in chapter 4. are listed and separated into phases.

sealed by Middle or Upper Miocene deposits. The related structures appear only on seismic sections. It is important to note, that this deformation was intense only in a narrow belt in the southern part of the study area, along the Balaton Zone (northern branch of Mid-Hungarian Fault zone).

D6) Miocene extension: This phase is represented by the first-order Zala half-graben and a number of second-order Miocene syn-sedimentary faults (Fig.5.1). Miocene extenional deformation started at 18 Ma (Fodor et al. 2013). The related faults show similar strike as D3 Senonian faults, therefore D6 structures are often reactivate older faults. A unique feature of the Miocene deformation is, that the area south of the Petri fault lacks any Miocene normal faults (Appendix III.b), and this part of the study area suffered syn-sedimentary folding during Miocene (Fig.4.18).

D7) Late Miocene – Quaternary inversion: This phase is represented by gentle E-W trending folds, which are coeval or younger than Late Miocene**.**

5.1. Pre-orogenic extension (D1)

5.1.1. Pre-orogenic extension on seismic data sets

5.1.1.1. Thickness variation of Permian to Middle Triassic succession

Significant thickness variation of Permian to Middle Triassic succession can be seen on a few seismic sections (Appendix I and II), which is probably the result of pre-orogenic syn-sedimentary extension. One example of thickness variation is directly related to F31 normal fault on Appendix II. In the case of F15 (Fig. 4.13) thickness variation could not be observed, however, the fault is sealed by Veszprém Marl, and overprinted by the Cretaceous F14 thrust. Strongly different seismic images of the footwall and hanging wall indicates different lithologies in the two sides of the fault, which may have developed due to syn-sedimentary normal faulting along F15 (Fig.4.13).

The resolution of seismic data does not allow detailed timing of this deformation. Possibly this normal faulting can be correlated with the Middle Triassic event, which is described from the Balaton Highland (Budai and Vörös 1992, 1993, 2006; Csicsek 2015; Fodor et al. 2017). Budai and Vörös (2006) gave a time constrain for this extensional event by Anisian facies differentiation.

Nevertheless, several indirect indications suggest that, Anisan deformation possibly represents the final stage of a longer "syn-rift" phase, which may have started already during Permian. The Upper Permian Balatonfelvidék Sandstone shows variable thicknesses in the Balaton Highland (Majoros 1983), which may be the result of Permian syn-sedimentary extension; however, direct evidences for fault activity has not been found, yet. Lower Triassic formations also show various thicknesses in the Balaton Highland (Budai 1999a). Fodor et al. (2017) suggested Early Triassic activity in the case of a map-scale fault near Zánka (Balaton Highland).

If we accept the possibility of Permian and Early Triassic extensional deformation, the question arises: why do not we see abrupt facies changes in the Permian – Lower Triassic succession. In my opinion, the sedimentation could take pace with extension-related subsidence during Permian and Early Triassic, and that is the reason why extension didn't lead to lateral facies changes during Permian and Early Triassic. Permian to Early Triassic fault activity therefore would be confirmed by identification of thickness changes based on cross-sections in the Balaton Highland, which need further analysis.

According to Gawlick et al. (2017) Anisian drowning of platforms in the Peri-Tethyan area is the result of oceanic break up and not the rifting of the continental crust. Theoretically,

oceanic break up accompanies with the termination of active extension on the continental margins (e.g. Decarlis et al. 2017). Vászoly Formation seals grabens and horsts (Budai & Vörös 2006), therefore the base of this formation possibly represents the syn-rift—post-rift boundary. Ladinian – Carnian outcrop scale normal faults, which were observed by Csicsek (2015) and Fodor et al. (2018), probably developed due to gravitational sliding.

5.1.1.2. Late Triassic and Jurassic syn-sedimentary normal faults

Significant thickness variations of Late Triassic formations are nicely visible on seismic sections. This variation can be connected to normal faults; the hanging-wall block always have thicker succession. Thickness variations of Hauptdolomit (F9 on Appendix I; F12 and F13 on Fig.4.12c; F25 on Fig. 4.15) suggest that extensional deformation started during its deposition, in the Norian. Initially, the rate of sedimentation could keep pace with the subsidence of the hanging wall, thus the depositional environment remained in the tidal zone, and no spectacular facies differentiation occur. However, subsequent normal faulting led to the formation of Late Triassic intra-platform basins filled with Rezi Dolomite and Kössen Formation (Budai and Koloszár 1987; Haas 1993b). The most spectacular Late Triassic grabens are shown on Figs. 4.11a and b. Besides thickness variations of Kössen Marl and Dachstein Limestone, the presence of talus cone breccias and internal discordance surfaces indicate further/continuous Rhaetian activity of the normal faults (F1, F2 and F3 on Fig. 4.11). Faults F4 and F5 (Fig.4.11b) demonstrate that some of the faults were active during Jurassic as well.

5.1.1.3. Pre-Senonian normal faults

Several normal faults are sealed by Upper Cretaceous strata (e.g. F9 on Fig. 4.11b; F24 on Fig. 4.15; F9 on Fig.4.16), or the separation at the pre-Senonian horizons are larger than the offset of the base-Senonian (F5 on Fig.4.11b; F19 on Fig.4.14). It cannot be proved, that the first increment of displacement along these faults are older, than the middle Cretaceous folding (D2). Theoretically, it is possible that these faults are coeval or younger than D2 folding, but older than Senonian. In this case, they would be syn-orogenic extensional structures. Nevertheless, in my view they more likely represent pre-orogenic structures, although that statement cannot be proved unambiguously.

5.1.1.4. Normal faults which are overprinted by subsequent Cretaceous folding and thrusting (D2)

A part of the pre-orogenic normal faults is represented by structures, which are overprinted or cut by Cretaceous thrusts (e.g. F1 is cut by a small thrust on Fig.4.11; F15 is cut

by F14 on Fig.4.13; F12 is cut by F23 thrust on Fig. 4.14). As I mentioned, fault F11 is sealed by the reflection of Rezi Dolomite. On Fig.4.12c, however, there are other indications, which suggest pre-Cretaceous activity. The Nagylengyel thrust shows curved geometry along the fault (Fig.4.12e). In other words, F11 restricted the development of the Nagylengyel thrust (for detailed discussion of structural inheritance see Chapter 5.2.7. Consequently, F11 fault had to exist before the development of the Nagylengyel thrust.

5.1.2. Pre-orogenic extension based on surface data from the Keszthely Hills

5.1.2.1. Coarse-grained breccias along the Late Triassic Cserszegtomaj Fault

Map-scale syn-sedimentary normal faults can be often outlined based on facies distribution and the presence of coarse-grained sedimentary breccias in the proximal hanging-wall of the fault (e.g. Bertotti et al. 1993). Dolomite breccias of the Rezi Dolomite described in the outcrops of the Keszthely Hills have dolomite matrix, which suggests that the formation of these breccias pre-dates early dolomitization, and they are likely to be sedimentary breccias (Fig. 4.1a, Fig. 4.2e, Fig. 4.4a, Figs. 4.5a and b). These breccias may have redeposited on a fault-controlled slope (Csillag et al. 1995). Such breccias could alternatively formed right after deposition, due to seismic shock of semi- or unconsolidated mud (Hips et al. 2015). In the study area, dolomite breccia outcrops of the Rezi Formation are limited to a NW-SE striking belt along the southwestern edge of the Keszthely Hills (Fig. 5.2c). Coarse-grained breccias of the Csókakő quarry and the Kőmell cliff can be interpreted as proximal talus breccia (Fig. 4.1a and Fig. 4.4a), while the more fine-grained breccia intercalation in the Pilikán quarry could be interpreted as a more distal lobe of fault-related mass movements (Fig. 4.5a and b). Probably, platform environment was the source of fossil-rich blocks in the Csókakő quarry (Csillag et al. 1995).

South of the dolomite breccia occurrence of Csókakő quarry the Hauptdolomit is exposed (Fig. 5.2a and 5.3a). The WNW-ESE trending contact of the two formations was identified already by former mapping (Bohn 1979; Budai 1999b), however, it was interpreted as a stratigraphic contact (Fig. 2.7c). In my interpretation, this contact represents a Late Triassic syn-sedimentary normal fault, which is referred to as the Cserszegtomaj fault in this study (Fig. 5.2a). Probably, the southern WNW-striking border of the Rezi Dolomite occurrences near Gyenesdiás represents further NNE-dipping segments of the Cserszegtomaj Fault. In map view, the fault segments do not constitute a continuous fracture, but are dissected into two or three segments. The overlapping fault segments of 1-3 km width were connected by ESE dipping relay ramps (Figs. 5.2a and c).

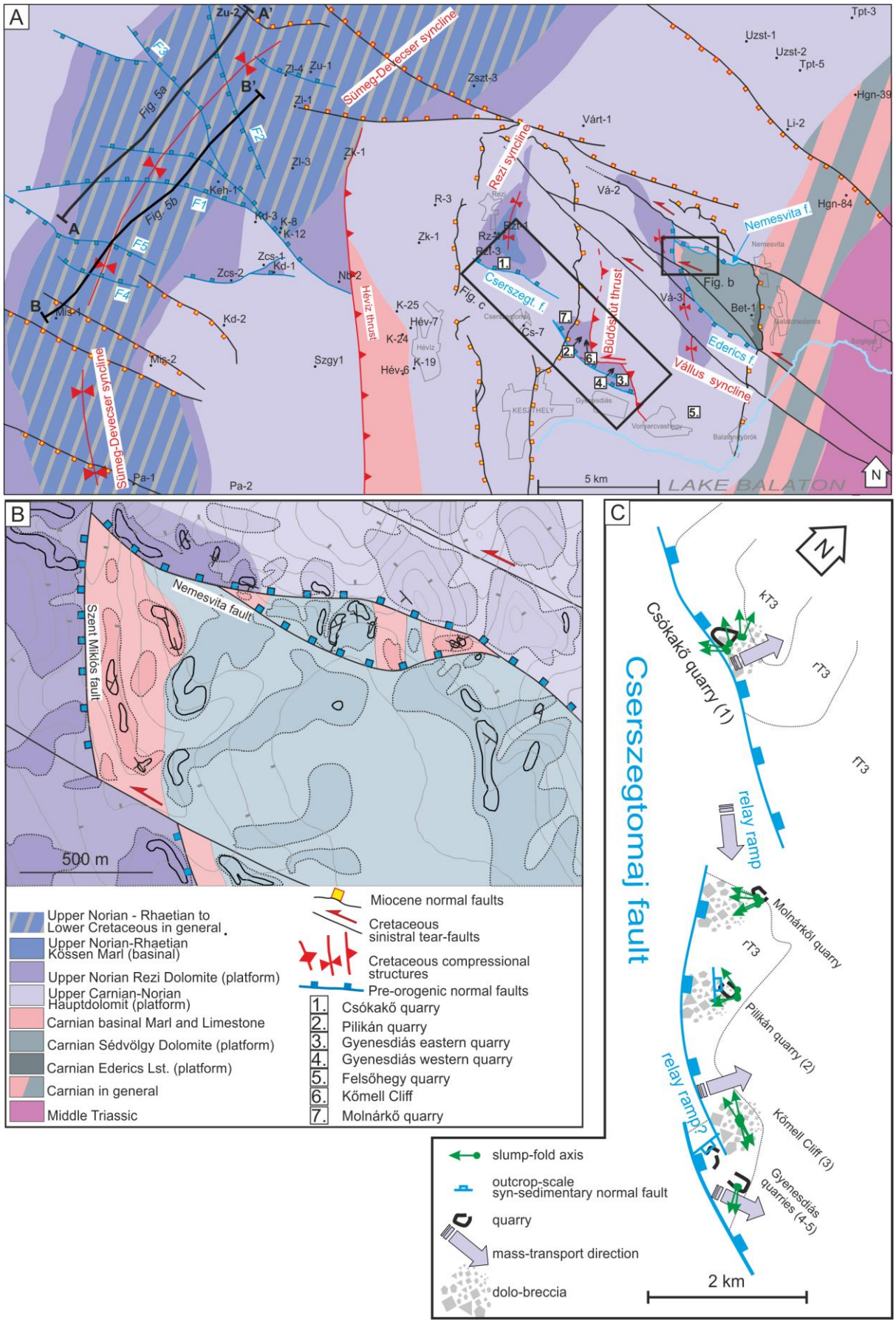

Fig. 5.2: (a) Pre-Miocene geologic map of the Keszthely Hills, and its NW foreland (b) Detailed map of the Eastern Keszthely Hills (c) Late Triassic syn-sedimentary structures along the Cserszegtomaj Fault.

Progradational tongue of dolomitized platform carbonates above the Rezi Dolomite was documented in the eastern part of the Keszthely Hills by Csillag et al. (1995). This pattern, fault-bounded talus breccia on the southwest and prograding platform carbonate on the northeast rather suggests an asymmetric half graben geometry for the Late Norian basin of the Keszthely Hill (Fig. 5.3a). Note, that the southward widening outline of the N-trending Rezi syncline also supports this asymmetric geometry, while it can be explained by (Cretaceous) E-W shortening of a NE-ward shallowing and thinning Late Triassic half graben (Fig. 5.3c).

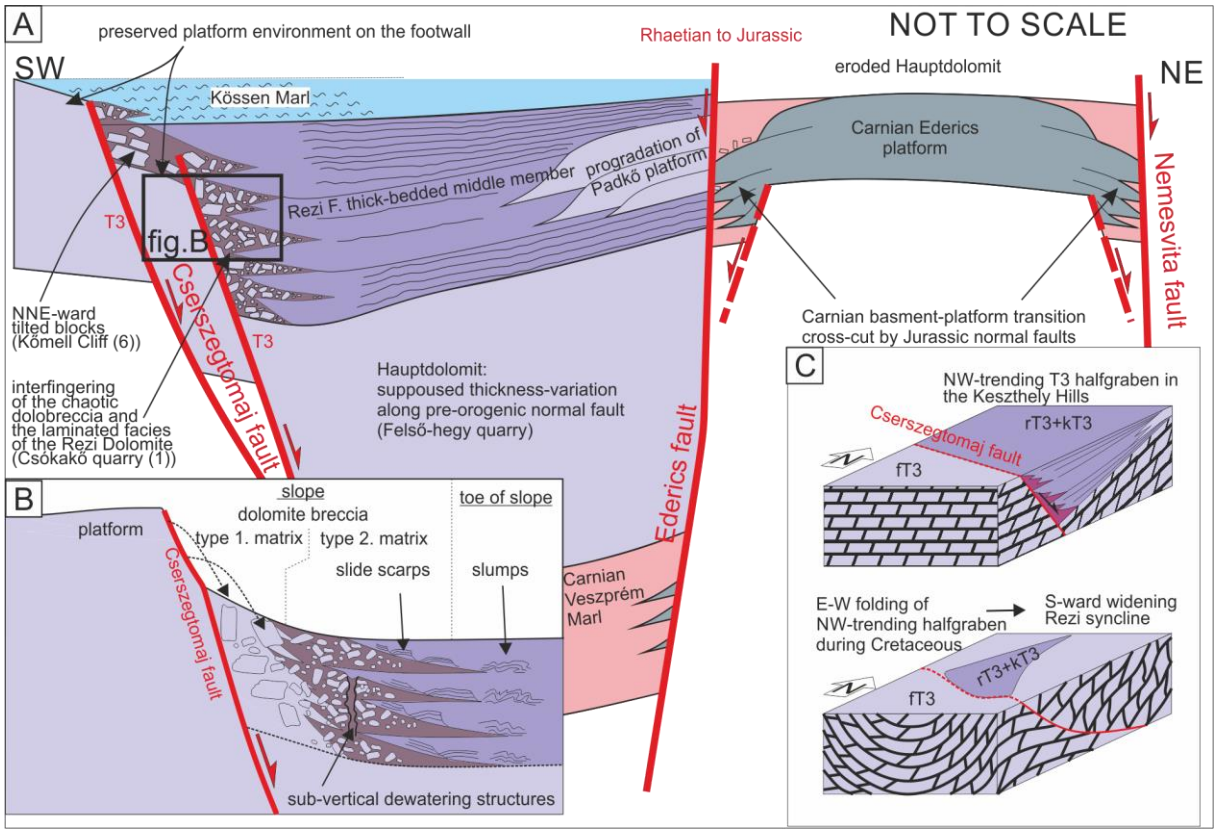

Fig. 5.3: (a) Model cross-section across the Keszthely Hills, showing the pre-orogenic basin geometry (b) Position of the structures exposed by the Csókakő quarry in relationship with the Cserszegtomaj fault (c) Simplified cartoon explaining the formation of the southward widening Rezi syncline, as a folded Late Triassic half graben.

The Cserszegtomaj fault can be correlated with faults F1 and F3 introduced on seismic sections (Fig. 4.11). The activity of these NE-NNE-dipping faults is evidenced by the main syn-tectonic deposits, which is represented by Rezi Dolomite in the Keszthely Hills (Figs. 5.3a and b), and Kössen Marl on the seismic section (Figs. 4.11). Probably, all of these faults were active simultaneously, although the resolution of seismic sections does not allow the investigation of syn-sedimentary deformation of the Rezi Dolomite. The extreme scarcity of Kössen Marl outcrops made the observation of its deformation problematic. However, the slumps and sedimentary breccias documented in cores indicate dynamic depositional environment during the formation of the Kössen Marl (Haas 1993b); this dynamism is at least partly due to tectonic deformation along graben margins.

5.1.2.2. Outcrop-scale pre-orogenic normal faults associated to map-scale features

Many of the described faults in the Keszthely Hills can be interpreted as syn-sedimentary Late Triassic structures, based on the following features: a) thickness variations of the beds along faults (Fig. 4.5a and c, Figs. 4.7a, b and d), b) presence of wedge-shaped syn-tectonic beds (Fig. 4.5.a, Figs. 4.7.a, b), c) faults sealed by younger beds of the Late Triassic succession (Fig. 4.5.c, Figs.4.7a, b).

In the Pilikán quarry small syn-sedimentary reverse faults occur besides normal faults (Fig. 4.5c). Certainly, all of these faults formed in the same extensional stress field, and the reverse faults formed due to space problems related to the movement along a non-planar normal fault plane.

Small steps of the beds in the western Gyenesdiás quarry (Fig. 4.7b) can be interpreted as healed normal faults, where the discrete faults disappeared due to diagenetic processes. These structures can be considered as pre-diagenetic faults.

Other faults have wider time constraints: tilted normal faults of the eastern Gyenesdiás quarry (Fig. 4.6b) represent such structures, which postdate deposition and diagenesis, on the other hand, they developed before Cretaceous tilting/folding.

Part of the observed syn-sedimentary normal faults detach at a layer parallel horizon. Probably these structures represent gravity-induced slide-scarps (e.g. Fcs1 set on Fig.4.1a).

The strike of outcrop-scale syn-sedimentary normal faults is in accordance with map-scale pattern (Fig. 5.2a), since most of these structures show WNW-ESE or NW-SE strike (Figs. 4.5d, 4.6f, 4.7f). This direction of extension is in accordance with the trend of other pre-orogenic normal faults, described in the central and north-eastern Transdanubian Range. The age of such structures are Middle Triassic (Budai & Vörös 2006) or Early and Middle Jurassic (Vörös & Galácz 1998; Lantos 1997; Fodor 2008). Perpendicular, WNW-ESE extension (Fig. 4.7c) was estimated only for syn-diagenetic small faults and slide planes of the western Gyenesdiás quarry; these unique features need specific explanation. In my model, they situated most probably on a relay ramp which connects two segments of the Cserszegtomaj Faults (Fig. 5.2c). Stress field can markedly be different in relay ramps, than in the “regular” faults (Fodor 2008).

5.1.2.3. Pattern of slumps and slides

The presence of millimetre to metre scale folds is widespread in the thin layered, laminated Rezi Dolomite. I considered most of these folds as slump folds, based on the following criteria. The thickness of the beds is varying on fold limbs (e.g, Apil1 on Fig.4.5a), which suggests syn-sedimentary folding. The folds are often restricted to one bed, and the upper strata cover these structures (e.g, Agy1 on Fig.4.6b). The folds show continuous deformation, the limbs of even isoclinal folds are not fractured (Ams and Sm1 on Fig.4.2d; Acs2 on Fig.4.1b). It means, that the dolomite is folded before diagenesis. In the Csókakő quarry (Fig. 4.1) an extensional and a compressional domain can be separated (Fig. 5.3b), similarly to many case studies (e.g. Farrell 1984; Debacker et al. 2009; Alsop & Marco 2011). I suggest, that the NNE-ward dipping beds of the southern part of the quarry represent the original dip of the slope (see next chapter). Slide scarps (Fcs1 set on Fig.4.1a) are present mostly in this part of the quarry (extensional domain). The northern side of the quarry, which can be characterized by horizontal dips, is dominated mostly by slump folds. This part of the quarry situated on the toe of the slope where the compressional domain of the gravitonally slided material developed.

The strike of slide-scarps and slump-fold axes may allow to determine the sedimentary transport direction. The strikes of slide-scarps are theoretically parallel to the strike of the slope. On the other hand, slump-fold axes can suffer notable rotation, after significant transport (Alsop & Marco 2011). During the early stage of slump formation, the slump fold shows symmetric geometry. In that stage, the axis of the slump is perpendicular to the dip direction of the slope (Bradley & Hanson 1998). Most of the slumps observed in Rezi Dolomite show symmetric or slightly asymmetric geometry, suggesting minor transport (e.g. Fig. 4.1b). Therefore, the transport direction is supposed to be sub-perpendicular to the fold axis. Of course, there are exceptions, such the isoclinal recumbent fold (Fig.4.2d) in the Molnárkő quarry. While most of the observed slump axes are NW-SE directed (Fig. 5.2c), the gravity slide transport direction is toward NE; into the direction of the hanging wall of the fault segments (Csókakő quarry, Kőmell Cliff; Fig. 5.2c). On the other hand, the slump fold axes pronouncedly different on relay ramps while having NE-trend; this may suggest southeast-ward mass transport. Such examples could be identified in the Molnárkő quarry and Gyenesdiás quarries (Fig. 5.2c).

Slump folds often show features resembling to metamorphic ductile structures. For example, the presence of stretching lineation is common in the case of soft-sediment folds (Ortner 2013). However, in the present case a completely different type of lineation was observed. On the polished surface of the samples it is visible that this lineation represents hinges of very fine microfolding (in the scale of 1-3 mm), thus the lineation derives from fold hinges of micro-folds (Figs. 4.1b and c).

5.1.2.4. Dewatering structures

An episode of talus-cone breccia formation probably provided considerable volume of sediments. The sudden load made the underlying unconsolidated thin-layered carbonate mud compacted, and de-watered. The chaotic zone of the Csókakő quarry (Fig. 4.1a) may indicate dewatering and fluidisation of originally laminated sediments, similarly to examples of Ortner (2007). Sediment fluidization occurred, where the original sedimentary features of the laminated dolomite was completely destroyed (Knipe 1986; Ortner 2007). The dewatering related compaction could be responsible for the collapse and subsidence (down-bending) of the overlying beds (upper laminated layer on Fig.4.1a). The vertically arranged few cm wide zones can be interpreted as dewatering pipes, where water was released and ascended from deeper beds (Fig. 4.1a). The inclined beds of the Csókakő quarry are dissected by sub-vertical dewatering pipes and fluidized zone (Figs. 4.1a, 5.3b). It confirms that the inclined layering in the Csókakő quarry predates diagenetic processes, such as dewatering, and the inclined strata represents the original dip of a talus breccia cone, positioned on the tectonically controlled slope.

The style of the above-mentioned early deformation was probably highly influenced by early diagenetic process such as dolomitization (Meister et al. 2013). Platform-derived redeposited blocks observed in the Csókakő quarry (Fig. 4.1a) probably underwent early dolomitization as well (Haas et al. 2012), which redound the "brittle" re-deposition, represented by blocks. On the other hand, the laminated Rezi Dolomite – which deposited in deeper marine environment – probably dolomitized later, during burial, therefore dolomitization did not obstruct/obscure soft-sediment deformation features, such as slump folds, or sediment fluidization and dewatering.

5.1.2.5. Rhaetian? to Jurassic extensional horst of the eastern Keszthely Hills

Reinterpretation of former geologic map (Budai et al. 1999b) suggests the presence of further map-view pre-orogenic structure in the Eastern Keszthely Hills. The easternmost part of the Keszthely Hills (Fig. 2.7c) is built up by Carnian formations (Csillag et al. 1995; Budai et al. 1999b). These formations are partly dolomitized platform carbonates (Ederics Fm.) intercalating with the pelagic Veszprém Marl (Csillag et al. 1995; Budai et al. 1999a; Haas et al. 2014). The Carnian formations have tectonic contact with the Rezi Dolomite and the Hauptdolomit. The fault system, bounding Carnian formations has a northern WNW-ESE trending segment (Nemesvita fault), a western N-S trending segment (Szent Miklós fault), and a southern NW-SE trending segment (Ederics fault) (Figs. 5.2a and b). The whole area is dominated by westerly dips, which formed during the mid-Cretaceous E-W shortening. There

are areas (e.g. along the Szent Miklós fault), where the Veszprém Marl is in direct contact with the Rezi F., thus the whole Hauptdolomit, which is more than 1 km thick, is tectonically omitted.

The Szent Miklós fault is sub-vertical based on the vertical electric sounding of Gulyás (1991). That is why it was interpreted by Dudko (1996) as a syn-orogenic, syn-folding strike-slip fault. In my interpretation, the large (km-scale) vertical displacement can rather be explained by normal or oblique-slip faulting (Figs. 5.2a and b). The actual sub-vertical dip of the fault (Gulyás 1991) can be the result of the later, general moderate westward tilting, associated with syn-orogenic Cretaceous folding, which steepened, but not overturned the originally west-dipping fault.

It is clear from map-view, that the Szent Miklós fault is dissected by NW-SE trending sinistral faults with few hundred meters of offset (Figs. 5.2a and b; Budai et al. 1999b; Dudko 1996). These faults have significant offset on the eastern mid-Cretaceous syncline (Vállus syncline), but they die out towards northwest, and do not crosscut the western syncline (Rezi syncline). Therefore, I suppose that these sinistral faults can be considered as syn-folding tear-faults. These sinistral faults also prove that the Szent Miklós fault is an older, pre-orogenic fault, which was overprinted by the structures of Cretaceous compression. On the other hand, no coarse breccia was observed along the Szent Miklós Fault, which may suggest that it is younger, than the Rezi Dolomite.

Although there are no data on the age of Nemesvita and Ederics faults, I suggest that these faults are coeval with the Szent Miklós fgault, and the area in between them represents a pre-orogenic extensional horst. The Ederics fault shows many similarities to fault F2 on seismic, which is slightly younger than faults F1 and F3 (Fig. 4.11). Fault F2 was moderately active during the deposition of Kössen Marl, but it was still active later, during the deposition of Dachstein and Kardosrét Limestone, when the southwestern boundary faults (Fault F1 and F3) were inactive (Fig. 4.11). The presence of Jurassic deposits in the hanging wall, and the Senonian seals suggest, that F3 was slightly active during the Jurassic, too. The same situation is suggested for the pre-orogenic horst of the eastern Keszthely Hills (Fig. 5.3a).

5.1.3. Significance of Late Triassic deformation

A second syn-rift phase is outlined based on the above described Late Triassic - Jurassic normal faults, which can be clearly separated from the Permian(?) to Middle Triassic normal faulting. A-A’ and B-B’ sections (Fig.4.11) suggest that main interval of this second rifting occurred during the Norian – Rhaetian, and just a few normal faults remained active during Jurassic. This statement somewhat contradicts with the opinion of e.g, Vörös and Galácz (1998)

and Fodor (2008). These authors suggest, that major pre-orogenic extension occurred during Early and Middle Jurassic in the Transdanubian Range. The lack of real “Jurassic syn-rift” sediments, like the several hundred meters or even km thick Allgau Formation in the Northern Calcareous Alps (Gawlick et al. 2009) also suggests that major extensional deformation terminated in the TR by the beginning of Jurassic. In this concept, normal and strike-slip faults reported by e.g. Vörös and Galácz (1998), Lantos (1997), Fodor (2008) Fodor et al. (2018) are rather minor structures.

5.2. Mid-Cretaceous orogenic deformations (D2)

5.2.1 Criteria of classification into D2 phase

Cretaceous folding and thrusting is one of the major deformations of the Transdanubian Range, which resulted in significant tilting of pre-Senonian beds. The entire study area is involved in this deformation, in contrast with D5 structures, which are restricted to a narrow belt (see later chapter 5.3.3). An important criterion of D2 phase is, that the related structures are sealed by Senonian deposits. This can be clearly established in the Zala Basin (Appendix I): the Sümeg-Devecser syncline, the Pölöske anticline, the Nagylengyel and Szilvágy synclines and the Nagylengyel thrust are sealed by Upper Cretaceous deposits. Aptian – Early Albian Tata Limestone appears in the core of Sümeg-Devecser syncline, which suggests that D2 deformation occurred during Albian – Coniacian time-interval (Haas et al. 1984).

Timing of D2 structures is much more problematic in the Keszthely Hills, since the oldest cover of compressional structures is the Cserszegtomaj Kaolinite, which is Badenian (Middle Miocene) in age (Kelemen 2018). Therefore, a very wide post-Triassic to pre-Middle Miocene time-span can be given for folding. However, sub-horizontal Senonian beds in the western and northern foreland of the Keszthely Hills can be projected into the Keszthely Hills, therefore, probably major synclines and anticlines of the Keszthely Hills are also pre-Senonian in age (Pajtika syncline and aPaj1 anticline on Fig.4.3; Molnárkő anticline on Fig.4.2; Pilikán anticline on Fig.4.5e; Gyenesdiás anticline on fig.4.6; Büdöskút anticline on Fig.4.10; Rezi and Vállus syncline on Appendix IV.b). It cannot be excluded, that a part of the folds in the Keszthely Hills are the result of Late Oligocen – Early Miocene D5 folding. Nevertheless, I don't think that this is a possible scenario, based on the following fact: according to seismic data D5 thrust and folds (e.g. F33 and Bak-Nova syncline on Fig.4.18) are E-W trending. Trend/strike of D2 structures of the Zala Basin is ranging from NE-SW to NW-SE, but N-S trend /strike is the dominant. That is true for the folds of the Keszthely Hills, which suggest rather classification into D2 phase. Moreover, according to seismic interpretation of the present study, D5 structures are restricted to a narrow belt along the southern edge of the study area. The continuation of this belt is most probably located south of the Keszthely Hills (see details in chapter 5.3.3). Therefore, north of this belt (e.g, in the Keszthely Hills) there was no significant D5 deformation, consequently, folds of the Keszthely Hills must have formed during D2 phase.

5.2.2. Style of folding in the outcrops of Keszthely Hills

5.2.2.1. Buckling folds vs. fault bend folds

The anticlines of the Pilikán quarry (Fig. 4.5.e) and the Gyenesdiás quarries (Fig.4.6) were interpreted by Héja (2015a) as fault-bend folds, which developed above a décollement located at the base of Rezi Dolomite (Fodor et al. 2017). In my former interpretation (Héja 2015a) the hanging wall ramps of the related thrust is exposed on the southern wall in the Pilikán quarry. The quarry was expanded in the last few years, and it turned out that major thrust of the southern wall cannot be followed on the northern wall (Fig.4.5e). The "major thrust" of the southern wall represents in fact a minor structure, and the formation of the anticline needs alternative explanation.

Reinterpretation of the stratigraphy in Gyenesdiás quarries suggests that the Hauptdolomit and not the Rezi Fm. is exposed in the core of the anticline (János Haas and Tamás Budai pers. comm.). Consequently, the anticline cannot be interpreted as a fault-bend fold above such a shallow décollement, like the base of the Rezi Dolomite. The existence of such décollement is problematic anyway, since there is not enough difference between the competency of Hauptdolomit and Rezi Dolomite.

In my new interpretation, the anticline exposed in the Pilikán and Gyenesdiás quarries represents rather buckling folds, whose amplitude is progressively increasing upward (Fig. 4.5e; Fig.4.10). The upward increasing amplitude and decreasing interlimb angle can be observed in the case of Pilikán anticline (Fig.4.5e). These folds probably gradually flatten downward in the Hauptdolomit, without any unequivocal detachment (Fig.4.10). Similar folding of the Hauptdolomit was described by Ortner (2013) in the Northern Calcareous Alps (Fig. 5.4a).

Due to the above described features, the Gyenesdiás and Pilikán anticline can't be considered as a simple detachment fold. In the case of simple detachment folds a basal "ductile" layer is needed: the space in fold core is filled up by this mobile material, and the overlying competent rocks suffer parallel folding, theoretically (Fig.5.4b; Mitra 2003). Such "ductile" layer cannot be expected in the Hauptdolomit, in which Gyenesdiás and Pilikán anticline probably flatten downward (Fig.4.10).

Alternatively, detachment folds can evolve due to strain accommodation due to second-order thrusting and folding under brittle condition (Fig.5.4c; Epard & Groshong 1995). In that case, no basal ductile layer is needed, and the fold forms due to second order structures, which developed in the competent unit (Fig.5.4c). Probably the well layered Hauptdolomit and Rezi Dolomite provide suitable lithology for the development of such second order structures (e.g.

fault bend folds limited to single layers). Therefore, I suggest that type of geometry in the case of Gyenesdiás and Pilikán anticline.

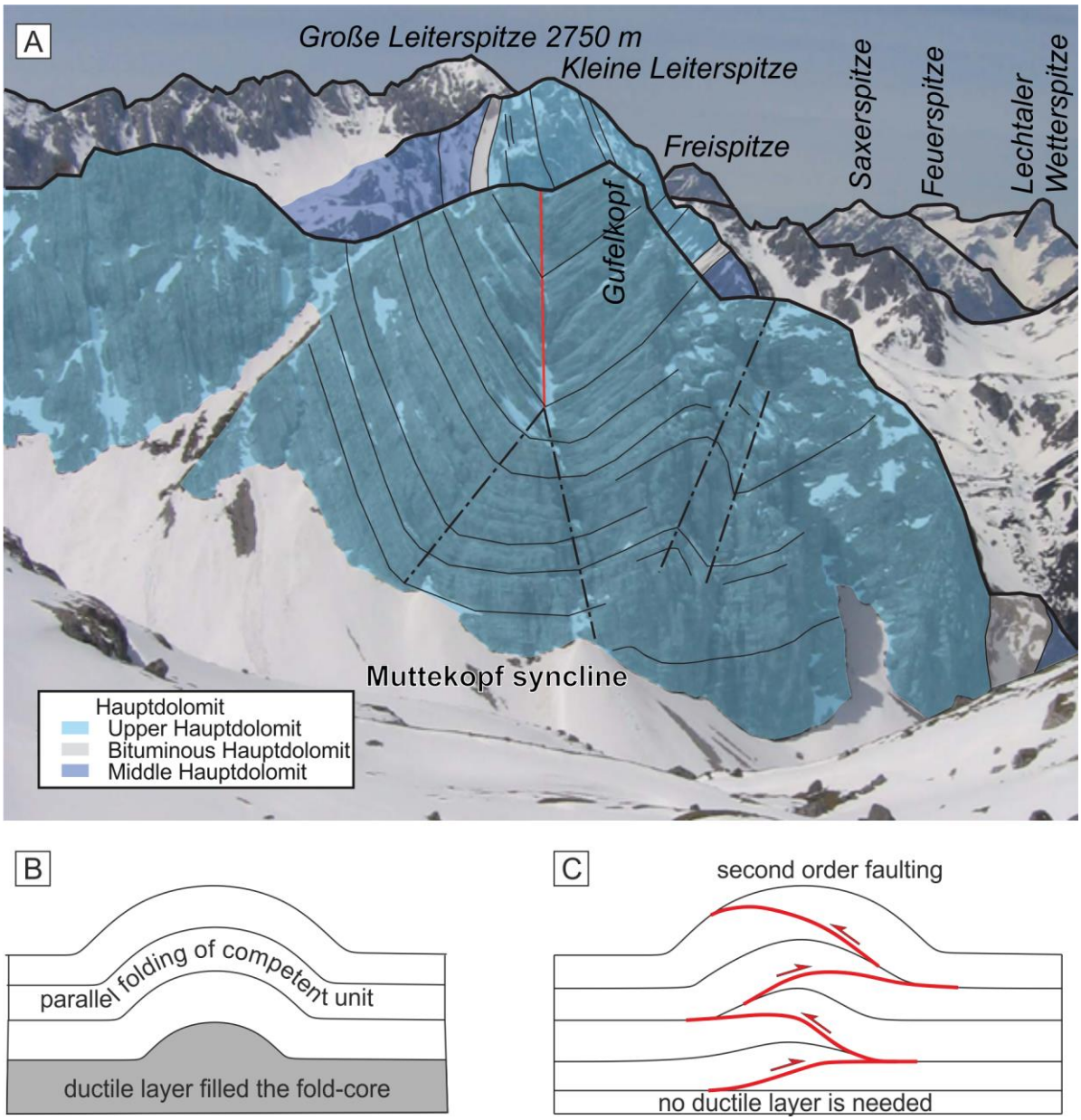

Fig.5.4. (a) Secondary anticline in Hauptdolomit in the core of Muttekopf syncline – Northern Calcareous Alps (Ortner 2013), the amplitude of the anticline is gradually increasing upward. (b) simple detachment folds forms above "ductile" layer, due to migration of incompetent material into the fold core (e.g., Mitra 2003) (c) detachment folds can form due to second order faulting, in that case no ductile layer is needed (Epard and Groschong 1995).

5.2.2.2. Mechanism of folding

Layer-parallel slicken-lines (Fig.4.3) and layer-parallel shear zones made up by powdered dolomite (Figs.4.6a and b; Fig.4.8) are commonly observed in the quarries of the Keszthely Hills. These structural elements can be considered as the result of flexural-slip folding (Suppe 1983), which is one of the main mechanisms of folding under brittle condition. Similar process is on, when cards slip over each other, when we bend a deck of card. In nature, cards are represented by beds, whereas the slip-surfaces are layer parallel shear zones. Layer

parallel shear zones dissect tilted pre-orogenic normal faults in the eastern Gyenesdiás quarry (Fgy2-5 on Fig.4.6b) giving a top to the west sense of shear on the eastern limb of the Gyenesdiás anticline. It can be seen, that pre-tilt normal faults (Fgy2-5 on Fig.4.6b) are not perfectly symmetric to bedding, and conjugate fault pairs (Fgy2-3 and Fgy4-5) are sheared in the same top to the west sense (Figs.4.6b and f). On one hand, this asymmetry in respect of bedding can be an initial feature, on the other hand, it can be possibly the result of shear along fold limb (flexural-slip folding). Conjugate normal faults can be used as reference object in estimation of the amount of layer parallel shear in different lithologies; however, this require a much bigger dataset of tilted normal faults.

Flexural slip folding occurs in case of low-friction bedding surfaces (Tavani et al 2015). In case of high-friction bedding surfaces, layer-parallel shear is confined, thus flexural slip folding mechanism is blocked. In such case, the layered unit can suffer tangential-longitudinal strain associated to folding. It means that layer-parallel extension develops in the outer arc of the fold and shortening occurs in the inner arc of the fold (Ramsay 1967; Tavani et al. 2015). These two areas are separated by the so called neutral line/surface, on which layer parallel strain is zero (Ramsay 1967; Frehner 2011).

Specially distributed small-scale faults, which were observed in the Keszthely Hills, can be explained by tangential-longitudinal strain. Fgy1 (Figs.4.6a and d) pop-up structure is possibly developed in the inner curve of the syncline bordering the Gyenesdiás anticline from the east. Thrusts of Fgy1 pop-up and layer parallel shear zones mutually overprint each other (Fig.4.6a), which suggests that, they developed coevally. Fb1-4 thrusts in the Balatongyörök quarry (Fig.4.8a) and Fm2 thrust in the Molnárkő quarry (Fig.4.2f) can be interpreted in a similar way. Fm1 normal faults, which are situated on the crest of Molnárkő anticline (Fig.4.2f), and Fgy6 and Fgy7 normal faults, which developed on the crest of the Gyenesdiás anticline (Figs.4.6c and d), are possibly syn-folding normal faults, which formed in the outer arc of the anticlines. It is also possible, that Fgy6 and Fgy7 faults are post-folding fault, as it was suggested by Héja (2015a). However, these faults do not dissect the Middle Miocene denudation surface (Fig.4.6c), so their Miocene age (D6) can be excluded.

To summarize, signs of flexural-slip folding and tangential-longitudinal strain both can be seen in the outcrops of Keszthely Hills, which may suggest that both of these mechanisms had a role in the D2 folding coevally.

5.2.3 Section view geometry of map-scale folds in the Keszthely Hills

Fig.5.5. is enlarged part of the regional restored section (Appendix IV). Fig.5.5 shows a possible interpretation for the geometry of map-scale folds and thrusts of the Keszthely Hills and surrounding areas. According to my interpretation the Rezi syncline is considered as hanging-wall, trailing syncline of the Hévíz thrust, which has an intermediate flat segment in the level of Carnian marl (Figs.5.5b and c). On the other hand, the Várvölgy anticline can be interpreted as a fault-bend fold above a deeper footwall ramp of the Hévíz thrust (Fig. 5.5c). In my opinion, initially, the pre-orogenic Cserszegtomaj fault confined the movement along the Hévíz thrust, therefore a passive roof thrust developed in the level of Carnian marl (Fig. 5.5.c). This roof thrust was blocked by the Szent Miklós fault and the Ederics fault. Due to this buttressing effect, buckling of the Hauptdolomit and Rezi Dolomite above the Carnian marl occurred (Büdöskút anticline on Fig. 5.5c). The Büdöskút anticline was localized by the Szent Miklós and Ederics faults (Fig.5.5c). Later on, due to additional shortening, the Hévíz thrust cross-cuts the Cserszegtomaj fault, creating a footwall short-cut (Fig. 5.5.c.). The Litér thrust is running probably in the basement of the Miocene Tapolca graben (Fig.5.5a), and it is represented by an E or ESE-vergent back-thrust in that area (Császár et al. 1978; Fodor et al. 2013b). The Vállus syncline is dissected by several NW-SE striking left-lateral strike-slip faults (Budai et al. 1999a). The offset of these strike slip-faults is gradually decreasing toward west, since they do not cross-cut the Rezi syncline. Therefore, they can be considered as syn-folding tear-faults accommodating different amount of folding. These tear-faults formed most probably coevally with folding, although I restored them in an individual step (Fig.5.5.b).

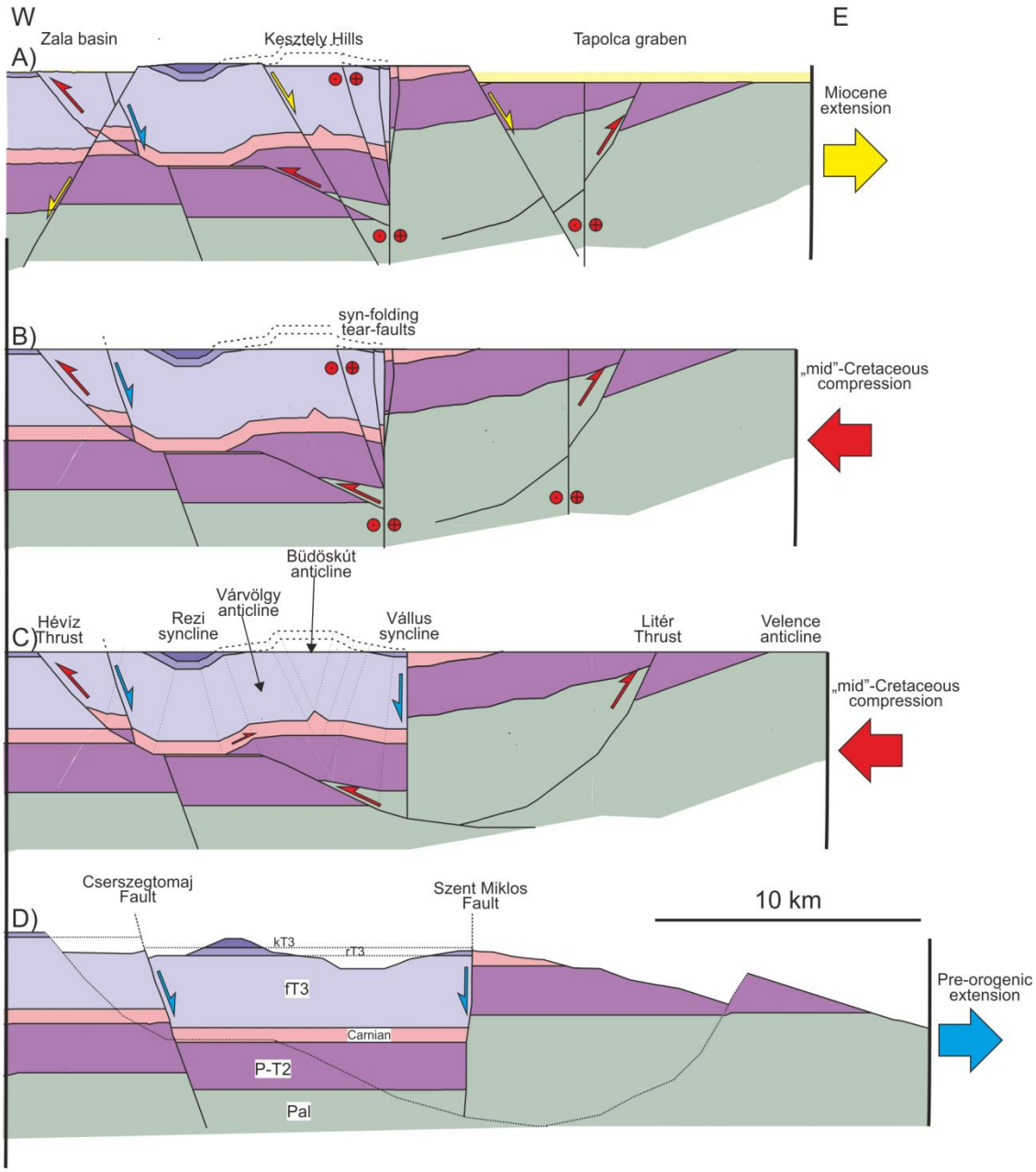

Fig.5.5 Restored E-W cross-section across the Keszthey Hills. (a) recent situation (b) restoration of D6 Miocene normal faults (c) restoration of D2 tear-faults (d) pre-folding situation after the restoration of D2 folds and thrusts.

5.2.4. Style of folding and thrusting based on seismic data (Zala Basin)

5.2.4.1. Section-view geometry of Nagylengyel and Sümeg-Devecser synclines

According to previous works, the middle Cretaceous contractional structures of the Transdanubian Range were interpreted as fault-bend folds or ramp anticlines (Tari 1994; Tari and Horváth 2010; Fodor 2010; Fodor et al. 2013b; Csicsek and Fodor 2016). According to these authors several décollement surfaces developed in different stratigraphic levels. These décollements formed in incompetent rocks such as the Paleozoic shales, the Lower Triassic Csopak Marl, the Middle Triassic Iszkahegy and Buchenstein Formation, the Carnian

Veszprém Marl, the Upper Triassic Kössen Marl and Jurassic to Lower Cretaceous succession (e.g., Tari 1994). In the fault-bend-fold model the thrusts are running along such décollement levels, and they cut upward in the stratigraphy along thrust ramps (e.g., Suppe 1983). These ramps form commonly in competent rocks: Tari & Horváth (2010) suggested that such competent unit is e.g., the Hauptdolomit in the Transdanubian Range. Fault-bend folds develop, when material is transported over a non-planar thrust, which forms due to the flat-ramp-flat geometry of the thrust (e.g., Brandes & Tanner 2014).

Tari (1994) was the first who applied this model explaining the geometry of the folds of the Zala Basin (Fig.2.7b). He proposed that the Nagylengyel and Sümeg-Devecser synclines of the Zala Basin are trailing synclines of west-vergent thrusts, which developed above a shallow level décollement at the base of Hauptdolomit (Fig.5.6a). The related ramps of the thrusts are cutting upward into the paleo-surface (base of Senonian), along which Hauptdolomit is thrust over the Jurassic – Lower Cretaceous succession (Fig.5.6a). Therefore, Tari (1994) proposed that the Nagylengyel syncline is bordered from the east by a west-vergent thrust. Moreover, in the model of Tari (1994) a part of the Triassic succession is duplicated along a far-travelled internal nappe with at least 50km displacement (Fig.2.7b). Although Tari (1994) and Tari & Horváth (2010) did not make estimation on the amount of shortening, their model implies more than 50% of shortening.

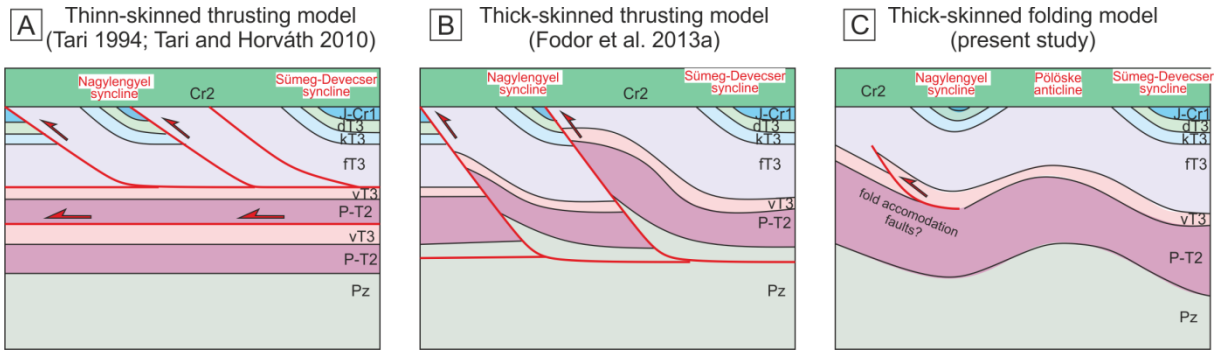

Fig.5.6: Structural models for the geometry of Nagylengyel and Sümeg-Devecser synclines. (a) According to Tari (1994) and Tari & Horváth (2010) these synclines are trailing synclines of WSW vergent thrusts above a shallow level décollement at the base of the Hauptdolomit. (b) According to Fodor et al. (2013a) these synclines are trailing synclines of west-vergent thrusts above a deep level décollement in the Paleozoic shales. (c) In this work I consider this synclines as thick-skinned folds.

Fodor et al. (2013a) considered the Sümeg-Devecser and Nagylengyel synclines also as trailing synclines of west-vergent thrust-ramps. Nevertheless, they proposed a deeper décollement for these thrusts in the Paleozoic shales (Fig.5.6b). Fodor et al. (2013a) proposed that the west-vergent Hévíz thrust is continuing into a flat segment in the level of Veszprém Marl, and it does not cut down in deeper stratigraphy.

According to my observations, the main D2 compressional structures of the Zala Basin are broad anticlines and synclines, such as the Nagylengyel and Sümeg-Devecser synclines.

True tightness of these folds are visible on the restored cross-section (Appendix IV.b). In my opinion there is no sign of any thrust, which cuts up to the paleo-surface (base Senonian) between the Nagylengyel and the Sümeg-Devecser synclines (Fig.5.6c). Therefore, the Nagylengyel syncline is not bordered from the east by a west-vergent thrust, and the Sümeg-Devecser syncline cannot be a trailing syncline of the same thrust, as it was proposed by Tari (1994), Tari & Horváth (2010) and Fodor et al. (2013a). Therefore, the Nagylengyel syncline and the Sümeg-Devecser syncline is separated by a simple anticline (Appendix IV.b), which is referred to as the Pölöske anticline in this work (Appendix I). While no major ramp was observed related to these folds, they cannot be considered as fault-bend folds which was suggested by Tari (1994) and Tari & Horváth (2010). I suggest that, these structures are rather thick-skinned buckling folds (Fig.5.6c), since Variscan unconformity is also involved in the folding (Appendix I; Appendix IV.b). I also suppose that the Velence anticline is a similar thick-skinned buckling fold, too. Applying this model, the restored regional section (Appendix IV.) results only approximately 10 % shortening for middle Cretaceous D2 deformation, which is significantly less than it was previously supposed (e.g., Tari & Horváth 2010).

5.2.4.2. The role of fold-accommodation faults

L-L'–Kapolcs-Balatonszepezd section (Appendix II) has a key role in the understanding of the relationship of map-scale thrusts and folds. In that section it is clearly visible that the Bakonybél thrust does not cut down into the stratigraphy below the Veszprém Marl. A logical scenario is that, the Bakonybél thrust has a sub-horizontal décollement at the base of Veszprém Marl (Tari 1994; Fodor & Koroknai 2000; Fodor 2010). On the other hand, I think it is a more realistic scenario that, the offset of this thrust gradually decreasing to zero downward (along dip). In that case, the Bakonybél thrust represents a fold-accommodation fault (more precisely an out-of-syncline thrust – Mitra 2002) in the core of the Bakony syncline, which is outlined based on the reflection of Variscan unconformity (Appendix II). Possibly the Ajka anticline is also the result of space problems in the core of Bakony syncline (Appendix II).

According to Mitra (2002) fold-accommodation faults are secondary faults, which mostly "develop due to increase in bed curvature within the fold cores". Regarding a kink-fold model, increase in bed curvature appears, where two converging axial plane join into one plane (A and B axial planes join in AB point on Fig.5.7a). For example, an out-of-syncline thrust is running from this junction point with upward increasing offset (Fig.5.7a).

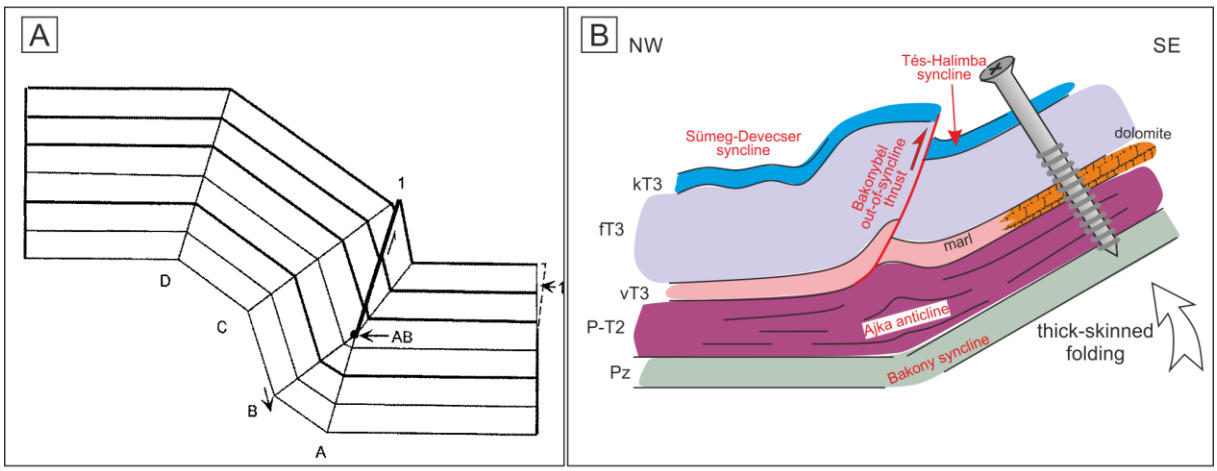

Fig.5.7 (a) Kinematic model of out-of-syncline thrust (Mitra 2002). The out-of-syncline thrust develops due to increased curvature in the fold core: the thrust is running from AB point, which is the junction point of A and B axial plane. (b) Schematic sketch of interpreted L-L' seismic section: the Bakonybél thrust is interpreted as an out-of-syncline thrust. In contrast of the model of Mitra (2002) I suppose that, the Bakonybél out-of-syncline thrust developed due to confined shear along the southeastern limb of the deep-seated Bakony syncline.

In my opinion mechanical stratigraphy is also responsible for the development of the Bakonybél "out-of-syncline thrust". The Veszprém Marl is probably interfingering with the coeval platform dolomite (e.g, Budaörs Fm.) on the southeastern limb of the Bakony syncline (Fig. 5.7b). The presence of competent dolomite, and the lack of incompetent Veszprém Marl on the fold limb possibly confined flexural-slip folding, which led to the formation of internal folds (Tés-Halimba syncline; Ajka anticline) and thrust (Bakonybél thrust), accommodating strain variation in the core of Bakony syncline (Fig.5.7b; Appendix II).

Similar relationships can be proposed between other map-scale thrusts and thick-skinned folds in the study area. According to my view the F29 fault set on Fig.4.17 represent similar out-of-syncline thrusts in the core of Sümeg-Devecser syncline. I suggest that, the Nagylengyel thrust (Appendix IV.b) and F23 thrust (Fig.4.14) are out-of-syncline thrusts of the Nagylengyel syncline.

The Litér thrust possible represents limb-wedge thrust. In that case wedging of the "competent" Permian-Triassic units results in the compenstanded for by layer-normal thickening of the Paleozoic shales (Appendix IV.b; Mitra 2002).

5.2.5 Defining first- and second ordered curvatures in the Transdanubian Range

Trend of D2 structures show large dispersion: their strike is ranging from NE-SW to NW-SE (Fig.5.1, Appendix III.a). Variation in trend along strike can be observed in the case of several individual folds or thrusts, which is resulting in a curved outline of the structures.

Large-scale curvature can be seen in the case of Sümeg-Devecser and Nagylengyel synclines across several tens of km, which have been described already by Tari (1994) and

Fodor et al. (2013b), although the geometry of this curvature differs in different works. Both the Nagylengyel and Sümeg-Devecser synclines are NE-SW trending in the central Transdanubian Range (eastern margin of the Danube Basin; Bakony). They change their strike gradually toward southwest, and they show N-S trend in the Zala Basin, forming the first-ordered salient of the western Transdanubian Range (Appendix III.a).

Tari (1994) proposed an approximately 180° curvature in the map-view strike of these structures. According to Tari (1994) WSW vergent middle Cretaceous thrusts of the Zala basin can be connected to SE-vergent thusts of the Balaton Highland (Fig.2.7a). However, my own observations (structural mapping based on 3D seismic block) clearly demonstrate that D2 compressional structures (e.g., Nagylengyel syncline) keep their N-S trend toward the south, and they do not curve toward but are cut by the Mid-Hungarian fault Zone and related D5 structures (e.g, F33 thrust on Appendix III). According to that, D2 thrusts do not "turn back" to join the NE-trending thrust faults and folds of the Balaton Highland area (Fig. 2.7c), as it was proposed by Tari (1994). Similar view was suggested by Fodor (2013a; Fig.2.4c) which is confirmed by the observations of the present work.

This first order curvature of the southwestern Transdanubian Range was explained by (Tari 1994) as the interference of an Aptian ENE-WSW and an Albian NNW-SSE compressional event. As it is shown later (chapter 5.2.7), I propose only one-phase folding in the study area during the Cretaceous, and therefore, I give an alternative explanation for the first-order salient of the western Transdanubian Range (chapter 6.4.4.).

Besides the large-scale curvature, there are examples of smaller curvatures in km-scale. Best example of such curved compressional structures is the Nagylengyel thrust, which forms a recess in the front of pre-orogenic horst, bounded by F11 and F12 normal faults (Fig.4.12). The Nagylengyel thrust outlines a salient north of this D1 extensional horst (Fig.4.12). Similar curvature can be observed in the case of Büdöskút thrust and Büdöskút anticline: these N-S trending structures become NW-SE trending approaching the WNW-ESE striking pre-orogenic Cserszegtomaj fault (Fig.5.8). The anticlines of the Molnárkő quarry, Pilikán quarry and Gyenesdiás quarries and the syncline of the Pajtika quarry show similar, various fold trend. This variation in fold trends appears also in km-scale. These second-order (km-scale) curves (salient and recess) appears along pre-existing normal fault (D1), therefore they should be in strong relationship. I suggest that, these second-ordered curves developed due to the interaction of contraction and pre-existing D1 normal faults (see details in chapter 5.2.7)

5.2.6. Structural inheritance of Triassic and Jurassic normal faults in section view

Pre-orogenic extensional structures and their effect on the later shortening are widely known from thrust-an-fold belts (e.g. Butler et al. 2006). I found several examples of such inheritances in the study area, which I discuss in the following two sub-chapters.

Pre-existing normal faults often localize thrust ramps (Butler et al., 2006; Schedl & Wilitschko 1987). In this case, the new ramp of the thrust develops in front of the pre-orogenic normal fault with identical dip direction but somewhat lower dip value (Fig. 1.1a). Numerical models pointed out that maximum stress values concentrate at basement corners (Schedl & Wiltschko, 1987; Wiltschko & Eastman, 1983). In the present study the Nagylengyel thrust provide a good example for ramp localization (Figs. 4.12a-d). The thrust is localized by the pre-orogenic F11 fault. Most authors only emphasized the role of crystalline basement rocks in ramp localization (Schedl & Wiltschko 1987) however, the example of Nagylengyel thrust shows that the same processes could work, when both the footwall and the hanging wall of the pre-existing normal fault are built up by sedimentary rocks.

There are examples where the footwall ramp of a thrust is emerging from the footwall of the pre-existing normal fault above the pre-existing graben (Fig.1.1b; Ustaszewski & Schmid 2006). I proposed similar situation in the case of F14 thrust, which ramps up from the footwall of the pre-orogenic F15 fault (Fig.4.13).

It is also possible, that the normal fault is reactivated as reverse fault during shortening (Bonini et al. 2012; Fig.1.1c). Sometimes, the thrust breaks across the footwall corner (footwall cut-off), thus isolated triangular blocks can develop (Tavarnelli 1999; Butler et al. 2006; Fig.1.1d). Small reverse fault running from the F1 fault represents such footwall cut-off (Fig. 4.11b). According to my interpretation the relationship of F9 pre-orogenic normal fault and the Nagylengyel thrust can be explained by the combination of reactivation and footwall cut-off (Appendix IVb). In my interpretation westward tilting made F9 more gently dipping on the western limb of the Pölöske anticline, which facilitated its inversion (Appendix IV.b). On the other hand, I suggest that only the lower segment of F9 fault was inverted, and the related thrust break through the footwall corner of F9 (Appendix IV.b). This more flat-lying segment of the thrust is continuing into the Nagylengyel thrust (Appendix IV.b).

Inappropriate steepness of the normal fault often does not facilitate inversion. In this case, the pre-orogenic normal faults have a buttressing effect on the shortening. If a décollement is blocked by a normal fault, several scenarios are possible to accommodate the shortening. The detachment can be refracted, which leads to development of back-thrusts (Colpron et al. 1998;

Fig.1.1e), passive roof duplexes, or triangle-zones (Konstantinovskaya et al. 2014). Similarly to this model, minor D2 back thrusts developed in the hanging wall of pre-orogenic normal faults F1 and F2 of the study area (Fig.4.11a).

Buttressing effect can also induce the development of buckle folds above a detachment in the front of the normal fault (Fig.1.1f). I propose similar process for the anticlines of the Keszthely Hills. The anticline of the Pilikán quarry (Fig. 4.5e) and Gyenesdiás quarries (Fig. 4.6d) are situated in the proximal hanging wall of the Cserszegtomaj fault (Fig. 4.10), whereas the Büdöskút anticline (Fig.4.10) developed in the hanging wall of Szent Miklós fault and Ederics fault (Fig.4.10).

Pre-existing normal faults may also confine flexural-slip folding (Butler et al. 2006). Therefore, pre-existing normal faults are sometimes precursor of the hinge of future folds, since in the hinges no layer-parallel shear is expected (Butler et al. 2006). My observations provide several examples where the pre-existing normal fault is situated in the hinge of the Cretaceous fold (e.g. Fpil7 fault in the core of Pilikán anticline – Fig. 4.5e; Szent Miklós fault in the core of Vállus syncline – Fig. 5.2b; F24 in the core of Nagylengyel syncline – Fig. 4.15; F9 in the core of Nagylengyel syncline – Fig. 4.16).

5.2.7. Structural inheritance of Triassic and Jurassic normal faults in map view

The general trend of map-scale folds and thrusts in the Keszthely Hills is N-S (Fig. 2.7c; Budai et al. 1999b; Fodor et al. 2013b), however, the documented mesoscale folds along southern Keszthely Hills have significantly different trends (Fig. 5.8a). It is clear that deviations in fold trend occur along map-scale pre-existing normal faults, which I described in chapter 5.1.2. I propose that this spatial coincidence is casual; folds with non-regular trends are due to the presence of former NW-SE trending Late Triassic to Jurassic extensional faults and connecting relay ramps; the way of influence is described below.

The Büdöskút anticline in the hanging wall of the Büdöskút thrust has N-S trend, but it become NW-SE trending southward, approaching the WNW-ESE striking Late Triassic Cserszegtomaj fault (Figs. 5.8a and b). I proposed that the anticline observed in the Gyenesdiás quarries is the southern continuation of the anticline of the Pilikán quarry (Pilikán anticline). The map-view pattern of this anticline shows similar geometrical change in the footwall of the Büdöskút Thrust; the anticline is N-S trending in the Pilikán quarry, but its postulated southern continuation in the Gyenesdiás quarries is NNW-SSE trending just in the vicinity of the Cserszegtomaj fault (Fig.5.8a). It is important to note that, the Gyenesdiás anticline and the Pilikán anticline is dissected by an E-W striking tear-fault based on map-view pattern. Probably

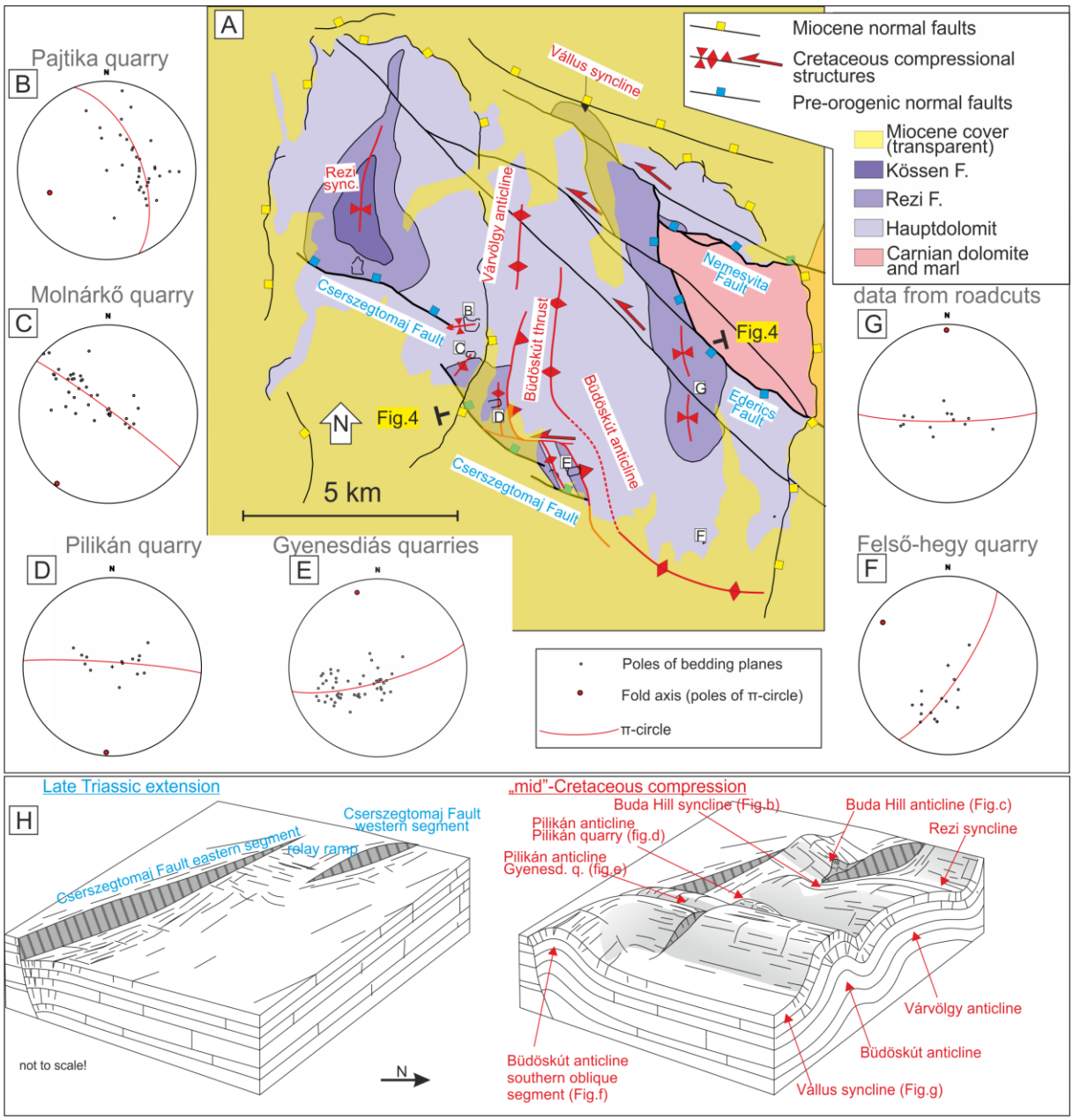

Fig.5.8: (a) Oblique folds along the pre-orogenic Cserszegtomaj fault (Keszthely Hills) (b) Schematic model of structural inheritance in the Keszthely Hills: left figure shows Late Triassic geometry of the Cserszegtomaj fault; right figure shows the geometry of middle Cretaceous folds.

the Büdöskút thrust is also dissected by this tear-fault, since there is a left-lateral step in the Rezi Dolomite – Hauptdolomit boundary. The curved strike of both the Pilikán-Gyenesdiás anticline and the Büdöskút anticline could be explained by the buttressing effect of the Cserszegtomaj fault which resulted in considerable drag of the fold hinges (Fig.5.8a).

Segments of the Cserszegtomaj fault are supposedly connected by relay ramps (Figs.5.2a and c). The NE-SW trending anticline of the Molnárkő quarry developed directly on one of these relay ramps (Fig.5.8a). The relay ramp between the two NNE-dipping normal faults had southeastern dip before the shortening, and this inherited dip domain contributed to the development of the formation of the NE-trending anticline in the Molnárkő quarry (Figs.5.8a and b). Close to the eastern tip point of the western Cserszegtomaj fault segment the steeply

WSW plunging syncline of the Pajtika quarry is situated (Fig. 5.8a). I suppose that this "transversal" syncline is also the result of the E-W compression. The transverse trend of the fold is the consequence of that the contractional deformation was inhibited by the eastern termination of the western segment of the Cserszegtomaj fault, and the Pajtika syncline represents actually the curved western limb of the Várvölgy anticline.

Similar style of deformation can be deduced from 3D seismic data of the Zala Basin. The curved Nagylengyel thrust can be considered as a recess which was developed in front of a pre-orogenic D1 extensional horst enclosed by F11 and F12 (Fig. 4.12). Based on Fig.4.12c this horst is sealed by the Rezi Dolomite, consequently this horst must exist before Cretaceous shortening. The curved geometry of the Nagylengyel thrust can be explained by that, the pre-orogenic extensional horst confined the propagation of Nagylengyel thrust, and it acted as an obstacle. Consequently, in the front of this obstacle a concave recess formed, whereas northward from F11 normal fault the Nagylengyel thrust forms a convex salient.

There are two end-member models for the formation of oblique thrusts/folds in fold and thrust belts (Fig.5.9):

1) Non-rotational salient represents such curved thrust/fold, which formed as an initially oblique or lateral structure (Fig.5.9b; Marschak 2004), and it is not suffered any rotation during its progressive development (that is oblique ramp sensu stricto). Theoretically the shortening is uniform across a non-rotational oblique ramp (Kwon & Mitra 2004).

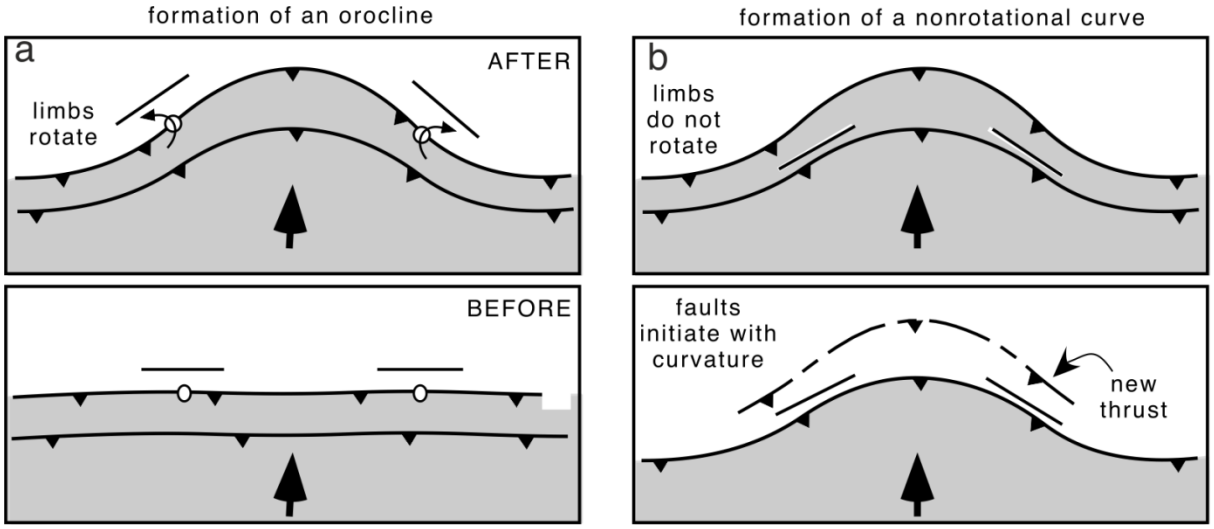

Fig.5.9: The contrast between rotational and non-rotational curves (Marschak 2004) (a) In rotational curves the trace of regional structures changes strike after thrusting and folding (orocline s.s.), or coevally with progressive deformation. The short line segments represent the trends of the thrusts. (b) In non-rotational curves, structures initiate with a curved trace.

2) Rotational salient is another end-member model, in which the curved thrust/fold was initially straight and perpendicular to the shortening, and it suffered rotation just later (5.9a; Marschak 2004), e.g., due to drag along a pre-existing normal fault. The modes of rotational

salient model can be further divided in respect of the relative timing of rotation and thrust or fold growth.

2a) On one hand, it is possible that first a straight thrust or fold develops, and it is bended just later in a separated event, in which the thrust or fold is not growing (that is equivalent to orocline sensu stricto; Hindle & Burkhard 1999).

2b) On the other hand, it is also possible that the initially straight thrust or fold become curved during its progressive deformation. In this case thrusting or folding is coeval with the bending of the curved belt (Hindle & Burkhard 1999).

Rotation of a thrust or fold can be accompanied by significant variations in the amount of tectonic transport / shortening along strike. There are several mechanisms to accommodate this kind of displacement gradient, such as the formation of transport-parallel simple shear or rigid rotation of thrust sheets (see more in Kwon & Mitra 2004, Hindle & Burkhard 1999).

Field and seismic examples of this study show evidences of significant displacement/shortening gradient along strike. The NE-SW trend of the Molnárkő anticline can partly be explained by that mechanism while the anticline reached larger amount of shortening on its northern part (Figs. 4.2a, f) approaching the fault tip of the westernmost segment of the pre-orogenic Cserszegtomaj Fault (Figs.5.8a, b). Similarly, the Pilikán anticline shows more significant amount of shortening along its oblique southern part (Gyenesdiás quarries), since there the anticline is much wider, and not only the Rezi Dolomite but also the underlying Hauptdolomit is exposed in the fold core (Fig.4.6d). Different amount of shortening along strike induced probably the formation of tear faults as well, which were observed in outcrops and on seismic sections, too (Fm3-5 on fig.4.2c and f; Fpaj3 on Fig.4.3a; F37 on Fig.4.19). The southern dragged part of the Pilikán anticline (Gyenesdiás quarries) is separated from the northern segment of the Pilikán anticline (Pilikán quarry) by a map-scale E–W trending sinistral fault which is interpreted as a tear fault (Fig.5.8a). This fault also contributes to the differential displacement of the two blocks, influenced by the buttressing effect of Cserszegtomaj fault (Fig.5.8a).

The Nagylengyel thrust points another nice example of displacement gradient along strike. Minimum offset of the thrust occurs in the front of the pre-existing horst, where a recess developed. On the other hand, displacement of the thrust is increasing away from the pre-existing horst, where a salient formed (Fig. 4.12).

The footwall cut-off line of the Nagylengyel thrust, which is outlined by the top reflection of the Veszprém-Sándorhegy Formation, point a similar curved geometry like the front of the Nagylengyel thrust (hanging wall cut-off line), nevertheless it has less curved amplitude (4.12e). If we propose that the footwall of the Nagylengyel thrust was a rigid block,

the footwall cut-off line of thrust will represent the initial map-view geometry of the Nagylengyel thrust. This suggests that the Nagylengyel thrust was initially curved (oblique ramp), where its oblique segment was localized by F11 pre-orogenic normal fault. On the other hand, the more arcuate hanging wall cut-off line of the Nagylengyel thrust suggests that, the curvature of the thrust increased further, during its progressive evolution (Fig.4.12e).

The example of the Nagylengyel thrust shows that these curved thrusts probably formed due to a mix of Marschak's (2004) end-member models: the thrust was initially arcuate (non-rotational salient), but it became more curved during its progressive deformation (rotational salient).

5.3. Post-orogenic deformations (D3-D7)

5.3.1. Senonian extension (D3)

Evidences of Senonian syn-sedimentary extension are provided by seismic sections (Fig 4.14; 4.18). Upward-decreasing offset along normal faults or the thickening of Senonian reflection packages in the hanging wall of normal faults indicate late Cretaceous syn-sedimentary normal faulting (F17 and F18 on Fig. 4.14; F32 and F17 on Fig. 4.18). The normal faults show mostly NW-SE trend (Fig.5.1), similarly like the D6 Miocene normal faults.

Faults having larger offset on the base-Senonian than on the base-Paleogene or base Miocene levels can also represent Late Cretaceous structures (e.g. F6 on Fig.4.11b and F10 on Fig.4.12; F22 on Fig.4.14; or F28; F26 on Fig.4.15, respectively). However, syn-sedimentary movement cannot be proved in these cases, since it is not obvious considering the geometry of hanging wall reflectors. In such cases younger, post-Senonian – pre-Miocene age cannot be excluded.

The observed Senonian extension is in accordance with the observation of Nyíri (2017) on seismic block A, and field study of Kiss (2009) in the Northern Bakony. In contrast of that Tari (1992; 1994) and Tari & Linzer (2018) supposed NW-SE compression as the origin of the Senonian basin. This contradiction can be solved if we take into account that in both cases the maximal horizontal stress axes are similar, lying in NW-SE direction. Therefore, it is possible that compressional stress field dominated during the Senonian, and the observed normal faults represent orogen-parallel extension. It is also possible that extensional stress field in the Zala Basin is replaced gradually by compressional stress field eastward, in the Southern Bakony.

The Senonian sedimentation was followed by uplift and subaerial exposure of the Transdanubian Range. Several authors propose the existence of an individual phase of NE-SW or ENE-WSW compression for this timespan based on fault-slip data (Sasvári 2008; Kiss 2009; Fodor 2010; Fodor et al. 2013b). Based on my observations this “phase” was not associated with significant deformations (e.g. folding) and this time span was probably a tectonically quiet period in the evolution of the southwestern Transdanubian Range. One important argument is that, no pronounced angular discordancy can be observed along the contact of Senonian and Paleogene beds, which contradict to the presence of considerable deformation (Fig. 4.15, Fig. 4.16, Fig. 4.18; Fig.4.19).

5.3.2. Paleogene transtension (D4)

The Paleogene succession is restricted more or less to an E-W trending belt in the Zala Basin, called as Bak-Nova graben (Kőrössy 1988). However, the kinematics of its boundary

faults have not been determined yet. The northern boundary of the graben is represented by steep normal faults (F36 and F38 on Fig.4.19) and steep reverse fault (F35 on Fig.4.18). However, these latter faults represent tilted normal fault (Fodor pers. com.) which was overtilted during subsequent shortening. The huge drag fold above F35 fault can be considered as extensional fault-propagation fold (e.g. Jin & Groshong 2006), along which the fault tip did not reach the paleo-surface. Onlap surfaces on the limb of this drag fold in the Paleogene succession indicate syn-sedimentary fault movement (Figs. 4.18). The WNW-ESE striking F36 and F38 faults (Fig. 4.18) join westward into a steep NE-SW striking fault (Appendix III), which also represents the westernmost border of the Bak-Nova graben.

I gave two possible explanations for the two populations of almost perpendicular faults (Fig.5.1; Appendix III). In the first scenario the major normal faults of the Paleogene Bak-Nova graben are represented by steep NE-SW striking fault, whereas WNW-ESE striking F36 and F38 faults are just breached relay ramps (Fig.5.1). This model is supported by the fact that F35 and F38 seem to detach on the top of Veszprém Marl (Fig.4.19), suggesting that they are rather minor structures. According to this first scenario the direction of extension would be NW-SE. In the second scenario the NE-SW trending faults are transfer faults, which are accommodating movement on the F36 and F38 normal faults. In this case the direction of extension would be NNE-SSW.

Despite all these geometric complexities, the Bak-Nova graben represents a Paleogene syn-sedimentary transtensional half graben. Therefore, this graben cannot be directly correlated with the Hungarian Paleogene basin, which has probably compressional or transpressional origin (Tari et al. 1993; Fodor et al. 1994). It is an unsolved question what was the original, pre-erosional extent of this basin, and where were the original depositional margins located.

5.3.3. Late Oligocene – Early Miocene transpression (D5)

The southern part of the study area is characterized by north-vergent thrusts (e.g. F33 on Fig.4.18 and Fig.4.19) and approximately E-W trending folds (Appendix III.b). The D4 Bak-nova Paleogene graben was folded into a syncline (Bak-Nova syncline), which is well pronounced on Fig. 4.18. The amount of related deformation is abruptly decreasing northward, and the area just north of the Bak-Nova graben is only slightly involved in this deformation; the Senonian succession is gently tilted toward SSE there, but only minor repetition was observed (Fig. 4.18). This intensively deformed D5 belt can be mapped precisely only in the western side of the study area (Appendix III.b), where seismic data are available. However, I propose that the front of this D5 thrust belt is continuing south of the Keszthely Hills (Appendix III.a), where the Veszprém Marl was reached by Balatonberény B-1 well. This well probably

drilled the hanging wall of the continuation of F33 thrust (Appendix III). Mapping and structural observations of this study suggest that north of this belt, including the Keszthely Hills, there was no significant D5 deformation, therefore folds of the Keszthely Hills must have formed during D2 phase.

The deformed Paleogene and gently deformed Miocene cover suggest that these E-W trending folds and thrusts were broadly coeval with the dextral shear of the sub-parallel Mid-Hungarian fault zone (Balla & Dudko 1989; Csontos & Nagymarosy 1998; Fodor et al. 1998).

This kinematic contradiction can be explained by strain partitioning (Platt 1993). It suggests that in major transpressional shear zones the strain is often separated into pure compressional and into a pure strike-slip domain. The narrow D5 thrust belt of the study area (Appendix III) can be considered as a minor, purely contractional domain, positioned parallel to the basically dextral Mid-Hungarian fault zone.

Palotai & Csontos (2010) and Palotai (2013) identified a very similar narrow ENE-WSW trending thrust-and-fold belt further to the northeast, near the Tóalmás segment of the broad Mid-Hungarian fault zone. Palotai & Csontos (2010) and Palotai (2013) explained this geometry in a similar way, by strain partitioning.

5.3.4. Miocene extension (D6)

5.3.4.1. Baján low-angle normal fault

The Pannonian back arc basin formed during the Miocene (Horváth 1993; Balázs et al. 2016), while significant extension reached the study area due to the roll back of the Carpathian subduction (Tari 1994; Fodor et al. 2003; Fodor et al. 2013a).

The major element of the related deformation is the Baján low-angle normal fault, which has been described already by Fodor et al. (2013a). This structure represents the westernmost boundary of the Transdanubian Range; the footwall of the fault is built up by high-pressure metamorphic rocks of the Koralpe-Wölz Nappe system (Schmid et al. 2004; Schmid et al. 2008; Fodor et al. 2013a). According to Fodor et al. (2008), the footwall of the Baján low-angle normal fault can be considered as a metamorphic core complex; its exhumation started already during Late Cretaceous based on thermochronology (Lelkes-Felvári et al. 2002). The Baján low-angle normal fault itself is represented by hundreds of meters thick mylonite zone, which can be characterized by ductile extensional deformation, overprinted by brittle extensional faults. The reflections of the related foliation can be seen on seismic (Appendix I). Occasionally, this type of foliation can be so strong, that totally overprint the structures related to the former compressional deformations (Brun and Sokoutis 2007).

The Baján low-angle normal fault dipping towards ENE in the western Zala basin (Appendix I), while it becomes flat toward west, lying above the Murska Sobota High in Slovenia. Small extensional allochtons of the Transdanubian Range were described by Fodor et al. (2013a) above the western flat segment of the detachment fault in this area.

Formation of metamorphic core complex occurs due to ductile flow of the lower crust (McKenzie et al. 2000). The flat lying segment of the detachment probably developed due to hinge rolling of the core complex, which made the former steep segment sub horizontal (Fig. 5.10; Brun et al. 2017).

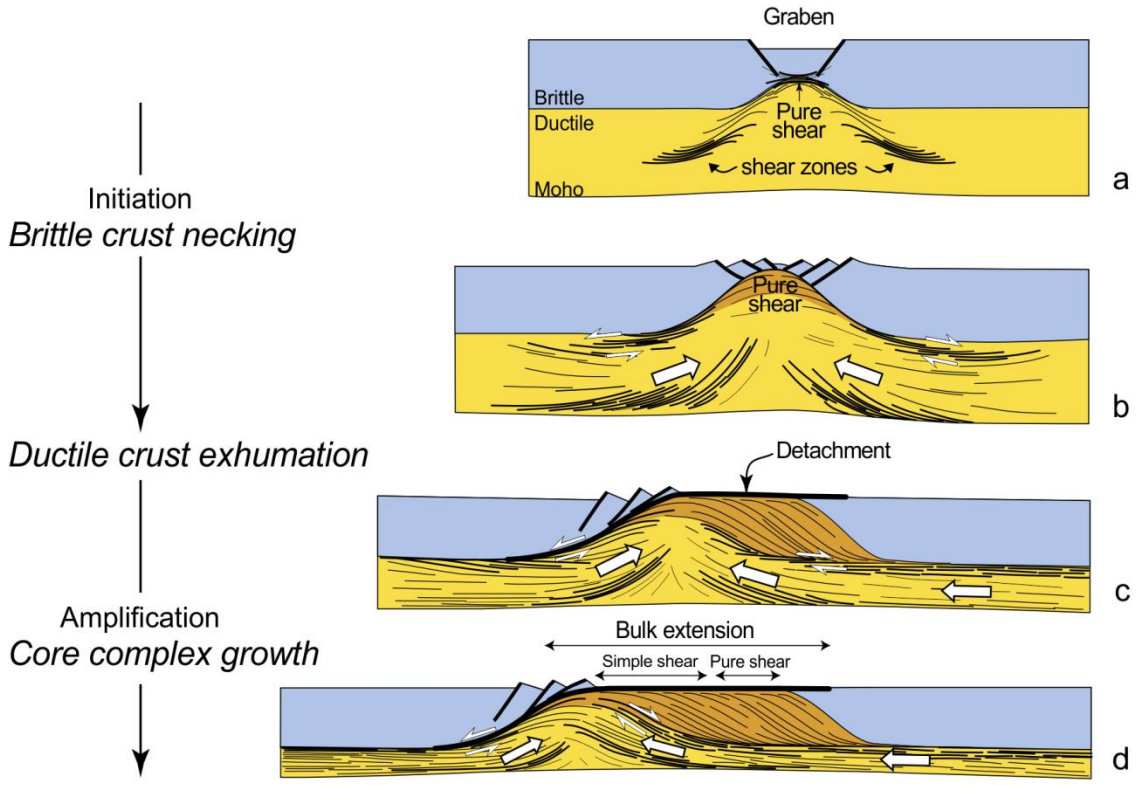

Fig.5.10. Four-stage deformation pattern of a metamorphic core complex (Brun et al. 2017).

The NNE- dipping segment of the Baján low-angle normal fault probably continues into a sub-horizontal detachment under the Zala Basin (Appendix IV.c). However, it is highly questionable, how deep this detachment is situated. Low-angle normal faults bordering metamorphic core complexes detach mostly along brittle-ductile transition, which is represented by a mid or lower crustal level (Brun et al. 2017). However, according to cross sections of Tari (1994) and Schmid et al. (2008) the Rába low-angle normal fault under the Danube Basin (which occupies the same structural position as the Baján detachment fault) is detaching at the level of the Moho. I followed this interpretation in the case of Baján low-angle normal fault as well (Appendix IV.c). It is also possible that the lower crustal flow was so significant, that the ductile crust is pinched out, and the brittle ductile transition overlaps with the Moho.

5.3.4.2. Zala half graben

The Zala basin can be considered as a huge half graben in the hanging wall of the listric Baján low-angle normal fault (Appendix IV.c). The basal Miocene strata represents a roll-over anticline of this half graben (Appendix I.; Appendix IV.c). The roll-over is dissected by a number of second order normal faults and grabens. Miocene syn-tectonic sediments in the hanging-wall of second order normal faults show various ages. For example, F13 or the Viszák fault was active during Karpatian, normal faults dissecting the Nagylengyel syncline were active mostly during Badenian, wheras normal faults in the neighborhood of Keszthely Hills show Sarmatian or Pannonian activity (Appendix I). According to that, the Miocene extensional deformation was diachronous, and the locus of deformation migrated toward the east. Similar migration of extensional deformation was described by Balázs et al. (2016) in the eastern part of the Pannonian Basin.

Note, normal fault segments can be observed frequently in Late Miocene post-rift succession above remarkable syn-rift normal faults (e.g. above Viszák fault, F12, F6 on Appendix I; above F22 on Fig. 4.14). These segments represent most probably non-tectonic faults, which developed due to compaction induced differential subsidence. Similar non-tectonic structures were described in detail by Balázs et al. (2018) in the central part of Pannonian basin.

Another important Miocene structure of the study area is the Petri fault (Fig. 4.18; Appendix III). The fault shows a clear dextral off-set based on the dissected Cretaceous synclines and Paleogene Bak-nova graben (Appendix III). Miocene normal faults of the study area are limited from the south by the WNW-ESE trending Petri fault (Fodor personal comm.). South of the Petri fault the "syn-rift" Miocene succession shows the sign of syn-sedimentary folding (growth syncline, onlap surfaces on Fig. 4.18), therefore the Petri fault accommodates total extension of Miocene normal faults in the study area (Fodor personal comm.).

The Petri fault can be correlated with the WNW-ESE trending strike-slip faults of the central Transdanubian Range (e.g. Telegdi-Roth fault in Bakony). These dextral faults of the Bakony are interpreted by several authors as the result of an individual transpressional event with late Middle Miocene (Sarmatian) age (Kókay 1966; Mészáros 1983; Tari 1991; Márton and Fodor 2003). The example of the Petri fault may suggest that, these dextral faults represents just simple transfer faults related to Miocene syn-rift extension, and they are not the result of an individual transpressional phase.

According to Fodor et al. (2013a) and Nyíri (2017) the NE-SW trending Viszák fault (Appendix I, IIIa) represents a sinistral transfer fault, which can be considered as the conjugate pair of the Petri fault. The Viszák fault can be correlated to the ENE-WSW trending sinistral

faults of the Eastern Alps (e.g. Inntal fault; SEMP), which accommodate movement of major N-S trending normal faults (Brenner fault; Katschberg fault) bordering the Penninic Window (Linzer et al. 2002; Ortner et al. 2006).

5.3.5. Late Miocene – Quaternary inversion (D7)

Gentle folds are outlined based on Upper Miocene reflections on N-S sections (e.g. on Fig. 4.18). The lack of thickness variation suggests that the folding took place after deposition. According to Uhrin et al. (2009) south of the study area E-W trending folds controlled the deposition of youngest Late Miocene sediments. On the basis of that, the front of compressional deformation migrated continuously northward.

Late Miocene beds dip toward west on the E-W trending regional cross section (Appendix I), except the westernmost part of the section, where they dip toward east. Gently dipping Late Miocene reflections are truncated by recent surface, however, the related tilting has probably been started already during deposition (e.g. the height of Late Miocene clinoforms are decreasing eastward on Appendix I). Westward thickening of Late Miocene succession can be the result of several combined processes, such as different amount of post-rift thermal subsidence and compaction related subsidence. Additionally, the uplift of the Transdanubian Range (sensu stricto) resulted the westward tilting of Late Miocene beds; however, it is not well known which processes are responsible for this uplift. According to Tari (1994), Horváth & Cloetingh (1996) and Cloethingh & Burov (2006) uplift of the Transdanubian Range (s.s.) can be explained by crustal scale folding.

On the other hand, the present-day NE-SW trend of the Transdanubian Range is not perpendicular to recent N-S sigma 1 directions (Ruszkiczay-Rüdriger et al. 2018; Ruszkiczay-Rüdriger personal comm.), therefore, the uplift of the Transdanubian Range may have induced by asthenosphere dynamics (Ruszkiczay-Rüdriger et al. 2018).

6. Mesozoic geodynamic evolution of the Transdanubian Range: review of previous works and the introduction of my speculations

6.1. Nomenclature of the Mesozoic oceanic realms in the vicinity of the TR

During the investigated time span, the Transdanubian Range was part of the Adriatic plate, which was situated between Laurasia and Gondwana (Stampfli & Borel 2004, Handy et al. 2010, Schmid et al. 2008, Haas et al. 1995). Post-Variscan deformation and basin evolution of this plate was controlled by the opening and the closure of two oceanic realms. One of them is the Meliata-Vardar Ocean, which may form an embayment of the Neotethys-system, and from its break-up, it formed the eastern passive margin of the Adriatic plate. On the other hand, from the Middle Jurassic, the Adriatic plate was separated from European plate by the Piemont-Ligurian Ocean (southern branch of the Alpine Tethys) from the west (Stampfli & Borel 2004, Handy et al. 2010, Schmid et al. 2008, Haas et al. 1995).

Haas et al. (1995) and Schmid et al. (2008) consider Meliata-Vardar Ocean as an oceanic branch of the Neotethys. According to Maffione & Hinsbergen (2018) the Neotethys is a back-arc ocean of the Adria-ward subducting Paleotethys. In contrast, Stampfli & Borel (2004) use the term Neotethys in a totally different context. They positionated Neotethys south to the Adriatic plate, and correlate it to the present day Ionian Sea. This concept considers Meliata and Vardar Oceans as totally independent back-arc oceans in the hanging wall of the Europe-ward subducting Paleotethys, and they do not have direct contact with the Neotethys. In the present work, I follow the nomenclature and model of Schmid et al. (2008) and I consider Melitata and Vardar Oceans as part of the Neotethys system.

6.2. Opening of the Neotethys Ocean

Extensive Permian – Early Triassic transgression in the Circum-Pannonian Region (Haas et al. 1995), Permian extensional grabens (e.g. Southern Alps; Bertotti et al. 1993; Bernoulli 2007) and Permian – Early Triassic HT metamorphism (Eastern Alps; Schuster et al.

2004; Stüwe & Schuster 2010) all indicate the continental rifting of the Neotethys Ocean (Csontos & Vörös 2004). Oceanic break-up of the Meliata Ocean was accompanied by volcanism and the drowning of Anisian platforms (Gawlick et al. 2017).

After Anisian oceanic break up, the Neotethys Ocean reached approximately 800-1000 km width (Schmid et al. 2008; Gaina et al. 2013). The Transdanubian Range was most probably situated in the northwestern edge of this ocean. The geometry of this embayment is strongly variant in different reconstructions. For example, according to Haas et al. (1995) and Velledits (2006) the Northern Calcareous Alps and the Transdanubian Range were situated in opposite margins of Meliata Ocean, which had aproximatelly E-W trending spreading centers. In contrast, other authors depict these units as part of the same continental margin (e.g. Csontos & Vörös 2004; Gawlick et al. 2017). Paleomagnetic analyses of Triassic sheeted dykes showed that the investigated part of the Neotethys dilated along approximatelly N-S oriented spreading centers (Fig.6.2; Maffione & Hinsbergen 2018). The passive margins of the Meliata (Neotethys) ocean was probably highly irregular due to transform faults, which will have significant consequences on the evolution of later subduction (e.g. Argnani 2018).

6.3. Opening of the Alpine Tethys

6.3.1. Alpine correlation of Late Triassic extensional grabens of the study area

The Late Triassic extensional graben system, which is described in details in this work (Chapter 5.1), can be correlated to other areas of the Alpine region (Fig.6.1). Similar Late Triassic extensional back-platform basins are known from the western Southern Alps (Lombardy) and from the Bajuvaric nappes of the Northern Calcareous Alps. On the basis of Late Triassic facies boundaries (namely Hauptdolomite/Dachstein Limestone boundary), several authors argued that facies boundary pattern of the Transdanubian Range refers to Triassic paleogeographic connections with nowadays more westernly located units. The Triassic paleo-position of the Transdanubian Range is proposed between the Northern Calcareous Alps, the Drau Range and Southern Alps (Haas et al. 1995; Mandl 2000). Following this correlation, the described Late Triassic extensional basins formed a continuous extensional basin-system, which is referred as Kössen Basin in this study (Fig. 6.2). The remnants of Kössen Basin became strongly fragmented due to later strike-slip movements. The stratigraphical-sedimentological correlation of the remnants of Kössen Basin was the topic of several

publications (Haas et al. 1995; Gale et al. 2015; Rožič et al. 2009), therefore in this study I compare these basin remnants from a structural point of view.

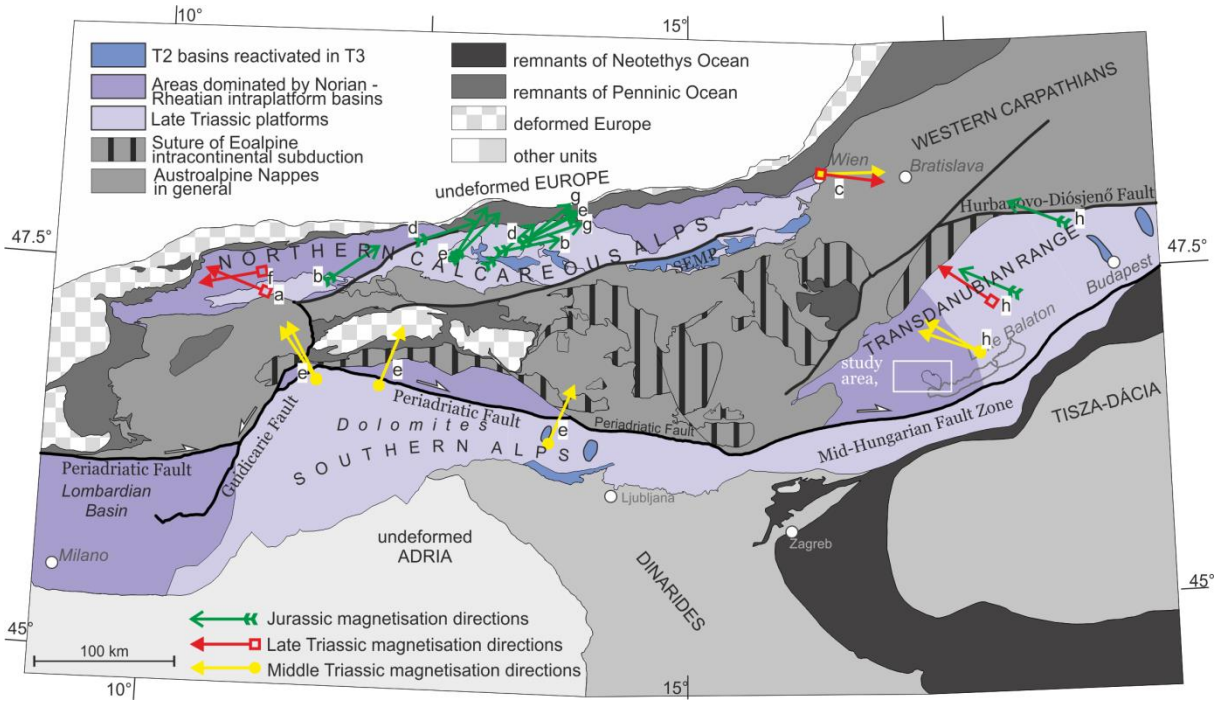

Fig.6.1: Tectonic map of the Eastern Alps and the Westerrn Carpathians (after Schmid et al. 2008), showing most important Late Triassic facies boundaries. Austroalpine cover nappes were coloured on the basis of their dominant Late Triassic depositional environment (basin/platform). The separation of the Kössen basin suggest approximately 500 km apparent dextral shear along the Periadriatic faults. Yellow arrows show the Middle, Rer arrow the Late Triassic and green aroows Jurassic magnetization directions based on the measurements of a) Becke and Mauritsch 1985, b) Channell et al. 1990, c) Gallet et al. 1998, d) Heer 1982, e) Mauritsch 1980, f) Mauritsch and Becke 1987, g) Mauritsch and Frisch 1978, h) Márton and Márton 1983.

The geometry of the Late Triassic extensional basins is well reconstructed in Lombardy, notwithstanding, it is strongly overprinted by south-vergent Cenozoic thrusts (Bertotti et al. 1993, Carminati et al. 2010, Jadoul et al. 2005). Approximately 10 km wide, N-S trending horsts and grabens were formed there (Bertotti et al. 1993), which show similar dimension to the Late Triassic grabens of the southwestern Transdanubian Range (Chapter 5.1, Appendix III.a). Some of the Norian–Rhaetian faults in the Lombardian region were still active during the Jurassic (Bertotti et al. 1993), which is also a common feature, compared to my observations. Back-rotating the units with the Mesozoic paleomagnetic data (Fig. 6.1. and references therein) the pre-orogenic normal faults of Lombardy and the study area had similar N-S strike (Fig. 6.2).

The pre-orogenic basins in the Northern Calcareous Alps were strongly overprinted by Cretaceous nappe stacking. Therefore, the Late Triassic basin geometry has not been reconstructed, yet. However, several authors propose the presence of Norian extensional deformation based on facies distribution and other sedimentological evidences (Satterley & Brandner 1995; Gawlick & Missoni 2013). An exception is the work of Behrmann & Tanner (2006), which reported the thickness variation of the Hauptdolomit along present-day N-S and

NE-SW trending faults based on restored cross-sections. According to this work, extensional deformation has been started already during the deposition of Hauptdolomit (latest Carnian – Norian), and formation of intraplatform basins (filled up by Plattenkalk and Kössen Marl) represents a later episode of Norian extension. That is what we see in the case of southwestern Transdanubian Range, since the thickness of the Hauptdolomit is changing apruptly in the study area as well (along F9 fault on Appendix IV.a). Considering paleomagnetic data (Fig.6.1 and references therein) the NE-SW striking segments reported by Behrmann & Tanner (2006) from the Northern Calcareous Alps also shows N-S paleo-strike, similarly, to the Late Triassic faults of the study area and the Southern Alps (Fig. 6.2).

6.3.2. Time constrains for the on-set of continental rifting within the Alpine Tethys

The Permian to Middle Triassic rifting of the Meliata Ocean was followed by another period of extensional deformation of the Adriatic plate during Late Triassic to Jurassic. Most authors relate this deformation to the continental rifting of the Alpine Tethys (Piemont-Ligurian Ocean), however, the exact timing of the onset of continental rifting is controversial in the different works. Suggestions range from Late Triassic to Middle Jurassic, therefore geodynamic background of Norian deformation of the Adriatic plate is still under debate. Bertotti et al. (1993) considered this deformation as first sign of rifting of Alpine Tethys. On the other hand, Cozzi (2000) suggests that Norian faults of the Southern Alps can be rather related to the opening of the Meliata (or Neotethys), although the distance is large, and extension within the passive margin, far from the sprading centres (mid-oceanic ridges) is not easy to explain.

Several recent works suggested that, continental rifting of the Penninic Ocean started just during Early Jurassic (Froitzheim & Manatschal 1996; Berra et al. 2009; Handy et al. 2010; Decarlis et al. 2015), but these models do not explain the observed Late Triassic extensional deformations, and interpret only Jurassic structures and sedimentological features.

Field observation and seismic interpretation of the present study shows that the main syn-rift sediments of the southwestern Transdanubian Range (Hauptdolomit, Rezi and Kössen Fm.) are Late Triassic in age, and extension was quasi continuous up to the Early and Middle Jurassic. This observation suggests, that the early, continental episode of the Penninic rifting should have started on the proximal Adriatic margin already during Norian, which has already been suggested by Bertotti et al. (1993) and Haas (1993b).

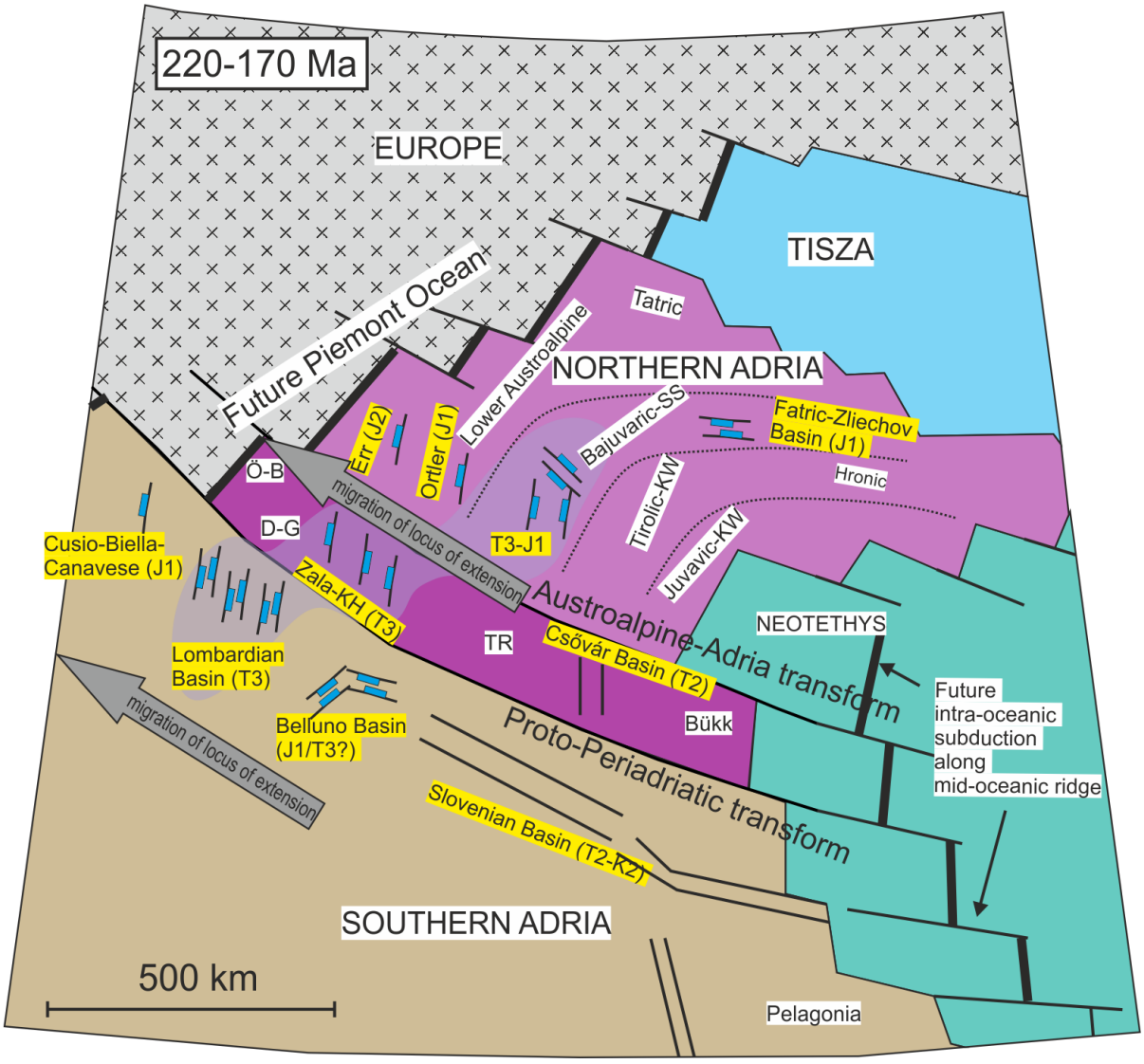

Fig.6.2. Late Triassic to Middle Jurassic reconstruction of the Transdanubian Range (TR) and neighbouring units applying plate-tectonic reconstruction of Handy et al. 2010 (redrawn, modified). Datails are based on the works of Schmidt et al. 1991, Haas et al. (1995), Froitzheim & Manatschal (1996), Mandl (2000), Gawlick et al. (1999) and Héja et al. (2018). The faults were simplified and back rotated based on the magnetization direction of Fig. 6.1.

6.3.3. Asymmetry of the Alpine Tethys rift

The Late Triassic Kössen basin was situated significantly to the east of the future Penninic Ocean, on the proximal Adriatic passive margin (Fig. 6.2). During Jurassic, westward migration of extensional tectonics was pointed out within the Austroalpine nappes (Froitzheim & Manatschal 1996). The proximal Adriatic margin was subject of dominantly Hettangian-Sinemurian extension, whereas in the distal Adriatic margin (later became proximal margin of the Alpine Tethys) Pliensbachian-Callovian extension occurred (Fig. 6.2). A similar situation was interpreted for the Southern Alps, west of Lombardy. In the Cusio-Biella-Canavese Zone extensional grabens formed just during the Early Jurassic (Decarlis et al. 2017). Coevally with that thining of lower crust started during Rhaetian at high temperature circumstance, and was

continuous during Early Jurassic, based on Zircon U-Pb dating of lower crustal shear zone of the Ivrea Zone (Langone et al. 2018).

In addition, further Early Jurassic normal faults and grabens are known east of the Lombardian basin (Fig. 6.2). In the Belluno Basin deep-water sedimentation and facies-differentiation started during the Early Jurassic. However, thickness changes suggest that significant extension initiated already during the Norian. However, in contrast with the Lombardian Basin, the sedimentation could keep pace with extension-related subsidence till the Early Jurassic (Masetti et al. 2012).

Most authors agree that the opening of the Piemont-Ligurian Ocean is the result of asymmetric rifting, where the Adriatic plate represents the lower plate, while the European plate is the upper plate (Froitzheim & Manatschal 1996). Alternatively, it is also possible that the rift system changed polarity along a major transform fault, such the paleo-Periadriatic fault (Decarlis et al. 2017). According to Lavier & Manatschal (2006) and Decarlis et al. (2017) the rift-system of the Alpine Tethys was initially symmetric, and it became asymmetric only after necking of the lithosphere. The transition from symmetric to asymmetric rifting occurred when the ductile lower or middle crust pinched out in the rift axis. According to Decarlis et al. (2017) the rift-system became asymmetric, when the residual crust did not contain any ductile level.

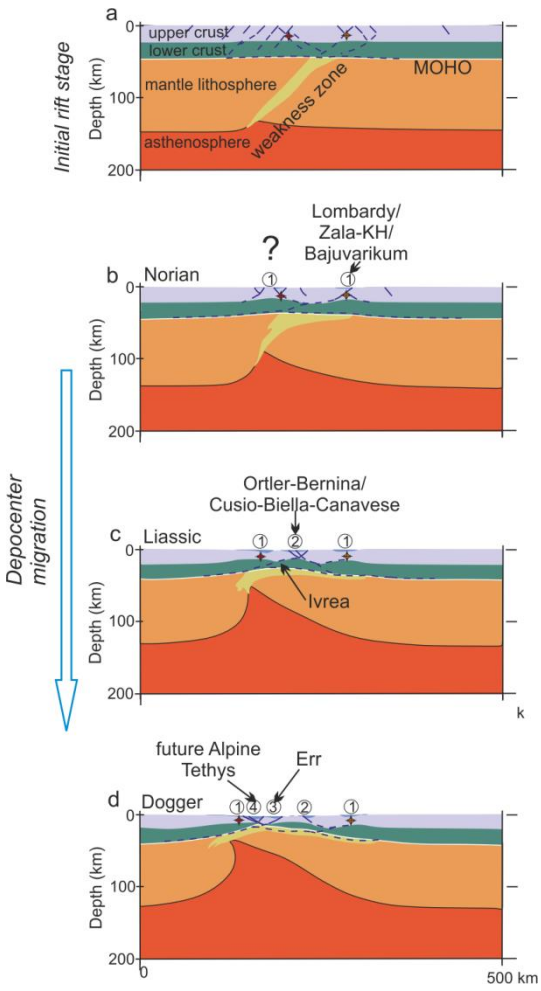

Fig.6.3. Applicaiton of the numerical model of Balázs et al. (2017) for explanation of migration of locus of Late Triassic to Jurassic extension within the lower plate of the Alpine Tethys (Adria). The location of some Alpine units are tentative, and correspond to documented migration of extension during the opening of Penninic Ocean. Purple stars represent reference points of the model.

As I mentioned, westward migration of extensional deformation started during Late Triassic on the Adriatic margin (Fig. 6.2). This feature is asymmetric, while such processes are not present, or not so pronounced on the adjacent European margin. Therfore, the rifting of the Alpine Tethys was initial asymmetric in my opinion (Héja et al. 2018). According to a numerical model of Balázs et al. (2017), the development of initially asymmetric rift-zones can be triggered by inherited weakness-zones (e.g. inherited suture; Fig. 6.3). In the present case the role of Variscan orogeny or its Permian collapse can arise (Manatschal et al. 2015). On the other hand, this relationship needs further investigation, and the description of Variscan orogeny beyounds the skope of this work.

After the mantle exhumation a magma-poor passive margin of the Alpine Tethys formed (Manatschal et al. 2015) during Middle Jurassic (170 Ma; Handy et al. 2010).

6.3.4. Transfer faults across the Adriatic plate

According to several plate tectonic model or paleogeographic reconstructions, the Adriatic plate was dissected by several transfer faults, which are related to the opening of the Meliata Ocean and Alpine Tethys (e.g. Mandl 2000; Schmid et al. 2008, Handy 2010). According to Mandl (2000) the Austroalpine-Adria transform was situated between the Northern Calcareous Alps and the Transdanubian Range, and probably the precursor of the Periadriatic Fault (proto-Periadriatic Fault in Handy et al. 2010; Iberia-Adria-Zone in Mandl 2000) was also active as a transfer fault, which separated the Southern Alps and the Transdanubian Range (Mandl 2000). In the following paragraph, I list the evidences for Mesozoic movements along these transfer faults.

The Periadriatic fault is one of the most important structural elements in Cenozoic evolution of the Alps (Handy et al. 2015), accommodating approximately 300 km of apparent Late Oligocene – Early Miocene dextral shear (Tari 1994; Fodor et al. 1998). On the other hand, Mesozoic facies markers (e.g, Late Triassic facies boundaries on Fig. 6.1) suggest larger, approximately 500 km of dextral off-set (Tari 1994), which suggest earlier movement along the Periadriatic fault. The Late Triassic succession is very similar in the Zala Basin (Transdanubian Range) and in the Lombardian Basin (Southern Alps). The main difference is the thickness of the basin-fill sediments. The thickness of Rhatian strata can reach 2500 m in the Lombardian Basin (Bertotti et al. 1993), while it is only few hundreds of metres thick in the Transdanubian Range. This difference in thickness suggests that, e.g, Rhaetian syn-sedimentary normal faults accommodated more significant extension in Lombardy than in the Zala Basin. Thus, larger upper crustal extension is proposed in the southern side of the Periadriatic fault, than on its northern side during Late Triassic (Fig. 6.2). This differential extension may have been accommodated in a transfer zone, which was possibly represented by the “proto”- Periadriatic fault. For similar reasons, the Periadriatic fault was an active transfer zone even earlier, during Permian to Middle Triassic.

Focusing on the northern boundary of the Transdanubian Range, a significant, aproximatelly 500 km shift of Late Triassic facies boundaries between TR and Northern Calcareous Alps occurs (Fig.6.1). It is important to note, that this 500 km off-set is appearent, and it was porbably significantly enlarged by Late Cretaceous and Miocene orogene parallel extension. This off-set can be explained by sinistral movement along the Austroalpine-Adria transform fault (Schmidt et al. 1991). Facies boundary shifts are not the only indications of strike-slip movement. Late Jurassic syn-sedimentary strike-slip faulting is supposed in the Northern Calcareous Alps based on stratigraphic (Frank & Schlager 2005) and structural

(Ortner 2017) evidences. This strike-slip tectonics can be probably strongly connected to sinistral movement on Austroalpine-Adria transform. Note, there are strongly different interpretations for the Late Jurassic tectonic evolution of the NCA, which suggest the onset of thrusting of continental margin even during Late Jurassic (e.g. Gawlick et al. 1999).

Time constraints for the Mesozoic transform faults

According to Stüwe & Schuster (2010) the mid-Cretaceous Eoalpine orogeny nucleated along the Austroalpine-Adria transfer fault, therefore its sinistral off-set must pre-dates Early Cretaceous (see Chapter 6.4.4). Based on this model, sinistral movement along the Adria-Austroalpine transform postdates Late Jurassic ophiolite obduction (see chapter 6.4.2), which give a Latest Jurassic – Earliest Cretaceous time span for left lateral strike slip faulting

According to Frank & Schlager (2006) transfer faults were active only during and after Late Jurassic. According to my oppininion, if transfer faults are present in a continental margin, their activity may have started even during continental rifting (Late Triassic in the present case). Therefore, I suppose that these major transfer faults were active during Norian (or even earlier, during the Neotethyan rifting) and Jurassic, and the first episodes of their activity pre-dates the obduction of Vardar ophiloites.

In plate-tectonic model of Handy et al. (2010) the proto-Periadriatic Fault is assigned as the major transfer fault. In contrast, I suggest, that tha Adria-Austroalpine transform has a much more significant role in the later evolution of the Adriatic plate (Stüwe & Schuster 2010; see chapter 6.4.4). In the following, I will refer to the two parts of Adriatic plate as Southern and Northern Adria, which were dissected by the Adria-Austroalpine transform fault.

6.4. Closure of Neotehtys

6.4.1. Intraoceanic subduction of the Neotethys

Coevally with the spreading of the Alpine Tethys, intraoceanic subduction started in the Neotethys Ocean. These two events were probably kinemathically related. By definition of Schmid et al. (2008) Melitata represented the lower oceanic part of the Adriatic plate in this intraoceanic subduction, while further spreading and production of juvenile oceanic crust took

place in the upper plate (Vardar). The subduction started during the late Early or Middle Jurassic, which is evidenced by radiometric ages from the metamorphic sole of the obducting oceanic lithosphere (Dimo-Lahitte et al. 2001), sedimentary age of the underlying mélange nappes (e.g. Đerić et al. 2007, Gawlick et al. 2017), and subduction-related blueschist-facies metamorphic rocks (Borka nappe) from the Western Carpathians, forming the same lower plate (Faryad & Henjes-Kunst 1997). Middle to Late Jurassic spreading of Vardar Ocean occurred in the hanging wall of this subduction as supra-subduction opening (Majer & Lugovic 1985, Ustaszewski et al. 2008). It is considered by many authors as back-arc basin (Stampfli & Borel 2004; Plašienka 2018).

6.4.2. Obduction related down-bending versus imbrication of the distal passive margin during Late Jurassic

After consumption of the oceanic crust in the intra-oceanic subduction of the Neotethys, the attenuated Adriatic continental margin entered the subduction zone. Onset of obduction of the Vardar Oceanic crust onto the Adriatic margin occurred during Kimmeridgian (Schmid et al. 2008). The obducted ophiolite nappe sheet is well preserved in the Dinarides and Hellenedis, while completely missing in those units, which derives from the Norhern Adria. That is why the role of obduction in the Late Jurassic evolution of the Northern Calcareous Alps, Transdanubian Range and Western Carpathians is much more questionable.

Late Jurassic redeposition of sediments was described by Gawlick et al. (1999) in the Northern Calcareous Alps. They interpreted the Late Jurassic successions of the so called ‘radiolarian flysch basins’ as foreland and piggy-back basins connected to obduction and imbrication of the distant passive margin. In this model, nappe tectonics reached the Northern Calcareus Alps as early as Oxfordian. In contrast, according to Frank & Schlager (2005) and Ortner et al. (2017) Late Jurassic evolution of the Northern Calcareous Alps can be better explained by strike-slip tectonics (See Chapter 6.3.4.).

Several authors arose the possibility of Late Jurassic thrusting in the Transdanubian Range based on sedimentary breccias from the central (Bakony) and northeastern (Gerecse and Pilis) TR (Csontos & Vörös 2004, Palotai et al. 2006a and b). However, the clasts of these breccias are redeposited from local sources, and no structural significance is available for Late Jurassic thrusting. According to structural analyses of Fodor et al. (2013b) Late Jurassic breccias of the Gerecse (northeastern Transdanubian Range) can be rather considered as talus breccias at the feet of normal faults. Following this concept, these normal faults developed due

to down-bending of the distal lower plate below obduction related load. In this model, the northeastern Transdanubian Range was in a distal foreland (bulge) position during that time.

Meliata unit of the Western Carpathians is interpreted by Schmid et al. (2008) as sub-ophiolitic mélange. Plašienka (2018) placed Melita unit in a different geodynamic context: in the model of Plašienka (2018) Meliata units thrusted onto northern Adriatic margin due to Late Jurassic collision of southern Adriatic plate (including Transdanubian Range and Bükk) and northern Adriatic plate (Centreal Western Carpathians). In my opinion, this collision took place only during middle Cretaceous Eoalpine orogeny (See Chapter 6.4.4) and Late Jurassic – Early Cretaceous evolution of the Western Carpathians and Northern Calcareous Alps was rather determined by Adria-ward migration of obduction related compression.

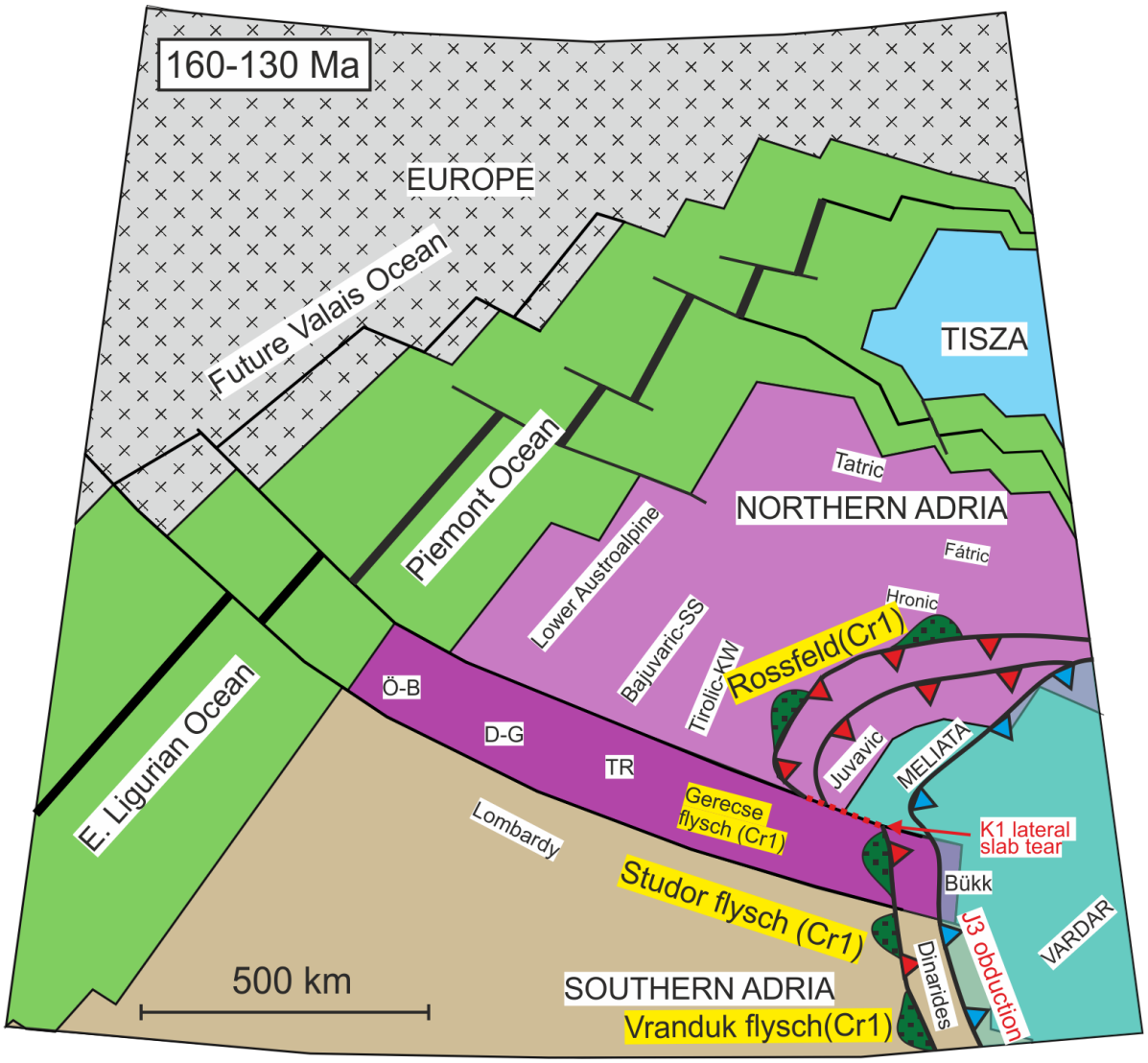

Fig.6.4. Middle Jurassic to Early cretaceous reconstruction of the Transdanubian Range (TR) and neighbouring units applying plate-tectonic reconstruction of Handy et al. 2010 (redrawn, modified). Datails are based on the works of Schmid et al. 2008; Stüwe & Schuster 2010; Argnani 2018; Tari 1994; Goričan et al. 2018; Faupl and Wagreich 2000; Jablonsky 1993 and Plasienka 1997, 2018.

6.4.3. Lateral tearing of Meliata slab during Late Jurassic – Early Cretaceous

As it was mentioned in the previous chapter, ophiolite obduction occurred in the Dinarides during Kimmeridgian-Berriasian (Schmid et al. 2008). Dinaric ophiolites are sealed by Tithonian-Berriasian (152-140 Ma) limestone, which shows the end or signifigant slowdown of obduction related deformation (Gawlick et al. 2017). The locus of deformation shifted into the northern Adriatic margin (north of the Austroalpine-Adria transform), which is indicated by for example the on-set of Early Cretaceous syn-orogenic sedimentation (Rossfeld Formation). Ophiolite obduction was followed by imbrication of the southern Adriatic crust south of the Austroalpine-Adria transform as well: thrusting and low-grade metamorphism of several lower-plate units occurred during Early Cretaceous (Schefer, 2012, Porkoláb et al. 2018).

Due to the existing sinistral Adria-Austroalpine transfer, the leading edge of southern Adriatic continental margin situated more to the east than the eastern edge of northern Adria. Consequently, the southern Adriatic margin (Dinarides) was underthrusted earlier below the Vardar oceanic crust during Kimeridgian-Beriasian. In my opinion this obductional zone continued northward into a intraoceanic subduction zone at that time east of the Northern Calcareous Alps. Since the subduction was driven at least partly by roll-back, subduction of the southern Adriatic plate during Kimeridgien made slow down the subduction in the Dinarides. In contrast of that, north of the Adria-Austroalpine transform still oceanic lithosphere was subducted at time, which enhanced further roll-back and latereal tearing along Adria-Austroalpine transform. Therfore, obduction-related deformation retreated faster along the northern Adriatic margin than along the slowdown Dinaridic (southern Adriatic) one during Earliest Cretaceous. This model is very similar to the model of Argani (2018) who proposed lateral tearing of Meliata slab north of the Pelagonian microcontinent (it represents southeastern Adria in Schmid et al. 2008). Similar lateral tearing due to the subduction of a rectangular continental margin or a microcontinent was described by analog model of Guillaume et al. (2013).

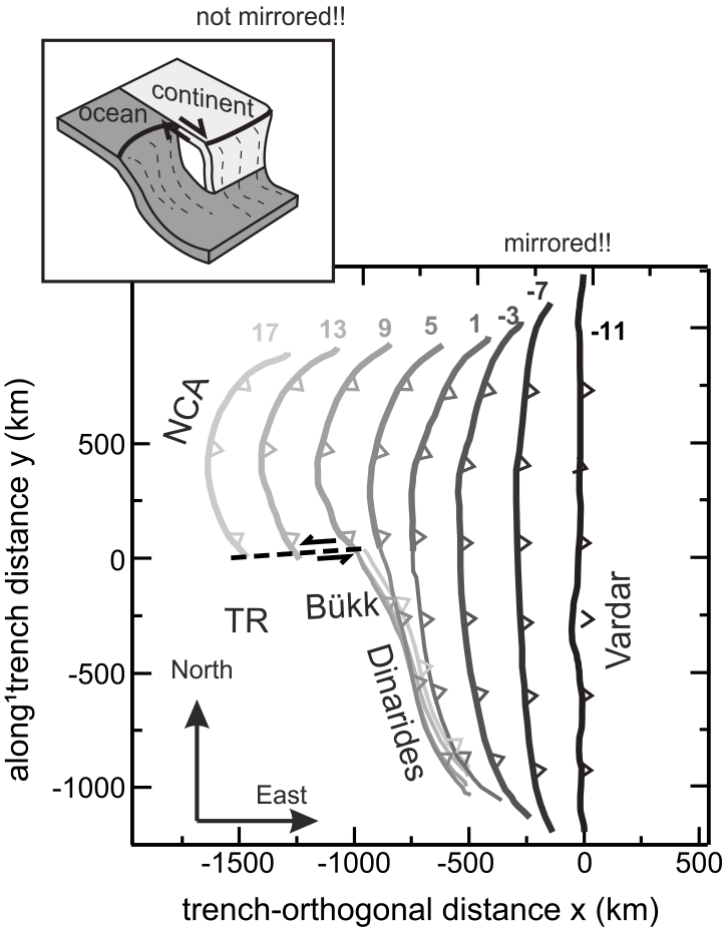

Fig.6.5. Applicaiton of the analogue model of Guillaume et al. (2013): "The dynamics of laterally variable subductions". The authors made an experiment to model subduction of two different materials, a positively buoyant one (defined as *continental* lithosphere) and a negatively buoyant one (defined as *oceanic* lithosphere). Thick and thin lines indicates locations of oceanic and continental subductions, respectively. Numbers at the top indicate the time after subduction of continental lithosphere in Myr. Dashed line indicates the location of the tear fault. Insets show 3-D sketches of the subducting plate shape at the end of experiment.

Subduction of dissected Meliata slab probably continued during Early Cretaceous, because foreland basins developed in the front of obducted ophiolites all along the eastern Adriatic margin. Adriatic continental crust was imbricated in the front of and below the ophiloitic nappe, meaning that the related deformation reached more internal part of the Adriatic plate. The syn-orogenic Valanginian to Aptian Rossfeld Basin of the Tirolic nappes (Faupl and Wagreich 2000), and Hautrivian syn-orogenic sediments of the Hronic nappe (Jablonsky et al. 1993; Plasienka et al. 1997; 2018) probably represented one continuous foreland basin sytem related to the Meliata slab. Similar Early Cretaceous foreland basin system evolved on the southern Adriatic plate too: the Berriasian to Aptian Gerecse basin of the northeastern Transdanubian Range (Szives et al. 2018) can be correlated to Valanginian to Early Albian Studor flysch in the Southern Alps (Goričan et al. 2018), and Valanginian to Cenomanian Vranduk flysch in the Dinarides (Goričan et al. 2018). Common feature of these Early Cretaceous foreland basins is the significant amount of detrial chromium-spinell (Császár &

Árgyélán 1994), which confirms that these basins are related to obducted ophiolite, and represent post-obducction deformation. The shift of facies, the locus of deposition and also the migration of the related forebulge (Mindszenty et al. 1994; Mindszety et al. 2000; Tari 1994) suggest that they were Adria ward migrating foreland basins in the front of overriding ophiolites.

6.4.4. Eoalpine orogeny

The Eolpine high-pressure belt is a rock series, containing high-pressure or even ultra high-pressure metamorphic rocks in the Eastern Alps (Janák et al. 2004). It forms part of the Koralpe-Wölz nappe system, which is part of Upper Austroalpine nappes (Schuster et al. 2004, Schmid et al. 2008). The age of the high- to ultra-high pressure metamorphism is around 100-90 Ma (Thöni 1999), which arises a lot of questions concerning geodynamic connections. This middle Cretaceous age is too young to be directly related to the subduction of the Neotethys ocean or adjacent attenuated continental margin (related blueschist ages are around 155 Ma; Faryad & Henjes-Kunst 1997), and too old to relate it to the subduction of the Alpine Tethys (on-set of subduction started at 94 Ma based on Handy et al. 2010). The high-pressure metamorphic rocks of the Eoalpine high-pressure belt have continental crustal material as protolith, and they lack any material of oceanic origin. Therefore, the existence of an individual intracontinental subduction zone was proposed (Janák et al. 2004, Stüwe & Schuster 2010). The earlier work suggested, that this intracontinental subduction zone developed along a Permian continental rift zone (Janák et al. 2004). According to Stüwe & Schuster (2010), the Eaolpine subduction zone devoleped along the sinistral Austroalpine-Adria transfer, and it was triggered by juxtaposition of continental lithospheres with strongly different buoyancy.

Besides different buoyancy, the pull of Meliata slab and the Aptian spreading of Valais Ocean could also trigger the development of Eoalpine intracontinental subduction (Handy et al. 2010). In this concept, the intracontinental subduction zone was continuing westward into the Ligurian (western part of Alpine Tethys) intraoceanic subduction zone (Fig.6.6). Based on that, the intracontinental subduction represented a connection between the northern Meliata and Ligurian slab (Fig.6.6).

The present-day Silvretta-Seckau and Koralpe-Wöltz nappe systems represented the lower plate of this intracontinental subduction zone (Schuster et al. 2004; Schmid et al. 2008). The Northern Calcareous Alps, which was imbricated into a thin-skinned thrust and fold belt during the orogeny, may represent the detached sedimentary cover of the above mentioned

basement nappes (Fig.6.7; Schmid et al. 2004). The Ötztal-Bundschuch and the Drauzug-Gurktal nappe systems formed the upper plate of this Eoalpine suture zone (Schuster et al. 2004, Schmid et al. 2004). The investigated Transdanubian Range is part of the Drauzug-Gurktal nappe system (Fig.6.7; Schmid et al. 2008).

Thin-skinned deformation is a characteristic feature of the lower plates during subduction, since sediments can be easily sheared off from their original basement on a subducted lower plate. In contrast, development of thin-skinned deformation is much rarer on upper plate position, where thick-skinned tectonics is widespread. The most common exception is an upper plate retro-wedge, where thin-skinned thrust and fold belt can more frequently develop (e.g. Subandean belt - Echavarria et al. 2003). Recently suggested thick-skinned folding of the Transdanubian Range (See chapter 5.2.4.1.) strenghten its upper plate position within the Eoalpine orogeny. Therefore, Eoalpine structural evolution of the Transdanubian Range (upper plate position) and the Northern Calcareous Alps (sheard off from the lower plate) can not be directly correlated. This new possibility challenges the model of Linzer and Tari (2012) suggesting similar tectonic position during the middle Cretaceous deformation.

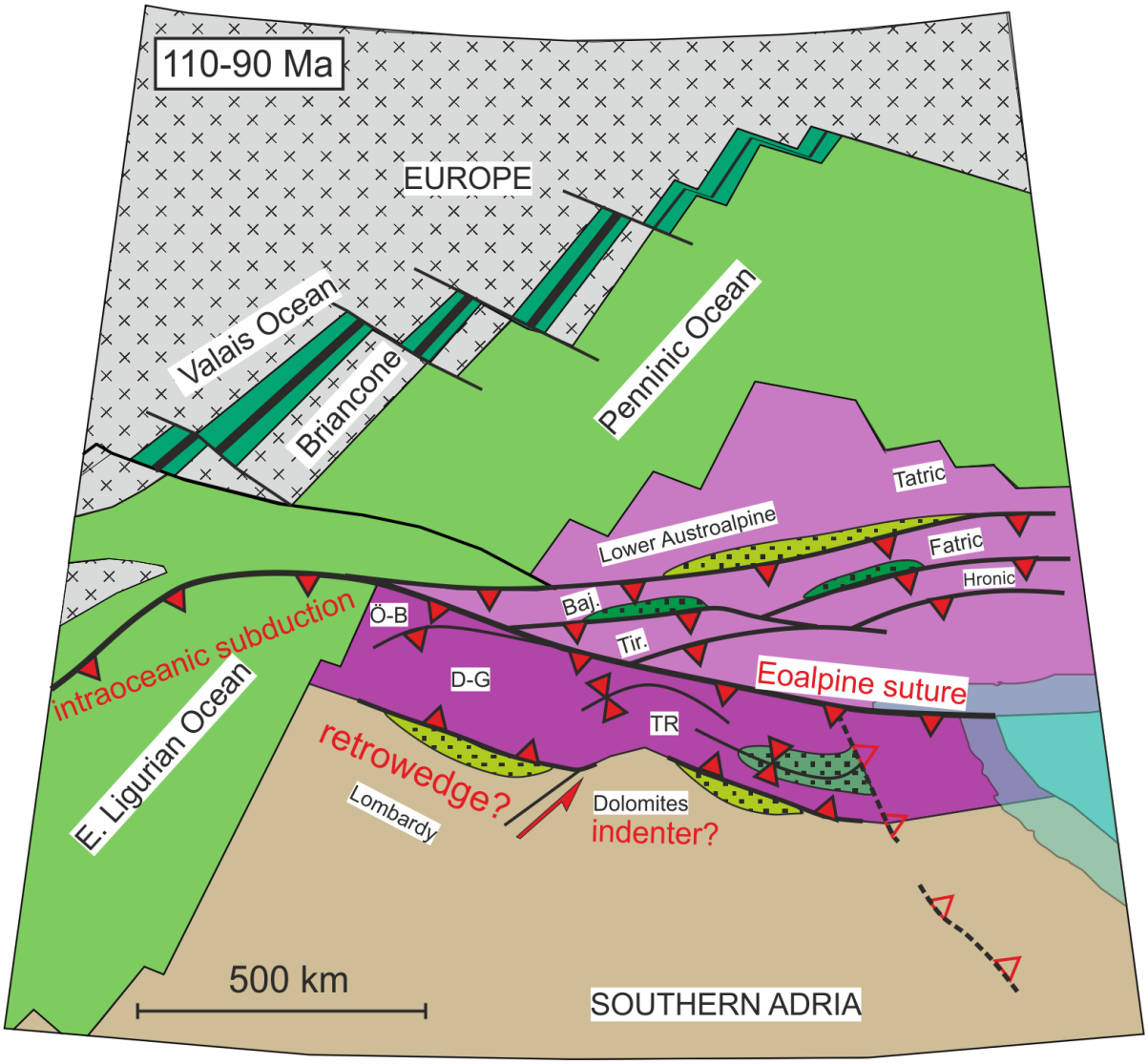

Fig.6.6: Early to Late Cretaceous reconstruction of the Transdanubian Range (TR) and neighbouring units applying plate-tectonic reconstruction of Handy et al. 2010 (redrawn, modified). Datails are based on the works of Ortner 2003 and Plašienka 2018.

Time constraints for the onset of subduction

Stüwe & Schuster (2010) dated the onset of the Eoalpine intracontinental subduction by the deposition of Rossfeld Fm. (135 Ma). However, peak metamorphism of Eoalpine high pressure metamorphic rocks show much younger age around 100-90 Ma (Thöni 1999). Based on the evolution of Transdanubian Range the timeout between the obduction-related (and post-obduction) versus the "Austroalpine" deformations is Aptian/Albian (Tari 1994; Tari & Horváth 2010; Sasvári 2009; Szives et al. 2018).

First-order salient of the Transdanubian Range: result of indentation of the Dolomites?

As it was discussed in Chapter 5.2.5., first-order salient of the southwestern Transdanubian Range was explained by Tari (1994) as interference of an Aptian ENE-WSW and an Albian NNW-SSE compressional events. I suggest an alternative explanation for the formation of this arcuate thrust belt (salient), since I propose only one phase folding before the Senonian (Chapter 5.2.7).

Formation of salients is often influenced by former basin geometry or indentation of a rigid block (basin-controlled and indenter-controlled salient of Marschak 2004, respectively). In the following, I try arguing for a new model on the formation of the salient of the southwestern Transdanubian Range. If we accept the Late Triassic facies boundaries as marker lines in the two sides of the Periadriatic-Balaton fault (Fig. 6.1), then the central Transdanubian Range (Bakony) was situated north of the Dolomites, whereas the study area – including the Keszthely Hills and Zala Basin – laid north of Lombardy (Haas et al. 1995). These facies boundaries were shifted significantly by the dextral Periadriatic fault during Late Oligocene – Early Miocene (e.g. Tari 1994, Kázmér & Kovács 1985).

Indentation of Dolomites as a rigid block may explain the development of first order salient of the Transdanubian Range. This model implies Cretaceous activity of a transfer fault between the Dolomites and Lombardy (proto-Giudicarie fault; Fig. 6.7), which is proposed by several authors (e.g. Doglioni 1987; Doglioni & Bosselini 1987; Schönborn 1992; Castellarin et al. 2006). Note, that exact timing motion along the Giudicarie fault is controversial; e.g, Pomella et al. (2012) proposed only Miocene movement on this structure, since Cretaceous bending of the Periadriatic fault by the Guidicarie Fault makes Late Oligocene – Early Miocene movement along the Periadriatic fault problematic.

However, if we accept the former model, the Lombardian flysch and Aptian-Albian flysch of the Dolomites (Castellarin et al. 2006) possibly represent retro-wedge foreland basins of the Eoalpine orogeny (Fig. 6.7). Somewhat different interpretation was given by Zanchetta et al. (2012), who considered these deposits as retro-wedge of the Penninic oceanic subduction.

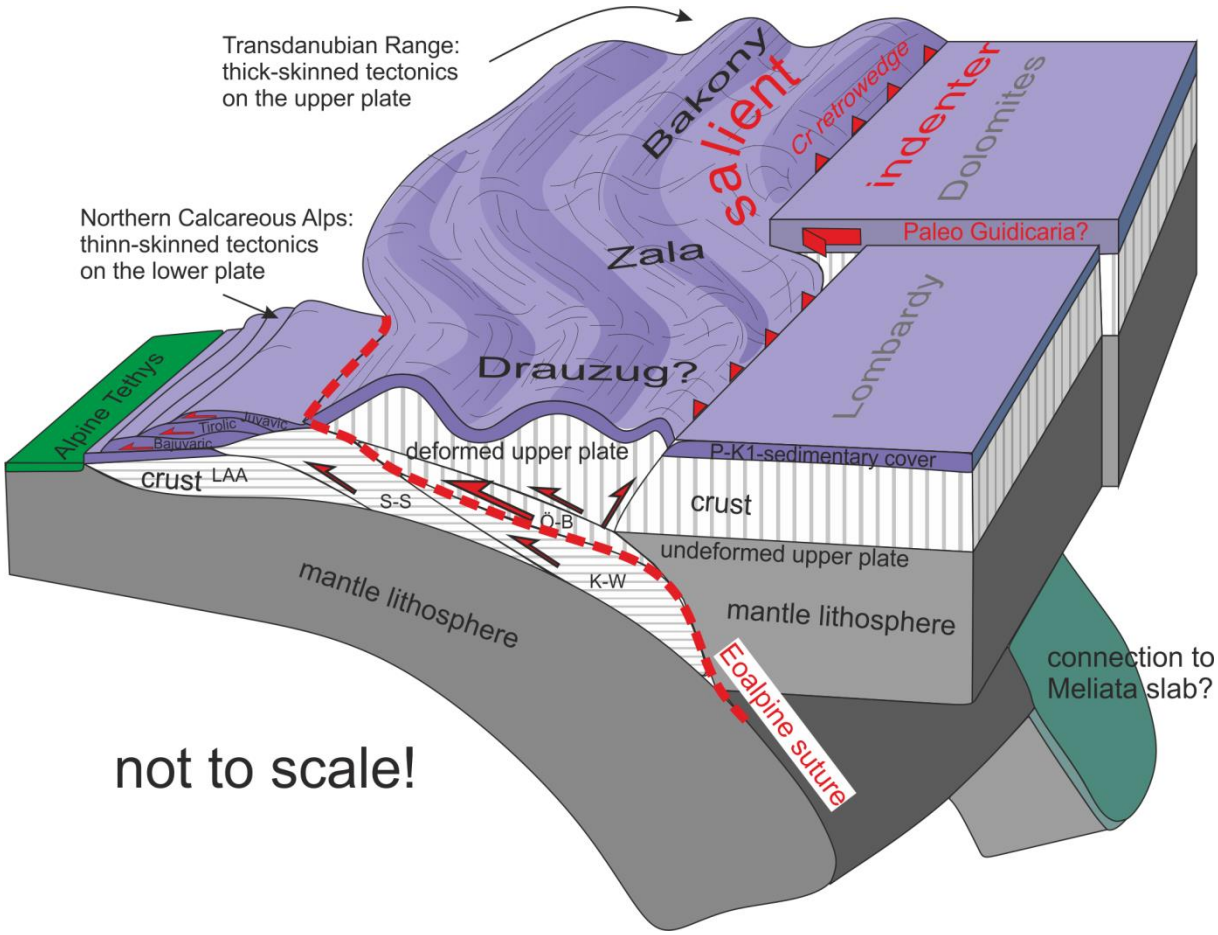

Fig.6.7: Schematic model interpreting the first order salient of the SW Transdanubian Range as an indenter controlled salient. This indenter is possibly represented by the rigid block of Dolomites. The figure is highly influenced by Stüwe and Schuster (2010)

6.5. Onset of subduction of the Alpine Tethys

Syn-orogenic sediments show gradual N-NW-ward migration of the deformation front in the Northern Calcareous Alps and Western Carpathians during Cretaceous (Ortner 2003, Plašienka 2018; Fig.6.6). During Cenomanian or Turonian, the compressional deformation front may have reached the eastern part of Alpine Tethys, and the onset of Alpine Tethys subduction started north of the Eastern Alps and Western Carpathians (e.g, Handy et al. 2010). Previous models supported the presence of two single slabs of the Penninic and the Meliata subduction (e.g, Neubauer et al. 2000). Recent models calculate with one single slab regarding Meliata and Penninic subduction (Stüwe & Schuster 2010; Handy et al. 2010; Plašienka 2018). According to these models, subduction shifted from the Meliata Ocean into the Alpine Tethys by the decoupling of Adriatic mantle lithosphere from the imbricating crustal part (Fig.6.8a; Stüwe & Schuster 2010; Handy et al. 2010; Plašienka 2018).

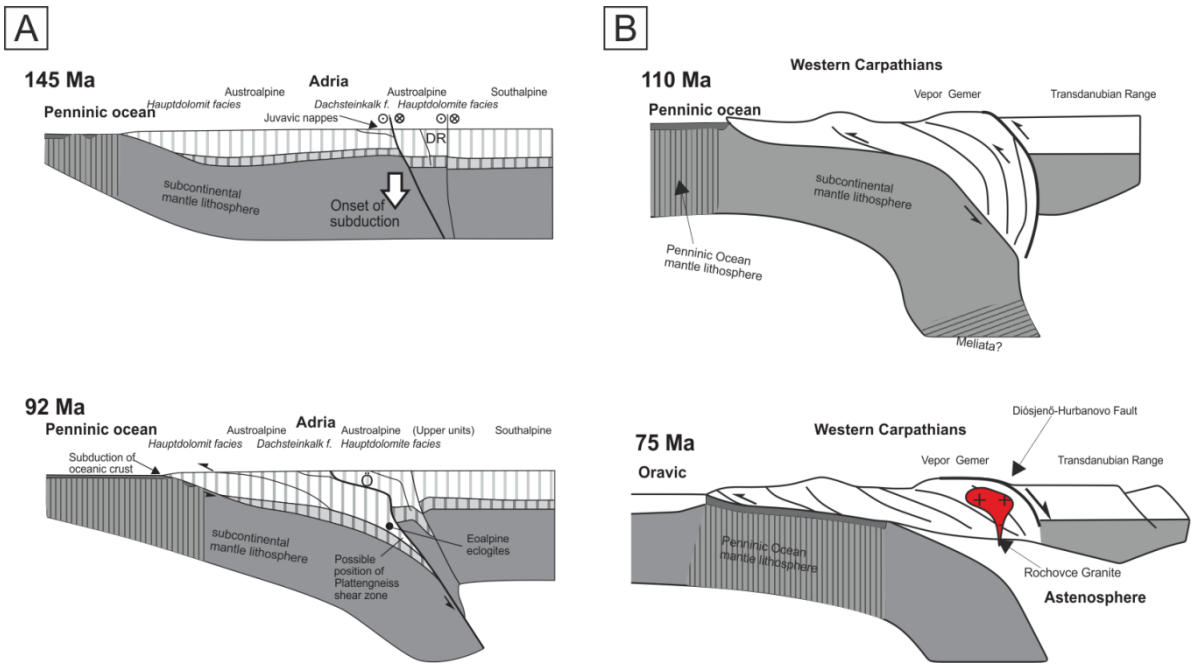

Fig.6.8: Cretaceous evolution of the Eastern Alps – Western Carpathians (a) decoupling of mantle lithosphere under the Eastern Alps (Stüwe & Schuster 2010) (b) supposed delamination of mantle lithosphere under the Western Carpathians (Plašienka 1997; and this work, applying the figure of Brun & Faccena 2008).

Late Cretaceous delamination of mantle lithosphere below the Western Carpathians has been already suggested by Plašienka et al. (1997). I would like to follow this idea, which can explain several features of the Carpathian orogenic wedge (Fig.6.8b). It is common, that metamorphic rocks exhume in the backstop of a thust-wedge due to delamination of subducted mantle lithosphere (Brun & Faccena 2008). In this case, metamorphic rocks exhume along a steep hinterland dipping normal fault, which was initially a thrust (Brun & Faccena 2008). In my view the Diósjenő-Hurbanovo fault, which represents the northern boundary of the Transdanubian Range (Fig. 1.4), may represent similar steep hinterland-dipping normal fault / reactivated thrust (Fig.6.8b) (smilar scenario was postulated by Fodor & Koroknai 2000). The Veporic unit exhumed in the footwall of this steeply south dipping fault during Senonian (90 to 80 Ma) based on thermochronlogy (Koroknai et al. 2001). Note, Jeřabek et al. (2012) explained the exhumation of the Veporic dome by the underplating of Fatric basement.

On the other hand, delamination-model explain the presence of Late Cretaceous plutons in the Western Carpathians. After delamination of lithospheric mantle the crust comes into contact with asthenosphere which often lead to magmatism. The Late Cretaceous (82-75.6 Ma) Rochovce Granite (Hraško et al. 1999; Poller et al. 2001) in the Veporic nappes may relate to this process (Plašienka et al. 1997).

Subduction of the delaminated continental lithosphere continued with the underthrusting of the oceanic lithosphere of the Alpine Tethys. Consumation of the oceanic

domain lead to to the underthrusting of Oravic microcontinent during Maastrichtian – Paleogene time (Plašienka 2018). I suggest, that Maastrichtian – Paleogene uplift of the Transdanubian Range can be explained by this process, which did not cause any significant deformation in the Transdanubian Range, since it was situated in distal hanging-wall position with respect to the subduction.

7. Conclusions

1) I recognized the widespread presence of Norian to Jurassic normal faults in the southwestern Transdanubian Range based on seismic and field data (D1 phase). The related normal faults are mostly WNW-ESE striking. Normal faulting started probably during the deposition of Hauptdolomit, and this process progressively led to the formation of Late Triassic intra-platform basins. are The graben infill of these intra-platform basins represent the main syn-tectonic deposits: namely the middle – late Norian Rezi Dolomite and the latest Norian - Rheatian Kössen Marl. Extensional deformation continued during Jurassic, however I suggest that the main pre-orogenic extension has been occurred during the Late Triassic (~225–201 Ma).

2) The observed Late Triassic extensional graben system is the first sign of the onset of the Alpine Tethys continental rifting. The investigated graben is situated on the proximal Adriatic margin of the future Alpine Tethys, and the locus of extension migrated gradually westward, toward the distal Adriatic margin, and this migration finally led to the opening of the Alpine Tethys during Middle Jurassic. According to my view this continental rifting was initially asymmetric, where Adria represented the lower plate, as it was suggested by a number of publications.

3) One of the most significant deformations of the study area was the D2 folding during the Albian to Coniacian time interval (113–87 Ma). My results suggest that there was only one phase of folding during the Cretaceous in the southwestern Transdanubian Range. The direction of compression was E-W in the Zala Basin and Keszthely Hills. The oblique, NE-SW and NW-SE strike of certain D2 folds and thrusts of the study area are the result of complex interplay between different structures, namely Late Triassic–Jurassic normal faults and the Cretaceous shortening. Structural inheritance of D1 normal faults and their connecting relay ramps induced the deviation of fold trends by dragging and formation of local folds on relay ramps

4) The main synclines of the Zala Basin (Nagylengyel syncline and Sümeg-Devecser syncline) appear as thick-skinned buckling folds, in contrast to previous interpretations, which interpreted them as trailing synclines of west-vergent fault-bend folds (Tari & Horváth 2010; Fodor et al. 2013b). Seismic evidences show that the Bakonybél thrust is a fold-accommodation fault (out-of-syncline thrust) in the sense of Mitra (2002). I suggest similar origin for most of the observed

thrusts in the study area (Nagylengyel thrust, Litér thrust). The development of these second-order structures is partly influenced by space problems, which derived from confined flexural-slip folding which was prohibited in massive dolomitic lithology.

4) Using balanced cross section, a rough estimation of Cretaceous shortening was carried out which suggest just approximately 10 % of internal shortening in the western part of the Transdanubian Range. This values suggests a significantly less amount off deformation, that was previously suggested (e.g, Tari and Horváth 2010)

5) Post-folding Senonian sedimentation was accompanied by syn-sedimentary NE-SW extension (D3). The study area was not reached by significant deformation during Latest Cretaceous – Early Paleogene timespan, since there is no significant angular discordancy between Senonian and Paleogene deposits. The Paleogene Bak-nova graben can be interpreted as a transtensional half graben (D4). I gave two possible explanations for the observed geometry. In the first case NE-SW striking D4 faults represent major normal faults, and WNW-ESE striking normal faults are breached relay ramps. In the second scenario, NE-SW striking normal faults are transfer faults, which accommodate normal faulting on WNW-ESE striking faults.

6) Narrow thrust-and-fold belt formed in the southern part of the study area which is coeval and strikes sub-parallel with the Late Oligocene–Early Miocene dextral Mid-Hungarian Shear Zone (D5). The observed NNW vergent thrust belt could develop due to strain partitioning.

7) The Miocene (D6) Zala half graben developed in the hanging-wall of the Baján detachment fault from 18 Ma. A huge roll-over anticline is outlined based on the base of Miocene horizon. This roll-over is dissected by a number of second-order Miocene normal faults, which have NW-SE strike. These normal faults are limited to the area north of the WNW-ESE striking Petri fault, which can be considered as a dextral transfer fault, which is accommodating movement on Miocene normal faults. South of the Petri fault the Miocene deformation can be characterized by gentle syn-sedimentary folding (D6). Due to the northward movement of the Adria indenter, the inversion of the Pannonian Basin is active since Late Miocene, which led to the formation of E-W trending gentle folds (D7).

8. Summary

The aim of the present study was the investigation of the structure of the Zala Basin and the Keszthely Hills, with particular attention to its Mesozoic deformations. The study area is the southwestern part of the Transdanubian Range unit, which represents the upper-most nappe of the Austroalpine nappe-stack (Tari 1994).

The Transdanubian Range suffered repeated pre-orogenic extension based on mostly thickness variations and facies-changes of the Triassic – Jurassic succession (Galácz & Vörös 1972; Galácz 1988; Budai & Vörös 2006; Haas 1993; Csillag et al. 1995; Vörös & Galácz 1998). However, the geometry of related map-scale faults, and their influence on later, Cretaceous shortening were just poorly identified.

In order to investigate this topic, I made structural observation in the Keszthely Hills, where Mesozoic basement is exposed. I compared surface data with interpretation of 2D and 3D seismic data from the Zala Basin, where Mesozoic basement is under thick Cenozoic cover.

In this work, I made a first attempt to identify map-scale pre-orogenic normal faults in the southwestern Transdanubian Range based on modern 2D seismic sections, 3D cubes, and surface observation. I put in a new light the geometry of Cretaceous compressional structures: in this new interpretation inherited, pre-existing normal faults (D1) have increased role. My results suggest, that there was only one phase of folding during Cretaceous. The direction of compression was E-W in the Zala Basin and Keszthely Hills. The oblique, NE-SW and NW-SE trend/strike of D2 folds and thrusts is the result of structural inheritance of the D1 normal fault – relay ramp system. I considered main synclines of the Zala Basin (Nagylengyel syncline and Sümeg-Devecser syncline) as thick-skinned buckling folds, in contrast with previous interpretations, which interpreted them as trailing synclines of west-vergent fault bend folds (Tari and Horváth 2010; Fodor et al. 2013a).

I illustrated the structural evolution of the study area by a restored E-W regional cross-section across the Keszthely Hills and Zala Basin. This restored section represents a first attempt of creating balanced cross-section regarding the Transdanubian Range.

9. Összefoglalás

Doktori kutatásom célja a Keszthelyi-hegység és a Zalai-medence szerkezetének vizsgálata volt, különös tekintettel annak mezozós deformációira. A kutatási terület a Dunántúli-középhegységi Egység délnyugati részén helyezkedik el. Ez a szerkezeti egység az Ausztroalpi takarórendszer legfelső helyzetű takarójaként értelmezhető (Tari 1994).

Számos szerző feltételez ismételt, pre-orogén extenziót a triász-júra időintervallumra (Galácz & Vörös 1972; Galácz 1988; Budai & Vörös 2006; Haas 1993; Csillag et al. 1995; Vörös & Galácz 1998). Ezen munkák többnyire üledékföldtani adatokra támaszkodnak, a kapcsolódó pre-orogén szerkezetek létét az üledékképződési környezetek laterális változékonysága alpján feltételezik a fent említett szerzők. Azonban a kapcsolódó triász-jura vetők geometriája nincs pontosan leképezve, és ezen korai vetőknek a későbbi kréta gyűrődésre gyakorolt hatása sem kellőképpen ismert a Dunátúli-középhegységben.

Ezen problémák vizsgálata képezi a fő célját jelen dolgozatnak. Munkám során szerkezeti megfigyeléseket tettem, kombinált szeizmikus és felszíni adatok alapján. Többek között felszíni megfigyeléseket végeztem a Keszthelyi-hegységben, ahol a mezozós közetek felszínre bukkanak, míg a szomszédos Zalai-medencében 2D és 3D szeizmikus adatok alapján vizsgáltam a mezozós aljzat felépítését.

Munkám során elsőként tettem kisérletet mezozós, pre-orogén normál vetők azonosítására szeizmikus szelvényeken a Dunántúli-középhegységi Egység területén. Új megvilágításba helyeztem a kréta során létrejött gyürt-pikkelyes szerkezeteket is. Az észlelt változatos redőirányokat (ÉK-DNY tól ÉNY-DK-ig) a pre-orogén normálvetők menti elhajlásként értékeltem. Ez alapján, véleményem szerint csak egy-fázisú gyűrődés érte a kutatási területet.

Új, az eddigi modellektől eltérő geometriai modellt dolgoztam ki a Zalai-medence térképi-léptékű szinklinálisait illetően. Ezalapján az észlelt szinklinálisok a Variszkuszi aljzatot is ért szimpla gyűrődés során jöttek létre, és nem rámpa-antiklinálisok háton-hordott szinklinálisai ként értelmezhetőek (Tari and Horváth 2010; Fodor et al. 2013a).

A kutási terület szerkezet fejlődését kiegyenlített földtani szelvényeken szemléltettem. Munkám során megtettem az első lépéseket egy, a Dunántúli-középhegység szerkezetét taglaló kiegyenlített szelvény létrehozásában.

10. References

Albert G. (2000). Az Északi-Bakony gyűrődései. (in hungarian, translated title: Folding of the Northern Bakony) *MSc thesis, manuscript, Eötvös University, Dept. of General and Applied Geology*, 89 p.

Alsop, G.I., Marco, S. (2011). Soft-sediment deformation within seismogenic slumps of the Dead Sea Basin. *Journal of Structural Geology* 33, 4, 433–457. http://doi.org/10.1016/j.jsg.2011.02.003

Angelier, J. (1990). Inversion of field data in fault tectonics to obtain the regional stress - III. A new rapid direct inversion method by analytical means. *Geophysical J. International*, 103, 363–373.

Argnani, A. (2018). Subduction evolution of the Dinarides and the Cretaceous orogeny in the Eastern Alps: Hints from a new paleotectonic interpretation. *Tectonics*, 37, 621–635. https://doi.org/10.1002/2017TC004632

Árgyelán, B. G. (1996). Geochemical investigations of detrital chrome spinels as a tool to detect an ophiolitic source area (Gerecse Mountains, Hungary). *Acta Geologica Hungarica*, 39/4, 341-368.

Bada G. (1994). A paleofeszültségtér fejlődése a Gerecse hegység és kelet-délkeleti előterének területén. *MSc thesis, Eötvös University*, Dept. of Applied and Environmental Geology, 147 p.

Badics, B., Vető, I. (2012). Source rocks and petroleum systems in the Hungarian part of the Pannonian Basin: The potential for shale gas and shale oil plays. *Marine and Petroleum Geology*, 31, 53–69.

Balázs, A., Matenco, L., Magyar, I., Horváth, F., Cloetingh, S., (2016). The link between tectonics and sedimentation in back-arc basins: new genetic constraints from the analysis of the Pannonian Basin. *Tectonics*, 35, 1526–1559. http:// dx.doi.org/10.1002/2015TC004109.

Balázs, A., Burov, E., Matenco, L., Vogt, K., Francois, T., Cloetingh, S. (2017). Symmetry during the syn- and post-rift evolution of extensional back-arc basins: The role of inherited orogenic structures. *Earth and Planetary Science Letters*, 462, 86–98. https://doi.org/10.1016/j.epsl.2017.01.015

Balázs, A., Magyar, I., Matenco, L., Sztanó, O., Lilla, T., & Horváth, F. (2018). Morphology of a large paleo-lake : Analysis of compaction in the Miocene- Quaternary Pannonian Basin. *Global and Planetary Change*, 171, 134–147. https://doi.org/10.1016/j.gloplacha.2017.10.012

Báldi, T. (1986). Mid-Tertiary Statigraphy and Paleogeographic Evolution of Hungary. *Akadémiai Kiadó*, Budapest, 293 p.

Balla, Z. (1987). Tertiary paleomagnetic data for the Carpatho-Pannonian region in the light of Miocene rotation kinematics. *Tectonophysics* 139, 67–98.

Balla, Z. (1988a). On the origin of the structural pattern of Hungary. *Acta Geologica Hungarica* 31, 1-2, 53–63.

Balla, Z. (1988b). A Kárpát-Pannon régió nagyszerkezeti képe a felsőeocénben és e kép hatása a mezozoós Tethys-rekonsrukciókra (Late Eocene tectonic pattern of the Carpatho-Pannonian region and its bearing on the Mesozoic reconsturctions of Tethys). *Földtani Közlöny*, 118, 11–26. (in Hungarian with English abstract)

Balla, Z. (1989). A Diósjenői diszlokációs öv újraértékelése (Reevaluation of the Diósjenő dislocation zone). *Annual Report of the Eötvös L. Geophysical Institute of Hungary for 1987*, 45–57. (in Hungarian with English abstract)

Balla, Z. Dudko, A. (1989). Large-scale Tertiary strike-slip displacements recorded in the structure of the Transdanubian Range. *Geophysical Transactions*, 35, 3–64.

Balla, Z. (1999). On the tectonic subdivisions of Hungary. *Annual Report of the Geological Institute of Hungary from 1992–93/II*, 9–14.

Balla, Z., Dudko, A., Redler-Tátrai, M. (1987). A Közép-Dunántúl fiatal tektonikája földtani és geofizikai adatok alapján (Young tectonics of Mid-Transdanubia based on geological and geophysical data, in Hungarian). *Annual Report of the Eötvös L. Geophys. Institute for 1986*, 74–94. (in Hungarian with English abstract)

Bárány, M. (2004). A jura–kréta határ gravitációsan átülepített képzõdményei az Északi-Gerecsében. *Diplomamunka, ELTE Általános és Történeti Földtani Tanszék,* 74 p.

Becke M, Mauritsch HJ (1985) Die Entwicklung der Nördlichen Kalkalpen ans palaomagnetischer Sicht, Archiv für Lagerstattenforschung der Geologisehen Bundesanstalt 6:113-116.

Behrmann, J., H., Tanner, D., C., (2006). Structural synthesis of the Northern Calcareous Alps, TRANSALP segment. *Tectonophysics*, 414, 225–240.

Benedek, K. (2002). Paleogene igneous activity along the easternmost segment of the Periadriatic-Balaton Lineament. *Acta Geologica Hungarica*, 45, 359-371.

Benedek, K., Pécskay, Z., Szabó, Cs., Jósvai, J., Németh, T. (2004). Paleogene igneous rocks in the Zala basin (Western Hungary): link to the Paleogene magmatic activity along the Periadriatic Lineament. *Geologica Carpathica*, 55, 1, 43–50.

Bergerat, F., Collin P., Y., Ganzhorn, A., C., Baudin, F., Galbrun, B., Rouget, I., Schnyder J. (2011). Instability structures, synsedimentary faults and turbidites, witnesses of a Liassic seismotectonic activity in the Dauphiné Zone (French Alps): A case example in the Lower Pliensbachian at Saint-Michel-en-Beaumont. *Journal of Geodynamics*, 51, 5, 344–357. https://doi.org/10.1016/j.jog.2010.10.003

Bernoulli, D. (2007). The pre-Alpine geodynamic evolution of the Southern Alps: a short summary. *Bulletin fuer Angewandte Geologie*, 12, 2, 3-10.

Berra, F., Galli, M., T., Reghellin, F., Torricelli, S., Fantoni, R., (2009). Stratigraphic evolution of the Triassic-Jurassic succession in the Western Southern Alps (Italy): The record of the two-stage rifting on the distal passive margin of Adria. *Basin Research*, 21, 3, 335–353.

Bertotti, G., Picotti, V., Bernoulli, D., Castellarin, A., (1993). From rifting to drifting: tectonic evolution of the South-Alpine upper crust from the Triassic to the Early Cretaceous. *Sedimentary Geology*, 86, 1–2, 53–76. http://doi.org/10.1016/0037-0738(93)90133-P

Billi, A., Salvini, F., (2003). Development of systematic joints in response to flexure-related fibre stress in flexed foreland plates: The Apulian forebulge case history, Italy. *Journal of Geodynamics*, 36, 4, 523–536. https://doi.org/10.1016/S0264-3707(03)00086-3

Bohn, P. (1979). The Regional Geology of the Keszthely Mountains. *Geologica Hungarica Series Geologica*, 19, 197 p.

Boldogh T. (2003). Az Észak-Zalai-medence senon képződményeinek szekvencia-sztratigráfiája. *MSc thesis, Eötvös University,* Department of Applied and General Geology, 87 p. (in Hungarian)

Bonini, M., Sani, F., Antonielli, B. (2012). Basin inversion and contractional reactivation of inherited normal faults: A review based on previous and new experimental models. *Tectonophysics*, 522–523, 55–88. https://doi.org/10.1016/j.tecto.2011.11.014

Böckh J. (1872). A Bakony déli részének földtani viszonyai. I. (in hungarianTranslated title: Geology of the southern Bakony part 1.) *Földt. Int. Évk.*, 2, 2, 31–166.

Bradley, D., Hanson, L. (1998). Paleoslope Analysis of Slump Folds in the Devonian Flysch of Maine. *The Journal of Geology*, 106, 3, 305–318. http://doi.org/10.1086/516024

Brandes, C., Tanner, D., C. (2014). Fault-related folding: A review of kinematic models and their application, *Earth-Science Reviews*, 138, 352-370. https://doi.org/10.1016/j.earscirev.2014.06.008.

Broglio Loriga, C., Góczán, F., Haas, J., Lenner, K., Neri, C., Oravecz-Scheffer, A., Posenato, R., Szabó, I., Tóth-Makk, Á., (1990). The Lower Triassic sequences of the Dolomites (Italy) and Transdanubian Mid-Mountains (Hungary) and their correlation. *Mem. Sci. Geol.*, 42, 41–103.

Brun, J., P., Sokoutis, D. (2007). Kinematics of the Southern Rhodope Core Complex (North Greece) *Int J Earth Sci (Geol Rundsch)*, 96, 1079. https://doi.org/10.1007/s00531-007-0174-2

Brun, J., P., Faccenna, C., (2008). Exhumation of high-pressure rocks driven by slab rollback. *Earth and Planetary Science Letters*, 272, 1–7. doi:10.1016/j.epsl. 2008.02.038.

Brun, J., P., Sokoutis, D., Tirel, C., Gueydan, F., Van Den Driesschea, J., Beslierf, M., O., (2017). Crustal versus mantle core complexes *Tectonophysics*, 10, 1016/j.tecto.2017.09.017.

Budai, T., Koloszár, L. (1987). Stratigraphic investigation of the Norian-Rhaetian formations in the Keszthely Montains (in Hungarian with English abstract). *Földtani Közlöny*, 117, 121–130.

Budai, T., Kovács, S. (1986). Contributions to the stratigraphy of the Rezi Dolomite Formation (Metapolygnathus Slovakensis (conodonta, Upper Triassic) from the Keszthely Mts (W Hungary)). *Annual Report of the Geological Institute of Hungary from 1984*, 175-191.

Budai, T., Vörös, A. (1992). Middle Triassic history of the Balaton Highland: extensional tectonics and basin evolution. *Acta Geologica Hungarica*, 35, 3, 237–250.

Budai, T., Vörös, A. (1993). The Middle Triassic events of the Transdanubian Central Range in the frame of the Alpine evolution. *Acta Geologica Hungarica*, 36, 1, 3–13.

Budai, T., Vörös, A. (2006). Middle Triassic platform and basin evolution of the Southern Bakony Mountains (Transdanubian Range, Hungary). *Rivista Italiana di Paleontologia e stratigrafia*, 112, 3, 359-371.

Budai, T., Lelkes, Gy., Piros, O., (1993). Evolution of Middle Triassic shallow marine carbonates in the Balaton Highland (Hungary). *Acta Geologica Hungarica*, 36, 1, 145–165.

Budai, T., Császár, G., Csillag, G., Dudko, A., Koloszár, L., Majoros, Gy. (1999a). Geology of the Balaton Highland. Explanation to the Geological Map of the Balaton Highland (1:50 000). *Geological Institute of Hungary*, Budapest

Budai, T., Csillag, G., Dudko, A., Koloszár, L. (1999b). Geological Map of the Balaton Highland (1:50 000). *Geological Institute of Hungary*, Budapest

Budai, T., Csillag, G., Vörös, A., Dosztály, L. (2001). Középső– és késő–triász platform- és medencefáciesek a Veszprémi-fennsíkon (Middle to Late Triassic platform and basin facies of the Veszprém Plateau (Transdanubian Range, Hungary). *Földtani Közlöny*, 131, 1–2, 37–70. (in Hungarian with English abstract).

Budai T., Fodor L., Sztanó O., Kercsmár Zs., Császár G., Csillag G., Gál N., Kele S., Kiszely M., Selmeczi I., Babinszki E., Thamóné Bozsó E., Lantos Z. (2018) A Gerecse hegység földtana – magyarázó a Gerecse hegység tájegységi földtani térképéhez (Geology of the Gerecse Mountains – Regional map series of Hungary Explanatory Book to the Geological Map of the Gerecse Mountains) *Geological Institute of Hungary*, (1:50000). 491 p.

Butler, R., W., H., Tavarnelli, E., Grasso, M. (2006). Structural inheritance in mountain belts: An Alpine–Apennine perspective. *Journal of Structural Geology*, 28, 1893–1908.

Carminati, E., Cavazza, D., Scrocca, D., Fantoni, R., Scotti, P., Doglioni, C. (2010). Thermal and tectonic evolution of the southern Alps (Northern Italy) rifting: Coupled organic matter maturity analysis and thermokinematic modeling. *AAPG Bulletin*, 94, 3, 369–397. http://doi.org/10.1306/08240909069

Castellarin, A., Vai, G., B., Cantelli, L. (2006). The Alpine evolution of the Southern Alps around the Giudicarie faults: a Late Cretaceous to Early Eocene transfer zone. *Tectonophysics*, 414, 203-223.

Channell JET, Brandner R, Spieler A (1990) Mesozoic paleogeography of the Northern Calcareous Alps—Evidence from paleomagnetism and facies analysis. Geology 18(9): 828–831. https://doi.org/10.1130/0091-7613(1990)018<0828:MPOTNC>2.3.CO;2

Cloethingh, S., Burov, E. (2011). Lithospheric folding and sedimentary basin evolution: a review and analysis of formation mechanisms. *Basin Research*, Wiley, 23, 3, 257-290.

Colpron, M., Warren, M., J., Price, R., A. (1998). Selkirk fan structure, southeastern Canadian Cordillera: tectonic wedging against an inherited basement ramp. *Bulletin of the Geological Society of America*, 110, 8, 1060–1074. https://doi.org/10.1130/00167606(1998)110<1060:SFSSCC>2.3.CO;2

Corrado, S., Di Bucci, D., Naso, G., Faccena, C. (1998). Influence of palaeogeography on thrust system geometries: an analogue modelling approach for the Abruzzi–Molise (Italy) case history. *Tectonophysics*, 294, 473-453.

Cozzi, A. (2000). Synsedimentary tensional features in Upper Triassic shallow-water platformcarbonates of the Carnian Prealps (northern Italy) and their importance as palaeostress indicators. *Basin Research*, 12, 133-146.

Császár G. (1986). Dunántúli-középhegységi középső-kréta képződmények rétegtana és kapcsolata a bauxitképződéssel. *Geologica Hungarica series*, 23, 295 p.

Császár G. (1995). A gerecsei és vértes-előtéri kréta kutatás eredményeinek áttekintése. (An overview of the Cretaceous research in the Gerecse and the Vértes Foreland.) *Általános Földtani Szemle*, 27, 133–152.

Császár G., Árgyelán B., G. (1994). Stratigraphic and micromineralogic investigations on Cretaceous Formations of the Gerecse Mountains, Hungary and their palaeogeographic implications. *Cretaceous Research*, 15, 417-434.

Császár G., Peregi Zs. (2001). Középső-jura korszakbeli mega-hasadékkitöltés a Vértes DNy-i peremén. (in hungarian, translated title: Middle Jurassic filled mega-crevice on the southern edge of Vértes.) *Földtani Közlöny*, 131, 3-4, 581–584.

Császár, G., Haas, J., Jocháné-Edelényi, E. (1978). A Dunántúli-középhegység bauxitföldtani térképe, 1:100 000. *Magyar Állami Földtani Intézet*,

Csicsek Á., L. (2015). A Veszprémi-fennsík Kádárta és Öskü közötti területének szerkezeti elemzése, különös tekintettel a kréta korú rátolódások vizsgálatára. (in hungarian, English title: Structural analisys of the Veszprém plateau between Kádárta and Öskü, with emphasize on Cretaceous thrusting.) *MSC thesis, ELTE Általános és Alkalmazott Földtani Tanszék*, 114 p.

Csicsek, Á. L. & Fodor, L. 2016: Középső-triász képződmények pikkelyeződése a bakonyi Öskü környékén (Imbrication of Middle Triassic rocks near Öskü (Bakony Hills, Western Hungary). *Földtani Közlöny,* 146,4, 355–370.

Csillag G., Haas J. (1993). Veszprémi Márga Formáció, Sándorhegyi Formáció, Edericsi Formáció. (in hungarian, translated title: Veszprém marl formation, Sándorhegy formation and Ederics formation.) In Haas J. (ed.): Magyarország litosztratigráfiai alapegységei. Triász. (in hungarian, translated title: Base units of the hungarian litostratigraphy. Triassic.). *Geological Institute of Hungary*, Budapest, 60-67.

Csillag, G., Budai, T., Gyalog, L., Koloszár, L. (1995). Contribution to the Upper Triassic geology of the Keszthely Mountains (Transdanubian Range), western Hungary. *Acta Geologica Hungarica*, 38, 2, 111–129.

Csillag G., Sztanó O., Magyar I., & Hámori Z., (2010). A Kállai Kavics települési helyzete a Tapolcai-medencében geoelektromos szelvények és fúrási adatok tükrében (Stratigraphy of the Kálla Gravel in Tapolca Basin based on multi-electrode probing and well data). — Földtani Közlöny, 140/2, 183–196.

Csontos, L. (1995). Cenozoic tectonic evolution of the Intra-Carpathian area: a review. *Acta Vulcanol.*, 7, 1–13.

Csontos, L., Nagymarosy, A. (1998). The Mid-Hungarian line: a zone of repeated tectonic inversion. *Tectonophysics*, 297, 51–72.

Csontos, L., Vörös, A. (2004). Mesozoic plate tectonic reconstruction of the Carpathian region. *Palaeogeography, Paleoclimatology, Palaeoecology*, 210, 1–56.

Csontos, L., Sztanó, O., Pocsai, T., Bárány, M., Palotai, M., Wettstein, E. (2005). Late Jurassic-Early Cretaceous Alpine Deformation Events int he Light of Redeposited Sediments. *Geolines*, 19, 29-31.

Csontos L., Tari G., Bergerat F., Fodor L. (1991). Evolution of the stress fields in the Carpatho-Pannonian area during the Neogene. *Tectonophysics*, 199, 73-91.

Csontos, L., Nagymarosy, A., Horváth, F., Kovac, M. (1992). Tertiary evolution of the intra-Carpathian area: a model. *Tectonophysics*, 208, 221-241.

De Vicente, G., Vegas, R., Muñoz,-Martín, A., Van Wees, J., D., Casas-Sáinz, A., Sopeña, A., Fernández-Lozano, J. (2009). Oblique strain partitioning and transpression on an inverted rift: The Castilian Branch of the Iberian Chain. *Tectonophysics*, 470, 3–4, 224–242. https://doi.org/10.1016/j.tecto.2008.11.003

Debacker, T., N., Dumon, M., Matthys, A. (2009). Interpreting fold and fault geometries from within the lateral to oblique parts of slumps: A case study from the Anglo-Brabant Deformation Belt (Belgium). *Journal of Structural Geology*, 31, 1525–1539. doi:10.1016/j.jsg.2009.09.002

Decarlis, A., Beltrando, M., Manatschal, G., Ferrando, S., Carosi, R. (2017). Architecture of the Distal Piedmont-Ligurian Rifted Margin in NW Italy: Hints for a Flip of the Rift System Polarity. *Tectonics*, 36, 11, 2388–2406. https://doi.org/10.1002/2017TC004561

Decarlis, A., Manatschal, G., Haupert, I., Masini, E. (2015). The tectono-stratigraphic evolution of distal, hyper-extended magma-poor conjugate rifted margins: Examples from the Alpine Tethys and Newfoundland Iberia. *Marine and Petroleum Geology*, 68, 54–72.

Đerić, N., Gerzina, N. Schmid, S., M., (2007). The age of the Jurassic radiolarian chert formation from the Zlatar Mountains (SW Serbia). *Ophioliti*, 32, 101–108.

Dimo-Lahitte, A., Monié, P., Vergély, P., (2001). Metamorphic soles from the Albanian ophiolites: Petrology, 40Ar/39Ar geochronology, and geodynamic evolution. *Tectonics*, 20, 1, 78-96.

Doglioni, C., (1987). Tectonics of the Dolomites (Southern Alps, Northern Italy). *Journal of Structural Geology*, 9, 181-193.

Doglioni, A. Bosellini, C. (1987). Eoalpine and Mesoalpine tectonics in the Southern Alps. *Geol. Rundsch.*, 76, 735–754.

Dohr, G. (1981). Geophysikalische Untersuchungen im Gebiet der Tiefbohrung Vorderriß 1. *Geologica Bavarica*, 81:55-64. 6 München.

Dudko A. (1991). A Balaton-felvidék szerkezeti elemei. Kirándulásvezető. *Kézirat. MÁFI*, Budapest. 1-61.

Dudko A. (1996). A Balaton-felvidék szerkezete (fedetlen földtani térkép alapján) (Translated title: Structure of the Balaton Highland (based on pre-Quaternary geological map)). manuscript, *Geological Institute of Hungary*, Budapest

Echavarira, L., Hernández, R., Allmandinger, R., Reynolds, J. (2003). Subandean thrust and fold belt of northwestern Argentina: Geometry and timing of the Andean evolution. AAPG Bulletin, v. 87, no. 6, pp. 965–985

Elliott, D., (1983). The construction of balanced cross sections. *Journal of Structural Geology*, 5, 101.

Erdélyi Fazekas, J. (1940). Hegyszerkezeti megfigyelések a Balatonfelvidéken (Jegyzőkönyv az 1940. június 5-i szakülésről). (in hungarian, translated title: Structural observations in the Balaton highlands) *Földtani Közlöny*, 70, 204–205.

Erdélyi Fazekas, J. (1943). A Balaton-felvidék geológiai és hegyszekezeti viszonyai a veszprémi fennsíkon és Vilonya környékén. (in hungarian, translated title: The geological and structural relationship of the Balaton Highlands, at Vilonya and the Veszprém plateau.) *MÁFI Évkönyv*, 36, 3–29.

Epard, J., L., Groshong, R., H. (1995). Kinematic model of detachment folding including limb rotation, fixed hinges and layer-parallel strain. *Tectonophysics*, 247, 85–103.

Farrell, S., G. (1984). A dislocation model applied to slump structures, Ainsa Basin, South Central Pyrenees. *Journal of Structural Geology*, 6, 727-736.

Faryad, S., W, Henjes-Kunst, F. (1997). Petrological and K-Ar and 40Ar-39Ar age constraints for the tectonothermal evolution of the high-pressure Meliata unit, Western Carpathians (Slovakia). *Tectonophysics*, 280, 141–156.

Faupl, P.,Wagreich M. (1996). Basin analysis of the Gosau Group of the Northern Calcareous Alps (Turonian-Eocene, Eastern Alps). In: Oil and Gas in Alpidic Thrust Belts and Basins of Central and Eastern Europe (Ed. by WESSELY, G. & LIEBL, W.). EAGE Spec. Publ. 5, 127–135.

Fodor, L. (2008). Structural geology. In: Budai, T., Fodor, L. (eds.): Geology of the Vértes Hills. Explanatory book to the Geological Map of the Vértes Hills 1:50000. *Magyar Állami Földtani Intézet*, 145–202, 282–300.

Fodor L. (2010). Mezozoos-kainozoos feszültségmezők és törésrendszerek a Pannon-medence ÉNy-i részén – módszertan és szerkezeti elemzés. *Doctoral thesis of the Hungarian Academy of Sciences*, manuscript, 129p.

Fodor, L. & Koroknai, B. 2000: Tectonic position of the Transdanubian Range unit: A review and some new data. *Vijesti Hrvatskoga geološkog društva,* 37, 38–40.

Fodor L., Magyari Á., Fogarasi A., Palotás K. (1994). Tercier szerkezetfejlõdés és késõ paleogén üledékképzõdés Budaihegységben. A Budai-vonal új értelmezése. *Földtani Közlöny*, 124, 129–305.

Fodor, L., Jelen B., Márton, M., Skaberne, D., Car, J., Vrabec M. (1998). Miocene-Pliocene tectonic evolution of the Slovenian Periadriatic fault: Implications for Alpine-Carpathian extrusion models. *Tectonics*, 17, 690–709.

Fodor, L., Csontos, L., Bada, G., Gyorfi, I., Benkovics, L. (1999). Tertiary tectonic evolution of the Pannonian Basin System and neighbouring orogens: a new synthesis of palaeostress data. *Geological Society, London, Special Publications*, 156, 295-334. 10.1144/GSL.SP.1999.156.01.15.

Fodor, L., Balogh, K., Dunkl, I., Pécskay, Z., Koroknai, B., Trajanova, M., Vrabec, M., Vrabec, M,. Horváth, P., Janák, M., Lupták, B., Frisch W., Jelen, B., & Rifelj, H. (2003). Structural evolution and exhumation of the Pohorje-Kozjak Mts., Slovenia. *Annales Universitatis Scientiarum Budapestiensis de Rolando Eötvös Nominatae*, 35, 118–119.

Fodor, L., Gerdes, A., Dunkl, I., Koroknai, B., Pécskay, Z., Trajanova, M., Horváth, P., Vrabec, M., Jelen, B., Balogh, K., Frisch, W. (2008). Miocene emplacement and rapid cooling of the Pohorje pluton at the Alpine–Pannonian-Dinaridic junction, Slovenia. *Swiss Journal of Earth Sciences*, 101, 1, 255–271. DOI 10.1007/s00015-008-1286-9

Fodor L., Uhrin A., Palotás K., Selmeczi I., Tóthné Makk Á., Rižnar, I., Trajanova, M., Rifelj, H., Jelen B., Budai T., Koroknai B., Mozetič, S., Nádor A., Lapanje A. (2013a). Geological and structural model of the Mura–Zala Basin and its rims as a basis for hydrogeological analysis (in Hungarian with English abstract). *Annual report of the Geological Institute of Hungary*, 2011, 47–92.

Fodor, L., Sztanó, O., Kövér, Sz. (2013b). Mesozoic deformation of the northern Transdanubian Range (Gerecse and Vértes Hills). *Acta Mineralogica-Petrographica*, Field guide series, 31, 1-52

Fodor, L., Héja, G., Kövér, Sz., Csillag, G., Csicsek, Á., L., (2017). Cretaceous deformation of the south-eastern Transdanubian Range Unit, and the effect of inherited Triassic–Jurassic normal faults. Pre-conference Excursion Guide, 15th Meeting of the CentralEuropean Tectonic Studies Group (CETeG) 5–8th April 2017 Zánka, Lake Balaton. *Acta Mineralogica-Petrographica*, Field Guide Series 32, 47–76.

Fodor L., Kercsmár Zs., Kövér Sz. (2018). A Gerecse szerkezete és deformációs fázisai (Structure and deformation phases of the Gerecse). In: Budai T. (szerk.): A Gerecse hegység földtana. 169–208. *Magyar Bányászati és Földtani Szolgálat kiadványa*, [In: Budai, T. (ed.): Geology of the Gerecse Mountains. *Mining and Geological Survey of Hungary, Budapest*, 169–208, 370–386. ISBN 978-963-671-312-6

Fogarasi, A. (1995a). Ciklussztratigráfiai vizsgálatok a gerecsei krétában: előzetes eredmények.(Cretaceous cyclostratigraphy of the Gerecse Mt. Preliminary results. *Általános Földtani Szemle*, 27, 43–58.

Fogarasi, A. (1995b). Üledékképződés egy szerkezeti mozgásokkal meghatározott kréta korú tengeralatti lejtőn a Gerecse hegységben – munkahipotézis (Sedimentation on tectonically controlled submarine slopes of Cretaceous age, Gerecse Mts., Hungary – working hypothesis). *Általános Földtani Szemle*, 27, 15–41.

Frank, W., Schlager, W. (2006). Jurassic strike slip versus subduction in the Eastern Alps. International *Journal of Earth Sciences*, 95, 431–450.

Frehner, M. (2011). The neutral lines in buckle folds – Journal of *Structural Geology, 33*, 1501-1508

Froitzheim, N., Manatschal, G. (1996). Kinematics of Jurassic rifting, mantle exhumation, and passive-margin formation in the Austroalpine and Penninic nappes (eastern Switzerland). *Bulletin of the Geological Society of America*, 108, 9, 1120–1133. https://doi.org/10.1130/0016-7606(1996)108<1120:KOJRME>2.3.CO;2

Fruth, I., Scherreiks, R. (1984). Hauptdolomit – Sedimentary and Paleogeographic Models (Norian, Northern Calcareous Alps). *Geologische Rundschau*, 73, 1, 305-319.

Fülöp, J. (1958). A Gerecsehegység krétaidőszaki képződményei. (Die Kretazeischen bildungen des Gerecse-gebirges.) *Geologica Hungarica, ser. Geologica*, 11, 1-123.

Fülöp J. (1990). Magyarország geológiája. Paleozoikum I. (*Geology of Hungary. Palaeozoic I.*). A *Magyar Állami Földtani Intézet* kiadványa, Budapest, 325 p. (In Hungarian)

Fülöp J., Dank V. (1987). Magyarország földtani térképe, 1:500 000. Magyarország Földtani Atlasza 2 [1986], (Translated title: Geological map of Hungary without Tertiary formations, scale 1:500,000, *Geological Atlas of Hungary 2*.) *Földt. Int. publ*

Gaina, C., Torsvik, T. H., van Hinsbergen, D.J.J.,Medvedev, S., Werner, S.C., Labails, C. (2013) The African plate: A history of oceanic crust accretion and subduction since the Jurassic. *Tectonophysics, 604*, 4-25.

Galácz A. (1988). Tectonically controlled sedimentation in the Jurassic of the Bakony Mountains (Transdanubian Central Range, Hungary). *Acta Geologica Hungarica*, 31, 313-328.

Galácz A., Vörös A. (1972). A bakony-hegységi jura fejlődéstöténeti vázlata a főbb üledékföldtani jelenségek kiértékelése alapján. (Jurassic history of the Bakony Mountains and interpretation of principal lithological phenomena.) *Földtani Közlöny*, 102, 122-135, Budapest. (In Hungarian, with English abstract)

Gale, L., Celarc, B., Caggiati, M., Kolar-Jurkovsek, T., Jurkovsek, B., Gianolla, P. (2015). Paleogeographic significance of Upper Triassic basinal succession of the Tamar Valley, northern Julian Alps (Slovenia). *Geologica Carpathica*, 66, 4, 269–283. http://doi.org/10.1515/geoca-2015-0025

Gallet Y, Krystyn L, Besse J (1998) Upper Anisian to Lower Carnian magnetostratigraphy from the Northern Calcareous Alps (Austria). Journal of Geophysical Research 103(B1):605–621.

Gawlick, H., J., Missoni, S. (2013). Triassic to Early Cretaceous geodynamic history of the central Northern Calcareous Alps (Northwestern Tethyan realm). *Berichte Geol. B.-A.*, 99, 178-190.

Gawlik, H., J., Frisch, W., Vecsei, A., Steiger, T., Böhm, F. (1999). The change from rifting to thrusting in the Northern Calcareous Alpl as recorded in Jurassic sediments. *Geologische Rundschau*, 87, 644–657.

Gawlick, H., J., Missoni, S., Schlagintweit, F., Suzuki, H., Frisch, W., Krystyn, L., Blau, J., Lein, R. (2009). Jurassic Tectonostratigraphy of the Austroalpine domain. *Journal of Alpine Geology*, 50, 1-152,

Gawlick, H., J., Sudar, M., N., Missoni, S., Suzuki, H., Lein, R., Jovanovic, D., (2017). Triassic—Jurassic geodynamic history of the Dinaric Ophiolite Belt (Inner Dinarides, SW Serbia). *J Alpine Geol*, 55, 1–167.

Gelabert, B., Sabat, F., Hardy, S., Rodriguez-Perea, A. (2004). Significance of Inherited Normal Faults during Inversion Tectonics: an example from the Tramuntana Range, Mallorca. *Geodinamica Acta*, 17, 6, 363–373. https://doi.org/10.3166/ga.17.363-373

Goričan, Š., Žibret, L., Košir, A., Kukoč, D., Horvat, A. (2018). Stratigraphic correlation and structural position of Lower Cretaceous flysch-type deposits in the eastern Southern Alps (NW Slovenia). *International Journal of Earth Sciences, 107*, 8, 2933–2953. https://doi.org/10.1007/s00531-018-1636-4

Guillaume, B., Husson, L., Funiciello, F., Faccenna, C. (2013). The dynamics of laterally variable subductions: laboratory models applied to the Hellenides. *Solid Earth, European Geosciences Union*, 2013, 4, 179-200. <10.5194/se-4-179-2013>. <insu-00914586>

Gulyás, Á. (1991). Jelentés a Keszthelyi-hegység és a Bakonyban 1990-ben a Plató program keretében végzett felszíni geofizikai mérésekről. (translated tilte: Report of near-surface geophysical measurement of Keszhely Hills and Bakony). *Plató project 1990*, manuscript, Budapest. (in Hungarian)

Haas, J. (1988) Upper Triassic carbonate platform evolution in the Transdanubian Mid-Mountains. *Acta Geologica Hungarica*, 31, 3-4, 299-312.

Haas J. (1993a). Budaörsi Dolomit Formáció, Fődolomit Formáció, Kösseni Formáció. (in hungarian, translated title: Budaörs Folomite Formation, Hauptdolomit Formation and Kössen Formation.) In Haas J. (ed.): Magyarország litosztratigráfiai alapegységei. Triász. (in hungarian, translated title: Base units of the hungarian litostratigraphy. Triassic.) *Geological Institute of Hungary*, Budapest. (in Hungarian)

Haas J. (1993b). Formation and evolution of the „Kösseni Basin" in the Transdanubian Range. *Földtani Közlöny*, 123, 1, 9–54.

Haas J. (1999). Late Cretaceous isolated platform evolution in the Bakony Mountains (Hungary). *Geologica Carpathica*, 50, 241–256.

Haas J. (2002). Origin and evolution of Late Triassic backplatform and intraplatform basins in the Transdanubian Range, Hungary. *Geologica Carpathica*, 53, 3, 159–178.

Haas J., Jocháné Edelényi E. (1978): A Dunántúli-középhegység bauxitföldtani térképe. Felsõkréta bauxitszint (1:200 000). — Issue of the Hungarian Geological Survay

Haas J., Jocháné-Edelényi E., Gidai L., Kaiser M., Kretzoi M., Oravecz J. (1984). Geology of the Sümeg Area. *Geologica Hungarica Series Geologica*, 20, 353.

Haas J., Tóth-Makk Á., Oravecz-Scheffer A., Góczán F., Oravecz J., Szabó I. (1988). Alsó-triász alapszelvények a Dunántúli-középhegységben. *Annals, of the Geological Institute of Hungary*, 45, 319 p.

Haas J., Kovács S., Krystyn L., Lein R. (1995). Significance of Late Permian-Triassic facies zones in terrane reconstructions in the Alpine-North Pannonian domain. *Tectonophysics*, 242, 1–2, 19–40. http://doi.org/10.1016/0040-1951(94)00157-5

Haas, J., Budai, T., (1999). Triassic sequence stratigraphy of the Transdanubian Range,Hungary. *Geologica Carpathica*, 50 (6), 459–475.

Haas J., Korpás L., Török Á., Dosztály L., Góczán F., Hámorné Vidó M., Oraveczné Scheffer A., Tardiné Filácz E. (2000a). Felső-triász medece- és lejtőfáciesek a Budai-hegységben a Vérhalom téri fúrás vizsgálatának tükrében (Upper Triassic basin and slope facies in the Buda Mts.- based on study of core drilling Vérhalom tér Budapest). *Földtani Közlöny*, 130, 371–421. (in Hungarian with English abstract)

Haas J., Mioć P., Pamić J., Tomljenović B, Árkai P, Bérczi-Makk A, Koroknai B, Kovács S, Felgenhauer E (2000b). Complex structural pattern of the Alpine-Dinaridic-Pannonian triple junction. *International Journal of Earth Sciences*, 89, 377–389.

Haas J., Budai T., Csontos L., Fodor L., Konrád Gy. (2010). Magyarország pre-kainozoos földtani térképe, 1:500 000 (Pre-Cenozoic geological map of Hungary, 1:500 000). *Geological Institute of Hungary*, Budapest. (In Hungarian and in English)

Haas J., Budai T., Raucsik B. (2012). Climatic controls on sedimentary environments in the Triassic of the Transdanubian Range (Western Hungary). *Palaeogeography, Palaeoclimatology, Palaeoecology*, 353–355, 31–44, https://doi.org/ 10.1016/j.palaeo. 2012.06.031

Haas J., Budai T., Győri O., Kele S. (2014). Multiphase partial and selective dolomitization of Carnian reef limestone (Transdanubian Range, Hungary). *Sedimentology*, 61, 3, 836–859. http://doi.org/10.1111/sed.12088

Handy, M., R., Schmid, S., M., Bousquet, R., Kissling, E., Bernoulli, D. (2010). Reconciling plate-tectonic reconstructions of Alpine Tethys with the geological – geophysical record of spreading and subduction in the Alps. *Earth-Science Reviews*, 102, 3–4, 121–158.

Handy, M., R., Ustaszewski, K., Kissling, E. (2015). Reconstructing the Alps – Carpathians – Dinarides as a key to understanding switches in subduction polarity , slab gaps and surface motion. *International Journal of Earth Sciences*, 104, 1–26. https://doi.org/10.1007/s00531-014-1060-3

Heer L (1982) Paläomagnetische Testuntersuchungen in den Nördlichen Kalkalpen im Gebiet zwischen Golling und Kössen. MSc. Thesis, Technical University, Munich

Héja G. (2015a). A Keszthelyi-hegység és nyugati előterének szerkezetfejlődése, különös tekintettel a kréta deformációkra. (in hungarian, English title: Structural evolution of the Keszthely hills and their western forelands, with aspect of the Cretaceous deformations.) *MSc work, manuscript, Eötvös University, Dept. of Applied and General Geology*, 118 p.

Héja G. (2015b). Az északi-bakonyi albai-cenomán üledékciklus tektonosztratigráfiai értelmezése. (in hungarian, english abstract: The tectono-sedimentological interpretation of the albian–cenomanian basin evolution of the Northern Bakony, Hungary.) *Földtani Közlöny*, 145, 3, 257-272.

Héja, G., Csizmeg, J., Kövér, Sz., Fodor, L. (2016). The effect of Late Triassic extension on eoalpine thrusting in the Keszthely Hills, West Hungary. *AAPG European Regional Conference and Exhibition, Bucharest, Romania, Abstract Volume*, 154 p.

Héja G., Csizmeg, J., Kövér, S., Németh, A., Fodor, L. (2017a). Structural inheritance of Triassic–Jurassic normal faults in a Cretaceous thrust and fold belt based on seismic and field data (western Transdanubian Range, Hungary) In: Abstracts of 'Fold and Thrust Belts: structural style, evolution and exploration'. *London, United Kingdom, Abstract Volume*: pp. 159-160.

Héja, G. Kövér, Sz., Csizmeg, J., Németh, A., Fodor, L., (2017b). The deformation of the SW part of the Transdanubian Range (West Hungary), based on balanced cross-sections. Acta Mineralogica-Petrographica Field Guide Series 32, *15th Meeting CETEG 2017, Abstract Volume*, 13 p.

Héja, G., Kövér, Sz., Csillag, G., Németh, A., Fodor, L. (2018). Evidences for pre-orogenic passive-margin extension in a Cretaceous fold-and –thrust belt on the basis of combined seismic and field data (western

Transdanubian Range, Hungary). *International Journal of Earth Sciences*, 107, 2955-2973. https://doi.org/10.1007/s00531-018-1637-3

Hetényi, M. (2002). Organic facies distribution at the platformward margin of the Kössen basin. *Acta Mineralogica-Petrographica*, Szeged, 43, 19-25.

Hindle, D., Burkhard, M. (1999). Strain, displacement and rotation associated with the formation of curvature in fold belts; the example of the Jura arc, *J. Struct. Geol.*, 21, 1089-1101.

Hips K., Haas J., Győri O. (2015). Hydrothermal dolomitization of basinal deposits controlled by a synsedimentary fault system in Triassic extensional setting, *Hungary. Int J Earth Sci (Geol Rundsch)*, 2016, 105, 1215–1231. 675 DOI 10.1007/s00531-015-1237-4

Horváth F. (1993). Toward a mechanical model for the Pannonian Basin. *Tectonophysics*, 225, 333-358.

Horváth F., Berckhemer, H. (1982). Mediterranean backarc basins, in Alpine-Mediterranean Geodynamics, *Geodyn. Ser., vol. 7, edited by H. Berckhemer, K. Hsü*, 141–173, AGU, Washington, D. C.

Horváth F., Cloetingh, S. (1996). Stress-induced late-stage subsidence anomalies in the Pannonian basin, *Tectonophysics*, 266, 287-300.

Horváth, F., Bada, G., Szafián, P., Tari, G., Ádám, A., Cloetingh, S., (2006). Formation and deformation of the Pannonian basin: Constraints from observational data. In: Gee, D., G., Stephenson, R., A. (Eds.), European Lithosphere Dynamics. *Geological Society, London, Memoirs*, 32, 1, 191-206.

Horváth F., Musitz B., Balázs A., Végh A., Uhrin A., Nádor A., Koroknai B., Pap N., Tóth T., Wórum G. (2015). Evolution of the Pannonian basin and its geothermal resources. *Geothermics*, 53, 328-352.

Hraško, Ľ., Határ, J., Huhma, H., Mäntäri, I., Michalko, J., & Vaasjoki, M. (1999). U/Pb zircon dating of the upper cretaceous granite (Rochovce type) in the Western Carpathians. Krystalinikum, 25, 163–171.

Jablonský, J., Michalík, J., Plašienka, D., & Soták, J. (1993). Sedimentary environments of the Solírov Formation and correlation with Lower Cretaceous turbidites in central West Carpathians, Slovakia. Cretaceous Research, 14(6), 613–621. https://doi.org/10.1006/ cres.1993.1043

Jadoul, F., Galli, M., T., Calabrese, L., Gnaccolini, M. (2005). Stratigraphy of Rhaetian To Lower Sinemurian Carbonate Platforms in Western Lombardy (Southern Alps, Italy): Paleogeographic Implications. *Rivista Italiana Di Paleontoligia E Stratigrafia*, 111, 2, 285–303.

Janák, M., Froitzheim, N., Lupták, B., Vrabec, M., Ravna, E., J., K. (2004). First evidence for ultrahigh-pressure metamorphism of eclogites in Pohorje, Slovenia: Tracing deep continental subduction in the Eastern Alps. *Tectonics*, 23, TC5014. https://doi.org/10.1029/2004TC001641

Jeřábek, P., Lexa, O., Schulmann, K., & Plašienka, D. (2012). Inverse ductile thinning via lower crustal flow and fold-induced doming in the west Carpathian Eo-Alpine collisional wedge. Tectonics, 31, TC5002. https://doi.org/10.1029/2012TC003097

Jin, G., Groshong Jr., R., H., (2006). Trishear kinematic modeling of extensional faultpropagation folding. *Journal of Structural Geology*, 28, 170–183.

Jósvai J., Németh A., Kovácsvölgyi S., Czeller I., Szurominé Korecz A. (2005). A Zala-medence szénhidrogén kutatásának földtani eredményei. *Földtani Kutatás*, 42, 1, 9–15.

Kázmér, M., Kovács, S. (1985). Permian-Paleogene Paleogeography along the Eastern part of the Insubric-Periadriatic Lineament system: Evidence for continental escape of the Bakony-Drauzug Unit. *Acta Geologica Hungarica*, 28, 71–84.

Kelemen, P. (2018). Provenance study of various continental sediments in the Transdanubian Range — implications for the Mesozoic to Cenozoic geologic and geodynamic evolution. *9th Assembly of Petrology and chemistry*, 79-80.

Kiss A. (2009). Az Északi-Bakony szerkezetalakulása. PhD Thesis, *Eötvös University, Dept. of Applied and Environmental Geology*, 120 p.

Knipe, R., J. (1986). Deformation mechanism path diagrams for sediments undergoing lithification. *Mem. Geol. Soc. Amer.*, 166, 151–160.

Kókay, J. (1966). A Herendi-medence földtana.(in hungarian, taranslated title: Geology of the Herend Basin.) *Geologica Hungarica, ser. pal.*, 36, 92 p.

Konstantinovskaya, E., Malo, M., Badina, F. (2014). Effects of irregular basement structure on the geometry and emplacement of frontal thrusts and duplexes in the Quebec Appalachians: Interpretations from well and seismic reflection data, *Tectonophysics,* Volume 637, 268-288.

Koroknai, B., Horváth, P., Balogh, K., Dunkl, I. (2001). Alpine metamorphic evolution and cooling history of the Veporic crystalline basement in northern Hungary: new petrological and geochronological constraints. *International Journal of Earth Sciences*, 90, 3, 740–751.

Kőrössy L. (1958). Adatok a Kisalföld mélyföldtanához (Some data concerning the subsurface geology of the Kisalföld, Little Hungarian Basin). *Földtani Közlöny*, 88, 291-298. (in Hungarian with English abstract)

Kőrössy L. (1988). Hydrocarbon geology of the Zala Basin in Hungary. *Általános Földtani Szemle*, 23, 3–162. (in Hungarian)

Kwon, S., Mitra, G. (2004). Strain distribution, strain history, and kinematic evolution associated with the formation of arcuate salients in fold-thrust belts : The example of the Provo salient, Sevier orogen, Utah. *Geological Society of America Special*, 205–223. https://doi.org/10.1130/0-8137-2383-3(2004)383

Lantos, Z. (1997). Karbonátos lejtő-üledékképződés egy liász tengeralatti magaslat oldalában, eltolódásos vetőzóna mentén (Gerecse). (in hungarian, English abstract: Sediments of a Liassic carbonate slope controlled by strike-slip fault activity (Gerecse Hills, Hungary) *Földtani Közlöny*, 127, 3-4, 291–320.

Lavier, L., Manatschal, G. (2006). A mechanism to thin the continental lithosphere at magma-poor margins. *Nature*, 440:324-328.

Lelkes-Felvári Gy. (1998). A Dunántúli-középhegység metamorf képződményeinek rétegtana. In: Bérczi I., Jámbor Á. (szerk.): Magyarország geológiai képződményeinek rétegtana, 73–86, Budapest.

Lelkes-Felvári Gy., Sassi, F.P., & Zirpoli, G. (1994). Lithostratigraphy and Variscan metamorphism of the Paleozoic sequences in the Bakony Mountains, Hungary. *Mem. Sci. Geol.* 46, pp. 303–312.

Lelkes-Felvári, Gy., Sassi, R., Frank, W. (2002). Tertiary S-C mylonites from the Bajánsenye-B-M-I borehole, Western Hungary. *Acta Geologica Hungarica*, 45, 29–44.

Linzer, H., G,. Tari, G. (2012). Structural correlation between the Northern Calcareous Alps (Austria) and the Transdanubian Central Range (Hungary). *American Association of Petroleum Geologists Memoir*, 100, 249–266.

Linzer, H., Decker, K., Peresson, H., Dell, R., Frisch, W. (2002). Balancing lateral orogenic float of the Eastern Alps. *Tectonophysics*, 354, 211–237.

Maffione, M., Van Hinsbergen D.J.J. (2018). Reconstructing Plate Boundaries in the Jurassic Neo-Tethys From the East and West Vardar Ophiolites (Greece and Serbia). Tectonics, 37, 858-887

Magyar, I., Radivojevic, D., Sztanó, O., Synak, R., Ujszászi, K., Pócsik, M. (2013). Magyar, I., Radivojevic, D., Sztanó, O., Synak, R., Ujszászi, K., Pócsik, M. (2013). Progradation of the paleo-Danube shelf margin across the Pannonian Basin during the Late Miocene and Early Pliocene. *Global and Planetary Change*, 103, 168–173.

Majer, V., Lugović, B. (1985). Metamorfne stijene u ofiolitnoj zoni Banije, Jugoslavija. II. Amfiboliti (metabaziti) (Metamorphic rocks in Banija ophiolitic zone, Yugoslavia. II. Amphibolites (metabasic rocks)). *Acta geol. JAZU*, 15, 25–49.

Majoros Gy. (1983). Lithostratigraphy of the Permian Formations of the Transdanubian Central Mountains. *Acta Geologica Hungarica*, 26, 1–2, 7–20.

Manatschal, G., Lavier, L., Chenin, P. (2015). The role of inheritance in structuring hyperextended rift systems: Some considerations based on observations and numerical modeling. *Gondwana Research*, 27, 140-164.

Mandl, G., W., (2000). The Alpine sector of the Tethyan shelf - Examples of Triassic to Jurassic sedimentation and deformation from the Northern Calcareous Alps. *Mitt. Österr. Geol. Ges.*, 92, 61–77.

Marshak, S., (2004). Salients, recesses, arcs, oroclines, and syntaxes—A review of ideas concerning the formation of map-view curves in fold-thrust belts, in K. R. McClay, ed., Thrust tectonics and hydrocarbon systems: *AAPG Memoir*, 82, 131–156.

Márton E, Márton P (1983) A refined polar wander curve for the Transdanubian Central Mountains and its bearing on the Mediterranean tectonic history. Tectonophysics 98:43–57.

Márton, E., Fodor, L., (2003). Tertiary paleomagnetic results and structuralanalysis from the Transdanubian Range (Hungary); sign for rotational disintegration of the Alcapa unit. *Tectonophysics*, 363, 201–224.

Márton E., Grabowski J., Tokarski A., K., Túnyi I. (2015). Paleomagnetic results from the fold and thrust belt of the Western Carpathians: an overwiev. *Geological Society, London, Special Publications*, 425.

Masetti, D., Fantoni, R., Romano, R., Sartorio, D., Trevisani, E. (2012). Tectonostratigraphic evolution of the Jurassic extensional basins of the eastern southern Alps and Adriatic foreland based on an integrated study of surface and subsurface data. *AAPG Bulletin*, 96, 11, 2065–2089. https://doi.org/10.1306/03091211087

Mauritsch HJ (1980) Palaomagnetische Untersuchungen an einigen Magnesiten aus der westlichen Grauwackenzone. Mitt. Österr. Geol. Ges. 73:1-4.

Mauritsch HJ, Becke M (1987) Palaeomagnetic Investigations in the Eastern Alps and the Southern Border Zone. In: Flugel HW, Faupl P (eds) Geodynamics of the Eastern Alps. 283-308, Deuticke, Vienna.

Mauritsch HJ, Frisch W (1978) Palaeomagnetic data from the Central part of the Northern Calcareous Alps, Austria. J. Geophys. 44:623-637.

Mauritsch, H., J., Márton, E. (1995). Escape models of the Alpine-Carpathian-Pannonian region in the light of palaeomagnetic observations, *Terra Nova*, 7, 44-50.

McKenzie, D., Nimmo, F., Jackson, J.A., Gans, P.B., Miller, E.L., (2000). Characteristics and consequences of flow in the lower crust. *Journal of Geophysical Research*, 105, 11,029–11,046, doi:10.1029/1999JB900446.

Meister, P., Mckenzie, J., A., Bernasconi, S., M., Brack, P. (2013). Dolomite formation in the shallow seas of the Alpine Triassic. *Sedimentology*, 60, 1, 270–291. https://doi.org/10.1111/sed.12001

Mészáros, J., (1983). Structural and economic geological significance of strikeslip faults in the Bakony Mountains. *Annual Report Geol. Institute Hung. from 1981*, 485–502. (in Hungarian with English abstract)

Mindszenty A., Deák F. (1999). Karbonátos paleotalajok a gerecsei felsó-triászban. (Carbonate palaeosols from the Upper Triassic of the Gerecse Mountains, Hungary). *Földtani Közlöny*, 129, 2, 213-248. (in Hungarian with English abstract)

Mindszenty, A., Knauer, J., Matei S. (1994). Superimposed paleokarst phenomena in the Halimba Basin (south Bakony, Hungary) – The anatomy of a multiple regional unconformity. *IAS 15th Regional Meeting, 13-15 April 1994, Ischia, Italy, Abstracts*, 285–286. (de Frede, Napoli).

Mindszenty, A., D'Argenio, B., Aiello,G. (1995). Lithospheric bulges at regional unconformities. The case of Mesozoic-Tertiary Apulia. *Tectonophysics*, 252, 137-161.

Mindszenty A., Csoma A., Török Á., Hips K., Hertelendi E. (2000). Flexura jellegű előtéri deformációhoz köthető karsztbauxit szintek a dunántúli középhegységben (Rudistid limestones, bauxites, paleokarst and geodynamics. The case of the Cretaceous of the Transdanubian Central Range). *Földtani Közlöny*, 131, 107–152. (in Hungarian with English abstract)

Mitra, S. (2002). Fold-accommodation faults. *AAPG Bull*, 86, 671–693.

Mitra, S., (2003). A unified kinematic model for the evolution of detachment folds. *J. Struct. Geol.* 25, 1659–1673.

Moustafa, A., R., Khalil, S., M. (2016). Control of compressional transfer zones on syntectonic and post-tectonic sedimentation: implications for hydrocarbon exploration. *Journal of the Geological Society*, https://doi.org/10.1144/jgs2016-030

Nagy, Z., R., Djeric, N., Kovács, S., Oravecz-Scheffer, A., Velledits, F., Piros, O., Csillag, G. (2014). Evidence for Ladinian (Middle Triassic) platform progradation in the Gyulakeszi area, Tapolca Basin, western Hungary: Microfacies analysis and biostratigraphy. *Rivista Italiana di Paleontologia e Stratigrafia*, 120, 2, 165-181.

Neubauer, F., Genser, J., Handler, R. (2000): The Eastern Alps: Result of a two-stage collision process. Mitt. Österr. Geol. Ges. 92 (1999), 117–134.

Nyíri, D. (2017). Az Őrség szekvenciasztratigráfiai és szerkezeti értelmezése, különös tekintettel a miocén üledéksor fejlődéstörténetére. *MSc thesis,Eötvös University, Dept. of Applied and General Geology,* 94 p.

Ortner, H. (2003). Cretaceous thrusting in the western part of the Northern Calcareous Alps (Austria) - evidences from synorogenic sedimentation and structural data. *Mitt. Österr. Geol. Ges.sterr. Geol. Ges.*, *94*, 2001, 63–77.

Ortner, H. (2007). Styles of soft-sediment deformation on top of a growing fold system in the Gosau Group at Muttekopf, Northern Calcareous Alps, Austria: Slumping versus tectonic deformation. *Sedimentary Geology*, 196, 1–4, 99–118. http://doi.org/10.1016/j.sedgeo.2006.05.028

Ortner, H. (2013). Deep water sedimentation on top of a growing orogenic wedge - interaction of thrusting, erosion and deposition in the Cretaceous Northern Calcareous Alps. *Geo. Alp.*, 13, 141–182.

Ortner, H. (2017). Geometry of growth strata in wrench-dominated transpression: 3D-model of the Upper Jurassic Trattberg rise, Northern Calcareous Alps, Austria. European Geosciences Union General Assembly 2017 Vienna, Geophysical Research, Abstracts, 19

Ortner, H., Reiter, F., Brandner, R. (2006). Kinematics of the Inntal shear zone–sub-Tauern ramp fault system and the interpretation of the TRANSALP seismic section, Eastern Alps, Austria. *Tectonophysics*, 414, 1-4, 241–258. doi:10.1016/j.tecto.2005.10.017

Ortner, H., Ustaszewski, M., Rittner, M. (2008). Late Jurassic tectonics and sedimentation: Breccias in the Unken syncline, central Northern Calcareous Alps. *Swiss Journal of Geosciences*, 17. https://doi.org/10.1007/s00015-008-1282-0

Pace, P., Di Domenica, A., Calamita, F. (2014). Summit low-angle faults in the Central Apennines of Italy: Younger-on-older thrusts or rotated normal faults? Constraints for defining the tectonic style of thrust belts. *Tectonics*, 33, 5, 756–785. https://doi.org/10.1002/2013TC003385

Palotai M. (2013). A Közép-magyarországi zóna középső részének oligocén-miocén szerkezetfejlődése. *PhD thesis, Eötvös University, Dept. of Applied and General Geology*, 148 p.

Palotai, M., Csontos, L. (2010). Strike-slip reactivation of a Paleogene to Miocene fold and thrust belt along the central part of the Mid-Hungarian Shear Zone. *Geologica Carpathica*, 61, 6, 483-493.

Palotai M., Csontos L., Dövényi P. (2006a). A kesztölci mezozoos (felső-jura) előfordulás terepi és geoelektromos vizsgálata (Field and geoelectric study of the Mesozoic (Upper Jurassic) occurrence at Kesztölc). *Földtani Közlöny*, 136, 3, 347–368. (in Hungarian with English abstract)

Palotai M., Csontos L., Dövényi P., Galácz A. (2006b). Az Eperkés-hegyi felső-jura képződmények áthalmozott tömbjei. (in hungarian, extended English abstract: Redeposited blocks in Upper Jurassic sediments on Eperkés Hill.) *Földtani Közlöny*, 136, 3, 325-346. (in Hungarian with English abstract)

Perez, N., D., Horton, B., K., Carlotto, V. (2016). Structural inheritance and selective reactivation in the central Andes: Cenozoic deformation guided by pre-Andean structures in southern Peru. *Tectonophysics*, 671, 264–280. https://doi.org/10.1016/j.tecto.2015.12.031

Plašienka, D., Grecula, P., Putiš, M., Kováč, M., & Hovorka, D. (1997). Evolution and structure of the Western Carpathians: An overview. In P. Grecula, D. Hovorka, & M. Putiš (Eds.), Geological evolution of the Western Carpathians (pp. 1–24i). Monograph: Mineralia Slovaca.

Plašienka, D. (2018). Continuity and Episodicity in the Early Alpine Tectonic Evolution of the Western Carpathians : How Large-Scale Processes Are Expressed by the Orogenic Architecture and Rock Record Data. *Tectonics*, 1–51. https://doi.org/10.1029/2017TC004779

Platt, J., P. (1993). Mechanics of oblique convergence. *J. Geophys. Res.*, 98, 16,239-16,256,

Pocsai, T., Csontos, L., (2006). Late Aptian–early Albian syn-tectonic faciespattern of the Tata Limestone Formation (Transdanubian Range, Hungary). *Geol. Carpathica*, 57, 15–27.

Pogácsás, Gy. (1985). Seismic stratigraphic features of Neogene sediments in the Pannonian Basin Geophysical *Transactions*, 30, 4, 373-410.

Poller, U., Uher, P., Janák, M., Plašienka, D., Kohút, M. (2001). Late Cretaceous age of the Rochovce granite, Western Carpathians, constrained by U-Pb single-zircon dating in combination with cathodoluminiscence imaging. *Geologica Carpathica*, *52*, 1, 41–47.

Pomella, H., Stipp, M., Fügenschuh, B. (2012). Tectonophysics Thermochronological record of thrusting and strike-slip faulting along the Giudicarie fault system (Alps, Northern Italy). *Tectonophysics*, 579, 118–130. https://doi.org/10.1016/j.tecto.2012.04.015

Porkoláb K., Kövér Sz., Benkó Zs., Héja G., Fialowski M., Soós B., Spajić, N.G., Đerić, N., Fodor L. (2018): Structural and geochronological constraints from the Drina-Ivanjica thrust sheet (Western Serbia): implications for the Cretaceous-Paleogene tectonics of the Internal Dinarides — Swiss Journal of Geosciences

Ramsay, J., G. (1967). Folding and Fracturing of Rocks. McGraw-Hill, New York. 568.

Royden, L., H. (1988). Late Cenozoic tectonics of the Pannonian basin system. In: L.H. Royden and F. Horváth (Editors): The Pannonian Basin, a Study in Basin Evolution. *Am. Assoc. Pet. Geol, Mem.*, 45, 27-48.

Rožič, B., Kolar-Jurkovšek, T., Šmuc, A. (2009). Late Triassic sedimentary evolution of Slovenian Basin (eastern Southern Alps): Description and correlation of the Slatnik Formation. *Facies*, 55, 1, 137–155. https://doi.org/10.1007/s10347-008-0164-2

Rumpler, J., Horváth, F. (1988). Some representative seismic reflection lines from the Pannonian basin and their structural interpretation. In: L.H. Royden and F. Horváth (Editors): The Pannonian Basin, a Study in Basin Evolution. *Am Assoc. Pet. Geol. Mem.*, 45, 153-169.

Ruszkiczay-Rüdiger, Zs., Balázs, A., Csillag, G., Drijkoningen, G., Fodor, L. (2018). Plio-Quaternary uplift of the Transdanubian Range, Western Pannonian Basin: How fast and why? *In: Šujan et al., (eds.) Abstracts of the 11th ESSEWECA Conference, 29-30th. November, 2018, Bratislava, Slovakia*, 94-95.

Saïd, A., Baby, P., Chardon, D., Ouali, J. (2011). Structure, paleogeographic inheritance, and deformation history of the southern Atlas foreland fold and thrust belt of Tunisia, *Tectonics*, 30, TC6004, doi:10.1029/2011TC002862.

Sasvári Á. (2008). Rövidüléshez köthető deformációs jelenségek a Gerecse területén. (in Hungarian with English abstract: Shortening-related deformation in the Gerecse Mts, Transdanubian Range, Hungary). *Földtani Közlöny*, 138, 4, 385-402.

Sasvári Á. (2009). Középső-kréta rövidüléses deformáció és szerkezeti betemetődés a Gerecse területén. *PhD thesis, Eötvös University, Dept. of Applied and General Geology*, 164 p. (in Hungarian)

Sasvári, Á., Kiss, A., Csontos, L.(2007). Paleostress investigation and kinematic analysis along the Telegdi Roth Fault (Bakony Mountains, western Hungary). *Geologica Carpathica*, 58, 477–486.

Satterley, A., K., Brandner, R. (1995). The genesis of Lofer cycles of the Dachstein Limestone, Northern Calcareous Alps, Austria. *Geologische Rundschau*, 84, 2, 287–292. https://doi.org/10.1007/BF00260441

Schedl, A., Wiltschko, D., V. (1987). Possible effects of pre-existing basement topography on thrust fault ramping. *Journal of Structural Geology*, 9, 8, 1029–1037. https://doi.org/10.1016/0191-8141(87)90011-3

Schefer, S., (2012) Tectono-metamorphic and magmatic evolution ofthe Internal Dinarides (Kopaonik area, southern Serbia) and itssignificance for the geodynamic evolution of the BalkanPeninsula: University of Basel

Schmid, S., M., Fügenschuh, B., Kissling, E., Schuster, R. (2004). Tectonic map and overall architecture of the Alpine orogen. *Eclogae Geologicae Helvetiae*, 97, 1, 93–117. https://doi.org/10.1007/s00015-004-1113-x

Schmid, S., M., Bernoulli, D., Fügenschuh, B., Matenco, L., Schefer, S., Schuster, R., Tischler, M., Ustaszewski, K. (2008). The Alpine-Carpathian-Dinaridic orogenic system: Correlation and evolution of tectonic units. *Swiss J. Geosci.*, 101, 139–183. doi:10.1007/s00015-008-1247-3

Schmid, S., M., Bernoulli, D., Fügenschuh, B., Georgiev, N., Kounov, A., Matenco, L., Oberhänsli, R., Pleuger, J., Schefer, S., Ustaszewski, K. Van Hinsbergen, D. (2016). Tectonic Units Of The Alpine Collision Zone Between Eastern Alps And Western Turkey. Map.

Schmidt, T., Blau, J., Kázmér, M., (1991). *Large-scale strike-slip displacement of the Drauzug and the Transdanubian Mountains in early Alpine history: evidence from Permo-Mesozoic facies belts. Tectonophysics*, 200, 1-3, 213-232. ISSN 0040-1951

Schönborn, G. (1992) Alpine tectonics and kinematic models of the central Southern Alps. *Mem. Sci. Geol.*, 44, 229–393

Schuster, R., Koller, F., Hoeck, V., Hoinkes, G., Bousquet, R. (2004). Explanatory notes to the map: Metamorphic structure of the Alps – Metamorphic evolution of the Eastern Alps. *Mitteilungen der Österreichischen Mineralogischen Gesellschaft*, 149, 175–199.

Siegl-Farkas, Á., Haas, J., (2002). Stratigraphic and sedimentological analysis of the Upper Cretaceous sequence of the Zala Basin on the basis of the investigation of the Szilvágy-33 well. *Acta Geologica Hungarica*, 45, 153–175.

Stampfli, G., M., Borel, G. (2004). The TRANSMED transects in space and time: constraints on the paleotectonic evolution of the Mediterranean domain. In: Cavazza, W., Roure, F.M., Spakman, W., Stampfli G.M. & Ziegler, P.A. (Eds): The TRANSMED Atlas: The Mediterranean Region from Crust to Mantle. *Springer, Berlin and Heidelberg*, 53–80.

Stüwe, K., Schuster, R. (2010). Initiation of subduction in the Alps: Continent or ocean? *Geology*, 38(2), 175–178. https://doi.org/10.1130/G30528.1

Suppe, J., (1983). Geometry and kinematics of fault-bend folding. *Am. J. Sci.*, 283, 684–721.

Szives O. (1999). Ammonite biostratigraphy of the Tata Limestone Formation (Aptian - Lower Albian), Hungary. *Acta Geologica Hungarica*, 42, 2, 401–411.

Szives, O., Fodor, L., Fogarasi, A., Kövér, Sz. (2018). *Integrated calcareous nannofossil and ammonite data from the upper Barremian–lower Albian of the northeastern Transdanubian Range (central Hungary): Stratigraphical implications and consequences for dating tectonic events. Cretaceous Research*, 91, 4, 229-250. ISSN 0195-6671

Sztanó, O. (1990). Submarine fan-channel conglomerate of Lower Cretaceous, Gerecse. *Neues Jahrbuch Geol. Paläont. Mh.*, 7, 431–446.

Sztanó O., Magyari Á., Tóth P. (2010). Gilbert-típusú delta a pannóniai Kállai Kavics Tapolca környéki előfordulásaiban (Gilbert-type delta in the Pannonian Kálla Gravel near Tapolca, Hungary). *Földtani Közlöny,* 140/2,167–182.

Sztanó, O., Kováč, M., Magyar, I., Šujan, M., Fodor, L., Uhrin, A., Rybár, S., Csillag, G., Tőkés, L. (2016). Correlation of Late Miocene (Pannonian) lithostratigraphic units in the Danube–Kisalföld Basin (Slovakia, Hungary). *Geologica Carpathica*, 67, 6, 525–542. ISSN online:1336-8052 / print: 1335-0552

Tari, G. (1991). Multiple Miocene block rotation in the Bakony Mountains, Transdanubian Central Range, Hungary. *Tectonophysics*, 199, 93-108.

Tari, G. (1992). Tectonic significance of the Senonian basin in the Transdanubian Central Range, Hungary. *ALCAPA Meeting, Terra Nova, vol 4, Abstracts supplement 2*, 66.

Tari, G. (1994). Alpine Tectonics of the Pannonian Basin. *PhD Dissertation Rice University, Houston,*.

Tari, G. (1995). Eoalpine (Cretaceous) tectonics in the Alpine/Pannonian transition zone. — In: Horváth, F., Tari, G., Bokor, Cs. (editors) Extensional collapse of the Alpine orogene and Hydrocarbon prospects in the Basement and Basin Fill of the Western Pannonian Basin. *AAPG International Conference and Exhibition, Nice, France, Guidebook to fieldtrip No. 6. Hungary*, 133–155.

Tari, G., Horváth, F. (2010). Eo-Alpine evolution of the Transdanubian Range in the nappe system of the Eastern Alps: revival of a 15 years tectonic model. *Földtani Közlöny*, 140, 4, 483–510.

Tari, G., Linzer, H., G. (2018). Austrian versus Hungarian bauxites in an Alpine tectonic context: a tribute to Prof. Andrea Mindszenty. *Földtani Közlöny*, 148, 1, 35-44.

Tari, G., Horváth, F., Rumpler, J. (1992). Styles of extension in the Pannonian basin. *Tectonophysics*, 208, 203-219.

Tari, G., Báldi, T., Báldi-Beke, M. (1993). Paleogene retroarc flexural basin beneath the Neogene Pannonian Basin: a geodynamical model. *Tectonophysics*, 226, 433–455.

Tavani, S., Storti, F., Lacombe, O., Corradetti, A., Muñoz, A., J., Mazzoli, S. (2015). A review of deformation pattern templates in foreland basin systems and fold-and-thrust belts: Implications for the state of stress in the frontal regions of thrust wedges. *Earth Sci. Rev.*, 141, 82–104.

Tavarnelli, E. (1999). Normal faults in thrust sheets: pre-orogenic extension, post-orogenic extension, or both? *Journal of Structural Geology*, 21, 1011–1018.

Thöni, M. (1999). A review of geochronological data from the Eastern Alps. Schweiz. *Mineral. Petr. Mitt.*, 79, 209–230.

Teleki, G. (1936). Adatok Litér és környékének sztratigráfiájához és tektonikájához. (Beitrage zur Stratigrahie und Tektonik der Umgegend von Litér im Balaton-Gebirge). *Földtani Intézet Évkönyve*, 32, 1, 3–60.

Teleki, G. (1941). Adatok Felsőörs és környékének földtani viszonyaihoz. (translated title:). *MÁFI Évi Jelentése 1936–1938-ról*, 295–310.

Uhrin, A., Magyar, I., Sztanó, O., (2009). Effect of basement deformation on the Pannonian sedimentation of the Zala Basin, SW Hungary., *Földtani Közlöny*, 139, 273-282.

Ustaszewski, K., Schmid, S., M. (2006). Control of preexisting faults on geometry and kinematics in the northernmost part of the Jura fold-and-thrust belt. *Tectonics*, 25, 5, 26. https://doi.org/10.1029/2005TC001915

Ustaszewski, K., Schmid, S., M., Fügenschuh, B., Tischler, M., Kissling, E., Spakman, W. (2008). A map-view restoration of the Alpine–Carpathian– Dinaridic system for the Early Miocene. *Swiss J Geosci*, 101, 1, 273–294

Ustaszewski, K., Schmid, S.M., Lugović, B., Schuster, R., Schaltegger, U., Bernoulli, D., Hottinger, L., Kounov, A., Fügenschuh, B., Schefer, S., (2009). Late Cretaceous intraoceanic magmatism in the internal Dinarides (northern Bosnia and Herzegovina): implications for the collision of the Adriatic and European plates. *Lithos*, 108.

Velledits, F. (2006). Evolution of the Bükk Mountains (NE Hungary) during the Middle-Late Triassic assymetric rifting of the Vardar-Meliata branch of the Neotethys Ocean. *International Journal of Earth Sciences 95*, 395-412.

Vörös, A., Galácz, A. (1998). Jurassic palaeogeography of the Transdanubian Central Range (Hungary). *Rivista Italiana di Paleontologia e Stratigrafia*, 104, 1, 69–84.

Wein, Gy. (1977). Tectonics of the Buda Mountains. *Földtani Közlöny*, 107, 329-347. (in Hungarian with English abstract)

White, N., J., Jackson, J., A., McKenzie, D., P. (1986). The relationship between the geometry of normal faults and that of the sedimentary layers in their hanging walls. *Journal of Structural Geology*, 8, 897-909.

Wiltschko, D., Eastman, D. (1983). "Role of basement warps and faults in localizing thrust fault ramps", In: Hatcher, R., D., Jr., Williams, H., Zietz, I. (1983). Contributions to the Tectonics and Geophysics of Mountain Chains. *Geological Society of America*, 158, 177-190. https://doi.org/10.1130/MEM158-p177

Yagupsky, D., L., Cristallini, E., O., Fantín, J., Valcarce, G., Z., Bottesi, G., Varadé, R. (2008). Oblique half-graben inversion of the Mesozoic Neuquén Rift in the Malargüe Fold and Thrust Belt, Mendoza, Argentina: New insights from analogue models. *Journal of Structural Geology*, 30, 7, 839–853. https://doi.org/10.1016/j.jsg.2008.03.007

Zanchetta, S., Garzanti, E., Doglioni, C., Zanchi, A. (2012). The Alps in the Cretaceous: A doubly vergent pre-collisional orogen. *Terra Nova*, *24*, 5, 351–356. https://doi.org/10.1111/j.1365-3121.2012.01071.x

Acknowledgement

First of all, I am grateful to Szilvia Kövér, who helped a lot in the improvement of this work. I would like to thank my supervisor, László Fodor for his help. All my research was supported by the Hungarian Oil Company MOL Plc, and particularly by András Németh who was my external consultant.

Collaboration with many experts of the Hungarian Oil Company MOL Plc (Géza Wittmann, Zsolt Nagy, Emese Milankovich, Judit Szalay) are thanked. Consultation with Gábor Csillag, János Haas, Tamás Budai, Attila Balázs, Zoltán Erdős, Soma Budai contributed to this work.

Benjamin Scherman and Éva Oravecz helped me through stressful times during completion of this thesis.

I learnt the balancing technique from different sources, from short courses of Kamil Ustaszewski (Jena, Germany) and from Hugo Ortner (Innsbruck, Austria) during my CEEPUS scholarship.

The research was also supported by and formed part of the basic research project NKFIH-OTKA 113013, led by my supervisor. I benefitted the frame and support of the Tectonic Research Group within the MTA-ELTE Geological, Geophysical and Space Science Research Group located in the Eötvös Loránd University. My studies were also supported by the Scholarship of ÚNKP.

Last but not least I would like to say thank you to my family and my wife: Köszönöm picike, hogy elbirtál viselni idegbeteg állapotomban is.